Biological and molecular characterization of a new virus infecting *Cucumis melo* (Musk melon)

Thesis submitted to the
University of Hyderabad for the award of

DOCTOR OF PHILOSOPHY

By

NAGA TEJA NATRA
(Enrolment No. 09LPPH20)

Department of Plant Sciences
School of Life Sciences
University of Hyderabad
Hyderabad, 500 046
India

NOVEMBER 2014

Biological and molecular characterization of a new virus infecting *Cucumis melo* (Musk melon)

Thesis submitted to the
University of Hyderabad for the award of

DOCTOR OF PHILOSOPHY

By

NAGA TEJA NATRA
(Enrolment No. 09LPPH20)

Department of Plant Sciences
School of Life Sciences
University of Hyderabad
Hyderabad, 500 046
India

NOVEMBER 2014

UNIVERSITY OF HYDERABAD
हैदराबाद विश्वविद्यालय

(A Central University established in 1974 by act of parliament)
HYDERABAD – 500046, INDIA

DECLARATION

I, **Naga Teja Natra** hereby declare that this thesis entitled **"Biological and molecular characterization of a new virus infecting *Cucumis melo* (Musk melon)"** submitted by me under the guidance and supervision of **Dr. Gopinath Kodetham** is an original and independent research work. I also declare that it has not been submitted previously in part or in full to this University or any other University or Institution for the award of any degree or diploma.

Naga Teja Natra
09LPPH20

Dr. Gopinath Kodetham
(Research Supervisor)

UNIVERSITY OF HYDERABAD
हैदराबाद विश्वविद्यालय

(A Central University established in 1974 by act of parliament)
HYDERABAD – 500046, INDIA

CERTIFICATE

This is to certify that this thesis entitled **"Biological and molecular characterization of a new virus infecting *Cucumis melo* (Musk melon)"** is a record of bonafide work done by **Mrs. Naga Teja Natra,** a research scholar for Ph.D. programme in the Department of Plant Sciences, School of Life Sciences, University of Hyderabad, under my guidance and supervision. The work presented in this thesis is original and plagiarism free, no part has been submitted for any degree or diploma of any other University.

Dr. Gopinath Kodetham
(Research Supervisor)

HEAD
Department of Plant Sciences

DEAN
School of Life Sciences

Acknowledgments

The completion of this thesis would not have been possible without the help and support of many important people in my life. I would like to thank each and every one of them for their contributions and encouragement. In particular:

First and foremost, I would like to thank my mentor, **Dr. Gopinath Kodetham,** *Associate Professor, Department of Plant Sciences, School of Life Sciences, University of Hyderabad, Hyderabad for welcoming me into his laboratory, accepting me as a PhD student, providing the invaluable guidance, constant encouragement and critical reviews. He is always accessible for the help and advice throughout my research inquiries. I can't forget his persistent support during the hard times in the research. I am thankful to him for teaching research and made to compete with the challenging environment.*

I equally grateful to my Doctoral Committee members, **Prof. Apparao Podile** *&* **Dr. Y. Sree Lakshmi,** *Dept. of Plant Sciences for their timely advices and immense support. I would also like to thank profusely for their kind help and support during hard times. I am thankful for their helping hand and permission for the usage of their lab in the initial stages of our laboratory establishment.*

I am really grateful to Prof. S. Dayananda, Department of Animal Sciences, School of Life Sciences, University of Hyderabad for providing me the opportunity in the UoH for my project work in MSc which enthuse me to join PhD.

I express my loyal thanks to Dr. Naresh Sepuri, Department of Biochemistry, School of Life Sciences, University of Hyderabad for extending their lab facilities to us in the initial stages of my research with full freedom.

My heartfelt gratitude to Prof. Ch. Venkatramana (Present Head), Prof. A. R. Reddy & Prof. A. R. Podile (Former Heads), Prof. A.S. Raghavendra (Dean) and Prof. Aparna Dutta Gupta, Prof. M. Ramanadham (former Deans) Department of Plant Sciences, School of Life Sciences, University of Hyderabad for given that common facilities accessibility at all the times without hindering the work.

I express my deepest gratitude to all faculty in the school of Life Sciences for inspiring me and helping me directly or indirectly during my research period

Heartfelt thanks to all my lab-mates, Soumya, Anil, Shilpa, Sankar for their support and making my stay as memorable one in HCU and hostel. Special thanks to Mr. Mahesh Kumar who helped me in PCR cloning in the initial stages of my work. I appreciate all the project students in the lab who helped me in my work.

I thank Dr. Rajesh from Prof. P.B. Kirti's student for his help and valuable suggestions in 5' RACE amplification.

I gratefully acknowledge the funding sources that made my Ph.D. work possible. I was funded from BBL fellowships initially then by DBT project and finally by the UGC-RFSMS-BSR fellowship. I also acknowledge the IPM-CRSP, DBT for the generous funding to laboratory. The financial support given to the Department of Plant Science and School of Life sciences from the DST, UoH, DBT-CREBB, DST-FIST, UGC-SAP- CAS and UGC-XI plan are gratefully acknowledged.

I forever beholden to my family: my mother, father, brother (Nirmala, Venkateswara rao, VenuGopal) and all my in-laws for their huge support, unwavering love and encouragement. Their affection and scarifies were always a source of inspiration to achieve my goals.

It gives me great pleasure in acknowledging my loving life partner, Mr. Gopichand, best counselor and well-wisher who cheers me up and stood by me through the good and bad times. I really appreciate his unending love, encouragement, support and understanding me in my hardships. Without him, I would not be able to accomplish this task. Thank you for believing in me.

I appreciate the work and help of Miss. Nalini, technician in confocal laser scanning microscopy and Mr. Durga Prasad, electron microscopy technician for their images in my thesis.

I would like to thank Mr. Mahender, field Assistant for carrying out the field work and maintaining the plants and laboratory in healthy condition.

I am obliged to non-teaching staff members of the Department, School and Administration for the valuable information provided by them time to time. I am grateful for their cooperation during the tenure.

I am grateful to Prof. T. Ohki for helping me in confirmation of my virus by providing MNSV antisera raised against the Japan MNSV isolates.

I am thankful to Prof. H. S. Savitri, IISc and Bengaluru for providing me SeMV and PhMV viruses which are used in my study.

Although there may be many who remain unacknowledged
in this humble note of gratitude but
there are none who remain unappreciated

…… Naga Teja Natra

*Dedicated to my **parents and husband** for their endless affection, support and encouragement*

Contents

Abbreviations

APS	Ammonium persulfate
ATP	Adenosine Tri Phosphate
bp	Base pair
BCIP	5-Bromo-4-Chloro-Indolyl-Phosphatase
BME	β-Mercaptoethanol
cDNA	Complementary DNA
Da	Dalton
DAC	Direct antigen coating
DMSO	Dimethyl Sulfoxide
DMFO	Dimethyl formaldehyde
DNA	Deoxy ribonucleic acid
dNTPs	Deoxy Nucleotide Triphosphates
DTT	Dithiothreitol
EDTA	Ethylene diamine tetra acetic acid
ELISA	Enzyme-linked immunosorbant assay
EtBr	Ethidium Bromide
ER	Endoplasmic reticulum
g	Gram
G	Guanine
h	Hour(s)
IPTG	Isopropyl β-D-thiogalactoside
kb	Kilobase
kDa	Kilodalton
L	Litre
LB	Luria-Bertani
M	Molar
mg	Milligram
min	Minute
ml	Milliliter
mM	Millimolar
MMLV	Moloney Murine Leukemia Virus
M_r	Molecular mass
NBT	Nitro blue tetrazolium chloride
nm	Nanometers
OD	Optical Density
ORF	Open Reading Frame
PAGE	Polyacrylamide Gel Electrophoresis
PCR	Polymerase Chain Reaction
PEG	Poly Ethylene Glycol
PMSF	Phenylmethylsulfonylfluoride
PPB	Potassium phosphate buffer
PBS	Potassium buffer saline
PVDF	Polyvinylidene Fluoride
RNA	Ribonucleic acid
RNase	Ribonuclease
rpm	Revolutions Per Minute
RT	Room temperature
RT-PCR	Reverse Transcriptase-polymerase chain reaction

SDS	Sodium dodecyl sulphate
sec	Seconds
T	Thymine
TAE	Tris acetate EDTA
TBS-T	Tris buffer saline – Tween
T-DNA	Transfer DNA
TEMED	N,N,N′,N′-Tetramethylethane-1,2-diamine
Tm	Melting temperature
V	Volts
V/V	Volume/Volume
W/V	Weight/Volume
X-gal	5-bromo-4-chloro-3-indolyl β-D- galactoside
µg	Microgram
µm	Micromolar
µl	Microlitre
°C	Degree celcius

CHAPTER-1

Introduction and literature review

1.1 Viruses

Plant viruses are obligate intracellular parasites, due to their sub microscopic nature and having relatively small genomes, represent an excellent model system with which to reveal how the genetic paradigm of host-pathogen interactions operates. The life cycles of plant viruses include phases of genome replication, virion assembly, cell-to-cell movement, systemic movement and plant to plant transmission. Progress of infection is accompanied by virus-host interactions and fierce competition between plant defences and viral counter defences, a wealth of information concerning each of these processes/viruses have been accumulates (Noueiry and Ahlquist 2003).

The viruses having smaller size than bacteria and are visible only under electron microscope. They range in size from 15 nm to 400 nm (1nm = 10^{-9} meters) (fig-1.1). In comparison with bacteria, the smallest bacteria are of 400 nm in size. The rod shaped virus particles size varies from 65-350 nm in length and 15-25 nm in width. Bacilliform viruses range from 30-500 nm in length and 3-8 nm in width. The largest filamentous virus is *Citrus tristeza clasterovirus* with 1000 nm in length and 3-20 nm in width (Citovsky *et al.,* 1992). Mimivirus was the largest known virus for the past decade (La Scola *et al.,* 2003).

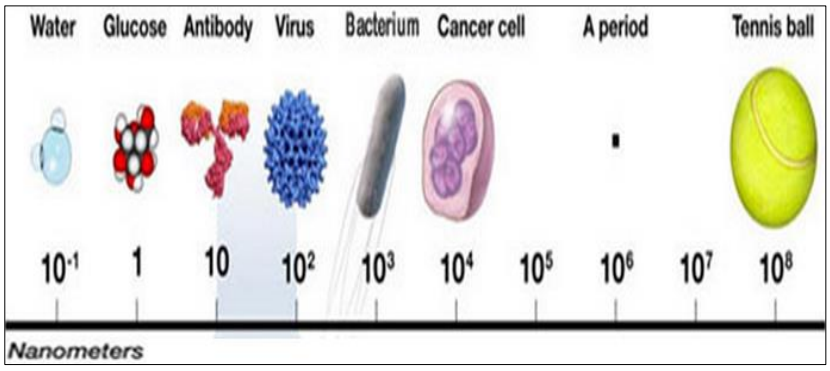

Fig-1.1: Representation of size of the viruses in comparison with other cells

In 2011, another virus larger than Minivirus known as Megavirus was identified with 680 nm of total particle diameter and 77 kb (6.5%) larger than Mimivirus (Arslan *et al.,* 2011) with 1200 genes, larger than parasitic bacteria. This showed that the limit has not charted for the viruses. This was challenged by the discovery of the Pandoravirus

having 1000 nm in length and 500 nm in width (Philippe *et al.,* 2013). Only the DNA polymerases of Pandoraviruses (*Pandoravirus salinus* and *P. dulcis*) are showing homology to DNA viruses and 93% of the genes are not known. Recently, the largest known virus is *Pithovirus sibericum* from Siberian region with 1500 nm length and 500 nm diameter (Matthieu *et al.,* 2014). The size of this virus is 50% larger than the previously reported virus.

The maximum diversity of the viruses was observed in the type of the nucleic acid. The nucleic acid of the viruses may be either DNA or RNA but never both. They may be in double stranded or single stranded and may be linear (ds DNA & ds RNA) or circular (ds DNA) forms. They may be positive sense, negative sense and ambisense. They might be monopartite, bipartite and multipartite genomes (fig-1.2). Most of the available plant viruses are positive sense RNA viruses in nature. They constitute about 34% among all the viruses (Hull, 2014). The nucleic acid of icosahedral viruses is partially ordered and crumpled as a ball inside the protein coat and whereas the nucleic acid of the helical viruses is highly ordered as the protein coat.

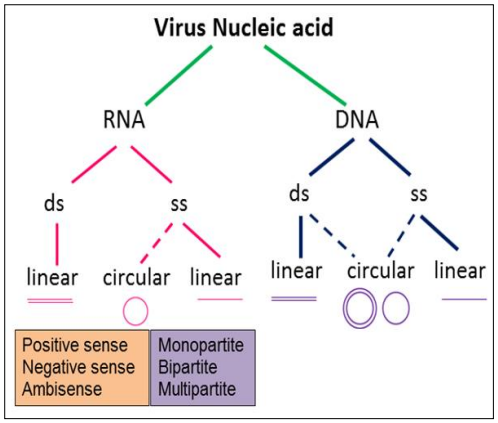

Fig-1.2: Diversity of the viral nucleic acid

The size of the RNA virus genome ranges from 3.5 to 30 kb (Koonin and Dolja, 1993). The International Committee on Taxonomy of Viruses (ICTV, 2000) officially declared that viruses are not living organisms; because of smaller genome sizes and they are not capable of producing proteins on their own. But this was challenged by discovery of Mimivirus and Mamavirus (slightly higher genome than Mimivirus) with 911 genes, which has genes that encode for DNA repair, produce mRNA transcripts from genes and translate these mRNAs into proteins (Forterre, 2010; Mary, 2012; Pearson, 2008). Later, with the discovery of pandoraviruses, a clear exemplar change was witnessed in the old

view that viruses are non-living. It also crossed the imaginary boundary of genome sizes between the viruses and cellular organisms (fig-1.3). One of the pandoraviruses has 1.91 million DNA bases and the other has largest genome with 2.47 million bases. Nonetheless, both lack genes for energy production and can't produce a protein on their own (Philippe *et al*., 2013; Pennisi, 2013). Recently, Pithovirus with 2.3 million bases was also reported (Matthieu *et al.*, 2014).

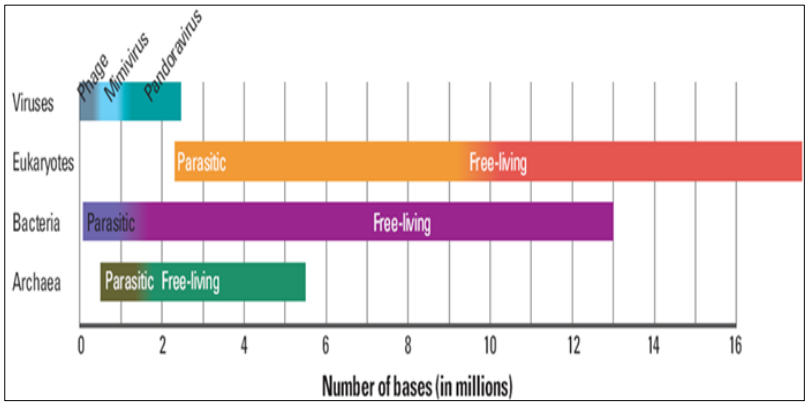

Adopted from Pennisi, (2013)

Fig-1.3: Pictorial representation of genome sizes of viruses in comparison to cellular organisms

1.2 Classification of plant viruses

Many plant viruses are characterized and described (www.dpvweb.net). Several hundreds of new viruses are reported and more and more are yet to be reported and several are at different stages of characterization (Roossinck, 2013). Whenever an unknown viral disease is detected, initially the concerned virus has to be checked with the already known virus characters. If it is a new virus, characterization was in two different stages. 'Diagnostic phase' is the first stage where the virus was assigned to a group based on the electron microscopy and serological tests. If it is not assigned based on the above characters then it has go into the 'descriptive phase'. In this every biological and molecular property is investigated to assure it as a new virus (Hamilton *et al.*, 1981). After characterizing the virus there is a need to classify the viruses for easy identification. Classification of viruses is important to make structural arrangement for easy comprehension, to enable prediction of properties of new viruses and possible evolutionary relationships.

According to the current classification (King *et al*., 2012), viruses are divided into 6 orders, 73 families, 19 subfamilies, 349 genera and 2284 species. ICTV, 1966 is the centralized repository of virus information and nomenclature. It collects data from

different databases around the world and facilitates the work of accurate identification and diagnosis of new and important virus diseases. Current classification of plant viruses was adopted from ICTV taxonomy web page (9th report of ICTV) and it was tabulated below (tab-1.1).

Genome	Family & sub family	Genus	Type member
ds DNA	Caulimoviridae	Caulimovirus	*Cauliflower mosaic virus*
		Badnavirus	*Commelina yellow mosaic virus*
		Cavemovirus	*Cassava vein mosaic virus*
		Petuvirus	*Petunia vein clearing virus*
		Soymovirus	*Soybean chlorotic mottle virus*
		Solendovirus	*Tobacco vein clearing virus*
		Tungrovirus	*Rice tungro bacilliform virus*
ss DNA	Geminiviridae	Becurtovirus	*Beet curle top Iran virus*
		Begamovirus	*Bean golden yellow mosaic virus*
		Curtovirus	*Beet curly top virus*
		Eragrovirus	*Eragrostis curvula streak virus*
		Mastrevirus	*Maize streak virus*
		Topocuvirus	*Tomato pseudo-curly top virus*
		Tuncurtovirus	*Turnip curly top virus*
	Nanoviridae	Babuvirus	*Banana bushy top virus*
		Nanovirus	*Subterranean clover stunt virus*
ds RNA	Reoviridae		
	Sub family: Sedoreovirinae	Phytoreovirus	*Wound tumor virus*
	Spinareovirinae	Fijivirus	*Fiji disease virus*
		Oryza virus	*Rice ragged stunt virus*
	Partitiviridae	Alphacryptovirus	*White clover cryptic virus 1*
		Betacryptovirus	*White clover cryptic virus 2*
	Unassigned family	Varicosavirus	*Lettuce big-vein associated virus*
(-) ssRNA	Rhabdoviridae	Cytorhabdovirus	*Lettuce necrotic yellows virus*
		Nucleorhabdovirus	*Potato yellow dwarf virus*
	Bunyaviridae	Tospovirus	*Tomato spotted wilt virus*
	Ophioviridae	Ophiovirus	*Citrus psorosis virus*
	-	Unassigned genus : Tenuivirus	*Rice stripe virus*
(+) ssRNA	Bromoviridae	Alfamovirus	*Alfalfa mosaic virus*
		Anulavirus	*Pelargonium zonate spot virus*
		Bromovirus	*Brome mosaic virus*
		Cucumovirus	*Cucumber mosaic virus*
		Ilarvirus	*Tobacco streak virus*
		Oleavirus	*Olive latent virus 2*
	Closteroviridae	Ampelovirus	*Grape vine leafroll-associated virus 3*
		Closterovirus	*Beet yellows virus*
		Crinivirus	*Lettuce infectious virus*
	Secoviridae	Cheravirus	*Cherry rasp leaf virus*
		Sadwavirus	*Satsuma dwarf virus*

		Sequivirus	*Parsnip yellow fleck virus*
		Torradovirus	*Tomato torrado virus*
		Waikavirus	*Rice tungro spherical virus*
	Sub family: Comovirinae		
		Comovirus	*Cowpea mosaic virus*
		Fabavirus	*Broad bean wilt virus 1*
		Nepovirus	*Tobacco ringspot virus*
	Alfaflexiviridae	Allexivirus	*Shallot virus X*
		Mandarivirus	*Indian citrus ringspot virus 7*
		Potex virus	*Potato virus X*
	Betaflexiviridae	Capillovirus	*Apple stem grooving virus*
		Carlavirus	*Carnation latent virus*
		Citrivirus	*Citrus leaf blotch virus*
		Foveavirus	*Apple stem pitting virus*
		Tepovirus	*Potato virus T*
		Trichovirus	*Apple chlorotic leaf spot virus*
		Vitivirus	*Grapevine virus A*
	Tymoviridae	Maculavirus	*Grapevine fleck virus*
		Marafivirus	*Maize rayado fino virus*
		Tymovirus	*Turnip yellow mosaic virus*
	Luteoviridae	Enamovirus	*Pea-enation mosaic virus 1*
		Luteovirus	*Barley yellow dwarf virus-PAV*
		Polerovirus	*Potato leafroll virus*
	Potyviridae	Brambvirus	*Blackberry virus Y*
		Bymovirus	*Barley yellow mosaic virus*
		Ipomovirus	*Sweet potato mild mottle virus*
		Macluravirus	*Maclura mosaic virus*
		Poacevirus	*Triticum mosaic virus*
		Potyvirus	*Potato virus Y*
		Rymovirus	*Ryegrass mosaic virus*
		Tritimovirus	*Wheat streak mosaic virus*
	Tombusviridae	Alfanecrovirus	*Tobacco necrosis virus*
		Aureusvirus	*Pothos latent virus*
		Avenavirus	*Oat chlorotic stunt virus*
		Betanecrovirus	*Tobacco necrosis virus D*
		Carmovirus	*Carnation mottle virus*
		Dianthovirus	*Carnation ringspot virus*
		Gallantivirus	*Galinsoga mosaic virus*
		Macanavirus	*Furcraea necrotic streak virus*
		Machlomovirus	*Maize chlorotic mottle virus*
		Panicovirus	*Panicum mosaic virus*
		Tombusvirus	*Tomato bushy stunt virus*
		Zeavirus	*Maize necrotic streak virus*
	Virgaviridae		
		Furovirus	*Soil born wheat mosaic virus*
		Hordeivirus	*Barley stripe mosaic virus*
		Pecluvirus	*Peanut clump virus*
		Pomovirus	*Potato mop-top virus*
		Tobamovirus	*Tobacco mosaic virus*
		Tobravirus	*Tobacco rattle virus*

	Unassigned family		
		Benyvirus	*Beet necrotic yellow vein virus*
		Emaravirus	*Rose rosette virus*
		Idaeovirus	*Raspberry bushy dwarf virus*
		Ourmiavirus	*Ourmia melon virus*
		Sobemovirus	*Southern bean mosaic virus*
		Tenuivirus	*Rice Stripe virus*
		Umbravirus	*Carrot mottle virus*

Tab-1.1: Classification of plant viruses according to the ICTV virus taxonomy (9th report of ICTV)

One of the major motivating forces to study about plant viruses is due to the devastating diseases caused by them on crops and affecting the productivity all over the world. The estimated crop loss due to plant viruses was around 6-7 x 10^{10} US$ annually around the world (Agrios, 2005; Hull, 2014). The documentation of the losses due to viruses is different due to their intriguing properties like diversity in their genomes and the amount spent to control the losses is also increasing day-by-day which became a major threat to the human life. The plant viruses can cross the host barrier and effect wide range of hosts by interacting with the host proteins. It has been reported that 30 X 10^6 new virus host combinations have to be evaluated (Hull, 2014). *Cucumber mosaic virus* (CMV) will infect different hosts and has the broadest host range of any known virus infecting more than 1200 plant species including monocots and dicots (Edwardson *et al*., 1991; Hull, 2014). Similarly, one plant species can be infected by different viruses ex: A complex group of viruses from different genera infects cucurbits, plant group that includes cucumber, pumpkin, squash, melon and watermelons. Comovirus, Cucumovirus, Potyvirus, Nepovirus, Carmovirus are major genus affecting cucurbits (Ghasemzadeh *et al.,* 2012).

We have identified a new virus on *Cucumis melo* plants, no fruits were observed in the infected plants. Initially we fail to diagnose the virus through initial characterization however, we have tentatively identified the virus as *Melon necrotic spot virus* (MNSV) and assay systems were developed in the laboratory. In view of the host in which it has been identified we give a brief literature related to *Cucumis melo* plants.

1.3 *Cucumis melo*:

It belongs to the family Cucurbitaceae and is commonly known as Tarbuja or Karbuja. The wild melons are originally from Africa and now grown in all continents. Asia is the largest producer of melons in the world. According to 2012 FAO statistics (faostat3.fao.org), India occupies 2nd rank in the production of vegetables and melons in the world after China. World share for India in the production of vegetables and melons is 9.7%. According to the 2012 reports of U.N. Food and Agriculture Organizations FAO STATS, India occupies 27th position in the world in production of melons with average of 353 thousand tons which is equal to 12.6% of the world production. In India, melon breeding programs were strengthened with the beginning of the All India Coordinated project on vegetable Crops (AICRP-VC) in 1971. Andhra Pradesh is one the major fruit producing states in India.

1.4 Nutritional Value

	Amount per serving (177 g)	(% of daily dietary value)
Calories	60.2 (252 KJ)	3%
Fat	-	0%
Potassium	473 mg	14%
Sodium	28 mg	1%
Total carbohydrade	16 g	5%
Dietary fiber	2 g	6%
Sugars	14 g	-
Protein	1.5 g	3%
Vitamin-A	5987 IU	120%
Vitamin C	65 mg	108%
Calcium & Iron	15.9 &0.4 mg	2%
Water	160 g	-

Table-1.2: Dietary value is based on a 2000 calories diet. (From Nutrition data.com)

Melon fruits have high nutritional value. Melons contain 92% of water, 6% of sugars, source of vitamin C and minerals. Vitamin C is capable of preventing heart diseases. In 2005 dietary guidelines stated that melons are highly rich in potassium that may help to control blood pressure, kidney stones and heart stroke. Notably the inner rind of the melon (white colored area) contains many hidden nutrients that most people

avoid eating due to its unique flavor. The amino acid 'citrulline' was first extracted from watermelon. In a recent study it has been found that the regular intake of melons can decrease risk of metabolic syndrome. Melon is rich in Vitamin-B & C, less acidic than many other fruits and gives very good results for facial masks. The nutritional values of the melons are tabulated below (tab-1.2).

1.5 Cucurbit diseases

Though, India occupies a rank in melon production, the production rate is very low when compared with major producing countries. Number of factors are responsible for the yield reduction in India and the most important constrain is the diseases caused by different types of pathogens. Plant pathogens are the major cause of the production and economic losses in the agriculture and horticulture worldwide. To have sustainable agriculture, monitoring the diseases and health of the plant is very important. The plant pathogens may be bacteria, fungi, nematodes or viruses which cause the devastating effects to the agriculture and there by directly effecting the country's economy.

Bacterial fruit blotch is major bacterial disease caused by *Acidovorax avenae* sp. Symptoms are mature fruit displaying typical bacterial fruit blotch symptoms including irregular shaped water soaked lesions with cracks. This bacterium is transmitted through seeds from generation to generations. Fusarium wilt is the major fungal disease that attack melon crops by *Fusarium oxysporum*. This can be controlled by use of registered fungicides and maintaining the hygiene of the crop. Other fungal diseases that cause major damage to the melon crops are powdery mildew and gummy stem blight. Root knot nematode is the one which infect most of the plant species. It can readily wilt the melon plant because the galled roots have limited ability to absorb and transport water and nutrients. Soil treatment is the only remedy for the disease management (Liu *et al*., 1995). As my thesis work is related to plant viruses, some important viral diseases of cucurbits are discussed briefly.

1.6 Viral diseases of cucurbits

Viral diseases are the major limiting factor for their production and cause damage mainly to squash and melon (Rodriguez-Hernandez, 2012). Recently, it was reported that 59 well-characterized different viruses are naturally infecting cucurbits (Lecoq and Desbiez, 2012; Ghasemzadeh *et al.*, 2012; Provvidenti, 1996). Usually several diseases of cucurbits are coupled with the multiple infections. Two or more

viruses that cause mild symptoms enhance the symptom severity through a process known as synergism in multiple infections (Lecoq, 1994; Lathman and Jones, 2001; Fattouh, 2003). Mostly potyviruses infecting cucurbits are involved in synergistic infections with viruses of other genera.

Major damage causing viruses to cucurbit crops are *Squash mosaic virus* (SqMV), *Cucumber mosaic virus* (CMV), *Watermelon mosaic virus* [WMV-1 (*Papaya ringspot virus* (PRSV)), & WMV-2], *Zucchini yellow mosaic virus* (ZYMV). Minor damage is caused by *Tobacco ringspot virus* (TRSV), *Tomato ringspot virus* (ToRSV), *Clover yellow vein virus* (CYVV), *Cucumber green mottle virus* (CGMV), and *Melon necrotic spot virus* (MNSV) (Rodriguez-Hernandez, 2012; Romay *et al*., 2014; Abou-Jawdah *et al*., 2000; Yuki *et al*., 2000; Massumi *et al*., 2007; Ali sevik and Toksoz, 2008). Recently, *Melon yellow spot virus* (MYSV) from genus Tospovirus is found to infect cucumber crops (Chao *et al.*, 2010).

Squash mosaic virus symptoms in the field condition are pronounced chlorotic mottle, green vein banding, leaf blistering, infects muskmelon (*Cucumis melo*) and the virus is seed borne that can be transmitted by cucumber beetles (Han *et al.*, 2002).

Cucumber mosaic virus is most widely known virus that infects cucurbits and belongs to family Bromoviridae, genus Cucumovirus. This virus is detected in mixed infection along with SqMV at the early stages of infection. Symptoms seen with the plants infected with CMV are leaf mosaic, yellowing, ringspots, stunting and distortion of flower, fruits and leaves. It is transmitted by aphids (ex. *Aphis gossypii*, *Myzus persicae* etc.) through non-persistent mode and mechanically by beetles (ex. *Diabrotica vittata* & *D.undecimpunctata*). The main diagnostic feature of the virus is that the plant tissues contain inclusion bodies and is mainly transmitted through aphids (Wang *et al.*, 2002).

Papaya ringspot virus infection is limited to cucurbits and is aphid transmitted. The foliage of affected plants shows strong mosaic, distortion and leaf serration. Fruits are malformed with knobby over growth. This virus is also known as *Water melon mosaic virus* (WMV-1). WMV-2 is also aphid transmitted virus and causes milder symptoms on foliage but fruit distortion and color breaking are common. Its host range is wide and not limited to cucurbits only. Mixed infections with CMV are common at the end of the season (Ghasemzadeh *et al.*, 2012).

Zucchini yellow mosaic virus is an aphid borne Potyvirus and affects all cucurbits and especially zucchinis. The symptoms include severe leaf mosaics, yellowing of leaves

and the fruits are stunted, twisted and deformed. Control is mainly dependent on use of proper insecticides and control of aphids (Coutts *et al.*, 2011).

Tobacco ringspot virus belongs to Secoviridae, genus Nepovirus. The infected plants are dwarfed with yellowish leaves, mottling and has deformed flowers and fruits. Small spots are observed on leaves with pin point centers and develop definite rings. Seed transmission is rare and mainly transmitted by nematodes. Other vectors are grasshoppers, mites, thrips and fleabeetles (Andret-link and Fuchs, 2005).

Tomato ringspot virus is also a member of *Nepovirus* under family Secoviridae causes ringspots and mosaic symptoms in tobacco, tomato and raspberries. Transmitted by vector nematode (*Xiphinema americanum*) and spread through seeds in few varieties (Rott *et al.*, 1991).

Clover yellow vein virus is a member of Potyvirus belongs to family Potyviridae. Symptomology includes vein clearing, yellowing and mottle. No seed transmission is observed and mainly transmitted by aphids (Bryan *et al.*, 1992).

Cucumber green mottle virus is classified under genus Tobamovirus, family Virgaviridae. The virus affects mainly young leaves of cucurbits with green and yellow-green spots. Veins of the infected leaf remain green. Leaves and fruits are small and aborted with the severity of the virus (Reingold *et al.*, 2014; Tian *et al.*, 2014).

Melon yellow spot virus is a related to member of genus Tospovirus. Diseased young plants show mosaic symptoms and matured leaves develop yellowing and yellow spots which gradually necrotize the leaves. It is an emerging thrips-borne threat in melons and watermelons in Taiwan (Peng *et al.*, 2011).

Melon necrotic spot virus is a Carmovirus in the family Tombusviridae. Host range is restricted to cucurbits and symptoms include necrotic spots and necrosis of stems and petioles. No seed transmission was observed. It is mainly transmitted by the fungus *Olphidium bornovanus* (Riviere and Rochon, 1990).

1.7 Stages of viral infection and their control strategies

The virus infection in a host cell was explained in different stages: a) introduction of the viral genome into the host cell either by mechanical inoculation or by vectors, b) replication in the introduced cell, c) intracellular movement to reach plasmodesmata (PD), d) intercellular movement from infected cell to healthy cell, e) systemic movement of virus through interaction with phloem proteins and f) finally transmission of virus from one plant to another by vectors (Kang *et al.*, 2005). The four possible stages where

the viruses can be controlled are: 1) Initial stages- uncoating of the virus, 2) replication within the infected cell, 3) during movement within the infected cell and 4) finally at the host cellular defenses in the infected cell (systemic movement of the virus).

Ours is a new laboratory started in 2008 in University of Hyderabad with main interest towards the study of host-pathogen interactions at molecular level and diverse viral processes like replication, translation, packaging/assembly at single cell level and in whole plant scenario using a model virus that can replicate in *Nicotiana benthamiana* or *Arabidopsis thaliana* whose genome sequences are known with a long term goal to develop anti-viral approaches. Towards this, extensive field surveys were conducted during the Kharif season of 2009, in and around Rangareddy district of Andhra Pradesh (newly formed Telangana state) and identified some peculiar mosaic leaf blisters, stem and leaf necrosis occurring predominantly on melon (*Cucumis melo*) crop. No fruits were observed in the infected plants. Those viral symptoms and are entirely different from the symptoms caused by *Cucumber mosaic virus* (CMV) or any other potyvirus on the cucurbit crops. Those infected leaves are collected and stored at -80 ºC for analysis. Initially, serodiagnosis was conducted with the available and heterologous antisera in the laboratory and no cross reactivity was observed in all the tested antisera. In order to characterize and gain insights into the genome organization of the unknown virus, we have set four challenging objectives in the present study where we would like to achieve to have a model virus in the laboratory and to develop an assay system where we can study the viral processes *in planta*.

1) Biological characterization of the field collected virus sample
2) Molecular characterization of the new virus through whole genome sequencing by reverse genetic approaches and diversity analysis
3) Construction of full length infectious cDNA cloning system (icDNA) to MNSV-Hyd and development of agroinfiltration approach
4) Elucidation and *in planta* analysis of virus encoded proteins as GFP chimeras

Based on the biological and molecular parameters the field collected sample was identified as the new virus and tentatively designated as *Melon necrotic spot virus* from Hyd (MNSV-Hyd).

As we have identified a new virus which is designated as MNSV-Hyd, which comes under the family Tombusviridae and genus Carmovirus. We have restricted our literature survey related to Carmoviruses and Melon necrotic spot virus (MNSV).

1.8 Classification of MNSV

According to the International Committee on Taxonomy of Viruses (ICTV) classification, *Melon necrotic spot virus* (MNSV) is a plant virus which belongs to the family Tombusviridae, which comprises of about 11 genera (tab-1.1). They are Aureusvirus, Avenavirus, Carmovirus (tab-1.3), Dianthovirus, Machlomovirus, Panicovirus, Tombusvirus, Gallantivirus, Macanavirus, Zeavirus, Alfanecrovirus and Betanecrovirus.

Sl.No	Genus Carmovirus members
1	*Ahlum waterborne virus* (AWBV)
2	*Angelonia flower break virus* (AFBV)
3	*Bean mild mosaic virus* (BMMV)
4	*Calibrachoa mottle virus* (CMoV)
5	*Cardamine chlorotic fleck virus* (CCFV)
6	*Carnation mottle virus* (CarMV)
7	*Cowpea mottle virus* (CPMoV)
8	*Cucumber soil-borne virus* (CuSBV)
9	*Hibiscus chlorotic ringspot virus* (HCRSV)
10	*Honeysuckle ringspot virus* (HRSV)
11	*Japanese iris necrotic ring virus* (JINRV)
12	*Melon necrotic spot virus* (MNSV)
13	*Nootka lupine vein clearing virus* (NLVCV)
14	*Pea stem necrosis virus* (PSNV)
15	*Pelargonium flower break virus* (PFBV)
16	*Saguaro cactus virus* (SgCV)
17	*Soybean yellow mottle mosaic virus* (SYMMV)
18	*Turnip crinkle virus* (TCV)
19	*Weddel waterborne virus* (WWBV)
	Tentative members
20	*Chenopodiun necrosis virus* (ChNV)
21	*Pelargonium line pattern virus* (PLPV)

Tab-1.3: List of viruses included in the genus Carmovirus according to ICTV classification.

The family consists of icosahedral virion particles of diameter varying from 25-34 nm with molecular weight of the virion ranges from 26-48 kDa. It consists of the linear single stranded positive RNA as the genome which ranges from 3.6-4.4 kb size and is monopartite except in the genus Dianthovirus (bipartite). The genome consists of 5 or 6 ORFs where mostly CP is at the 3' proximal end except for three genera, Aureusvirus, Tombusvirus and Zeavirus (http://www.ictvonline.org/virusTaxonomy.asp). The genus Carmovirus consists of 19 definitive members and 2 tentative members as listed in the tab-2.1.

1.9 Symptomology

MNSV has narrow host range which is limited to Cucurbitaceae members (Ohki *et al*., 2008; Diaz *et al*., 2003; Gonazalez-Garza *et al*., 1979). It infects mainly cucurbit crops like *Citrullus lanatus*, *Cucumis melo* and *Cucumis sativus* with symptomology ranging from chlorotic lesions to the severe necrotic symptoms on leaves and stems (Choi *et al*., 2003; Diaz *et al*., 2003), occasionally on petiole (Ohki *et al*., 2008) and severe stunting (Gonazalez-Garza *et al*., 1979). The small chlorotic rings/spots are formed at the early stages of infection which slowly develop, coalesce and form brown coloured necrotic lesions. Necrotic stripes were also observed in few cases on stems and fruit stalk and later slowly whole plant was weakened (Choi *et al*., 2003). The major threat to the melon fields is the production of fruits with sponge like tissue formation, interstitial space formation within the fruit and there by severe economic losses (Kishi 1966; Yoshida *et al*. 1980; Avgelis 1985). The affected plant will wilt and losses the fruit vigour. The fruits consist of brown colour spots on the surface and the inner rind shows the discolouration and brown colour staining. The fruits are unmarketable when the pulp will be watery and hallow with air spaces entrapped in it (Matsuo *et al*., 1991). Differences in the symptoms of MNSV host rang were reported (Diaz *et al*., 2003). MNSV symptoms are indistinctable from the bacterial disease symptoms, watermelon blotch (Padil, 2013, MNSV).

1.10 Geographical distribution of MNSV

This disease was first reported in Japan in 1960's (Kishi, 1966) and later, it is reported from Crete (Avgelis, 1985), Spain, Europe, Asia, Africa, America, Korea (Choi *et al*., 2003), Panama, UK, U.S.A, Guatemala (Herrera *et al*., 2006), China (Gu *et al*., 2008) and Tunisia (Yakoubi *et al*., 2008), Taiwan (Chen *et al*., 2008) Caribbean (CABI, 2010).

1.11 Strains of MNSV

Different strains of MNSV are reported (mainly from Japan and Spain) and the homology of the isolates is also very less (Ohki *et al*., 2008). Difference in the nucleotides and amino acid identity of MNSV strains was also reported (Riviere and Rochon, 1990). MNSV- NK & NH strains (Ohshima *et al*., 2000; Matsuo *et al*., 1991), Malfa5 (Diaz *et al*., 2003); MNSV-264 (Diaz *et al*., 2004); MNSV-A1, MNSV-Dutch (Riviere and Rochon, 1990); MNSV-S (Kishi, 1966; Matsuo, 1991), MNSV-KS, YS

(Kubo *et al*., 2005); MNSV-Chi, W, NW1, Y1, Kochi, Tottori (Ohki *et al*., 2008, 2010), MNSV-C (Gonazalez-Garza *et al*., 1979), MNSV-MN (Choi *et al*., 2003), MNSV-Chiba, Chiba prefecture, Yamaguchi, Chiba prefecture, Kouchi, prefecture (Kido *et al*., 2008), MNSV-N (Miras *et al*., 2014), and nucleotide sequence data was available for many strains in pub med (http://www.ncbi.nlm.nih.gov/nuccore).

1.12 Transmission

MNSV virus is highly stable and survives in the soil for several years without host. MNSV is transmitted by seeds in very low frequency (Gonazalez-Garza *et al*., 1979; Ohki *et al*., 2008) and virus was also extracted from seeds (Coudriet *et al*. 1979). The seed transmission can be controlled by treating the MNSV infected seeds at 70˚C for 144 hr without affecting the germination was reported by Herrera-Vasquez *et al*., 2009. It was shown that MNSV is transmitted by cucumber beetles (*Diabrotica undecimpunctata*, *D. balteata*) in crops in U.S.A (Coudriet *et al*. 1979). MNSV is mainly vector transmitted in the soil by the fungus *Olphidium bornovanus* and *O. virulentus* (Campbell *et al*., 1995) which is a soil born moisture dependent chytrid. These fungi are obligatory intracellular parasites which form motile zoospores and resting spores in root tissues. Zoospores of the fungus play a major role in the attachment of the virus and transmission to the host plant (Rochon *et al*., 2004). This type of transmission is known as vector mediated seed transmission (Campbell *et al*., 1996) because the virus can be detected on the seed irrespective of the presence of fungus but transmitted in presence of fungus. Soil fumigation with methyl bromide prevents the virus transmission. The coat protein of MNSV has a major role in the attachment of the virus to the fungal vector by acting as a ligand (Mochizuki *et al*., 2008).

1.13 dsRNA profiling

Double stranded RNA (ds RNA) profiling is one of the diagnostic tools for characterization of the unknown virus (Morris and Dodd, 1979; Tzanetakis and Martin, 2008). It is a characteristic feature of all RNA viruses during replication in the host cell. It is observed mainly during replication of positive RNA viruses and ambisense RNA viruses. ds RNA is associated with plant viruses in two modes. First one is that the viruses having ds RNA as genetic material (Reoviruses and Cryptoviruses) and secondly, in ss RNA viruses where dsRNA is present as a replication intermediate which is twice the size of genomic RNA. During genome replication, viral RdRp copies the positive

strand RNA in to a full length negative strand and this could result in the formation of double stranded molecule. It could be complete (replicative form) or incomplete (replicative intermediate, RI) (Kovalev *et al*., 2014). These are thermodynamically stable and act as a versatile tool for the characterization of viruses (Tzanetakis and Martin, 2008). In most cases this will be unstable, otherwise, this acts as strong silencing inducer and involves in the silencing of transgene, viral RNA (Weber *et al*., 2006).

1.14 Genome organization of MNSV

MNSV is isometric in nature with 30 nm diameter, single stranded positive sense, non-capped and non-polyadenylated monopartite with 4.3 kb RNA genome. The genome contains five open reading frames; p28, p89, p7A, p7B & p42 (fig-1.4) (Ohki *et al*., 2010). The first protein translated from the genome is p28 or p29 protein which is 28/29 kDa in size. The 89 kDa protein was translated from the ORF-1 by the read through stop codon of p29 gene which is involved in replicase activity (known as read through protein, RTP). These two proteins were translated from the genomic RNA. Centrally located two ORF's encode two movement proteins (7A & 7B) of 7 kDa which are translated from sub-genomic RNA1. If the read through stop codon is located at the end of the 7A, then it leads to the fusion protein of 14 kDa and its function was not known (Riviere and Rochon, 1990). The 3' proximal end of the genome encodes coat protein of 42 kDa and translated from sub-genomic RNA2. The 5' proximal end of the genome consists of less than 100 nt as non-coding region and the 3' proximal end of the genome consists of around 300 bp of NCR. (Canizares *et al*., 2001).

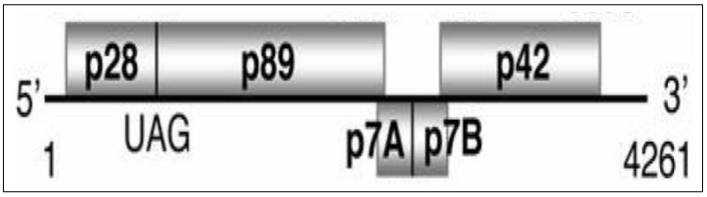

Fig-1.4: The genome organization of MNSV encoding five ORFs. ORF-1: p28/29 protein; ORF-2: p89 protein, read through stop codon after p28; ORF-3: 7A; ORF-4: 7B; ORF-5: p42 protein. MP and CP are translated through the sub-genomic RNA molecules (1.9 kb & 1.6 kb). Small NCR regions are present at the 5' and 3' ends of the genome. The ends are non-polyadenylated and non-capped. Adopted from Ohki *et al*., (2008)

1.15 RNA dependent RNA polymerase (RDRP)

Proteins, p28 and p89 are essential from the replication activity as in comparison with the other members in the genus. The presence of GDD signature motif in RTP also

confirms its involvement in replicase activity (O'Reilly and Kao *et al*., 1998; Wang *et al*., 2007). Motif-A and motif-GDD are placed in juxtaposed and the aspartic acids of these motifs are to bind to Mg2+ / Mn2+. The studies of the RDRP investigations of the Tombusviridae members TCV (Rajendran *et al*., 2002), TBSV (Boonrod *et al*., 2005), CNV (Panaviene *et al*., 2003) and PMV (Batten *et al*., 2006) have shown that the N-terminal auxiliary protein, p28 is important and is the master regulator of the replication process. Alanine scanning mutagenesis in TCV in the important motifs in the C-terminal region of RDRP have shown the significant decrease in the RNA synthesis and the mutation of second aspargine in GDD motif was lethal in *N.benthamiana* (Fang and Coutts, 2013).

The positive sense RNA viruses from Tombusvirus like TBSV, CNV are used for the study of viral replication complexes (VRC) which are membrane bound (Nagy and Pogany, 2010, 2011). This VRC complex consists of the auxillary protein and RDRP proteins and many other proteins required for the replication and it is membrane bound (Serva and Nagy, 2006, Romero-Brey and Bartenschlager, 2014). Apart from these proteins it also contains the viral positive strand RNA which serves as an assembly platform for the proteins (Pathak *et al*., 2012) and the interactions among them were studied (Nagy *et al*., 2012). The interaction between the auxiliary protein and read through protein (RTP), p89 was also important for the replication process (Pathak *et al*., 2013). The 3' proximal end of the genome also plays a major role in the transcription and translation processes where the upstream hair pin H4 in the 3' NCR and ribosome binding tRNA-shaped structure play a key role in efficient transcription initiation also (Yuan *et al*., 2010). Even though the tombusvirus and carmovirus RDRP are of the same family, their template usage is similar but not identical in comparison with TCV and TBSV RDRPs (Nagy and Pogany, 2000).

Several pathogenic factors of the plant viruses are identified that cause the necrosis in the host (Carette *et al*., 2002a; Diveki *et al*., 2004; Fernandez-Salas *et al*., 1999; Kiraly *et al*., 1999; Ozeki *et al*., 2006; Tribodet *et al*., 2005; Van Wezel *et al*., 2001). The RNA silencing suppressor protein of TBSV, p19, in Tombusviridae family was identified to cause necrosis in *N. benthamiana, N.clevelandii* and TBSV-CP induces necrotic lesions in the leaves of *N. glutinosa* and *N. edwardsonii* (Scholthof *et al*., 1995). The p33 product from ORF-1 of *Cymbidium ringspot virus* (CymRSV) induces systemic necrotic lesions in *N. benthamiana* (Burgyan *et al*., 2000). Even though full mechanism of the lethal necrosis was not demonstrated, the induction of necrosis of

MNSV in *N. benthamiana* is by the viral encoded protein, p29. The second transmembrane domain (TMD) and the extra amino acid region before TMD-2 of p29 have a role in mitochondrial targeting and induction of necrosis in *N.benthamiana* (Mochizuki *et al*., 2009). The presence of the proteins from ORF-1 (p33) & read through protein (RTP) (p92) in a particular ratio is also important for the replication of TBSV, the type member of the family, Tombusviridae and these are membrane associated (Scholthof *et al*., 1995).

1.16 Movement proteins

The Carmovirus genus consists of two movement protein genes known as double gene block proteins (DGB) (Gosalvez-Bernal *et al*. 2008). These two proteins are involved in the cell-to-cell movement of virus in the host. The virus movement from cell to cell was through the specialized cell organelles in the plant kingdom known as plasmodesmata (PD), membrane lined channels that contain appressed ER (Lucas, 2006; Christensen *et al*., 2009).

1.17 Movement of plant viruses

The plant viruses have special encoded proteins for their movement in the host cell. The concept of virus movement was in two distinct modes and the movement through phloem was firstly concluded by Samuel in 1934. This was further confirmed by the use of temperature sensitive mutants of TMV (Nishiguchi *et al*., 1978, 1980). Once a plant virus is introduced in to a host cell, the virus enters the outer most layers of cells, epidermal cells. To infect the whole plant, virus has to move from infected cell to healthy cell and from there consecutively it moves to mesophyll, bundle sheath and phloem parenchyma cells. The systemic infection from one leaf to another was through the vascular parenchymal cells into sieve cells from there it moves to the sink leaves (fig-1.5) (Carrington *et al*., 1996; Kehr and Buhtz, 2008; Harries and Ding, 2011). This movement is connected by the intricate symplastic complex (Lucas, 1995; Wang and Ding, 2010). It utilizes the plant cell organelle, plasmodesmata for its movement (Lucas, 2006).

The three major steps involved in the virus systemic movement are:

1) Synthesis and movement of freshly synthesized genomes to intracellular transport system from the site of synthesis

2) Intracellular transport of viral proteins
3) Inter cellular movement through plasmodesmata

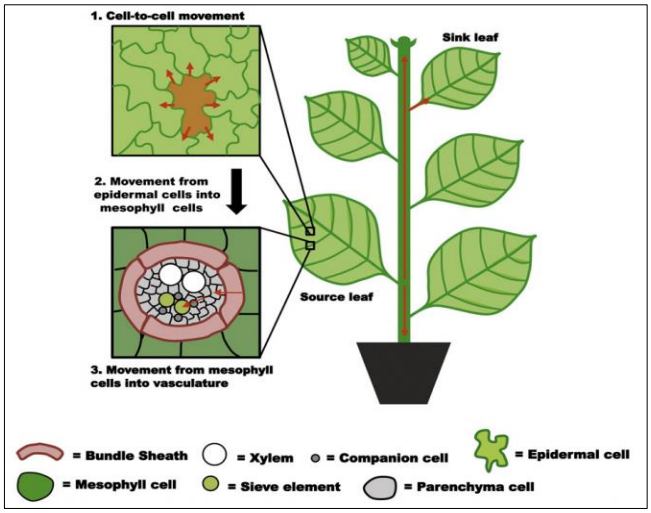

Adopted from Harries and Ding, (2011)

Fig-1.5: Cell-to-cell movement and long distance symplasmic transport in plants for proteins, RNAs, viruses, viroids and photo assimilates. After entry of virus into the host cell (source leaf), 1) to spread the infection it has to move from cell-to-cell, 2) for the systemic spread, it has to move the mesophyll cells and pass through the bundle sheath, parenchyma, companion cells and finally into sieve elements 3) Systemic movement of the virus into the upper non-inoculated leaf through vasculature from source to sink leaves. The virus-host interactions and the virus movement are represented in arrows.

1) <u>Synthesis and movement of freshly synthesized genomes to intracellular transport system from the site of synthesis:</u>

Positive sense RNA viruses constitutes the maximum percentage of viruses, they directly act as mRNA molecules and translated on ribosomes in the cytoplasm where there is direct access for the molecular network to traverse. In case of DNA and negative sense RNA viruses, the replication of the genome takes place in the nucleus and the newly synthesized genome molecules have to escape from the nucleus to the cytoplasm through nuclear pores. Some of the viral replication proteins are involved in this transfer. In case of BMV, the replication protein 2a deletion affects the systemic spread of the virus apart from the replication deficiencies in the protoplasts and 1a and 2a proteins were identified in the ER network by using reporter genes (Traynor *et al*., 1991; Restrepo-Hartwig and Ahlquist., 1996, 1999). The size exclusion limit of plasmodesmata can allow one 1 kDa protein to pass through it. The TMV-MP associates with ER and interacts with ER derived vesicles. Both RDRP and MP help in the control of actin and myosin dependent movement of viral replication complex (VRC) through plasmodesmata (PD) size exclusion (Harries *et al*., 2009a, b). But the interaction of the movement was not yet understood clearly

either with cytoskeleton or microfilaments (Harries *et al*., 2009a; Hofmann *et al*., 2009). The *Cowpea mosaic virus* (CPMV) MP targets the PD through tubule formation without affecting the secretory pathway or cytoskeleton pathway (Pouwels *et al*., 2002). The *potato leaf roll virus* targets the PD through actin and secretory pathway dependent manner (Vogel *et al*., 2007).

1) Intracellular transport of viral proteins:

In order to reach the cell periphery the synthesized viral proteins from the site of replication two processes are reported (fig-1.6).

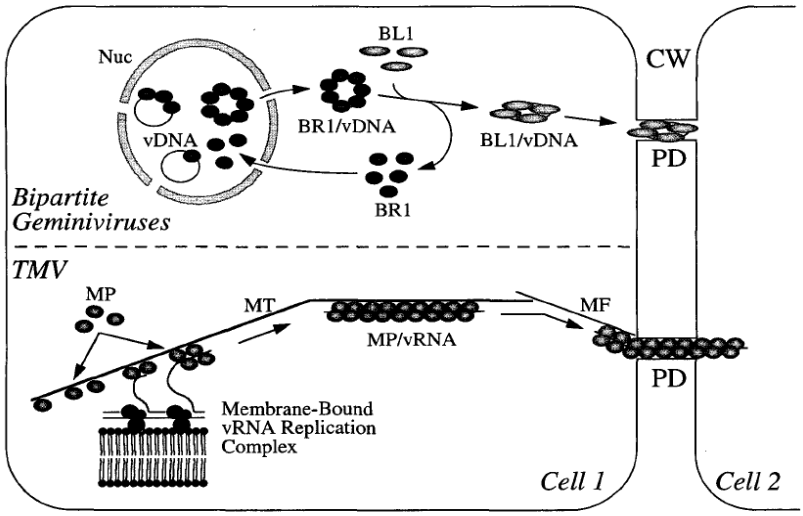

Adopted fromCarrington *et al*., 1996.

Fig-1.6: Pictorial representation of models of intracellular transport of the viruses. CW-cell wall; MF-microfilament; MP-movement protein; MT-microtubule; Nuc-Nucleus; PD-plasmodesmata; vDNA-viral DNA; vRNA- viral RNA.

a) The most studied MP of TMV, p30 which is 30 kDa protein and has RNA-binding function. It is an integral membrane protein that can bind to the RNA and translocate through ER network which is extended through the PD into neighbouring cell where the desmotubules are also involved for its activity (Maule, 2008; Epel, 2009). The hydrophilic region of TMV-MP associates with the ER and helps in the movement of virus but not integrates into the lumen of ER (Peiro *et al*., 2014).

b) Few viruses have been reported more than one movement protein known as double gene block (DGB) (Carmoviruses) or triple gene block proteins (TGB). `The Gemiviruses (fig-2.3), potex-like and hordei-like viruses have three small proteins which help in the movement of the viruses which are known as triple

gene block proteins (TGB). The TGBp1 is an RNA binding protein with helicase activity. TGBp2 &TGBp3 are membrane-bound proteins which help in viral movement to cell periphery by means of ER derived vesicles which move along the actin and myosin filaments (Samuels *et al*., 2007; Jackson *et al*., 2009; Schepetilnikov *et al*., 2008; Lim *et al*., 2009).

3) Inter cellular movement through plasmodesmata:

ER is extended into the plasmodesmata known as appressed ER (desmotubule) and forms connections with the neighbouring endo membranes. The viruses move between cytoplasmic sleeve, the space between the plasma membrane and desmotubule. The association of the MPs with the interior of plasmodesmata increases the size exclusion limit (SEL) of the channel and helps in the passage of the virus (Waigmann *et al*., 2004; Wright *et al*., 2007). Some viruses move as MP-genome complexes (Herranz and Pallas, 2004) and some as virion particles (Lucas, 2006). Some traverse by the formation of tubules across the cells which are approx. 50 μm in length (ex; Como, Caulimo, Nepo and tospoviruses; Kasteel *et al*., 1997). In *Tomato spotted wilt virus* (TSWV) apart from MP, glycoproteins are also observed at the ER-export sites (Ribeiro *et al*., 2008). It was shown that the TMD of glycol proteins plays a role in the localization of glycoproteins (Ribeiro *et al*., 2009).

For the long distance transport of the viruses they have to enter into the sieve elements (Oparka, 2004). As the sieve elements lacks the protein synthesis capacity and viral replication process the gating mechanism of the plasmodesmata is also different from that of the mesophyll cells. Some viruses require CP for its systemic movement in the host (ex: TSV, AMV). Tombusviruses encode two MPs and help in the cell-to-cell movement (Carrington *et al*., 1996; Lucas *et al*., 2006). In TGB proteins, TGBp2 & TGBp3 proteins act as integral membrane proteins. Sub cellular localization studies of TGB proteins reveals that the proteins target to the endomembrane system mainly to ER (Cowan *et al*., 2002). Mutational analysis of the TMD also revealed the association of the TGB proteins with ER and blocked the viral movement (Morozov and Solovyev, 2003; Mitra *et al*., 2003). The fluorescent motile molecules along the ER network are also observed which are moving towards the cell periphery (Haupt *et al*., 2005). All the three proteins in the TGB are required for their localization to PD where one alone cannot target the organelle (Zamyatnin *et al*., 2004).

The complementary studies of MNSV-7A & 7B proteins revealed that they are involved in the cell-to cell movement of the virus. In vitro analysis of membrane association requires TMD (Navarro *et al*., 2006). Biochemical studies of p7B protein revealed the presence of the transmembrane domain and cotranslational insertion into ER translocon (Martinez-Gil *et al*., 2007). They play a critical role in helix membrane protein topology, controlling and insertion orientation (Hessa *et al*., 2005). MNSV-MPs are not working in trans in systemic infection as in case of TCV but enough for the local infection (Cohen *et al*., 2000; Genoves *et al*., 2006). The MNSV-7B protein is a transmembrane protein (Navarro *et al*., 2006) was confirmed and it interacts with the ER after being synthesized on RER and moves to PD through the golgi apparatus (GA) in *N. benthamiana* using GFP and RFP chimeras and with proper control marker (Genoves *et al*., 2010). The hydrophobic region contribution to the insertion of the 7B and about the orientation of the insertion was shown by using GFP-7B chimeras. The TMD of 7B controls the insertion of MP into ER and also next cellular destination of the MP to target PD. The Y13A at the end of TMD and Y28A were the residues that properly target the MP destination. The aromatic amino acids presence at the interface (membrane-cytoplasm) helps in the positioning and orientation of the TMD in the lipid bilayer. The 7B localization to GA is essential for the MNSV cell-to-cell movement (Genoves *et al*., 2011). The computer based analysis of p7A protein, highly positively charged protein secondary structure consists of N'-terminal sequence variation among the different strains, conserved in the central α-helical region which is the RNA-binding region and C-terminal sequence consists of β-sheets in all the strains. The α-helical region consists of the conserved region "AKDAIRK" in all the strains along with some conserved amino acids besides it (Vilar *et al*., 2005; Navarro *et al*., 2006). Apart from the RNA binding property and cell-to-cell movement function of the 7A it was also proven that the primary and secondary elements appear to form an interaction between these two functions. The *in planta* analysis of sub-cellular localization and bimolecular fluorescence assays showed that 7A localizing to cytoplasmic granules with actin microfilaments and targeting to PD for intra and intercellular movement. Therefore it was demonstrated that the viral movement proteins are multifunctional agents involved in many aspects of viral infection process (Genoves *et al*., 2009). They include viral RNA translation, mediating cell-to-cell in long distance transport of viral genomes, viral RNP complexes and suppression of gene silencing. To elucidate these functions the MP has to interact with various host proteins (Lucas, 2006) for the viral genome trafficking.

1.18 Coat protein

The structural protein of the virus is the coat protein which plays a major role in the infection. The dot matrix comparisons of the coat proteins of Carmoviruses, MNSV, TCV, CNV and Tombusviruses, TBSV-BS, TBSV-chi have shown that extensive amino acid similarities in the coat protein among all 6 viruses. The similarity of MNSV is more to Tombusviruses than to Carmoviruses (Riviere *et al*., 1989). After determination of 3D structure of MNSV also it was proved that the CP of MNSV is more similar to TBSV than to Carmovirus members, CarMV, TCV, CPMoV. The coat protein structure was composed of 180 copies of coat protein sub units with triangulation of T=3 lattice (Lommel *et al*., 2005). The 3D structure of MNSV consists of 3 domains: the surface domain (S-domain), the RNA-binding domain (R-domain) and the P-domain. The differences between the 3D structure of Tombusviruses and Carmoviruses was also explained clearly (Wada *et al*., 2008). The three sub units A, B, C consists of two domains S and P. These two domains were connected by the hinge region (Ile262 to Met265). The R-domain was known to interact with RNA inside. The S-domain is highly conserved and the P-domain is very less conserved. It was also shown that MNSV CP structure is more similar to TBSV in comparison with other Carmoviruses (Riviere *et al*., 1989; Wada *et al*., 2008).

It was demonstrated that the amino acid substitution in the viral coat protein at position 300 from Ile-Phe, resulted in the loss of specific binding of the virus to the vector and also fungal transmission (Mochizuki *et al*., 2008). The chimeric constructs of Chi & W strains of MNSV constructed by exchanging the CP region have shown the contribution of CP in attachment to zoospores. Mainly the protruding domain of MNSV-CP is the region that is compatible with the zoospores. Many differences in the amino acid residues on the surface of virus are the cause for the recognition of the fungal vector, Y1 but not by NW1 (Ohki *et al*., 2010). The p42 protein was also able to give the local infection where it was also proven that the p42 is the factor controlling the symptoms and it was also important for the systemic transport. It was also able to delay RNA silencing in transient assay systems in the *N. benthamiana* plants (Genoves *et al*., 2006).

1.19 Infectious clones

An infectious clone helps us to gain knowledge on the functional genomics, replication, expression of viral proteins and in delineating host-virus interactions. In modern day biological infectious clones are the basic need of any laboratory to study the functional genomics of the pathogen. The cDNA clones, generated through RT-PCR were used for the construction of infectious clones, which are first assembled in bacterial plasmids. The manipulations of the clones for a particular investigation will be easier in bacteria. The construction of infectious clone is difficult task though several infectious clones are in use (Boyer and Haenni, 1994). The assembly of the infectious clone should be carefully designed in such a way that the clone should remind you of the wild type. Care should be taken to eliminate the non-viral nucleotides during the assembly of the infectious clone from the cDNA clones especially at the 5' end reduce the infectivity. Constructed clones are also enroute for mutations during cDNA synthesis, assembly and when transformed into *E. coli*. In bacterial cells, clones are toxic or unstable, which leads to point mutations or rearrangements turn the clone to non-infectious. These problems can be conquered by high fidelity long template PCR, introducing eukaryotic intron genes at critical genome regions and inclusion of frameshifts (Satyanarayana *et al.*, 2003; Marillonnet *et al*., 2005; Yamshchikov *et al.*, 2001; Yu and Wong, 1998).

The major and critical steps in construction of infectious clones are: conversion of the RNA genome into first cDNA strand with reverse primer at 3' end by reverse transcriptase enzyme, removal of RNA, synthesis of second strand by DNA polymerase with forward primer at 5' end of the genome. The promoter sequence was mostly added to the primer in the 5' end. It is notable that the synthesis of the first strand cDNA was hampered mostly by the strong secondary structures (Boyer and Haenni, 1994).

1.20 Types of infectious clones

Infectious clones are of two types based on the transcribing nature

a) Generation of run-off transcripts (*in vitro*)
b) Infectious cDNA which can result *in vivo* transcripts

Both contain same viral genome but variant at the 5' end flanking promoter sequence. The infectious clones that can produce infectious RNA consists of bacterial phage promoter sequence T7/SP6 but also λpm and T3. The phage promoter is used to transcribe large quantities of viral RNA from DNA. To guarantee the infectivity, RNA should resemble wild type RNA without nucleotide additions. One of the main advantages of the system is that the transcribed RNA can act as mRNA directly in the

cytoplasm instead of introducing it into the nucleus. The disadvantage of the infectious RNA approach is that the sensitivity (RNA is fragile and amenable for the RNase contamination) of the transcribed RNA to degradation and the problems with the inoculation on to plants. So, maintenance will be a bigger challenge in the form of RNA.

The infectious RNA can be transcribed *in vivo* from the infectious clone is achieved by CaMV-35S promoter. It requires the use of self-cleaving ribozyme at 3' end of the viral genome, which removes the unwanted non-viral nucleotides. *In vivo* transcription is easier, less expensive and RNA is not prone to degradation also. Delivery of the DNA into nucleus of the cell and symptoms are delayed when compare to *in vitro* RNA inoculation are the disadvantages in *in vivo* transcription (Van Bokhoven *et al.*, 1993). Agrobacterium T-DNA based approach was used which is DNA based and all the steps involved will be taken care by the agrobacterium machinery after transformation of constructed infectious cDNA into agrobacterium.

1.21 Different Transfection techniques

Several methods are available for the transfection of plants and plant tissues. Among them mostly widely used and cheapest ways for transfecting plants are

a) Mechanical inoculation is used to infect transcribed RNA (*in vitro*) on to plants. In this method leaf surface is abraded by an abrasive agent (carborundum/celite) and nucleic acids are applied on the surface with finger as the way we inoculate plant viruses (Hull, 2014). This method is less expensive and fast.

b) Agroinfection: The most effective method of transfecting plants is by the use of *Agrobacterium*, which is used as most favoured tool in genetic engineering. It helps in the stable integration of foreign gene into plant genome and production of transgenics (stable transformation). Using *Agrobacterium* as a vector, foreign gene was introduced into the nucleus of the plant cell, by transferring its tumor-inducing (Ti) DNA into the host cell (Tzfira *et al*., 2006; Gelvin, 2003). If we transfer bacterial genes into T-DNA of agrobacterium and infect the plant cell, it causes neoplastic growth and tumors are produced on the plant, indicates the successful transfection process. Now-a-days, this property is exploited by the modern day molecular virologists for transferring the foreign gene of interest which forms the basis for the agrobacterium mediated genetic transformation. It is being used for transient expression of the genes where we can introduce the foreign gene into the nucleus of the host cell and made more favourable for the transcription. This skill is

termed as 'agroinfection'. By mobilizing the infectious clone into T-DNA of *Agrobacterium tumifaciens* and infiltrating the plant cell with agrobacterium culture make certain that it is transcribed in the nucleus. Agrobacterium can be infiltrated into plant tissue by a syringe or vacuum infiltration or agrodrench methods. With the development of this technology introducing the foreign gene into nucleus was made easy, major disadvantage in *in vivo* transcription.

1.22 Transient expression

This method has a number of advantages over stable transformation procedures. It is very simple, cost effective and fast process. One can efficiently express the unlimited size of gene once it is cloned in between the right and left boarders and the minimal rearrangements are observed in the cloned inserts. This technique was most efficiently applied for plants (*N. benthamiana*) (Joensuu *et al*., 2010). The produced transformants are highly stable (Boyer and Haenni, 1994) but the transgene is not passed on to the progeny, because stable transformation was not observed (Gleba *et al*., 2007). Since 1980's foreign genes have been introduced into plants using plant viral vectors (Marillonnet, 2005). Many improvements have been made to expression systems through recent advances in the field of plant virology and molecular biology for study of gene silencing. (Min-Ryu *et al*., 2004; Liu and Lomonossoff, 2002; Vaghchhipawala and Mysore, 2008; Sang-Min *et al*., 2005; Johenson and Carrington, 2001; Yang *et al*., 2000). It can be adaptable to different cell types, culture procedures and the process can be applied in the Pharmaceutical industries for production of hormones, antibodies *etc* in larger volumes (Gils *et al*., 2005; Hefferon, 2012). Multiple proteins could be expressed using viral vectors (Bedoya *et al*., 2010). This process is also bio containment (Gleba *et al*., 2007).

1.23 Agrobacterium

Agrobacterium tumefaciens, is a gram negative soil resident phytopathogenic bacterium that causes crown gall disease on many dicotyledonous plants. It belongs to family *Rhizobiaceae*; genus: *Agrobacterium*, (Hellens, 2000; Gheysen, 1998). The crown gall disease is caused by the T-DNA released from Ti (tumour inducing) plasmid. The tumour-inducing plasmid is a large double stranded circular DNA of approximately 200 kb size, consisting of a specific region (T-DNA, approximately 20 kb). The Ti plasmid requires another plasmid that contains virulence genes (*Vir*) which helps in the transfer

process of T-DNA (Stewart, 2008). These two regions, vir region and T-DNA regions are important for the agrobacterium mediated genetic plant transformation. The T-DNA region in the Ti-plasmid is completely dispensable and clearly demarcated by 25 nucleotides of inverted repeats called right and left boarders. There are at least six essential vir operons, *Vir*A, *Vir*B, *Vir*C, *Vir*D, *Vir*E, *Vir*G and two non-essential operons- *Vir*F, *Vir*H and each has its own number of genes. All these are resided in Ti-plasmid and these vir genes will act *in trans* and involved in the transfer of the single strand T-DNA into the host cell nuclei (Gelvin, 2003).

With the interaction of *Agrobacterium* on to plant tissue, the bacterium recognizes and attach to the wounded tissue by identifying chemicals released from the injured tissue. Immediately, *Vir*A and *Vir*G genes are activated by the phenolic compounds (such as acetosyringone and some monosaccharides). *Vir*G is phosphorylated by *Vir*A, starts the transcription of other *Vir* genes. The activated *Vir* genes generates a new copy of single stranded (ss) molecules from the DNA fragment located between the right and left boarders of T-DNA (Tzfira and Citovsky, 2008).The genes, *Vir*D1 and *Vir*D2 nick the T-DNA border sequences at end of the boarders and excise the T-region from the Ti plasmid. After excising the ssDNA strand, *Vir*D2 binds covalently to the 5' end of the nicked DNA strand (Stewart, 2008). To this complex, *Vir*E2 is coated around to prevent degradation and along with other *Vir* proteins transported through the plant cell wall and cellular spaces to the nuclear genome by a system called *Vir*B/D4 (fig-1.7).

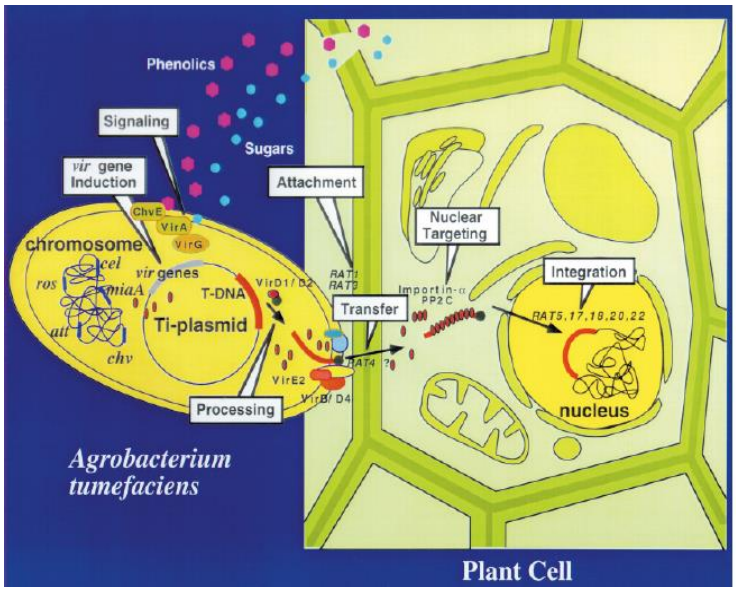

Adopted from Gelvin, 2003

Fig-1.7: Transformation of T-DNA region from Ti-plasmid of agrobacterium to the plant cell.

The last step in the transformation process is the integration of T-DNA to the plant nucleus, where the attachment of *Vir*D2 and the coat of *Vir*E2 are removed prior to the integration of T-DNA into the plant genome. During the integration process, T-complex interacts with the VIP1, CAK2M (plant ortholog of cyclin dependent kinase-activating kinases) and TATA-box binding protein (TBP) and other host machinery necessary for transcription to guide it to the site of integration (Tzfira and Citovsky, 2006; Gelvin, 2003) (fig-1.7). In transient expression system, the gene doesn't integration onto host cell genome but it will directly transcribe the gene with its own promoter sequence at the 5' end and translate. Therefore agrobacterium is a useful bacterium and it became a landmark event in the modern biology (Yuan and Williams, 2012).

1.24 Cell biology studies

The study of cell biology has been revolutionized by the early 20th century with the discovery of green fluorescent protein (GFP) which is isolated from the Jelly fish, *Aequorea victoria* (Prasher *et al*., 1992; Chalfie *et al*., 1994; Yang *et al*., 1996). GFP has around 238 amino acids and molecular weight of 27 kDa. Wide range of GFP-like proteins were identified recently ranging from cyan to red (different types) were discovered in marine organisms (Wiedenmann *et al*., 2009). All these fluorescent proteins were used as reporter genes in gene expression studies. They are indicators to study intracellular physiological changes, for monitoring cell organelle and protein dynamics, as probes for investigation of protein-protein interactions and as fusion proteins in studies of subcellular organelle.

The variants of fluorescent proteins are fused to the gene of interest to analyse the function of the protein in the living cell. With this new insights were gained in cellular processes in the cell and protein functions. Mutagenesis of GFP, yielded various variants which are helpful in the studies. The GFP enhanced version (eGFP) was also developed by amino acid substitution Ser^{65} to Thr^{65}, where the chromophore formation was accelerated (Gerdes and Kaether, 1996). Since plants contain large number of muti-gene families, comparison of subcellular localization of individual members are important for the cell biology study. Different fluorescent proteins are applied in dual labelling to study the proteins localization as well as its function (Forner and Binder, 2007). For example, individual viral proteins are fused with the fluorescent proteins (GFP, YFP,

BFP etc) to study their site of action, intra and intercellular trafficking etc (Harries *et al*., 2009, 2010; Niehl and Heinlein, 2011).

1.25 Subcellular localization of various viral proteins

Different viral encoded proteins target to different organelles during replication, movement and symptom expression. One of the replication proteins present at the 5' end of the genome in Carmoviruses target to mitochondria whereas the complete replicase protein targets nucleus for the transcription of the remaining viral proteins (Martinez-Turnio and Hernandez, 2012; Mochizuki *et al*., 2009). It has been proved that viral encoded proteins use different host cell organelles for the replication in the process of infection. BMV, CPMV, ToRSV targets endoplasmic reticulum (ER) for their replication. The regions important for the their targeting are also identified in many viruses (Carette *et al*., 2002 a, b; den Boon *et al*., 2001; Zhang and Sanfacon *et al*., 2006; Pouwels *et al*., 2002). The *Cauliflower mosaic virus* movement protein (CaMV-p6) can form motile inclusion bodies associating with ER that traffic along the microfilaments and stabilize microtubules (Harries *et al*., 2009a). TMV-MP associates and accumulates the microtubules during its movement (Curin *et al*., 2007).

Different types of movement protein trafficking intracellular was explained by Carrington *et al*., 1996. The C-terminal hydrophobic domain of the *Papaya ringspot virus* (PRSV) P3 protein (plays role in formation of viral replication complex) has shown to target ER (Eiamtanasate *et al*., 2007). *Tobacco vein mottle virus* (TVMV) P3 protein interacts with CI protein in cytoplasm (Rodriguez-Cerezo *et al*., 1993). The P3 protein of *Tobacco etch virus* (TEV) is associated with viral NIa and NIb proteins in the nucleus (Langenberg and Zhang, 1997). TEV-P3 protein forms mobile inclusions and traffics along actin microfilaments. P3 plays a dual role in virus movement and replication (Cui *et al*., 2010). It was shown that *Potato virus*-Y coat protein (PVY-CP) has action in chloroplasts may contribute to symptom development in infection (Naderi and Berger, 1997). The replication proteins (P1&P2) of *Alfalfa mosaic virus* (AMV) are localized into tonoplasts for the virus replication process even P1 is found in other organelles (Heijden *et al*., 2000). The replication protein, P33 of *Tobacco bushy stunt virus* (TBSV) localizes to peroxisomes to ER sorting pathway (McCartney *et al*., 2005). The 66 kDa replication protein of TYMV targets to chloroplast envelope for its action (Prodhomme *et al*., 2003). The cytopathological vesicles formed from the outer nuclear membrane were also observed in *Pea enation mosaic virus* (PEMV) (Powell *et al*., 1977). The

localization of 36 kDa protein of *Carnation Italian ringspot virus* (CIRSV) to mitochondria was also shown using GFP chimeras (Rubino *et al*., 2001). The membrane modifications that are required by the viruses in the plant cell are like: alpha-like viruses replicate along the ER invaginations, flavi-like viruses replicate along organellar membranes, Bromoviruses and Tombusviruses need ESCRT for their replication.

With this literature survey, the field collected virus attempted to characterized biologically (chapter-2), deduced the complete genome sequence through molecular manipulations, classified as the Carmovirus based on the molecular phylogenetic trees (chapter-3), constructed the infectious clone and developed agroinfiltration approach of transfection (chapter-4) and different viral proteins were localized in the host cell (*N. benthamiana*) through GFP chimeras (chapter-5).

CHAPTER-2

Biological characterization of the new virus collected from the field

2.1 Introduction

New viral reports are increasing every day in the Pubmed (http://www.ncbi.nlm.nih.gov/pubmed) all around the world. About 200 or more viruses are uncharacterized or at various stages of characterization and remained ungrouped (Hamilton *et al*., 1981). The crop losses due to the uncharacterized viruses are increasing due to various factors like change in soil, climate, vectors and also global warming (Zell *et al.*, 2008). As a pathologist, the frequent field surveys to the farmer's field are very important to identify the new diseases and their causative organisms to decrease the yield loss. Several virus diseases are described in the plants by using several methods for the identification and detection of plant viruses. Viruses are the most primitive organisms and the range of characteristics available for identification; detection and diagnosis are very limited. Even though, single biological and molecular diagnostic test is highly sensitive, we cannot completely rely on single test but a combination of different methods are needed for non-ambiguous results and diagnosis. Most of the diagnostic tests used for the detection of plant viruses are highly sensitive, rapid and inexpensive. However, the diagnostic tests used for the virus detection depends on various factors like type of the sample, number of samples to be tested, availability of reagents, facilities, level of sensitivity required, expertise and skill in the particular test and also on the availability of the information on the virus on detection (Naidu and Hughes, 2003).a

Diagnosis of the disease is the identification of the nature and cause of the disease whereas detection is the identification of the target organism associated with the disease (Narayanaswamy, 2008). Virus identification is very difficult and unsuccessful if the symptom expression in the host is not clear. Conversely, if a single host is affected by two or more pathogens then the symptom expression is different than the symptom expressed by individual pathogen and often synergistic effects can be described. So, the virus identification is broadly divided into two methods: a) Biological methods (discussed in the present chapter) and Molecular methods (discussed in chapter-3).

The biological methods used for the detection are time consuming, labor-intensive and require more green-house space. Biological methods are the basic methods that relays on the symptomology of the infected material. Even though symptoms provide the adequate information about the disease and the causative organism more field experience is required as plants will exhibit virus like symptoms in unfavorable climatic conditions (Narayanaswamy, 2008). The biological methods employed in the present chapter for the characterization of the field collected sample is single lesion assay, host range, virus purification, electron microscopy, nucleic acid extraction, ds RNA extraction, seed transmission tests and serology tests like ELISA, western analysis, dot-blot etc.

In single lesion assay, multiple infections occurring in the field samples through vectors are eliminated and pure virus was obtained which is very important for the study of characteristics to obey Koch's postulates (Hamilton, 1981).

The host species that a virus infects and induces symptoms naturally and experimentally represent the host range of a virus. The experimental host range study gives the probable natural infections for the virus. Major objective of host range study is to find a suitable assay/indicator host for analysis of the diverse viral processes in the laboratory and a systemic host to study viral infection processes in single cell and in whole plant scenario.

Plant viruses are to be separated from the host constituents without affecting the structure and infectivity of the virus to study the physic-chemical characteristics of the virus. Stanely demonstrated the TMV purification in 1935. After that several protocols to several viruses were reported. Purified virus is required to determine the structure, biochemical and molecular properties of a particular virus by various techniques without the background reactions.

The phenomenon of separation of biological molecules based on the charge under the influence of electric field is called electrophoresis. It's a simple, rapid and highly sensitive analytical tool. The proteins were treated with Sodium dodecyl sulfate (SDS), an anionic detergent in the presence of reducing agent; all the polypeptides are denatured and are linearized with negative charge. Then the proteins are separated by performing Laemmli discontinuous system of PAGE.

Extraction of the virus genetic material from the purified virus is important to understand the functional genomics and to classify the virus based on the molecular parameters. Detection of double stranded RNA (dsRNA) profile, a hallmark for the plant

RNA virus infection is used as screening tool for the identification and classification of the virus.

Serological techniques like Enzyme linked immunosorbent assay (ELISA), western blotting, dot immunobinding assay (DIBA) are also employed for the appropriate classification of the virus. Clark and Adams (1977) showed that the microplate method of ELISA is very effectively applied for the detection and assay of plant viruses. It is most sensitive, economical and rapid method for screening and identification of viruses with the mixed infections.

Western blotting technique is a widely recognized technique to detect specific proteins in the sample of tissue homogenate or extract or in a mixture of proteins. It is a combination of SDS-PAGE and immunodetection of separated proteins by transferring them from polyacrylamide gels to stable solid immobilized media (Polyvinyl diflouride (PVDF) membrane) with specific antisera against the antigen under detection.

Dot immunobinding assay (DIBA), is relatively easy technique that is performed with in 24 hrs and more number of samples can be screened using this technique.

Electron microscopy is an important tool for the determination of the morphology of the virus. The virus particles are visualized under electron microscope; there it makes the use of electron beam in order to magnify the viral particle. Kausche was the first to made the rough estimation of the rod shaped structure of the TMV in 1939 and It was later improved by Muller (1942) by using shadow casting with heavy metals like lead to obtain greater resolution. Negative staining of the virus with phosphotungstic acid (PTA) and uranyl acetate (UA) improved the resolution of the appearance and nature of virus particle (Milne, 1984).

In the present chapter, different biological and serological parameters are employed for the characterization of the field collected virus sample and there by assigning the virus to a particular group in the ICTV classification.

2.2 Materials and methods

2.2.1 Single lesion assay and virus maintenance

The virus collected from the fields of Rangareddy district has to be characterized through biological assays and it was initially maintained on *Phaseolus vulgaris* in the laboratory through single lesion assay. Towards this, isolated single lesion on the infected

leaf was selected; excised with sterile scalpel and ground in inoculation buffer pH-7.4 (Appendix (A), A1.11) and mechanically inoculated on to the fully expanded cotyledonary leaves of healthy plant using carborundum, as an abrasive. Single colony from each passage was passed to six passages and the virus from the last passage (where we are sure that as pure virus) was used to study the biological characteristics of the virus.

2.2.2 Host range

Host range for the field collected virus sample was conducted with the pure virus culture obtained after single lesion assay (2.2.1) by inoculating the leaf sap on to different herbaceous hosts (tab-2.1) by mechanical inoculation (2.2.1). The herbaceous plants at two leaf stage (cotyledon leaves were inoculated in case where plants were germinated directly from seeds) and 6 week old plants in case of *N. benthamiana* were dusted with carborundum (sometimes celite based on the availability) prior to the inoculation. Inoculum was prepared in inoculation buffer and inoculated on to the leaves with the help of two fold muslin cloth. The plants were maintained at controlled conditions in growth chamber at 24ºC temperature with 16 h light and 8 h dark. These inoculated plants were observed for 1 month and the results were scored on the basis of the visual symptoms obtained on the inoculated leaves as well as on the upper systemic leaves. Symptoms on all the hosts were confirmed by back inoculation on to indicator host (*Phaseolus vulgaris*).

2.2.3 Virus Purification

The purification procedures for each and every virus vary as no two viruses are identical and the procedure varies based on the host plant used in the extraction process. Initially the virus purification in this chapter was performed by following the basic protocol mentioned by Prof. M.V.Nayudu (2008). After identifying the virus, it was improved according to the protocol mentioned by Diez *et al.*, (1998).

Virus was purified from the local lesion host, *Phaseolus vulgaris* and systemic host, *N. benthamiana* to study the bio-physico-chemical and molecular properties of the virus. The virus infected leaf sample was harvested, weighed (200 gm) and homogenized (1 gm in 2 ml buffer) in an electric blender with 0.5 M potassium phosphate buffer (A1.20) (ice-cold) pH-7.4 containing 0.1% ß-mercaptoethanol in short pulses. The homogenate was sieved through two layers of muslin cloth; the filtrate was clarified by adding chloroform to 10%

(v/v) and mixed gently using magnetic stirrer at 4˚C for 30 min. The debris was separated by subjecting it to centrifugation at 10,000 rpm for 10 min at 4˚C. Supernatant was collected, divided into three equal fractions and subjected to the following parameters.

1) Precipitation with poly ethylene glycol (PEG) – 6000: The first fraction of the clarified supernatant was precipitated by adding 8% PEG-6000 (w/v) to the total volume and allowed to dissolve it completely by continuous mixing at 4˚C. 1% of NaCl was added as an additive to increase the efficiency of precipitation and stored the mixture at 4˚C for 2 h. The mixture was centrifuged at 10,000 rpm for 15 min and the supernatant was discarded. The pellet was re-suspended in 6 ml of 50 mM potassium phosphate buffer pH-7.0 and used in the later parts in sucrose density gradient ultra-centrifugation.
2) Precipitation with Ammonium sulphate: The second fraction was precipitated with 55% (w/v) of powdered ammonium sulphate by continuous mixing on magnetic stirrer in cold condition and stored for 2 h at 4˚C. The mixture was spun down at 10,000 rpm for 15 min and the supernatant was discarded. The pellet was re-dissolved in 6 ml of 50 mM potassium phosphate buffer and clarified at low speed 8,000 rpm for 10 min. The clarified supernatant was subjected to sucrose density gradient ultra-centrifugation.
3) Direct ultracentrifugation: The third fraction was directly subjected to ultracentrifugation at 24,000 rpm for 4 h at 4˚C in SW28 swing out rotors. The supernatant was discarded and the pellet was re-suspended in 6 ml of 50 mM potassium phosphate buffer. The mixture was clarified at low speed 8,000 rpm for 15 min and used in sucrose density gradient ultra-centrifugation.

By layering 5, 8, 8 and 4 ml of 40%, 30%, 20% and 10% respectively sucrose (dissolved in 50 mM potassium phosphate buffer) density gradients were prepared and stored the gradients undisturbed at 4˚C for overnight. Three fractions from the above steps were layered on individual sucrose gradients and subjected for ultra-centrifugation at 24,000 rpm for 2 h. The tubes were observed in dark by a beam of light for the light scattering zone of virus. The opalescent band was collected with the help of a syringe and diluted with equal volume of 50 mM potassium phosphate buffer. The virus was concentrated by subjecting to centrifugation at 40,000 rpm for 4 hrs. The purity of the virus was checked by analyzing the coat protein by SDS-PAGE.

The purified virus was diluted (1:100) and mechanically inoculated on to *Phaseolus vulgaris* to check the infectivity (data not shown). The purified virus sample was used further in different techniques like SDS-PAGE, electron microscopy, isolation of nucleic acid, seed transmission and serodiagnosis.

Quantification of purified virus particles

The purified virus particles were quantified according to Diez *et al*., (1998), based on the extinction coefficient for Carmoviruses is reported as 1 OD_{260} = 5 mg/ ml.

2.2.4 Sodium dodecyl sulphate-polyacrylamide gel electrophoresis (SDS-PAGE)

The separation of coat protein was carried out by 12% slab gel electrophoresis system as described in Sambrook *et al*., (2001). The resolving gel of 12% (A1.21), pH-8.8 and stacking gel of 5%, pH-6.8 (A1.25) were used. The polyacrylamide gels of acrylamide to bisacrylamide at 29.1:0.8 ratio (A1.2) and SDS of 0.1% was used. The protein samples were prepared by mixing equal volume of protein sample and 2X Laemmli sample loading dye (LSD) (1.12). The samples were incubated in boiling water bath for 5 min, subjected to brief spin to remove the debris and loaded on to the prepared gel using loading tips. Electrophoresis was conducted at 120 V in 1X SDS running buffer (A1.24). Quick staining of the gel was performed by adding staining solution (A1.26) with help of microwave oven in 4 short pulses of 10 sec each and destained with destaining solution (A1.10) was done in short pulses until the gel was de-stained properly, revealing the bands clearly against a faint background. The molecular weight of the unknown sample was estimated by using the known pre-stained molecular weight marker/protein ladder (Fermentas).

2.2.5 Electron microscopy

Electron microscope uses electromagnets to focus a beam of electrons produced from a tungsten rod by high voltage. The negative staining of the virus with uranyl acetate (UA, pH-5.0) or potassium phosphotungstic acid (KTA, pH-7.0) gives the better resolution of appearance and nature of the virus particle in electron microscope (De Carlo and Harris, 2011). The purified virus from the sucrose density gradient was used to study the morphology of the virus. Two drops of 10 µl of purified virus sample was placed separately on parafilm and one carbon coated grid was placed on each drop in inverted position for 2 min. The grids were removed with the help of fine forceps and excess sample was cleaned

with lint free filter paper. After allowing the grids to dry for a minute, one was placed on a droplet of 1% PTA and other was on 2% UA droplet separately for 30sec. The excess stain was removed and the grid was dried. The grids were observed under transmission electron microscope at 200 KV for the topology determination.

2.2.6 Total nucleic acid extraction from purified virion

The nucleic acid extraction protocol for the unknown virus was standardized with few modifications of the protocol mention by Nayudu (2008). Briefly, 200 µg of purified virus (2.2.3) was mixed with equal volume of nucleic acid extraction buffer (A1.23) and incubated at 42˚C for 20 min. To the incubated tubes equal volume of water saturated phenol and chloroform (1:1 ratio) was added. The contents of the tube were mixed vigorously and subjected to centrifugation at 14,000 rpm for 15 min at 4˚C. The upper aqueous phase was collected into sterile microfuge tube slowly with the help of 10 µl pipette without disturbing the phenol phase. To this, $1/10^{th}$ volume of 3M sodium acetate and equal volume of isopropanol was added. The nucleic acid was pelleted by centrifugation at 13,000 rpm for 15 min. Supernatant was discarded and the pellet was washed twice with 70% alcohol by centrifugation at 13,000 rpm for 10 min. The pellet was air-dried and dissolved in 30 µl of sterile milli-Q water. Using the same protocol, nucleic acids were extracted for two known viruses whose molecular sizes are reported which are *Sesbania mosaic virus* (SeMV) and *Physalis mottle virus* (PhMV). The molecular size of the nucleic acid molecules was analyzed by agarose gel electrophoresis (2.2.7) along with the known controls. The purity was analyzed by 260/280 ratios spectro-photometrically (1.8-2.0, 1.8-1.9 for RNA and DNA respectively).

2.2.7 Agarose gel electrophoresis

This technique was performed as described in Sambrook *et al.*, (2001). Nucleic acids were separated on 1% agarose gel in 1X TAE buffer (A1.29) at 100 V for 60 min. The samples were loaded on to gel with the help of 6X loading dye (A1.13), with final concentration of 1X. The RNA samples were mixed with 1 µl of 6M urea along with the 6X loading dye and heated at 65˚C for 5 min and loaded into the gel. The gels were visualized under UV-transilluminator and documented using gel documentation unit.

2.2.8 Sensitivity of nucleic acid to nucleases

Based on the activity of nucleases (DNase and RNase) the type of viral nucleic acid can be determined, which is helpful in virus characterization. The type of the viral nucleic acid of the unknown virus was confirmed by treating the extracted RNA with both DNase and RNase enzymes individually. About 200 µg of isolated viral nucleic acid was aliquoted in two sterile microfuge tubes. 1 U of the modifying enzymes, DNase and RNase were added to the tubes separately and incubated at 37˚C. After 30 min of incubation, the samples were loaded on 1% agarose gel as described in section 2.2.7 along with proper controls. The gel was visualized under UV-trans illuminator and documented.

2.2.9 Double stranded RNA extraction

The extracted of dsRNA was performed by following the protocol described by Dodds (1993) with few modifications and without the use of cellulose columns. The purified virus was mechanically inoculated on healthy *P. vulgaris* and *N. benthamiana* leaves and leaves were collected (on the 2, 3 and 4 dpi from *P. vulgaris* and from *N. benthamiana* on 2 to 6 dpi). One gram of infected leaf material was homogenized to fine paste in 10 gm of extraction buffer (A1.23). The homogenate was collected into centrifuge tube and incubated at 42˚C for 20 min. To the incubated sample, equal volume of phenol chloroform mixture (v/v) (1:1 ratio) was added and vortexed vigorously for 3 min. The nucleic acids were separated into the aqueous phase from the mixture by subjecting it to centrifugation at 13,000 rpm for 20 min at 4ºC. The upper aqueous layer was separated into sterile microfuge tube slowly with the help of pipette, and precipitated with equal volume of 2.5 M ammonium acetate and 2.5 volumes of cold ethanol. Precipitation can be enhanced by incubating the samples in -80˚C for 1 h. The nucleic acids can be pelleted by centrifugation at 15,000 rpm for 20 min at 4˚C. The pellet was washed with 70% ethanol, air-dried and re-suspended in 3 ml of milliQ water. The sample was re-precipitated by adding equal volume of 4 M LiCl and incubated at -80˚C for 30 min. The samples were subjected to centrifugation at 15,000 rpm for 20 min at 4˚C. dsRNA was precipitated from the supernatant with 2.5 volumes of ethanol and the tubes were placed in liquid nitrogen for 5 min prior to the centrifugation at 15,000 rpm for 15 min at 4˚C. Supernatant was discarded and the pellet was washed with 70% ethanol and spun down at 15,000 rpm for 10 min. The pellet was air-dried and dissolved in 2 ml of milli-Q water. Healthy leaves also collected and

processed in the same way to serve as control. The profiling of the ds RNA was evaluated by performing 1% agarose gel electrophoresis (2.2.7) along with healthy control.

2.2.10 Seed Transmission

The purified virus (2.2.3) was mechanically inoculated on to the *N. benthamiana* plants (100 plants) as described under the section 2.2.1. All the plants were covered with polythene covers individually. The infected plants were maintained in growth chamber under controlled conditions until they set flowers, fruit formation and seed formation. These seeds were tested in two ways. In the first method, the collected seeds from individual plants were tested directly by DAC-ELISA (100 plants X 10 seeds from each plant). In the second method, seeds from individual plants were allowed to germinate (100 seeds from each plant) and observed for the visual symptom expression and as well as the seedlings (10-20 seedlings were ground together from each plant) were tested by DAC-ELISA (2.2.12) using the raised poly clonal antisera (2.2.11). The leaf sap from the seedlings was also tested by back inoculation on to indicator host (2.2.1).

2.2.11 Polyclonal antibody production

2.2.11 (a) Polyclonal antibody production against the native virion particles

Polyclonal antibodies were produced against the native virion particles obtained in ultra-centrifugation. About 200 µg of antigen and equal volume of Freund's complete adjuvant was emulsified using 1 ml syringe and injected subcutaneously into New Zealand inbred male white rabbit. Pre-immune serum was collected prior to the injection to serve as control. After 21days, first booster dose was given with same concentration of antigen by emulsifying with Freund's incomplete adjuvant. Four booster doses were given for every 21 days interval with Freund's incomplete adjuvant and 1ml of blood samples were collected prior to each and every booster dose. Serum was collected from the blood and antibody titer was tested with DAC-ELISA, DIBA and western analysis. After last booster dose blood was collected from the rabbit by making a small cut from the ear vein. Serum was prepared from the clotted blood and traces of red blood cells are removed by centrifugation at 5000 rpm for 10 min at 4ºC. The serum was collected and tested for the antibody titer. Serum aliquots were diluted with sterile glycerol to a final concentration of 20% and stored at -20ºC for future use. The antisera titer was checked by DIBA, ELISA and western blot.

2.2.11(b) Polyclonal antibody production against the denatured virion particles

Similarly another set of polyclonal antibodies were produced against the denatured virus to detect the denatured coat protein (CP) in western analysis. Virion coat protein was separated on SDS-PAGE and the band of interest was excised from the gel, washed with TBS-T (5 times in 5 min interval) (A1.31) and final two washes with 1X TBS (A1.30) and sterile milli-Q water respectively. The gel pieces were ground in sterile motor and pestle into fine powder with the help of liquid nitrogen. Then it was properly emulsified with Freund's complete adjuvant and injected into rabbit subcutaneously. Except the preparation of the antigen, the procedure for production of polyclonal antibodies is same as mentioned in 2.2.11(a).

2.2.11(c) Cross absorption

Though we have used sucrose density gradient purified virus for polyclonal antibody production, there is a possibility of host proteins contamination in the virus particles. So, the antisera raised against the pure virus may also contain antibodies for the host proteins and gives the background reactions in the experiments due to that the results may be misleading. To avoid this scenario, the raised antiserum was mixed with equal volume of healthy host total soluble proteins (A1.33) and incubated at 4˚C for overnight (Hobbs *et al.,* 1987). The mixture was centrifuged at 5000 rpm for 15 min at 4˚C and the precipitated pellet was removed. The supernatant is more specific to antigen without background reaction.

2.2.12 Direct antigen coating-Enzyme Linked Immunosorbent Assay (DAC-ELISA)

The protocol was performed as described in Sambrook *et al.,* (2001). Briefly, 1 gm of infected leaf sample was ground in 2 ml of carbonate buffer (200 µl loaded) (A1.9) or appropriately diluted 200 µl of purified antigen was coated on to the ELISA plate. The coated plate was incubated at 4˚C for overnight. Then the plate was emptied by inverting it and washed by flushing the wells with a jet of PBS-T (A1.15) with a wash bottle. The above washing step was repeated thrice with 5 min interval. After the third wash, the plate was emptied completely by taping it on a pad of filter papers and 200 µl of primary antibody (raised polyclonal antibody) diluted in PBS-TPO (A1.16) was added to the required dilutions (1:5000, 1:10,000, 1:20,000, 1:40,000, 1:80,000 & 1:1,60,000) and incubated at room temperature for overnight. After incubation, the plate was emptied as done in the

earlier step and washed thrice with PBS-T with 5 min interval. The traces of the wash buffer was removed by tapping the plate forcibly on pad of filter papers and 200 µl of secondary antibody (Goat anti-rabbit-ALP, Biorad) was added by diluting in PBS-TPO at 1: 10,000 dilution. The plate was incubated for about one and half hour and repeated the washing step with PBS-T as above and the last wash was with 1X PBS (A1.14). Then 200 µl of substrate buffer (A1.28) was added and the plate was incubated in dark. Within 30-60 min yellow color development was observed indicating the positive result. The results were analyzed according to the prepared program sheet.

2.2.13 Western analysis

In this technique, the proteins were separated by slab gel electrophoresis as described under the section 2.2.4. The gel was removed from the holder (without staining the gel) and was placed in transfer buffer for 5 min. PVDF membrane was first placed in methanol for a minute and then dipped in transfer buffer (A1.32). The Whatmann No.1filterpaper and pads were cut in 1 cm extra to that of gel size and placed in transfer buffer. Pre-soaked gel was placed on 3-4 wet filter papers then PVDF membrane was placed on gel and another set of 3-4 wet filter papers were placed over the membrane. Air bubbles were removed between the membrane and gel by rolling a glass rod gently over the arrangement without disturbing. Whole arrangement was set in the gel holder and immersed in the western blot tank containing 1X transfer buffer (A1.32) with membrane on the anode side. The whole tank was surrounded with ice to avoid heating of the proteins due to electric current. The tank was covered with the lid and connected it to power pack with 100 V for 1 h. After the blotting run was completed the membrane was removed and placed it in 5% blocking buffer (A1.7) for 30 min at room temperature with gentle shaking. Then primary antibody was added in the blocking buffer for overnight at room temperature with shaking on a rocker. The membrane was washed with TBS-T (A1.31) thrice, 5 min each. Then secondary antibody (goat anti-rabbit ALP IgG) was added in 1:10,000 dilution in blocking buffer, membrane was incubated for 90 min at room temperature. Once again membrane was washed thrice with TBS-T and final wash with 1X TBS with 5 min interval. Substrate buffer (BCIP-NBT, Fermentas) was added and developed until prominent bands were visible in purple color. The reaction was stopped by placing the membrane in milli-Q water, dried and results were analyzed.

2.2.14 Dot Imunobinding assay (DIBA)

The PVDF membrane was pre-soaked in methanol for a min and then placed on wet filter papers. Before the membrane was dried off, 10 µl drops of antigen to be screened was placed as on the membrane by diluting to the required concentrations (virus-1 ng, 10 ng, 25 ng, 100 ng, 250 ng, 500 ng and 1 µg & infected leaf-serial dilution- 1:1,000; 1:10,000; 1:1,00,000; 1:1,50,000; 1:2,00,000; 1:2,50,000 and 1:3,00,00) along with healthy control of same concentrations. As soon as the droplets were absorbed, the membrane is placed in the 5% blocking solution at room temperature for 30 min on rocker. The working concentration of primary antibody (1:5000) specific to the antigen was added in the blocking solution. The membrane was incubated in the solution for overnight on gentle rocking. The membrane was washed thrice with TBS-T for every 5 min interval. Now the membrane was incubated in enzyme linked secondary antibody (goat anti-rabbit - ALP) specific to primary antibody in 1:10,000 dilution at room temperature for 1 h on gentle shaking. The membrane was washed thrice with TBS-T and final wash with 1X TBS. The washing solution was drained off completely and added 5 ml of substrate buffer (BCIP/NBT- Fermentas) and incubated in dark until the purple color reaction was visible clearly.

In case of denatured virus sample detection (fig-2.6), the purified virus in native condition was diluted from 1ng to 5 ng with phosphate buffer pH-7.4. The virus was denatured by heating the sample for 5 min in boiling water bath. The denatured virus sample was also diluted in the same concentrations as that of native virus sample. Now both the test samples were blotted on PVDF membrane by placing 10 µl drops. Remaining process of detection was same as above.

2.3 Results

2.3.1 Single lesion assay

Initially, the field collected sample was inoculated on to several indicator hosts which gave local necrotic lesions on *Phaseolus vulgaris* (French bean) after 3 days of post inoculation (dpi) (fig-2.1) and on *Vigna unguiculata* (Cowpea) after 6 dpi in green house conditions. So, we have selected *P. vulga*ris as the local lesion host for the virus and performed single lesion assay as described in the protocol mentioned under 2.2.1. Assuming that after the six successive passages of the single lesion the obtained virus was homogenous various biological parameters were performed (discussed in the following sections).

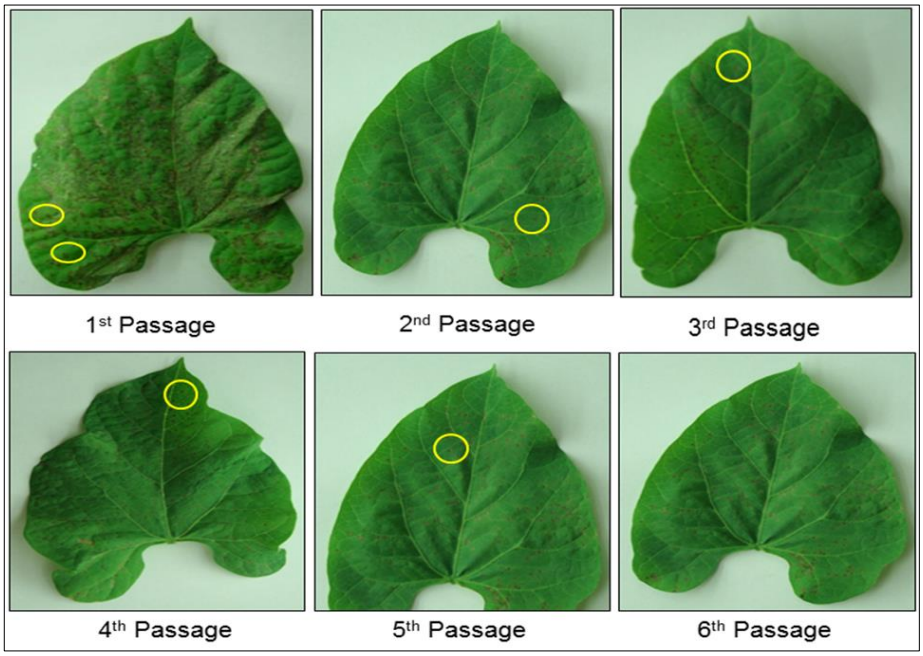

Fig-2.1: Single lesion assay performed on *Phaseolus vulgaris* showing the local necrotic lesions for six generations. Single lesion excised and re-inoculated for the next passage was shown in yellow color circle.

2.3.2 Host range studies

Using the resultant pure virus culture from the single lesion assay as inoculum, extensive host range studies were performed with various herbaceous hosts (tab-2.1). Based on the expression of symptoms the results were analyzed and documented (fig-2.2 and tab-2.1). Local chlorotic lesions were observed in 6-8 days on the inoculated leaves of *Cucurbitaceae* members like *Cucurbita maxima* (fig-2.2E), *C. pepo* (fig-2.2C), *Cucumis lanatus* (fig-2.2D), *C. sativus* (fig-2.2A), *Luffa acutangula* (fig-2.2G), *Momordica charantia* (fig-2.2F). Local necrotic symptoms were observed on *Fabaceae* hosts in 3-5 dpi like *Phaseolus vulgaris* local variety (fig-2.2L), *P. vulgaris* cv.S9 (fig-2.2M), *P. vulgaris* cv.

Plant species	Family	Symptoms	No. of days for symptom appearance
Phaseolus vulgaris (local variety)	Fabaceae	NLL	3
P.vulgaris cv.S9		NLL	4
P.vulgaris cv. Naveen		NLL	4
Dolichos lab lab		NLL	4
D. lab lab cv. puspak		NLL	4
Vigna radiata		NLL	1 (24 hr)
V. unguculata		NLL	5
V. unguculata (cv. C-152)		–	–
Chenopodium quinova	Chenopodiaceae	CLL	3
Chenopodim amaranticolor		CLL	3
Gomphrena globosa	Amarantaceae	NLL	2
Cucurbia maxima	Cucurbitaceae	CLL	5
Citrullus lanatus		CLL	6
Cucumis sativus		CLL	6
Cucurbita moschata		CLL	5
Luffa acutangula		CLL	6
Momordica charantia		CLL	5
Lagenaria siceraria		CLL	5
Nicotiana benthamiana	Solanaceae	chlorotic rings in 5 days and slowly necrotized	local lesions 6 days and systemic infection 10-15 days
N. tabacum (cv. Xanthi)		–	–
N. tabacum (cv. rustica)		–	–
N. bigelovii		–	–
N. plumbaginifolia		–	–
N. megalosiphon		–	–
N. clevelandii		–	–
N. glutinosa		–	–
N. edwarsonii		–	–
N. Samsun		–	–
N.tabacum (cv .Samsun NN)		–	–
N.tabacum (cv. White burley)		–	–
Capsicum annum		–	–
Datura stramonium		–	–
Digitalis purpuria		–	–
Pertunia hybrida		–	–

Tab-2.1: List of hosts tested in the host range study of the new virus. NLL-necrotic local lesion, CLL-chlorotic local lesion, '-' indicates no visual symptoms.

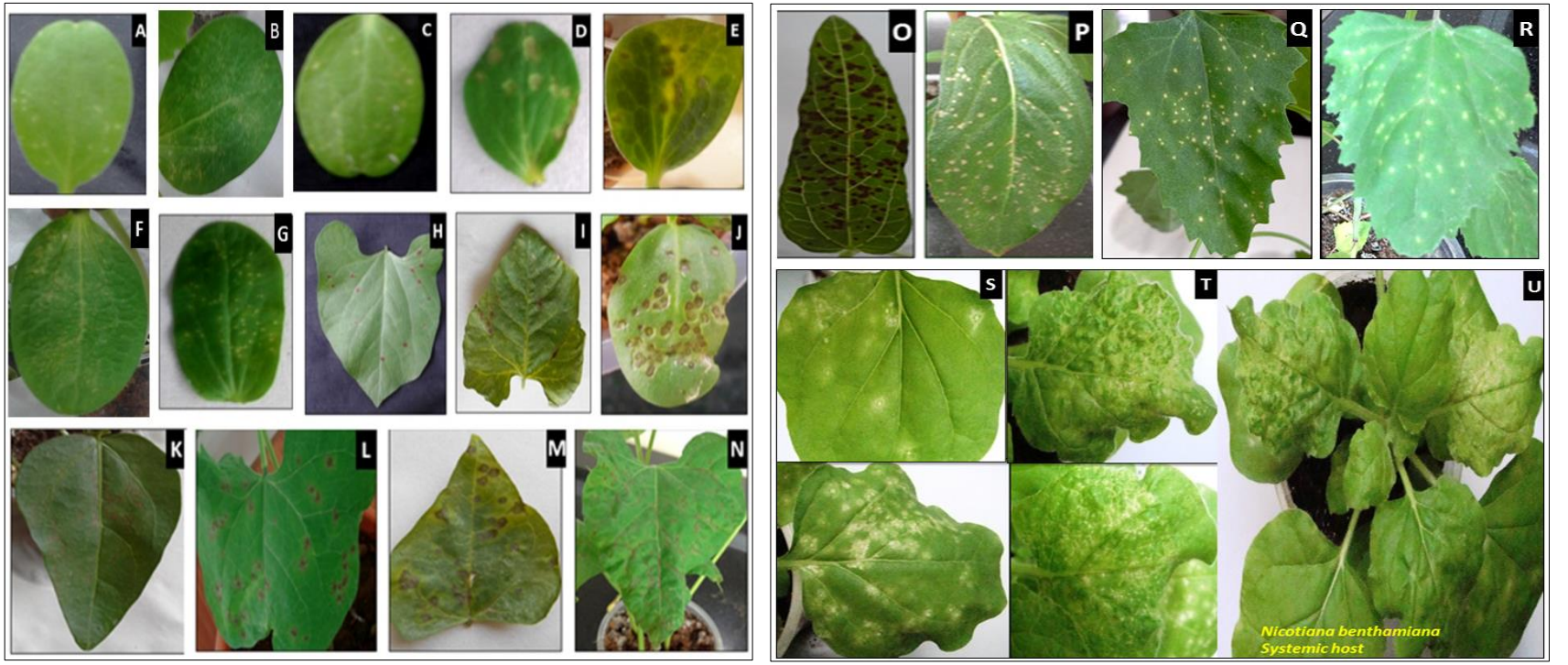

Fig-2.2: Host Range studies of the new virus in different herbaceous hosts (inoculated leaves). A) Local chlorotic lesions on *Cucumis sativas* (5 dpi), B) Local chlorotic lesions on *Lagenaria siceraria* (5 dpi), C) Local chlorotic lesions on *Cucurbita pepo* (5 dpi), D) Local necrotic lesions on *Cucumis lanatus* (6 dpi), E) Local chlorotic lesions on *Cucurbita maxima* (5 dpi), F) Local chlorotic lesions on *Momordica charantia* (5 dpi), G) Local chlorotic lesions on *Luffa acutangula* (6 dpi), H) Local necrotic lesions on *Dolichos lab lab* (3 dpi), I) Local necrotic lesions on *D. lab lab* cv. puspak (3 dpi), J) Local necrotic lesions on *Cyamopsis tetragonoloba* (4 dpi), K) Local necrotic lesions on *Vigna unguiculata* (5 dpi), L) Local necrotic lesions on *Phaseolus vulgaris* local variety (3 dpi), M) Local necrotic lesions on *P. vulgaris* cv. S9 (4 dpi), N) Local necrotic lesions on *P. vulgaris* cv. naveen (4 dpi), O) Local necrotic lesions on *Vigna radiata* (24 hr post inoculation),P) Local necrotic lesions on *Gomphrena globosa* (2 dpi), Q) Local chlorotic lesions on *Chenopodiun quinoa* (4 dpi), R) Local chlorotic lesions on *Chenopodiun amaranticolor* (3 dpi), S) upper panel-chlorotic rings on *N. benthamiana* on inoculated leaves (5-6 dpi), lower panel showing necrotized chlorotic lesions (10 dpi), T) both the panels showing chlorotic lesions and leaf blistering on systemic leaves of *N. benthamiana* (13-14 dpi), U) *N. benthamiana* whole plant showing systemic infection of the virus.

Naveen (fig-2.2N), *Vigna unguiculata* (fig-2.2K), *Vigna radiate* (fig-2.2O), *Cyamopsis tetragonoloba* (fig-2.2J) and *Dolichos lab lab* (fig-2.2H), *D. lab lab* cv. puspak (fig-2.2I). The virus was able to multiple and express the symptoms on *Vigna radiate* within 24 hr of post inoculation. Local chlorotic symptoms were observed on *Chenopodium quinoa* (fig-2.2Q) and *C. amaranticolor* (fig-2.2R) were observed. Chlorotic lesions were slowly turned to necrotic lesions with time. *Gomphrena globosa* belongs to family, *Amaranthaceae* showed large local necrotic lesions on the 2nd dpi (fig-2.2P). In all the observed hosts, the infection was restricted to the inoculated leaves only but the whole plant (systemic infection) was not observed even after one month of post inoculation. In *Nicotiana benthamiana* is the only host that showed systemic infection for the virus under investigation. The virus expressed local chlorotic ring like symptoms in the early stages of infection (7 dpi) in the inoculated leaves (upper panel, fig-2.2S), later slowly turned to necrotic lesions (lower panel, fig-2.2S). In the upper uninoculated leaves leaf puckering/blistering was observed after 10-15 dpi (fig-2.2T, both panels). To our surprise, blistering symptoms were observed in the first two emerging leaves after inoculation and the remaining emerging leaves are symptomless after 30 dpi (fig-2.2U). The presence of virus in the symptomless leaves was confirmed by back inoculating the symptomless leaf sap on to indicator host (data not shown). The local necrotic symptoms were developed within 3 dpi indicating the presence of the virus in the symptomless leaves and also confirmed the systemic infection of the virus (blistering symptoms) by back inoculation (data not shown). No visible symptoms were observed on few of the tested varieties (tab-2.1). For each species 15-20 plants were tested and 100% infectivity rate was observed in case of susceptible species.

2.3.3 Virus purification

The virion particles were initially purified from indicator host, *Phaseolus vulgaris* and systemic host, *N. benthamiana* infected material (100 gm) by differential centrifugation followed by sucrose density gradient through three different procedures mentioned under section 2.2.3 and the virus was observed as single light scattering zone at 20% - 30% interphase (under the monochromatic light Fig-2.3A). Out of the three different methods used for virus purification, more virus yield was obtained in direct ultracentrifugation method (data not shown).

The purified virus was quantified according to Diaz *et al*., (1998) that 1 OD_{260} unit is equal to 5 mg/ ml of virus concentration in the case of Carmoviruses. With 100 gm of leaf material we have obtained 5-10 mg of virus in case of *P. vulgaris* and 10-20 mg for *N. benthamiana*, systemic host. Virus yield was high in systemic infected host (*N. benthamiana*) in all the three methods when compared to the local lesion host, *P. vulgaris* (data not show).

The purity and molecular weight determination of the virion coat protein was analyzed by SDS-PAGE. The coat protein monomer resolved as a bulk band with a molecular weight of approximately 44 kDa (fig-2.3B). No major or minor bands are observed either above or below the 44 kDa protein indicating the highest purity of the virus. The infectivity test for the purified virus was conducted by inoculating the purified virion particles on indicator host. After 3 dpi, local necrotic lesions were developed on the inoculated leaves same as that of the virus infected leaf material (data not shown).

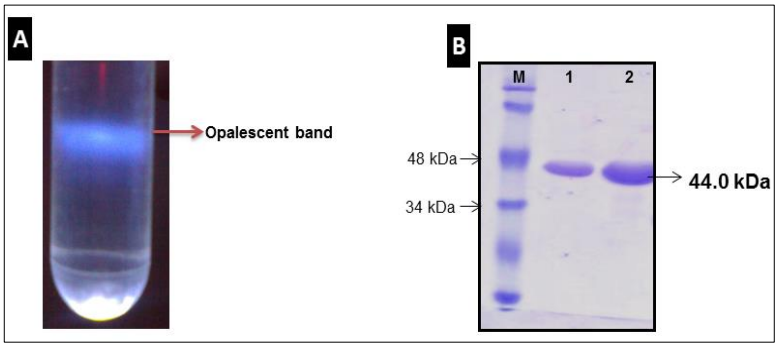

Fig-2.3: Purification of virion particles and purity analysis of the new virus by SDS-PAGE. A) The purified virus showing single light scattering region in linearized sucrose density gradient at 20-30% interphase under monochromatic light in dark room. B) SDS-PAGE analysis of the purified virus showing monomeric coat protein at 44 kDa molecular size. M) Molecular protein marker 1) Purified virus from *P.vulgaris* and 2) *N.benthamiana*.

2.3.4 Electron microscopy

The purified virion particles (2.3.3) were negatively stained with 2% UA and 1% PTA by following the procedure mentioned in section 2.2.5. In both the cases, the virion particles under TEM were appeared as icosahedral morphology with approximately 28 nm in diameter (fig-2.3A, B). The morphology of the virus was uniform all over the grid in case of 2% UA staining (fig-2.3A) but the virion particles aggregated and formed chains like pattern in PTA staining indicating that the virus particles are more stable in 2% UA staining (fig-2.4A) and clumping and aggregates are formed with PTA (fig-2.4B).

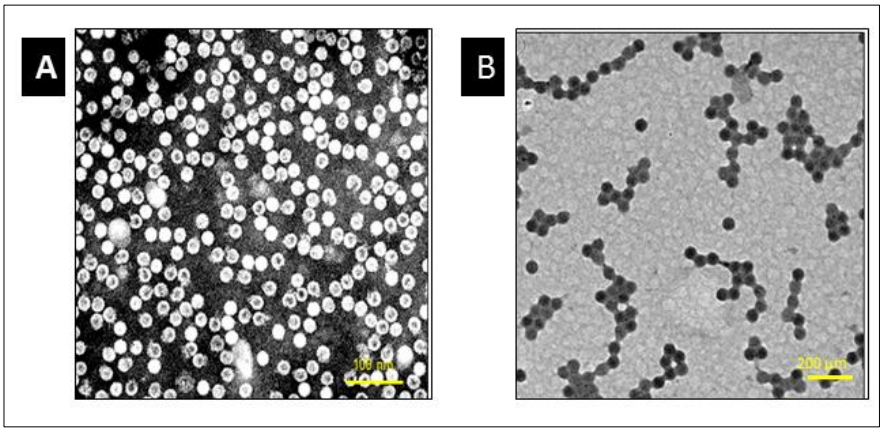

Fig-2.4: Electron microscopic view of purified virus particles negatively stained with A) 2% Uranyl acetate showing spherical particles with 28 nm diameter and B) 1% Phospho tungstic acid showing spherical 28 nm diameter particles. All the virion particles formed clumps with PTA.

2.3.5 Virion nucleic acid isolation and analysis

Viral nucleic acids were isolated from the purified unknown virus (2.3.3), *Sesbania mosaic virus* (SeMV,~4.2 kb; Lokesh *et al.,* 2001) and *Physalis mottle virus* (PhMV,~6.6 kb; Ranjith *et al.,* 1998) was used for the isolation of genetic material (DNA/RNA) by following the protocol mentioned under section 2.2.6. The integrity and molecular size of the extracted nucleic acids were analyzed by 1% agarose gel electrophoresis along with the internal controls. In the test sample, a single nucleic acid band of~4.3 kb size was observed on the agarose gel and was resolved little higher to SeMV RNA and lower to PhMV RNA (fig-2.5A).

Isolated nucleic acids were analyzed by nanodrop ND-100 from NanoDrop technologies. 260/280 ratios of the positive controls (SeMV and PhMV) are 1.82 and 1.85 respectively and it is 1.95 in the case of the unknown virus.

2.3.5 (a) Sensitivity test

The nucleases sensitivity test was carried out for the isolated nucleic acid with DNase and RNase enzymes as mentioned in the methods with the proper controls. The results were analyzed by agarose gel electrophoresis. The nucleic acid band of our unknown virus was not observed in the samples treated with the RNase enzyme when compared with the untreated sample and positive controls (SeMV and PhMV as they are ss RNA viruses) (fig-2.5B) indicating that the genetic material in unknown virus as RNA.

2.3.5 (b) Infectivity test

The infectivity test for the isolated genetic material (RNA) was performed by mechanically inoculating the purified RNA directly on to the carborundum dusted leaves of *Phaseolus vulgaris* and as well as *N. benthamiana*. After 2 dpi, small necrotic local lesions were observed on the inoculated leaves of *Phaseolus vulgaris*, same as that of virus inoculum (fig-2.5C1) and after 5 dpi chlorotic lesions were observed on *N. benthamiana* inoculated leaves (fig-2.5C2). The systemic infection was also observed as wild type virus inoculation. The symptoms were confirmed by performing the back inoculation, virus purification and confirmation of coat protein with SDS-PAGE and later by Dot Immunoblot Assay (DIBA) with raised polyclonal antisera (data not shown).

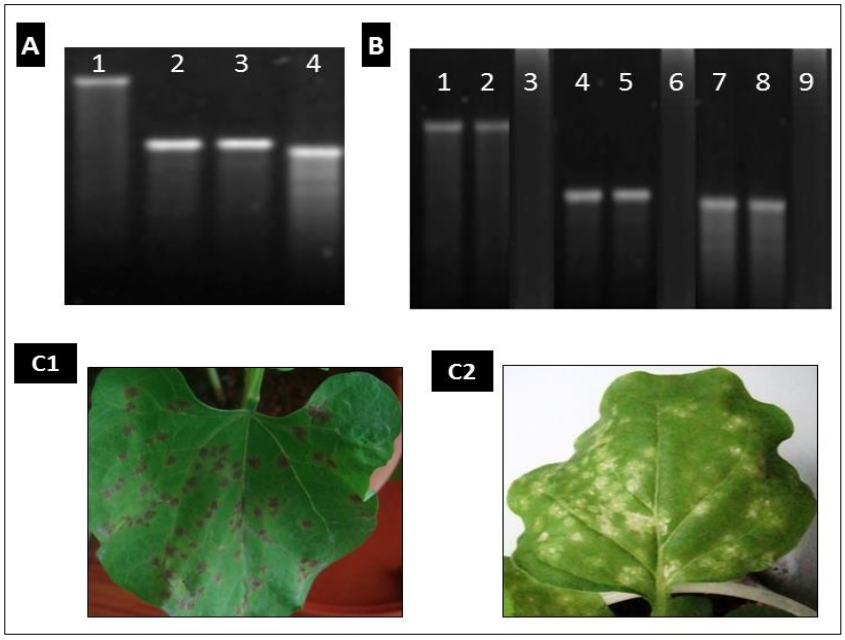

Fig-2.5: Nucleic acid analysis, sensitivity assay and infectivity analysis. A) Agarose gel analysis of the isolated nucleic acids; 1) PhMV-RNA (~ 6.6 kb), 2) Nucleic acid from unknown virus, *P. vulgaris* source; 3) *N. benthamiana* source; 4) SeMV-RNA (~4.2 kb). B) Sensitivity test with nucleases; 1) untreated PhMV-RNA, 2) DNase treated PhMV-RNA, 3) RNase treated PhMV-RNA, 4) untreated unknown viral nucleic acid, 5) DNase treated unknown viral nucleic acid, 6) RNase treated unknown viral nucleic acid, 7) untreated SeMV-RNA, 2) DNase treated SeMV-RNA, 3) RNase treated SeMV-RNA. Infectivity test to the isolated unknown viral RNA; C1) Small local necrotic lesions on *P.vulgaris on* 2 dpi; C2) local chlorotic rings on *N.benthamiana* inoculated leaf on 5 dpi.

2.3.6 Double stranded RNA analysis

Double stranded RNA (dsRNA) was extracted from the virus inoculated leaf material from *P. vulgaris* and *N. benthamiana* according to the protocol mentioned in 2.2.9. The ds RNA profile was resolved as three distinct bands in 1% agarose gel along with the healthy

control. At the moment we presume that the largest band corresponds to the genomic RNA (gRNA) and the smaller bands corresponds to sub-genomic RNA (sg1 & sg2) (fig-2.6) (need to be confirmed by northern analysis at the later part). The genomic DNA in the samples was removed by DNase treatment.

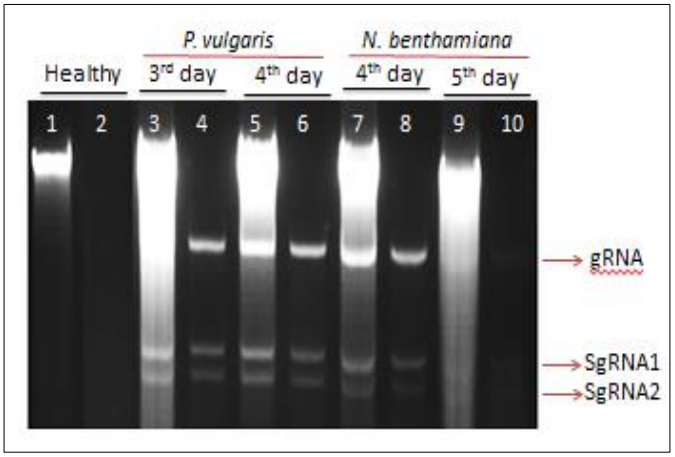

Fig-2.6: dsRNA profiling of the new virus on 1% agarose gel. ds RNA bands are clearly visible on 3 and 4 dpi in case of *P. vulgaris*, local lesion host and on 4 dpi (faintly on 5 dpi sample) in case of *N. benthamiana*, systemic host. Lanes- 1, 3, 5, 7 & 9 are DNase untreated samples, lanes- 2, 4, 6, 8 & 10 are DNase treated samples. Lanes-1, 2: Healthy control; 3-6: samples from *P.vulgaris* and 7-10: samples from *N. benthamiana*.

2.3.7 Serology and serodiagnosis

2.3.7 (a) Polyclonal antibody production

The polyclonal antibodies were raised against the purified virion particles in male New Zealand white rabbit as mentioned in methods section 2.2.11a and cross absorbed as described in 2.2.11c. The produced antisera titer was tested using DAC-ELISA, Dot-blot (DIBA). 1ng concentration of antigen, the antisera could able to react positively upto 1: 1, 60,000 antisera dilution in ELISA (fig-2.7A) (Two fold higher than the buffer controls).

In DIBA at 1:10,000 dilution the purified virus was detected up to 1 ng/µl concentration and in infected leaf sample. No color development was observed in case of healthy antigens (fig-2.7B).

When we performed western analysis with this set of polyclonal antisera, we found that the antiserum was not able to detect the denatured coat protein antigen in western analysis (data not shown). This was also confirmed by DIBA with native antigen and as well as the denatured antigen simultaneously where we have positive signals in the case of native virion particles and not with the denatured virion particles (fig-2.7C).

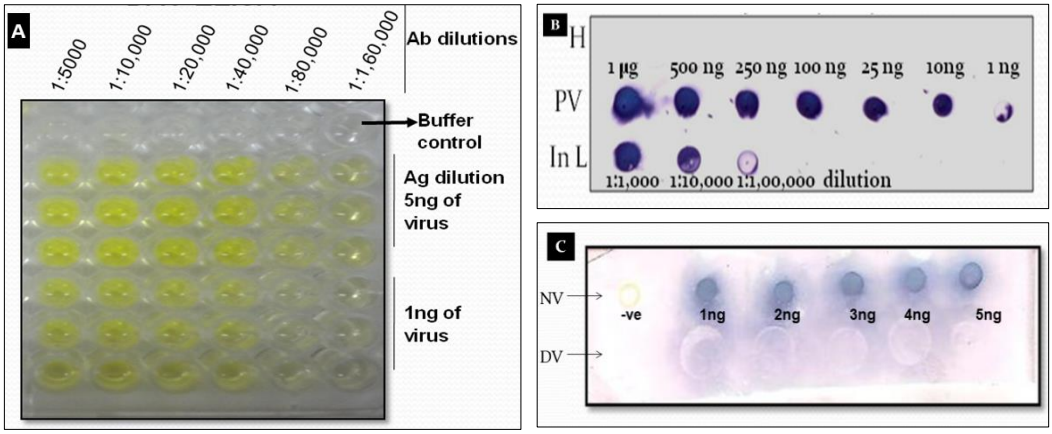

Fig-2.7: Assessment of the raised polyclonal antisera titer. A) DAC-ELISA with antiserum against native virion particles, B) Dot immune-binding assay (DIBA) with antiserum against native virion particles; PV- purified virus, H-Healthy control, In L- Virus infected leaf sample, used concentrations of antigen are mentioned in the diagram, C) DIBA with antiserum against native virion particles, NV- pure virus (native virus), DV- denatured virion particles. –ve –negative control (buffer), 1ng-5ng different concentrations of antigen in both native form and denatured form.

To overcome this obstacle, we have raised another set of polyclonal antibodies against the denatured antigen to use as mentioned in methods section 2.2.14. Unlike the polyclonal antibodies raised against the native virion, this set of polyclonal antibodies readily detected the denatured coat protein in the western blotting (fig.2.8B).

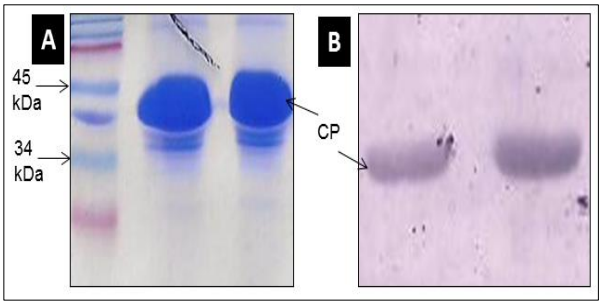

Fig-2.8: Serodiagnosis of the polyclonal antisera raised against denatured virion particles. A) SDS-PAGE for the purified virus particles, B) Western analysis for confirmation of denatured CP.

2.3.7 (b) Serodiagnosis of the unknown virus with heterologous antisera

ELISA and DIBA techniques were used to screen large number of samples. The purified virus was tested with antisera procured from different research groups to confirm the identity of the virus. The purified virus was diluted to 3 ng/µl concentration and used as antigen source for the experiment. The procured antisera against different viruses *Tobacco*

ring spot virus (TRSV), *Tobacco bushy stunt virus* (TBSV), *Tomato streak virus* (TSV), *Peanut bud necrosis virus* (PBNV), *Peanut seed-borne mosaic virus* (PsbMV), *Peanut clump virus* (PCV), *Peanut green mottle virus* (PGMV), *Pigeon pea sterility mosaic virus* (PPSMV), Tospovirus and potyvirus (generous gift by Prof. Sreenivasulu, SVU, Tirupati), CMV and SeMV (generous gift by Prof. Savitri, IISC, Benguluru), *Melon necrotic spot virus* (MNSV-generous gift by Takehiro Ohki, Japan) were tested in ELISA and DIBA (data not shown) and western analysis.

In western analysis the purified virus particles reacted with heterologous antiserum procured to Carmoviruses and in particular to MNSV indicating its relation (fig-2.9A). Homologous reaction of the virus with raised antisera against denatured virion was performed as a control (fig-2.9B). No positive results were observed in any of the other tested antisera (data not shown).

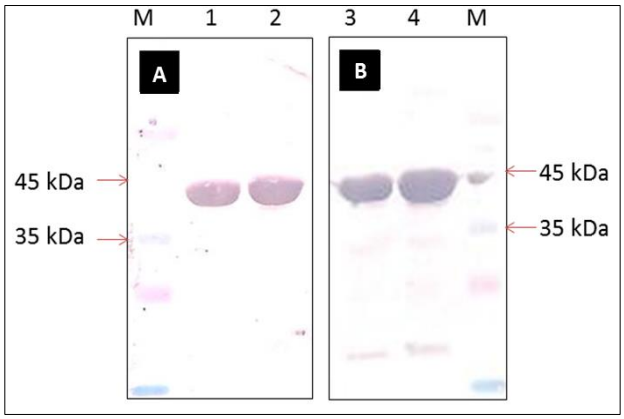

Fig-2.9: Western analysis of the unknown virus CP with the A) heterologous antisera from Japan against MNSV; B) homologous polyclonal antisera against the unknown virus. M-pre-stained protein marker from Fermentas, Marker sizes are denoted in the figure; 1, 2, 3, 4- Purified virus sample from sucrose gradient in two different concentrations (2 µl & 5 µl of 5 µg of purified virus).

2.3.8 Seed Transmission test

Seed transmission tests were performed in the laboratory in two different ways with the available techniques in the laboratory as mentioned under 3.2.10. In the first method, seeds from *N. benthamiana* plants with viral symptoms were tested through DAC-ELISA with virus as positive control where we haven't observed any positive result (data not shown). In second method also neither viral symptoms were observed nor was the virus

detected in ELISA from the plants raised from the seeds collected from virus infected plants (data not shown) indicating that the new virus we are working is not seed transmittable.

2.4 Discussion

Based on the symptomology, similarities in the host range, physical properties, particle characteristics and serological relationship parameters, the unknown virus was identified as *Melon necrotic spot virus* (MNSV) that belongs to the genus Carmovirus which comes under family Tombusviridae. From here after in the whole thesis the unknown virus was designated as MNSV-Hyd.

Habitually, plants are infected with more than a single virus in the field conditions as several viruses are transmitted by arthropod vectors. So, we used single lesion assay for the elimination of mixed infections in the laboratory by mechanically inoculating the single lesion and passing successively to obtain pure virus culture. Local lesion host for the virus was identified as *P. vulgaris* in the present study and the virus was maintained on the local host in pure form.

Host range is not an accurate technique for the identification of the virus and its interpretation should be attended with more care (Hamilton *et al*., 1981; Horvath, 1993; Naidu and Hughes, 2003). Since ours is a newly established laboratory, we need to have a model virus to work on which can replicate in *N. benthamiana* host for functional genomics. It is our model host in the laboratory as the genome sequence was known; most widely accepted experimental host in plant pathology and it is highly susceptible for all plant pathogens and (Goodin *et al*., 2008).

We have conducted host range for MNSV-Hyd in the laboratory in the present work for the identification of the susceptible hosts and for the virus diagnosis. Host range study of the new virus revealed that out of the 17 plant species tested 11 species were susceptible (tab-2.1). It has a limited host range infecting Cucurbitaceae, Fabaceae, Amaranthaceae and Chenopodiaceae members with local lesions and a systemic host *N. benthamiana*, Solanaceae member. The virus was able to replicate and express the symptoms within 24 hr of post inoculation in *V. radiata,* which can be used as diagnostic host for the virus. The virus replicates in *V. unguiculata*, local cultivar but not in *V. unguiculata* cv. C-152.

Minor differences between strains can lead to lot of difference in the symptom expression even some isolates have similar symptoms. For ex: ‘yellow type’ symptoms are

caused by different viruses and by mycoplasmas as well. MNSV-Hyd was distinct from the other reported MNSV strains in host range context. The previously reported MNSV strains have narrow host range confining themselves to Cucurbitaceae members (Ohki *et al*., 2008; Choi *et al*., 2003; Avgelis, 1985) but MNSV-Hyd is unique in infecting non-cucurbits, mostly Fabaceace members, Amarantahceae and a Solanaceae member, *N. benthamiana* (Diaz *et al*., 2004). The susceptibility of MNSV-Cretan isolate to *G. globosa* was reported earlier (Avgelis, 1985) however later MNSV-264 was also included in this (Diaz *et al*., 2004). Though systemic infection is only observed in *Cucumis melo* species in most of the reported MNSV strains (Ohki *et al*., 2008; Choi *et al*., 2003), MNSV-264 and MNSV-N are infecting *N. benthamiana* which might be due to difference in the genotype (Choi *et al*., 2003, Diaz *et al*., 2004; Miras et al., 2014) (discussed in chapter-3). MNSV-Hyd is unable to systemically infect *Cucumis melo* and *Citrullus lanatus* experimentally which is same as observed in case of W-isolate from Japan but both of these are efficiently replicating in *Lagenaria siceraria* (Ohki *et al*., 2008).

The Fabaceae members were not recognized as the hosts for any of the reported MNSV strains (Ohki et al., 2008; Choi *et al*., 2003; Avgelis, 1989). Based on the Fabaceous host range of MNSV-Hyd was identified as distinct from all the identified MNSV strains/isolates, further demonstrating the uniqueness of MNSV-Hyd. This is reliable to Gibb's theory in Tobamoviruses that individual viruses are adapted to specific families for their survival (Gibbs, 1999).

As demonstrated by Kido *et al*., (2008b) that higher temperatures restrict the expression of systemic symptoms in MNSV infected hosts, systemic symptoms of MNSV-Hyd in *N. benthamiana* were also observed at 22-24°C (controlled conditions) but not at higher temperatures (glass house/green-house conditions) (Need to be confirmed in protoplast experiments).

Working with the purified virus to obey the Koch's postulates is also important step in the plant virology. Towards this, we have purified the virus from the indicator host and systemic host by differential centrifugation followed by sucrose density gradient ultra-centrifugation. The quality analysis was performed by SDS-PAGE analysis whose molecular size was determined as~44 kDa which is higher than the reported MNSV strains (Choi *et al*., 2003; Diaz *et al*., 2003; Genoves *et al*., 2006).

Morphology of MNSV-Hyd was icosahedral as that of reported strains; the diameter was less (28 nm) in comparison to that of the reported strains (30 nm) diameter (Kishi, 1966; Gonazalez-Garza *et al*., 1979; Diaz *et al*., 2003, 2004; Kido *et al*., 2008a).

Based on the infectivity assay of the nucleic acid molecules of MNSV-Hyd was confirmed as monopartite positive sense, single stranded RNA genome which is~4.3 kb long same as the other reported MNSV isolates (Riviere and Rochon, 1990; Diaz *et al*., 2003, 2004; Genoves *et al*., 2006).

Double stranded RNA (ds RNA) profiling is one of the diagnostic tools for characterization of the unknown virus. The double stranded RNAs are formed as replicative forms or as replicative intermediates as a result of viral genome replication process. ds RNA profile of our virus is same as that of the reported MNSV strains with one genomic and two sub-genomic RNA molecules there are above posts that there are more than subgenomic dsRNAs reported in other strains (Choi *et al*., 2003; Ohki *et al*., 2008) and only the genomic RNA was encapsulated into the virion particle.

Literature pertaining to MNSV showed that MNSV is not seed transmissible as has been reported by us. It is mainly transmitted by fungus *Olphidium bornovanus* (Campbell, *et al*., 1996; Ohki *et al*., 2010).

The purified virion particles are good immunogens where we can produce high titer antisera. Viruses in the family Tombusviridae are distinct and are not detected by the other members in the genus (Gonzalez-Garza, 1979; Morris, 2001). The higher titer of the antisera was produced in the rabbit against the native virion particles of MNSV-Hyd. It was reported that the antisera produced against the native antigen will not detect the denatured antigen (Ohki *et al*., 2010) and the same was observed in case of the MNSV-Hyd (fig-2.7C). Presumed degradation of the coat protein of the virus was also observed when loaded on to the SDS-PAGE and smaller fragments were also confirmed by western analysis (fig-2.9B) (Robertson, 2004).

No positive reaction was observed for MNSV-Hyd when tested with different groups of heterologous antisera. Serodiagnosis has given us leads (fig-2.9B) that the new virus is related to MNSV as our antigen reacted strongly with MNSV antibodies procured for a Japanese strain.

Finally, to conclude this chapter that the determined properties of the causal agent satisfies the described properties of the Tombusviridae. All the discussed properties are

more closely related to genus, Carmovirus among the eight genera in the family (Van Regenmortel *et al*., 2000) and however serodiagnosis demonstrated it as MNSV from Carmovirus genus. Based on these criteria the causal agent was assumed to be a new member of Carmovirus and distantly related to MNSV and it was further confirmed by molecular parameters in the next chapter.

CHAPTER-3

Molecular characterization of the new virus through whole genome sequencing by reverse genetic approaches and diversity analysis

3.1 Introduction

More than one third of the virus genera consist of positive sense RNA viruses and they cause various diseases in plants and animals with high rate of variability (Malpica *et al*., 2002). Tombusviruses are one of the notable groups that cause various diseases in plants. Viruses also contain the same coding sense as the host mRNAs and function directly as templates for the viral protein translation. RNA viruses are more diverse because of their error-prone genome replication that change frequently and short generation times. The diversity of the plant viruses was marked from 1920s (Burdon, 1987) but it was over looked due to several reasons. It came in to light from past 10-15 years with the advancement of the molecular techniques to analyze the variability by sequencing the genome. Even though the RNA viruses recombine and produce the potential variants, genetic conservation is a rule, that virus genes are not more variable than their hosts and common conserved genes of a virus family are stable without variation. The diversity of the isolate can be determined through the phylogenetic or taxonomic levels (Garcia-Arenal *et al*., 2001).

These variants were first observed in the typical systemic infected plants (Mc Kinney, 1935). Because of this variation, the virus can change the host which is known as host adaptation. Mutation rate during the replication of RNA viruses is increasing in several magnitudes which results in the quasispecies (Hull, 2014). These mutants are genetically and phenotypically vary based on the biological factors. These RNA viruses have capacity to produce more variants that differ in genome size, sequence and biological activity. The nutrient depletion in the environment is also a major cause of mutants with revised biological characters (Domingo, 1997) and they affect the natural host range of the strain (Rua *et al*., 2011).

A single nucleotide change in the "cachexia expression motif" of *Hop stunt viroid* (HSVd) modulates cachexia symptoms in citrus trees was reported by Serra *et al*., (2008). A

single nucleotide change i.e. Adenine to Guanine at 627th position of the HC-Pro cistron of the *Potato virus Y* leads to the loss of vein necrosis phenotype in tobacco (Hu *et al*., 2009). The difference in the strains can be identified only by molecular characterization. However, the levels of variation depend on the virus-host interaction (Rua *et al*., 2011). Hence, the most reliable techniques are employed in the process of molecular characterization of the virus and its variants. The determination of the complete nucleotide sequence of the virus is an important step to study host-pathogen interactions for the study of its biology, functional analysis and helps in the mutational studies as well as to use it as a viral vector. The complete nucleotide determination of a virus is the important step for construction of full length infectious clones. Different steps involved in the sequence determination are a) RNA isolation, b) primer designing, c) first strand complementary DNA (cDNA) synthesis, d) PCR amplification, e) cloning techniques, f) sequencing the clones and comparison using NCBI-BLAST search tools and g) knowing the variants of virus based on the multiple sequence alignment (MSA) and by phylogenetic tree comparisons.

RNA isolation is the first step in molecular characterization of the virus. The viral nucleic acid is to be purified from the virus which is used for the determination of the sequence by reverse genetics approaches.

A primer is a single stranded oligonucleotide of 15-30 bases in length, complementary to template strand and is initiative for the DNA replication process. The sense (positive) primer is same as that of the template strand and anti-sense (negative) primer is anti-complementary to the template strand. So, both the primers will bind to the template in different directions and helps in the amplification of the desired gene/ fragment.

Important step in the reverse genetics approach is the conversion of RNA genome to a cDNA molecule. Reverse transcriptase (RTase) is an enzyme that transcribes cDNA using RNA template. Reverse genetics revolutionized with the discovery of RTase enzyme. It was first discovered by Howard Temin and independently isolated by David Baltimore in 1970. This enzyme transcribes the RNA template to complementary DNA (cDNA) and the removal of the RNA strand with intrinsic RNase-H activity was performed.

Polymerase chain reaction (PCR) was first developed by Kary Mullis in 1983 and was awarded noble prize in 1993 in chemistry. PCR is used to amplify the gene of interest in several folds of magnitude, generating millions of copies of particular DNA sequence. Now-a-days it is an indispensable molecular technique used in biology and medical research

applications like DNA cloning, DNA finger printing, DNA based phylogeny, detection and diagnosis of infectious and hereditary diseases. This depends on the thermal cycling conditions consisting of repeated heating and cooling steps.

Gel extraction is the process to purify the desired PCR fragment from 1% agarose gel, which will be devoid of agarose and non-specific PCR products.

The process of covalent linking of two/more desired PCR fragments using the modifying enzyme, DNA ligase is known as ligation.

Transformation is the process of genetic alteration of the cell resulting from direct uptake and incorporation of exogenous genetic material from its surroundings and taken up through the cell membrane. It was first demonstrated by Frederick Griffith (1928).

Plasmids are the extra chromosomal, circular DNA molecules that are able to replicate independent of chromosomal DNA. Plasmids were isolated from the transformed colonies and the positive plasmids for the desired gene of interest were confirmed by restriction analysis and sequenced.

National center for biotechnology information (NCBI) is a center where all the available nucleotide sequences are deposited in a common data base. Using this online database one can easily find the similarity of the desired gene with other available variants. The similarity will be at nucleotide as well as at protein level where the domains are easily identified.

Phylogenetic trees are the branching tree diagrams that deduce the evolutionary relationship among the biological species which are identified through molecular sequencing data and morphological data matrices. The taxa joined at the node in a tree are descended from common ancestor. These trees are helpful to assign the virus to particular group and to identify the new strain based on the values in the branches of a tree.

Once we are successful in identifying the field collected viral sample as MNSV-Hyd, we decided to develop this virus as a model virus in the laboratory. Towards this, first step is the determination of complete genome sequence of MNSV-Hyd using reverse genetic approaches and molecular techniques. The deduced sequence was used in the analysis of relationship of the particular virus with the other reported strains of MNSV by constructing phylogenetic trees using MEGA version-6 software.

3.2 Methods

3.2.1 Primer designing

In order to obtain the complete genome sequence of biologically characterized MNSV-Hyd (chapter-2) different primer sets were designed. All the primers are designed manually using the bioedit version 5.0 comparison data and synthesized from IDT oligos synthesis (Hall, 1999). Using Bioedit sequence aligner software all the type members of *Tombusviridae* family were aligned and degenerate primers were designed in most conserved regions of the family members (tab-3.1). Second set of specific primers were designed taking MNSV-A1 (accession number DQ339157) strain as template (tab-3.2). Two sets of degenerate primers were designed in the CP region of the MNSV. Apart from these two sets, specific primers were designed in the sequenced regions that were used in the 5' race and 3' race techniques in the sections 3.2.11 and 3.2.12 (tab-3.3).

3.2.2 First strand cDNA synthesis

The first strand cDNA was synthesized taking phenol chloroform purified RNA as template using EPICENTRE BIOTECHNOLOGIES kit by following the manufacturer's instructions. Briefly, 1 µg of RNA was mixed with 1 µl (100 ng/µl) of antisense specific primer and made up the volume to 10 µl with sterile milliQ water. The mixture was incubated at 65˚C for 5 min and then cooled down to room temperature slowly. Then, 2 µl of 10X RT buffer, 2 µl of 10 mM deoxynucleotides (dNTPs, Fermentas), 2 µl of 0.1 M DTT (Fermentas), 1 µl of RTase enzyme were added and the constituents in the tube were mixed properly. Reverse transcription reaction was carried out at 42˚C for 90 min and the synthesized cDNA was stored at -20˚C for future use.

3.2.3 Polymerase chain reaction (PCR) and agarose gel electrophoresis

Polymerase chain reaction is a technique used to amplify small target DNA molecules in many folds with two oligonucleotide primers that hybridize to template strand in opposite direction. The location of the primers in the template determines the length of the amplicon. The desired fragment was amplified with the specific sets of primers in combinations and appropriate cycling conditions with DNA polymerases (Pfu, Taq or Vent). The different steps in PCR amplification are: a) denaturation b) annealing and c) extension. The extended product in one cycle serves as template for the next cycle.

PCR was performed according to Sambrook *et al*., (2001) to amplify the target gene in 50 µl reaction. In 50 µl, 1 µl of template (cDNA/diluted plasmid) was mixed with 5 µl of 10X PCR buffer, 2 µl of 5 mM dNTP's (individual nucleotide sets from fermentas), 1 µl of 25 mM $MgCl_2$, 0.5 U of polymerase enzyme (Taq, fermentas), 2 µl of 10 mM forward and reverse primers. PCR reaction was performed in Eppendorf Thermal cycler and cycling conditions will vary based on the melting temperature (Tm) of the primers. The amplified product was analyzed by agarose gel electrophoresis.

It was performed as described in Sambrook *et al*., (2001). Briefly, 1% agarose solution was prepared in 1X TAE (A1.29) and poured in the gel casting unit with appropriate combs. After 30 min, the solidified agarose gel was placed in the tank containing 1X TAE buffer. The DNA samples were mixed with 6X loading dye (A1.13) which gives density to the samples to the final concentration of 1X and loaded in to the wells. The molecular size of the desired fragment can be determined with the commercially available 1kb ladder from Thermo Scientifics. Electrophoresis was performed at 120 V for 30 min and the samples were visualized under UV-trans-illuminator and photographed in the gel documentation unit.

3.2.4 Gel extraction

Gel extraction is the process of extracting the desired DNA fragment intact followed by the agarose gel electrophoresis. Gel purification kits (Qiagen) were used for extraction of desired DNA fragments from the agarose gel by following the manufacturer's instructions. Desired PCR amplified products or DNA fragments were excised from the agarose gel using sterile scalpel, and weighed in the microfuge tube. Gel solubilizing buffer was added to the tube having gel piece in 1:3 (w/v) ratio and incubated at 70˚C until the gel piece was solubilized completely. The solubilized mixture was passed through the column by centrifuging at 3,000 rpm for 1 min at room temperature. The flow through collected in the collection tube was passed through the column once again at 3000 rpm for 1 min and then the flow through was discarded. This step was repeated until whole gel mixture was passed through the column. Wash buffer of 750 µl was added to the column and centrifuged at 10,000 rpm for 1 min. The flow through was discarded and the column was dried by subjecting the empty column to centrifugation at 13,000 rpm for 2 min. DNA was eluted by transferring the dried column to sterile 1.5 ml microfuge tube; 30 µl of pre-heated elution

buffer was added, incubated at room temperature for 5 min then centrifuged at 13,000 rpm for 2 min. The eluted DNA was agarose gel analyzed and further used in ligation.

3.2.5 Ligation reaction

The purified PCR product from 3.2.4 was used for ligation into T/A cloning vectors. pGEMT-Easy vector from Promega or pTZ57R/T T/A vector from Fermentas were used for T/A cloning process in this study by following the manufacturer's specifications. Most of the ligation reactions were performed in 10 µl or 15 µl reaction based on the insert concentration. In most of the cases, ligation reaction was performed with 10X buffer (fermentas) /2X buffer (promega) at 4˚C for overnight in insert vector ratio of 3:1. Sometimes ligation mixture was incubated at 16˚C for 5-6 h or at 22˚C for 4 h. In case of most difficult ligations (three point ligations) were performed with few changes, reactions were incubated at room temperature for an hour and then incubated at 4˚C for overnight.

3.2.6 (a) Preparation of chemical competent cells (DH5α cells)

Laboratory glycerol stock of DH5α cells of *E.coli* strain was streaked on plain LB plate (without antibiotic) for the single isolated colonies. A single isolated colony was inoculated in LB broth without antibiotic and incubated for overnight at 37˚C. The overnight grown culture was used to inoculate 500 ml of LB broth without antibiotic and allowed to grow at 37˚C for 3-4 h until the OD reaches 0.5-0.6 at 600 nm (readings were taken for every 30 min after 2 h of incubation). After reaching required OD, the culture was incubated on ice for 1h and the cells were harvested by centrifugation at 4,000 rpm for 20 min at 4˚C. Supernatant was discarded carefully and the pellet was resuspended in 10 ml of buffer-A (A1.5) solution and made up to 200 ml finally, and incubated on ice for 1 h by mixing intermittently. Again the culture was harvested by subjecting it to centrifugation at 3,700 rpm for 20 min. Supernatant was discarded and the final drops were removed by inverting the centrifugation tube for 2 min on towel of tissue papers. The pellet was re-suspended in appropriate volume (5 ml) of buffer-B (A1.6) and 100 µl of culture were aliquoted in sterile 1.5 ml microfuge tubes, and stored at -80˚C freezer for further use.

3.2.6 (b) Competency checking

To check the competency of the prepared competent cells, known concentration of

plasmid DNA was transformed (mentioned under section 3.2.8) into one tube of the freshly prepared competent cells (100 µl) (3.2.7a). The efficiency of the cells (i.e., total number of viable cells in a given tube) can be calculated by the following formula

$$\text{Transformation efficiency (Or) Transformants/µg of DNA} = \frac{\text{Number of colonies on plate}}{\text{ng of DNA plated}}$$

The competence of the cells should range from $1x10^8$- 10^{11} in order to get the best results in case of *E.coli* strains.

3.2.7 Transformation

Transformation is the process of insertion of exogenous genetic material from the surroundings through cell membrane in to the cell. Generally heat shock method of transformation was carried out to introduce the gene of interest ligated in vector into bacterial cell. It was performed according to the protocol described by Sambrook *et al*., (2001). Stored chemical competent cells were removed from -80˚C and thawed them on ice. The ligated mixture (3.2.6) was added into 100 µl of thawed chemical competent cells; the tube was gently tapped with index finger and incubated on ice for 20 min. After heat shock treatment was given at 42˚C for 90 sec, immediately the tube was returned on to ice. After 5 min, 900 µl of plain LB broth was added to the tube and incubated at 37˚C with shaking for 1 h. The transformed culture was centrifuged at 8000 rpm for 2 min. The resulting pellet was suspended in 100 µl of LB broth and plated on LB plate containing appropriate antibiotic [For blue-white selection, prior to plating of bacterial cells 0.016 mg/ml of X-gal (Himedia) and 0.16 mg/ml of IPTG (Himedia) was spread on LB ampicillin plates]. The plates were incubated at 37˚C for 12-16 h in an inverted position.

3.2.8 Plasmid isolation

Single colony from freshly transformed plate was inoculated in 5 ml of LB medium containing appropriate antibiotic and incubated at 37˚C for overnight with vigorous shaking (180 rpm). The bacterial cells were harvested in microfuge tube at 10,000 rpm for 1 min at 4˚C. The supernatant was drained completely and 200 µl of re-suspension buffer (P1; A1.17) containing 100 µg/ml of RNase was added to the pellet and re-suspended it by vortexing the tube. To the re-suspended culture, 250 µl of lysis buffer (P2; A1.18) was

added and mixed thoroughly by inverting the tubes 3-4 times. The cell lysis was allowed to complete by incubating the tubes at room temperature for 5 min. To the lysate, 300 µl of neutralization buffer (P3; A1.19) was added, mixed by inverting the tubes several times and incubated at 37˚C for 1 hr. The tubes were centrifuged at 13,000 rpm for 10 min at 4˚C. Pelleted bacterial lysate was removed using sterilized tooth pick and to the supernatant equal volume of isopropanol was added. The contents of the tube were mixed properly and nucleic acid was precipitated and concentrated by centrifugation at 13,000 rpm for 15 min at 4˚C. Supernatant was discarded and 1 ml of 70% alcohol was added to the pellet, mixed well and centrifuged at 13,000 rpm for 10 min. The pellet was air dried by inverting the tubes on a towel of sterile tissue papers for 15 min. The pellet was dissolved in 50 µl of 10 mM tris pH 7.0 and 2 µl of plasmid was checked by agarose gel electrophoresis (3.2.3).

3.2.9 Restriction digestion analysis

Restriction enzymes are the endonucleases that recognize specific sequence on double stranded DNA molecules (palindromic sequences), cut the DNA and generate sticky ends or blunt ends. The isolated plasmids were confirmed by digesting the samples with restriction enzymes or by PCR amplification with specific sets of primers. 5-10 µg of isolated plasmid DNA was mixed with 1 U of restriction enzyme and respective 10X buffer to 1X concentration and incubated at 37˚C or optimum temperature of respective enzyme for 2 h. Double digestion was also performed to release the insert with selective restriction enzymes on either side of the insert. In this case, the digestion was carried out in the compatible buffer for both the enzymes. The restriction pattern of the clones was analyzed by agarose gel electrophoresis (3.2.3).

3.2.10 5' RACE (Rapid amplification of cDNA ends)

Specific reverse primers (tab-3.3; 1 and 2 primers) were designed in the sequenced region of MNSV-Hyd are used to determine the 5' authentic end nucleotide of the viral genome. The isolated RNA from the section 3.3.4 was used as template and primer M1043- was used for the first strand cDNA synthesis (Epicenter Biotechnologies) following the manufacturer instructions as mentioned under section 3.2.2. The synthesized cDNA was purified using PCR cleanup kit from Nucleospin by following the manufacturer's protocol. The purified cDNA was used as template for polyadenylation with dATP at 3' end with the

enzyme terminal deoxynucleotidyl transferase (TdT) (Fermentas) by following the manufacturer's specifications. The enzyme, TdT is a DNA polymerase that catalyzes the addition of nucleotides to the 3' terminus of DNA molecule independent of the template. Nested PCR was performed with the two different specific primers designed in the sequenced region. In the first round of PCR, specific primer M1043- & OliodT primer (tab-3.3) that can bind in the polyadenylated region of the cDNA, which was used as template for PCR amplification with Taq polymerase. Approximately, 1 kb fragment was amplified with the following PCR cycling conditions: 95˚C for 5 min of one cycle, 95˚C for 50 sec, 55˚C for 1 min & 72˚C for 1 min (30 cycles from the step-2) and one cycle of final extension at 72˚C for 10 min. The PCR product was agarose gel analyzed and purified from the gel using the PCR cleanup kit from Nucleospin by following the manufacturer's protocol. The purified PCR product resulted from the first PCR was used as a template to perform the second round of PCR with the specific primer (tab-3.3, 2nd primer). PCR conditions used for the amplification were denaturation step at 95˚C for 5 min, 30 cycles of (95˚C for 5 min, 60˚C for 1 min and 72˚C for 0.8 min) and one cycle at 72˚C for 10 min the amplified PCR product was agarose gel analyzed.

3.2.11 3' RACE

The viral RNA isolated in the section 2.3.4 was used for the determination of authentic nucleotides at 3' end of the viral genome. The RNA was polyadenylated with poly (A) polymerase tailing kit from Epicenter biotechnologies by following the manufacturer's specification. Briefly, 2 µg of RNA was used as a template for polyadenylation and the RNA was mixed with 2 µl of 10X Poly (A) polymerase buffer, 4 µl of 10 mM ATP, 2 µl of RNase inhibitor, 1µl of Poly (A) polymerase enzyme. The reaction contents were mixed and incubated at 37˚C for 1 h. The polyadenylated RNA was used as template to perform cDNA synthesis with OligodT primer by following the protocol mentioned in section 3.2.2. First round of PCR was performed with *Taq* polymerase with specific primers 8 and 9 from tab-3.3 under PCR conditions as follows: 95˚C for 5 min for one cycle; followed by 30 cycles of 95˚C-50 sec, 47˚C-1 min, 72˚C-2 min; ending with the final extension as 72˚C for 10 min. Second round of PCR was performed under the above cycling conditions with specific primer 7 and 9 from tab-3.3. Agarose gel electrophoresis was performed to analyze the PCR products.

3.2.12 Sequencing

The confirmed positive clones after restriction digestion and PCR amplification were sent for sequencing to Ocimum Biosolutions and Biosquare biotechnologies private limited, Hyderabad. The obtained sequencing results were in FASTA format was directly subjected for the nucleotide blast (blastn) and protein blast (blastp) search in NCBI database (http://www.ncbi.nlm.nih.gov). The sequences were aligned and compared for nucleotide changes with Bioedit sequence alignment editor software (Hall, 1999). Minimum of 5 individual clones were sequenced on both the strands for all the fragments and 10 individual clones were sequenced in case of 3' RACE and 5' RACE techniques.

3.2.13 Construction of phylogenetic trees

Phylogenetic trees are used to find the correlation of the complete viral sequence with other available strains of a particular virus, with the genus members and as well as with the family members. The sequences were assembled and analyzed with the aid of Molecular Evolutionary Genetic Analysis version 6.0 (MEGA6). Sequence similarity searches were performed using NCBI-BLAST (http://www.ncbi.nlm.nih.gov). The sequences were aligned using clustal W/muscle program that was inbuilt in MEGA6 software. The aligned sequences were subjected for the phylogenetic trees construction. All the parameters are left for the default settings. Phylogenetic trees were constructed with full optimum alignment and neighbor joining method options with 1000 bootstrap replications. Output appeared in the form of tree was saved in PDF format. *Sesbania mosaic virus* (SeMV) from Sobamovirus group was chosen as out member for the analysis. The bootstrap values of the branches represent the number of times the sequence appeared while constructing the phylogenetic tree. This analysis was focused on the comparison of MNSV-Hyd sequence with type members of family, *Tombusviridae*, genus, Carmovirus and different strains of MNSV at nucleotide level and deduced amino acid levels. The type members of each genus in the family, different *Carmovirus* members and MNSV isolates used in the study are listed with their accession number (tab-3.4).

3.3 Results

3.3.1 Primers

Sl.No	Name of the primer	Sequence (5'-3')	purpose
1	Tombus 3700+	GAA TAC GAA CAA GTC AAT AAA CC	Used to amplify 300 bp fragment from CP region
2	Tombus 4200	CCG CAA GAG TTC GCG ACC CTC C	
3	TBSV Rep 900+	GCT TGT TGC CAG GGT ACA AGG CC	Used to amplify 900 bp fragment from RdRp region
4	TBSV Rep 1800-	GCG TCA GGT ATG TTG ACA GGG ATG	
5	TBSV Rep 1317+	CAC GGC GGA GTC AAG GAT GCT GGG	Used to amplify 1243 bp fragment from RdRp region
6	TBSV Rep 2560-	GGA CGT CTT TCC CCG TTC AGG AAA G	
7	TBSV P19-	CGA AGG TCT CAG TAC CTT CAG	Used to amplify 500 bp fragment from MP region
8	TBSV P19+	ATG GAA CGA GCT ATA CAA GG	
9	CLSV P17-	CTG ATT GTG GGA GAC GCC CTT GG	Used to amplify 500 bp fragment from MP region
10	CLSV P17+	ATG GAA AAT ACC CAA GGC GGG G	
11	PoLV P14-	GGT TGT AAT TTC ATC GCT GG	Used to amplify 500 bp fragment from MP region
12	PoLV P14+	ATG GAA AAT TCC CAA CA GGG G	

Tab-3.1: Degenerate primers designed to the different *Tombusviridae* family members. TBSV- *Tobacco bushy stunt virus* (Acc No: M21958), CLSV- *Cucumber leaf spot virus* (EU127904), PoLV- *Pothos latent virus* (NC0009939), RdRp- replicase gene, MP-movement protein, CP-coat protein. + indicates forward primer, - indicates reverse primer.

Three different sets of primers to family members (tab-3.1), specific to MNSV-A1 template (tab-3.2) and specific primers to MNSV-Hyd (tab-3.3) were designed according to the procedure mentioned under 3.2.1 and used for the determination of complete nucleotide sequence of MNSV-Hyd.

Sl.No	Name of the primer	Sequence (5'-3')	Purpose
1	MNSV 1-24	GGG ATT ACT CTA GCC GAA TCC CCG	All the primers were used in different combinations to amplify MNSV-Hyd genome and to determine complete genome sequence in different sized fragments
2	MNSV Start+	GAT TAC TCT AGC CGG ATC CCC	
3	MNSV 854-880+	TGG TCT TCC TGA CTG GAA GGC CTT	
4	MNSV 1280+	GGA GGG GTT AAG TGT TCA ACG	
5	MNSV 1821-1847	TTC TTC CGT AGT CGT GGC ATC AGG GCG	
6	MNSV 2260+	GGA GTT AGC GCG ATT GGG TAA C	
7	MNSV 2668-2689+	GCC CCG GGG ATT ACT CTG GAG	
8	MNSV 2865-2888	AAG CAG GCC CTG CCC CTG CTA ACG	
9	MNSV 933-	GGT CAT GTC TGG GTG TGT CCC TC	
10	MNSV 1821-	CGC CCT GAT ACC ACG ACT ACG GAA G	
11	MNSV 2011-2024	CAT ATT TTT CCC CGT CGT ACA CAG	
12	MNSV 2401-2424	TAG TTC CCT GGG GCA CGA AAC CCC	
13	MNSV 3001-	CAG GAG CTG ATA TTG CAC CCG G	
14	MNSV 4247-4261	GGC GGG ATG GGC CTA TAA CCC ATC	
15	Md start	NNG AWW WCT CTA GCC GRT CCC CGR CTY TS	
16	Mdp89start	GGY TAG CAA TGG AWA CTG GWT TG	
17	M207+	CAT CCA TGG GTC TTG GAC TAG TGC TAT C	
18	M353+	CTA TGG GGA AGA AGT GGT TGA GCA AGT G	
19	M557+	GGT GGA TGC CCC GAC TCT AGT AAA TCG	
20	M118+	CTG GGN GTT TAG CCA CCT CAT CTG TTA TTA G	
21	M 220-	CGT GGC TGA TAG CAC TAG TCC AAG ACC CAT GG	
22	M 557-	CAC GTT CGA TTT ACT AGA GTC GGG GCA TCC ACC	
23	CIR1+	GAC TCC GCC GTA GCT TGA CC	amplified CP region
24	CIR2-	GGT TTA TTG ACT TGT TCG TAT TCA G	amplified CP region
25	MA32+	ATG GCG ATG GTT AAA CGC	amplified RdRp region
26	MA34-	TTA GGC GAG GTA AGC AGT TTC	amplified RdRp region
27	MNSV End-	AAA GGG ATG GGC CTA TAA CCC ATC	amplified CP region
28	MNSV 4089-4116	GAT ACG CCA(G) TTA CGG T(G)TA GCC	amplified CP region

Tab-3.2: Specific and degenerate primers designed to MNSV-A1 isolate (Genbank accession number DQ339157). + indicates forward primer, - indicates reverse primer.

Sl.No	Name of the primer	Sequence (5'-3')	Purpose
1	M1043-	CGA ACC GTA CGC TAG TTC CAA	Reverse primer used in 5' RACE
2	M725 *Eco*RI-	CA GAA TTC AAA AGA GCC CGA CTC GTG	Reverse primer used in 5' RACE
3	M2955 *Sma*I-	CCT TTA ATC GGA TCC CGG GCC CGT CGA	Reverse primer used for amplification
4	M3355 *Bam*HI-	CAGA CTC CAG AGT AAT CCC CGG GGC	Reverse primer used for amplification
5	M1747*BamsmaI*+	GGG AGG GGA TCC TGA GAA TCC TTA TCC CAG	Forward primer used for amplification
6	M1261*Hind*III+	GCA AGC TTG CGA ATC GCT TGA AGG ACT GGC	Forward primer used for amplification
7	MCP ODT1 @ 3679	TTG TAT AGT CCT TCA CGT TCTT	Forward primer used in 3' RACE
8	MCP ODT2 @3983	TAT ATC TCT GAT GCT GAT GTT AAA	Forward primer used in 3' RACE
9	OligodT *Eco*RI	GAA TTC TTT TTT TTT TTT TTT TTT	Reverse primer used in 3' RACE

Tab-3.3: Specific primers to MNSV-Hyd sequence. Used in amplification process of different products.

3.3.2 cDNA synthesis

The viral RNA isolated in section 2.2.1 was treated with DNase enzyme, phenol chloroform extracted and used for the first strand synthesis as mentioned in section 3.2.2. As RNA is positive sense, negative primers from each set of primers that can bind to template were used for the cDNA synthesis in all three sets of primers, assuming that the complete sequence is obtained by amplifying the whole genome in one of the combinations. The prepared cDNA was used as template for PCR analysis.

3.3.3 PCR amplification, cloning strategy and sequencing result of each fragment

The complete genome sequence of MNSV-Hyd was obtained from different PCR amplified fragments by cloning into T/A cloning vectors. Out of all the sequenced clones five mother clones were identified that can encompass the complete MNSV-Hyd sequence and the detailed cloning strategy for those five fragments was discussed. The number of the fragment was based on the sequence of their identification. The same cloning process was followed for all the fragments as: PCR amplification, gel extraction, ligation into T/A vector, transformation, plasmid isolation, confirmation of the positive clones by restriction digestion (methods were followed as mentioned under 3.2 section) and sequence determination by sequencing minimum of five positive clones for each fragment in both the directions.

The NCBI-blastn (nucleotide blast) result in most cases has no significant blast except for the non-coding regions. Thus, the blastp (protein blast) result was shown for the fragments where nucleotide blast was not obtained and nucleotide blast for the fragments with significant results.

3.3.3 (a) Fragment-1

Using the first set of primers designed in the conserved regions of *Tombusviridae* family members (tab-3.1; 3 and 4 primers), we were able to amplify 250 bp fragment (fig-3.1A) with *Taq* polymerase enzyme and at 57°C of annealing temperature with 1 min extension time. The amplified fragment was purified from the gel (fig-3.1B) and cloned into pTZ57R/T T/A cloning vector by following all the cloning steps as mentioned above. The positive clones were confirmed by restriction digestion with *Eco*RI and *Hind*III to release the cloned fragment (fig-3.1C).

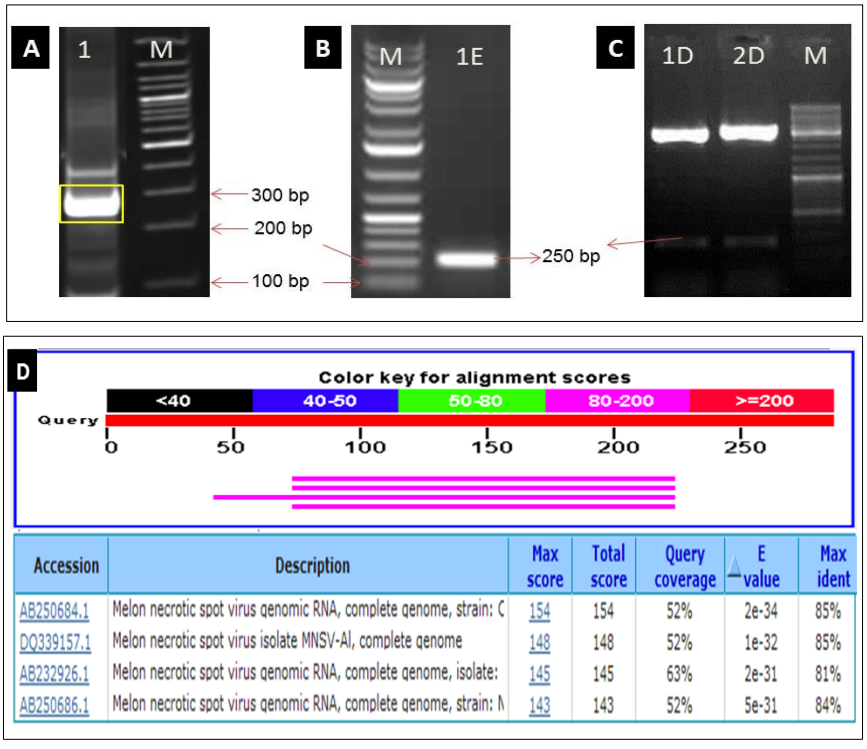

Accession	Description	Max score	Total score	Query coverage	E value	Max ident
AB250684.1	Melon necrotic spot virus genomic RNA, complete genome, strain: C	154	154	52%	2e-34	85%
DQ339157.1	Melon necrotic spot virus isolate MNSV-Al, complete genome	148	148	52%	1e-32	85%
AB232926.1	Melon necrotic spot virus genomic RNA, complete genome, isolate:	145	145	63%	2e-31	81%
AB250686.1	Melon necrotic spot virus genomic RNA, complete genome, strain: N	143	143	52%	5e-31	84%

Fig-3.1: RT-PCR and cloning strategies for fragment-1. A) PCR amplification of fragment-1 with family specific primers, TBSV 3700+ & 4200- primers and excised fragment was outlined with yellow box; B) gel extraction of the desired PCR fragment, 1E- gel extracted PCR amplified fragment; C) restriction digestion confirmation of the cloned fragment in pTZ T/A cloning vector with *Eco*RI & *Hind*III enzymes. Approximate 325 bp of insert (insert size-250 bp+75 bp multiple cloning site of pTZ T/A vector) was released after restriction digestion analysis, D) blastn result of fragment-1 in NCBI database, showing homology to different isolates of *Melon necrotic spot virus* (MNSV) with 52% of sequence coverage and homology of 85%.

The confirmed fragment was sequenced from Ocimum Biosolutions private limited in Hyderabad. The obtained sequencing result was subjected to online NCBI-blastn and the fragment-1 has 85% homology to MNSV complete genome (fig-3.1D). Once we got a lead that it has homology to MNSV virus by 250 by fragment-1, we went ahead by designing the specific primers to MNSV-A1 isolate (tab-3.2; 1-23 primers) and degenerate primers to amplify CP region (tab-3.2; 24-28 primers). With these specific primers to MNSV we tried to amplify MNSV-Hyd genome in different combinations for the next fragment.

3.3.3 (b) Fragment-2

With the second set of degenerate primers (tab-3.2; primer no. 15 & 28) were used to synthesize the first strand cDNA and CP region (1.3 kb fragment) was amplified in PCR with primer set 26 & 27 (PCR product named as CP1) , 24 & 25 (PCR product named as CP2) primers (fig-3.2A) amplified 1.2 kb fragment with *Taq* polymerase. PCR cycling conditions used for annealing of primers was 68˚C for 1 min and extension for 2 min 10 sec. Though we got nonspecific bands in PCR, only desired CP bands were agarose gel extracted (fig-3.2B) and cloned into pTZ T/A cloning vector by following the cloning steps. The plasmids were isolated from the transformed colonies and confirmed by restriction digestion with *Eco*RI and *Hind*III (fig-3.2C). The digestion pattern released from clone CP1 was different from clone CP2 digestion. So, we selected six individual positives clones from each set (CP1 & CP2) and sequenced from Ocimum Bio Solutions private limited on both the strands with universal primers (M13 forward and reverse).

The obtained results were aligned using Bioedit software and subjected for the NCBI-blast. As significant blast search was not observed in blastn, the nucleotide sequence result was translated using the Bioedit software and subjected to NCBI-blastp. The blastp result of CP2 showed 92% similarity to MNSV coat protein domain with 95% of sequence coverage (fig-3.2D) and CP1 product showed 80% homology to RdRP like super family of MNSV (fig-3.2E).

With the CP1 and CP2 results, the CP region present at the 3' end of the genome and part of RdRp region at the 5' end were deduced in the whole viral genome (fig-3.2F). Specific primers were designed (tab-3.3) in these sequenced regions (based on the reported genome map of MNSV strains) and amplified the remaining part of viral genome.

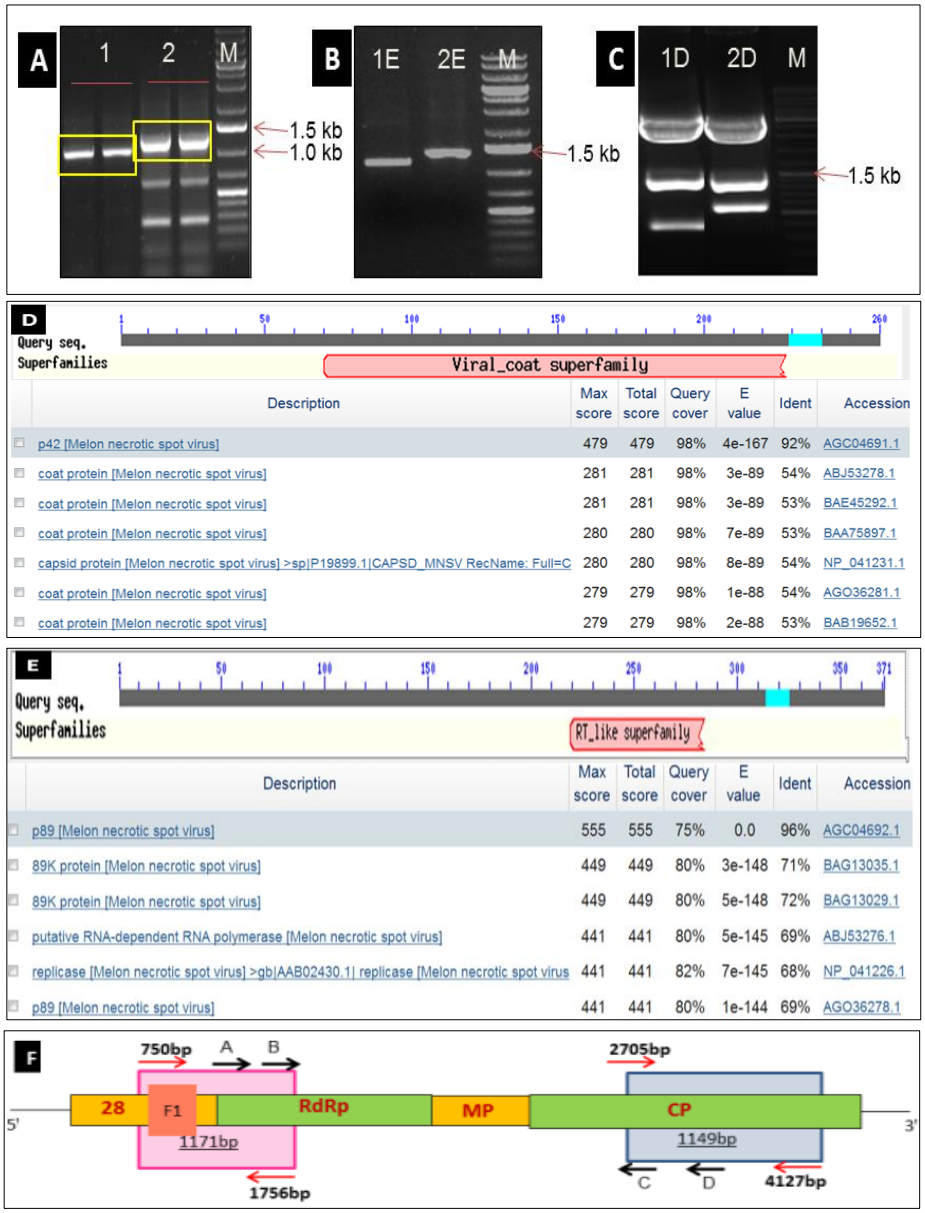

Fig- 3.2: RT-PCR and cloning strategies of fragment-2. A) PCR amplification of fragment-2, CP1- MA32+ & MA34- primers, CP2- CIR1+ & CIR2- primers and excised fragment was outlined with yellow box, M- 1 kb DNA ladder from Fermentas/Thermo scientific; B) gel extracted desired PCR products CP1 & CP2; C) Restriction digestion confirmation of the cloned fragments in pTZ T/A cloning vector with *Eco*RI restriction enzyme. According to the MNSV-A1 isolate, *Eco*RI is present as internal site at 769 bp. Two fragments of 800 bp and 631 bp should release in case of positive clones. In 2nd clone the digestion pattern was different; D) NCBI-blastp result of the CP1 clone having to MNSV-CP as expected, 92% homology to MNSV-CP with 98% of query coverage; E) NCBI-blastp result of CP2 clone having homology to MNSV-RdRp region with 96% of identity in 75% of the query coverage; F) Coverage of the sequenced two fragments on the whole genome map. 28: p28 gene, RdRp gene, MP gene, CP gene. F1: fragment-1 coverage representation, pink colored box- representation of CP2 sequence coverage. Blue colored box- representation of CP1 fragment coverage. Red arrows-primers used for the amplification of the fragments and sizes on red arrows represent homology of the fragment from the respective nucleotide in whole genome context. Black arrows- represent the specific primers designed to sequence fragments for fragment-3 amplification (region between the two fragments). A, B, C, D - 6, 5, 3 and 4 primers from tab-3.3.

3.3.3 (c) Fragment-3

Once we got the clue on the coverage of the sequenced fragments in the whole genome, we have designed two specific forward primers at 3' end of CP2 fragment and two reverse primers were designed at 5' end of CP1 fragment and used in combinations to obtain the sequence between the CP1 and CP2 fragments (fig-3.2F). The reverse primers (3 & 4; tab-3.3) were used for the first strand cDNA synthesis to the viral RNA template. Using *Taq* polymerase enzyme the PCR fragment of 1.5 kb & 2 kb size were amplified with the primer combinations 6 & 3 and 6 & 4 respectively (tab-3.3) at 57˚C annealing temperature for 1 min 10 sec and extension for 2 min 20 sec. Yet we got the non-specific fragments in PCR amplification, only the desired PCR amplicons were agarose gel purified (fig-3.3A, B) and cloned into pTZ T/A cloning vector. The positive clones were selected by restriction digestion with *Eco*RI (fig-3.3C). The sequencing results of both the fragments are matching to MNSV RdRp and movement protein (MP) genes in NCBI-blast result at protein level (fig-3.3D and E).

3.3.3 (d) Fragment-4

With the above amplified fragments, the viral genome sequence was determined of approximately 3.3 kb out of 4.3 kb (fig-3.4F). As single nucleotide is also important for the viral replication, 5' RACE and 3' RACE techniques were performed in conventional methods to identify the authentic start and end nucleotides at 5' and 3' ends respectively. The 5' end sequence was determined by 5' RACE technique as specified in under section 3.2.10. The 5' end of the viral genome was amplified (~ 800 bp) by performing nested PCR (fig-3.4A). The amplified PCR product was gel extracted (fig-3.4B), cloned into T/A cloning vector (pTZ57R/T), transformation was performed and the plasmids were confirmed by restriction digestion (fig-3.4C). Minimum of ten positives clones were sequenced for the confirmation of the authentic nucleotide. The sequencing results of the confirmed clones were showing homology to MNSV in NCBI-blastx to 54% identity with 55% of sequence coverage (fig-3.4D).

Fig-3.3: RT-PCR and cloning strategies for fragment-3. A) PCR amplification of MNSV-Hyd fragments with specific primers in the sequenced regions (tab-3.3), 1-6 & 3 primers (1.5 kb), 2-6 & 4 primers (2.1 kb), and excised fragment was outlined with yellow box M- 1kb DNA ladder ; B) Gel extraction of the PCR amplified fragments, 1&2 respectively, C) Confirmation of the transformed clones by restriction digestion analysis with restriction enzyme, *Eco*RI, these fragments have the internal *Eco*R*I* restriction site at 943 bp. 943 bp or 795 bp size fragments (based on the orientation) have to be released in case of first set of clones (1.5 kb clones) and 1189 bp or 795 bp fragments with the second set of clones (2 kb); D) NCBI-blastp result of the first fragment have homology to RdRp region of MNSV strains; E) NCBI-blastp result of the second set of clones have homology to RdRp & movement protein (MP) regions of MNSV. Even though the identity percentage is of 76% the sequence coverage is very less (16%).

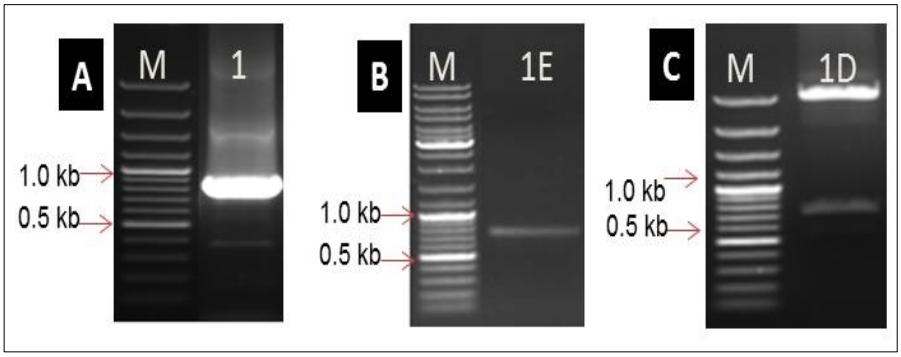

D

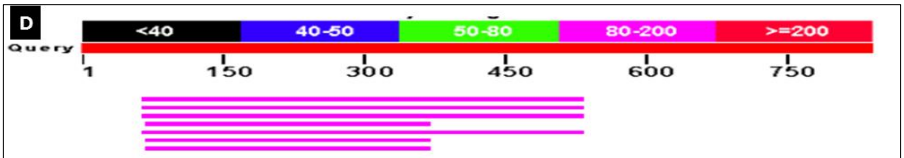

Accession	Description	Max score	Total score	Query coverage	E value	Max ident
BAG13030.1	29K protein [Melon necrotic spot virus]	135	135	55%	8e-36	54%
BAG13036.1	29K protein [Melon necrotic spot virus]	135	135	55%	2e-35	55%
BAG13029.1	89K protein [Melon necrotic spot virus]	135	135	55%	3e-33	54%
AAM83189.1	p29 [Melon necrotic spot virus]	129	129	36%	4e-33	70%
BAG13035.1	89K protein [Melon necrotic spot virus]	135	135	55%	5e-33	55%

E

>Naga.Teja.Natra_MD8_m13Forward_T314.P1,Trimmed Sequence(462 bp)
CGATGTCGACTTTTTTTTTTTTTTTGGGATAGCTAGCCACTATTCCCGTGCTCTCAGTG
TTCGAGATCCCGTGTCGGCAGGTTACTTTGATCGTAATATCGGCGGACCTAAACGTAAC
AGCGTATGGCTACTGCAATGAATACTATGGGGTTAACTGTGCTTAACTTAGCTCCCGTG
CAATCTTCTCATATAATAACTAGATGCTTTGCTGCGAGAAGTGTTGATAGTACTCTACCT
AGTAAAGATATATGTACTAGGTTGTCAAATAGTTTATGTGAGAATGTCAAATCTGATATC
GCTTCTATTGTTAAAGTCGGACTTGGAGCCGCTGTTTGTTATGGTGCTTATAGGTTGGC
AAAGAACTTTTGGTACAACCAGCGGAAACACTCTAAGGGTAAGATTGACAAATTAGG
GCAGGCCGTTTTGAAATGCATTGAAGATGTGGCAAACGGCAACGATGA

Fig-3.4: Determination of 5' authentic end nucleotide of viral genome by 5' RACE technique. A) PCR amplification of 5' end of the viral genome by nested PCR, M-1kb DNA ladder from Fermentas / Thermo scientific, 1- PCR amplified product on 1% agarose gel (~800 bp); B) 1E- gel extraction of PCR amplified product; C) 1D – restriction digestion confirmation of the cloned fragment in pGEMT-Easy (Promega) cloning vector with *Eco*RI restriction enzyme. Expected 800 bp fragment was released in digestion; D) NCBI- blastn result of the fragment-4 having identity of 54% to p29 gene of MNSV with 55% of query coverage.

3.3.3 (e) Fragment-5

3' terminal sequence of the viral genome was determined by 3' RACE technique as described in methods section 3.2.11 by using Poly (A) polymerase enzyme. The final product of PCR amplification is about 600 bp size (fig-3.5A). The PCR amplified product was gel extracted (fig-3.5B), cloned into pGEMT-Easy T/A cloning vector by following the standardized protocols and the positive clones were confirmed by restriction digestion with

*Eco*RI (fig-3.5C) and ten clones were sequenced. The tail, poly (T) added was observed in the sequenced result (fig-3.5D). The nucleotide blast result haven't shown significant homology search with the sequenced results. The sequence was confirmed by the overlapping sequence of fragment-2 and by aligning the sequence with CP sequence using BioEdit sequence aligner (data not shown).

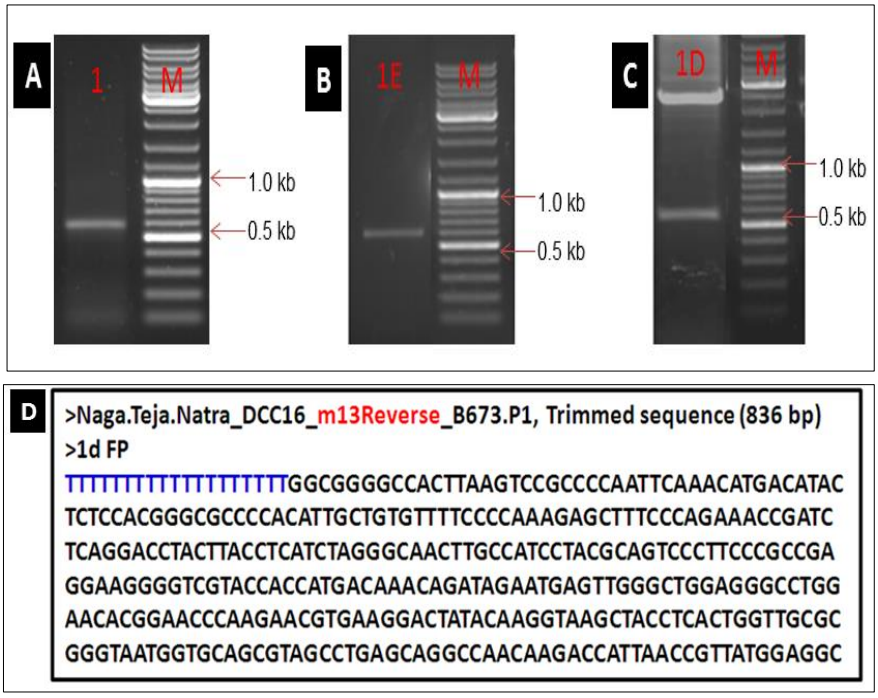

Fig-3.5: Confirmation of viral 3' end authentic nucleotides by 3' RACE. A) PCR amplification of the 3' end of the genome with specific primers ODT1 & OliodT *Eco*RI (tab-3.3), approximately 600 bp product; B) gel extraction of the PCR amplified product with Qiagen columns by following the manufacturer's protocol; C) confirmation of the cloned gene in pTZ T/A cloning vector with restriction enzymes, *Eco*RI and *Hind*III; D) Sequencing result of the clones showing the poly (T) tail after the end nucleotide.

3.3.4 Overview of complete sequencing

With all the sequencing clones, we are successful in identifying the five overlapping mother clones that encompass the complete genome sequence (fig-3.6) of MNSV-Hyd. For our convenience each clone from 5' end of the genome was nomenclature in respect of my supervisor, parents & husband that was followed by my name Teja (T) in all the clones (tab-3.4). Clone-1 (named as p5' TGN, supervisor's name Dr. Gopinath) obtained as a result of from 5' RACE contains the sequence from 1st nucleotide to 770 nt. Clone-2 (p5' TVR, father's name, Venkateswara Rao) overlaps the clone-1 of 20 nt and contains sequence from

750 –1756 nt. Overlapping the clone-2 of 456 nt clone-3 (pTNVR, mother's name Nirmala and father's name) starts from 1298 and goes up to 3405 nt. Clone-4 (pTGCP, husband's name Gopi chand) has overlapping of 697 nt in clone-3 and extents up to 4127 nt. By using 3' RACE method determined the 3' terminal sequence in clone-5 (p3' NCR, non-coding region); starts from 3719-4274 overlapping the clone-4 of 409 nt (tab-3.4).

The sequences from all the clones were aligned using BioEdit aligner software and the deduced complete viral genomic sequence comprises 4274 nucleotides (Appendix, A2). The complete genome sequence of MNSV-Hyd was deposited in Genbank under the accession number JX879088. The NCBI-blastn result of complete genome sequence was showing 75% homology to MNSV-Kochi (AB232926.1) & Tottori (AB232925.1) with 52% & 50% of sequence coverage (fig-3.7) respectively. The maximum identity of MNSV-Hyd to the other MNSV strains was observed in RdRp region but not the complete sequence coverage (fig-3.7).

Sl.No	Fragment	Designated name	Encompassing nt in complete genome
1	Fragment-4	p5' TGN	1-770
2	Fragment-2, CP2	p5' TVR	750-1756
3	Fragment-3	pTNVR	1298-3405
4	Fragment-2, CP1	pTGCP	2705-4127
5	Fragment-5	p3' NCR	3719-4274

Tab-3.4: The five mother clones that encompass the complete MNSV-Hyd genome sequence with their designated names.

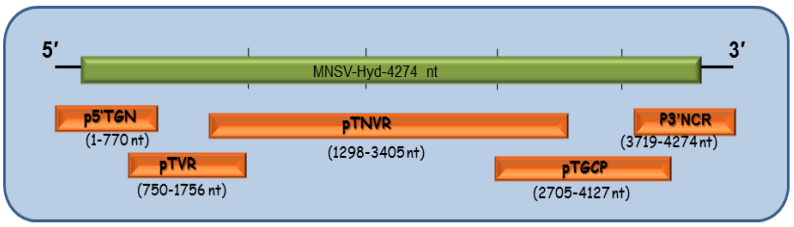

Fig-3.6: Pictorial view of the five mother clones which overlap the whole genome sequence. Clones were named from the 5' end and the encompassing nucleotides of each clone were shown below the respective clones. P5' TGN clone was obtained by 5' RACE technique; pTVR clone is fragment-2, CP2; pTNVR clone is fragment-3; pTGCP clone is fragment-2, CP1 and last one, p3'NCR by 3' RACE method.

3.3.5 Genome organization

Using the complete genome sequence and insilico analysis through MEGA5

software the genome organization of the virus was deduced as shown in the figure and matching to the Carmovirus genome organization. The virus, MNSV-Hyd consists of five open reading frames same as that of Carmoviruses (fig-3.8). The 5' terminus of the genome starts with the non-coding region of 1-98 nt. The first or the 5' proximal ORF-1 starts from 99 nt and ends with an amber stop codon at 926 nt (275 amino acids) encodes ~ 28 kDa protein (p28). The read through of the amber stop codon at 924-926 result in ORF-2 which encodes 89 kDa protein (797 amino acids, p89) and terminates at 2493-2495 nt with an amber codon. The p89 protein consists of amino acid sequence of Gly-Asp-Asp, commonly called as GDD motif at 1893-1901 nt, characteristic feature for RNA dependent RNA polymerase (RdRp).

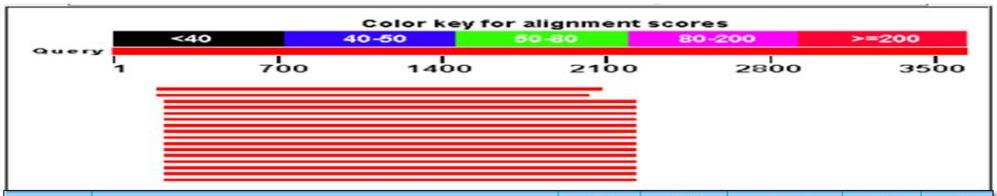

Accession	Description	Max score	Total score	Query coverage	E value	Max ident
AB232926.1	Melon necrotic spot virus genomic RNA, complete genome, isolate: Koch	793	793	52%	0.0	75%
AB232925.1	Melon necrotic spot virus genomic RNA, complete genome, isolate: Totto	778	778	50%	0.0	75%
DQ339157.1	Melon necrotic spot virus isolate MNSV-Al, complete genome	778	778	55%	0.0	74%
AY330700.1	Melon necrotic spot virus isolate MNSV264 29K protein, 89K protein, p7	761	761	55%	0.0	74%
D12536.2	Melon necrotic spot virus genomic RNA, almost complete sequence	756	756	55%	0.0	74%

Fig-3.7: Nucleotide blast result of the complete MNSV-Hyd genome sequence having 75% identity with only 52% of sequence coverage. The blast result has more homology to MNSV isolates Kochi and Tottori (watermelon strains) from Japan.

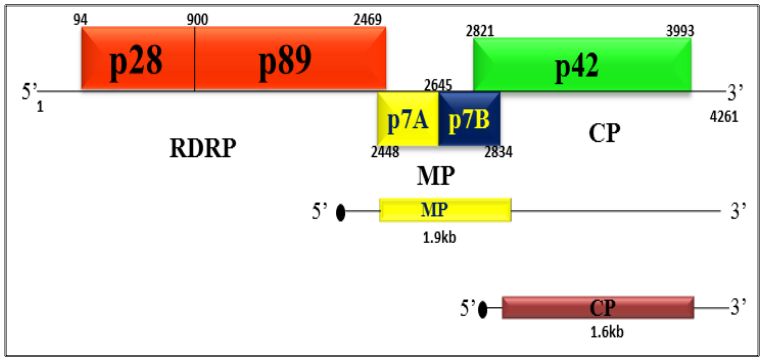

Fig-3.8: Genome organization of MNSV-Hyd with reference to the available MNSV isolates. The replicase gene (p89) & p28 are translated from the genomic RNA and the MP and CP are translated from the two sub-genomic RNAs.

ORF-3 is located centrally overlapping 22 nt from ORF-2 but in a different frame than that of ORF-1 & 2. It is located in between 2478-2677 nt and encodes (67 amino acids) 7 kDa protein (p7A), which stops with opal codon. ORF-4 is also centrally located from 2680 nt and terminates with an ochre stop codon at 2866-2868 nt. It is in the same frame as that of ORF-1 & 2 and encodes (62 amino acids) 7 kDa protein (p7B). The last and the 3' proximal ORF-5 starts from 2855 overlapping 14 nt of ORF-4 in same frame as that of ORF-3. It encodes 391 amino acids protein with a molecular mass of 42 kDa (p42; coat protein) and terminates with an amber stop codon at 4028-4030 nt. The 3' NCR region at the 3' proximal terminus consists of 244 nt (Appendix, A2).

3.3.6 Comparison studies

MNSV-Hyd complete genome sequence and individual ORFs at nucleotide and deduced amino acid sequence were compared with 12 different Carmovirus members and 12 MNSV strains whose complete genome sequence was available (tab-3.5). The complete genome sequence shows more identity to MNSV- Kochi and Tottori (75%) (fig-3.7). It shows very less homology to CarMV, CPMoV, PLPV, AnFBV and PSNV among the Carmovirus members (data not shown) and this clearly observed in the phylogenetic trees. Individual genes were also compared at both nucleotide and protein levels. P28 shows identity ranging from 68-72% with sequence coverage of 42-43%. The closest similarity was found to Malfa5 (72%) at nucleotide level and to Malfa5, Kochi & Tottori strains (51%) with 97% sequence coverage at protein level (tab-3.6).

Sl. No	Virus	Abbreviation
1	AnFBV	*Angelonia flower break virus*
2	CarMV	*Carnation mottle virus*
3	CbMV, CMoV	*Calibrachoa mottle virus*
4	CCFV	*Cardamine chlorotic fleck virus*
5	CLSV	*Cucumber leaf spot virus*
6	CPMoV	*Cowpea mottle virus*
7	FNSV	*Furcraea necrotic streak virus*
8	GaMV	*Galinsoga mosaic virus*
9	HCRSV	*Hibiscus chlorotic ringspot virus*
10	HSRV, HRSV	*Honeysuckle ringspot virus*
11	JINRV	*Japanese iris necrotic ring virus*
12	MCMV	*Maize chlorotic mottle virus*
13	MNeSV	*Maize necrotic streak virus*
14	NLVCV	*Nootka lupine vein clearing virus*
15	OCSV	*Oat chlorotic stunt virus*
16	PFBV	*Pelargonium flower break virus*
17	PLPV	*Pelargonium line pattern virus*
18	PMV	*Panicum mosaic virus*

19	PoLV	*Pothos latent virus*
20	PSNV	*Pea stem necrosis virus*
21	SCV	*Saguaro cactus virus*
22	SYMMV	*Soybean yallow mottle mosaic virus*
23	TBSV	*Tomato bushy stunt virus*
24	TCV	*Turnip crinkle virus*
25	TNV-A	*Tobacco necrosis virus A*
26	TNV-D	*Tobacco necrosis virus D*

Tab-3.5: List of the Carmoviruses used in the present comparison study

The post read through region (PRTR), p89 exhibits more identity to MNSV strains Kochi & Tottori of 74% with sequence coverage of 100% at nucleotide comparison and at protein level, 70% similarity with sequence coverage of 98%. The movement protein p7A & p7B at nucleotide level exhibits more identity to MNSV strain SP-16 of 77% with sequence coverage of 98% and at protein level p7A shows 76% identity to Yamaguchi, Kochi & Tottori strains with 100% sequence coverage whereas p7B shows only 57% identity to SP-16 with 98% of sequence coverage. p7B doesn't show any homology with Yamaguchi, Chiba & Nagasaki strains of MNSV at protein level. The coat protein region (CP) shows highest homology to MNSV-Kochi strain at nucleotide and protein levels of 64% & 53% with sequence coverage of 51% & 99% respectively (tab-3.6).

The nucleotide and deduced amino acid sequences of different ORFs of MNSV-Hyd was compared with other members of Carmovirus. At nucleotide level p28 region doesn't have any identity with Carmovirus members but at protein level shows identity ranging from 29% (HSRV) & 37% (PSNV) in the selected viruses from Carmovirus group (tab-3.6) with sequence coverage of 41 & 77% respectively.

The PRTR shows 69% (PSNV) and 72% (HCRSV) with sequence coverage of 45 & 54% respectively at nucleotide level. At protein level shows more homology to PSNV – 58% with sequence coverage of 91% and least homology to CarMV-44% with 85% of sequence coverage. At nucleotide level out of p7A, p7B & CP only p7A shows 69% of homology to PSNV with 53% of sequence coverage where as 7B and CP doesn't have similarity with other Carmoviruses. At protein level all the three proteins shows 56%, 63% and 36% of identity towards PSNV in the selected viruses (tab-3.6) with sequence coverage of 88%, 48% and 77% respectively (tab-3.6).

virus	Accession no #	Complete nucleotide(nt) Identity (%)	P28		PRTR		7A		7B		CP	
			nt (%)	aa (%)	nt (%)	aa (%)	nt (%)	aa (%)	nt (%)	aa (%)	nt (%)	aa (%)
Carmovirus												
PFBV	AJ514833	-	-	33/46	65/16	46/81	-	-	-	-	-	-
CarMV	AF192772	66/11	-	32/58	66/30	44/85	-	-	-	-	-	-
CPMoV	U20976	71/4	-	30/51	71/13	47/81	-	-	-	-	-	-
HCRSV	DQ392986	-	-	32/76	72/45	49/82	-	-	-	-	-	-
NLVCV	EF207438	-	-	34/59	-	50/62	-	-	-	-	-	-
PLPV	AY613852	67/11	-	33/48	67/31	44/82	-	-	-	-	-	-
TCV	M22445	-	-	36/49	-	48/85	-	-	-	-	-	-
HSRV	NC014967	-	-	29/47	-	43/86	-	-	-	-	-	-
AnFBV	DQ219415	66/12	-	34/47	66/34	47/80	-	-	-	-	-	-
CbMV	GQ244431		-	34/41	65/30	46/81	-	-	-	-	-	-
SCV	U72332		-	29/47	65/30	45/82	-	-	-	-	-	-
PSNV	AB086951	69/28	-	37/77	69/54	58/91	69/53	56/88	-	63/48	-	36/77
MNSV strains												
Yamaguchi	AB250687	81/63	70/43	50/97	72/100	68/99	76/98	76/100	73/85	-	81/33	51/99
Chiba	AB250684	81/63	71/42	50/97	73/100	68/99	76/98	73/100	73/85	-	81/33	52/99
Nagasaki	AB250686	83/62	70/42	50/97	72/100	68/99	76/98	75/100	73/85	-	83/33	51/99
NH	AB044291	83/62	69/42	50/97	71/100	68/99	76/98	75/100	73/85	56/100	83/33	51/99
HM	GU480022	72/62	69/43	50/97	73/100	69/98	76/98	74/100	73/85	56/100	68/29	52/99
Israel	DQ922807	71/61	68/42	50/97	72/100	68/99	75/98	72/100	73/84	56/100	67/27	52/99
A1	DQ339157	69/71	69/42	50/97	73/100	68/99	76/98	74/100	76/84	52/100	67/29	52/99
264	AY330700	69/71	68/42	50/97	73/100	69/98	74/98	74/100	73/83	57/100	65/47	51/99
Malfa5	AY122286	72/65	72/43	51/97	72/100	69/98	74/98	75/100	75/85	59/100	65/40	52/99
Kochi	AB232926	72/67	71/43	51/97	74/100	70/98	72/99	76/100	80/32	58/98	64/51	53/99
Tottori	AB232925	72/62	71/43	51/97	74/100	70/98	74/99	76/100	80/32	58/98	66/29	52/99
SP-16	FJ621527	73/9	-	-	-	-	77/98	-	77/98	57/98	-	51/99

Tab-3.6: Homology of MNSV-Hyd with different Carmovirus members and with MNSV isolates in NCBI-blast. First numerical (numerator) indicates the percentage of homology and the denominator indicates the sequence coverage, nt- homology at nucleotide level; aa- homology at amino acid level and '–'indicates no homology.

3.3.7 Genetic diversity through phylogenetic analysis

The homologous sequences that are conserved form the informative sites and are used for constructing the phylogeny using MEGA6 software. The tree representing the evolutionary relationship was determined for the CP, MP, RdRp genes and as well as non-coding regions at 3' & 5' ends.

3.3.7 (a) Relationship of complete genomic sequence of MNSV-Hyd

n comparison of complete nucleotide sequence with the type members in a family (fig-3.9A), the tree was clustered into three groups. Group-I includes GaMV and FNSV on one hand of the branch and TNV-A and TNV-D on the other hand of the branch with boot strap value of 99. In group-II, PMV stands on one hand and MNSV-Hyd & CarMV on the other hand of the branch with 85 replicates of boot strap value. MNSV-Hyd has boot strap

value of 97 with CarMV. PoLV, CLSV, TBSV, MNeSV are under group-III with boot strap value of 100. OCSV was branched out as a separate branch from group-I (Mo *et al*., 2011).

In comparison with Carmovirus members, in the tree (fig-3.9B), CPMoV, SYMMV, PSNV, MNSV-Hyd were grouped together tightly with boot strap value of 100 on separate branch. MNSV-Hyd was more related to PSNV among all the Carmoviruses. JINRV, AFBV were branched as separate groups. MNSV-Hyd branched as an individual branch.

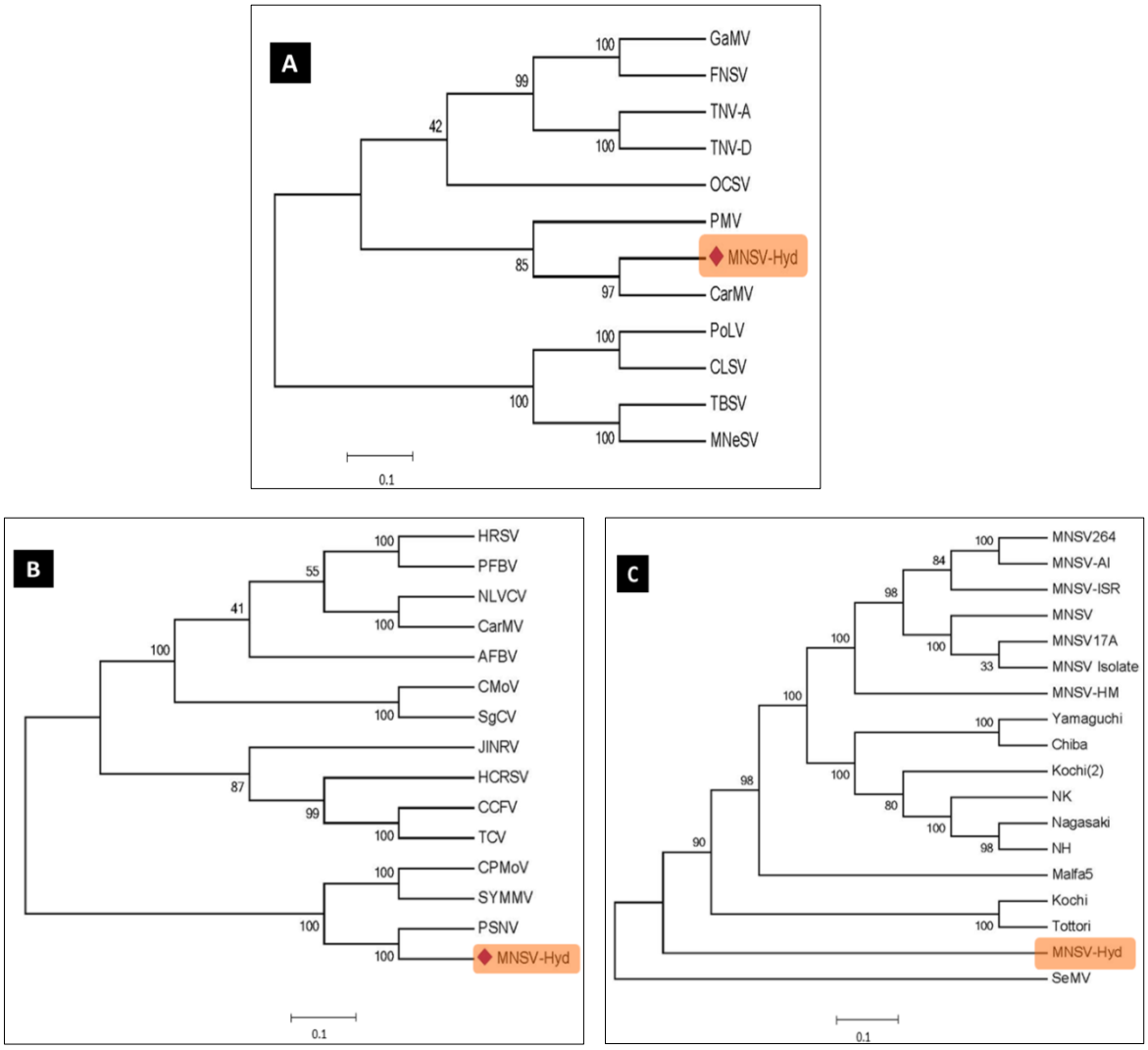

Fig-3.9: Phylogenetic tree showing relationship of MNSV-Hyd constructed using MEGA-6, neighbor joining bootstrap method. A) homology with type members in the family; B) with Carmovirus members and C) with MNSV isolates listed in the tab-3.5. Bootstrap values are represented at the branch points.

In comparison with MNSV isolates (fig-3.9C), our virus (MNSV-Hyd) relates to watermelon isolates of Japan (Kochi & Tottori) with bootstrap value of 90. All Spain

isolates, except MNSV-HM and Malfa5, and all the Japan isolates are paired together on two individual groups.

3.3.7 (b) Taxonomic relationship of replicase sequence

The complete RdRp gene (read through protein, p89) was used for constructing phylogenies. In comparison with Tombusviridae members, MNSV-Hyd clusters with CarMV with boot strap value of 100 on one hand of the clade at nucleotide level and other hand consists of MCMV & PMV with bootstrap value of 94 at branch point. OCSV & CRSV are separated as different individual branches (fig-3.10A). The RdRp tree with family members at protein level also represents the same as nucleotide tree (fig-3.10B). MNSV-Hyd clusters with CarMV with bootstrap value of 92. The trees constructed with Carmovirus members at nucleotide and protein levels are different unlike the family trees. MNSV-Hyd clusters with PSNV with bootstrap value of 100 in both the nucleotide and protein levels. CPMoV & SYMMV are strongly clustered on the other hand of the clade in both the trees (fig-3.10C, D). The type member of the genus, CarMV was branched as separate branch in protein tree but clustered with NLVCV with 50 bootstrap value at nucleotide level. The phylogenetic analysis of MNSV-Hyd with MNSV isolates shows its homology to Kochi and Tottori strains of Japan with 62 bootstrap value (fig-3.10E, F). But it branches out in protein tree from Kochi & Tottori with bootstrap value of 80. In both trees, all the Japan strains are grouped on one branch and Spain isolates on another branch whereas Malfa5, ISR & HM are branched individually.

3.3.7 (c) Taxonomic relationship of MP sequence

In individual gene comparison, MP gene relates to CarMV on one hand to GaMV & TNV-A on another hand at nucleotide level in a family tree (fig-3.11A). In protein tree MNSV-Hyd clusters with TNV-A. GaMV & PMV are branched separately in protein tree unlike the nucleotide tree (fig-3.11B). MNSV-Hyd clusters with PSNV more strongly in comparison with Carmoviruses at both nucleotide and protein levels (fig-3.11C, D). It also relates to CCFV and TCV on one hand of the clade in protein tree with 67 bootstrap value. Remaining viruses also related to each other differently at nucleotide and protein levels. MNSV-Hyd branches out separately and shows its diversity among MNSV isolates

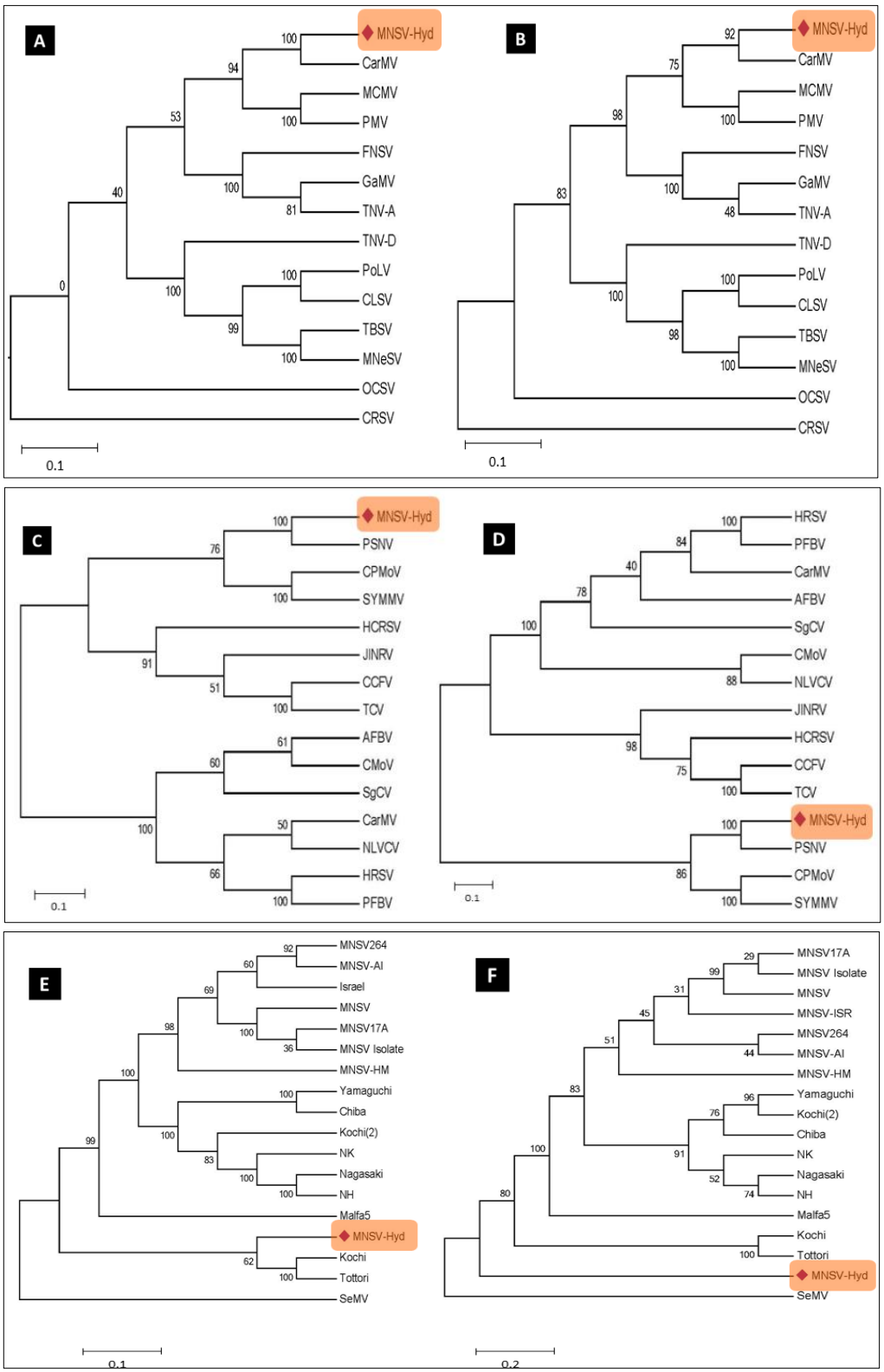

Fig-3.10: Representation of phylogenetic trees for replicase gene sequence with family, genus and MNSV isolates constructed by neighbor-joining (NJ) method with 1000 bootstrap replicates using MEGA6. A, B is with family, tombusviridae members; C, D is with genus, carmovirus members; E, F is with MNSV isolates. A, C, E are at nucleotide level and B, D, F are at protein level. MNSV-Hyd is highlighted in all the cases. The distance bar is represented at the bottom of the tree. SeMV was used as out member.

(fig-3.11E, F). In both the trees representing MNSV strains, MNSV-Hyd relates to watermelon strains of Japan with 47 & 95 boot strap values respectively. Two separate groups for Japan and Spain isolates were observed same as with RdRp homology tree.

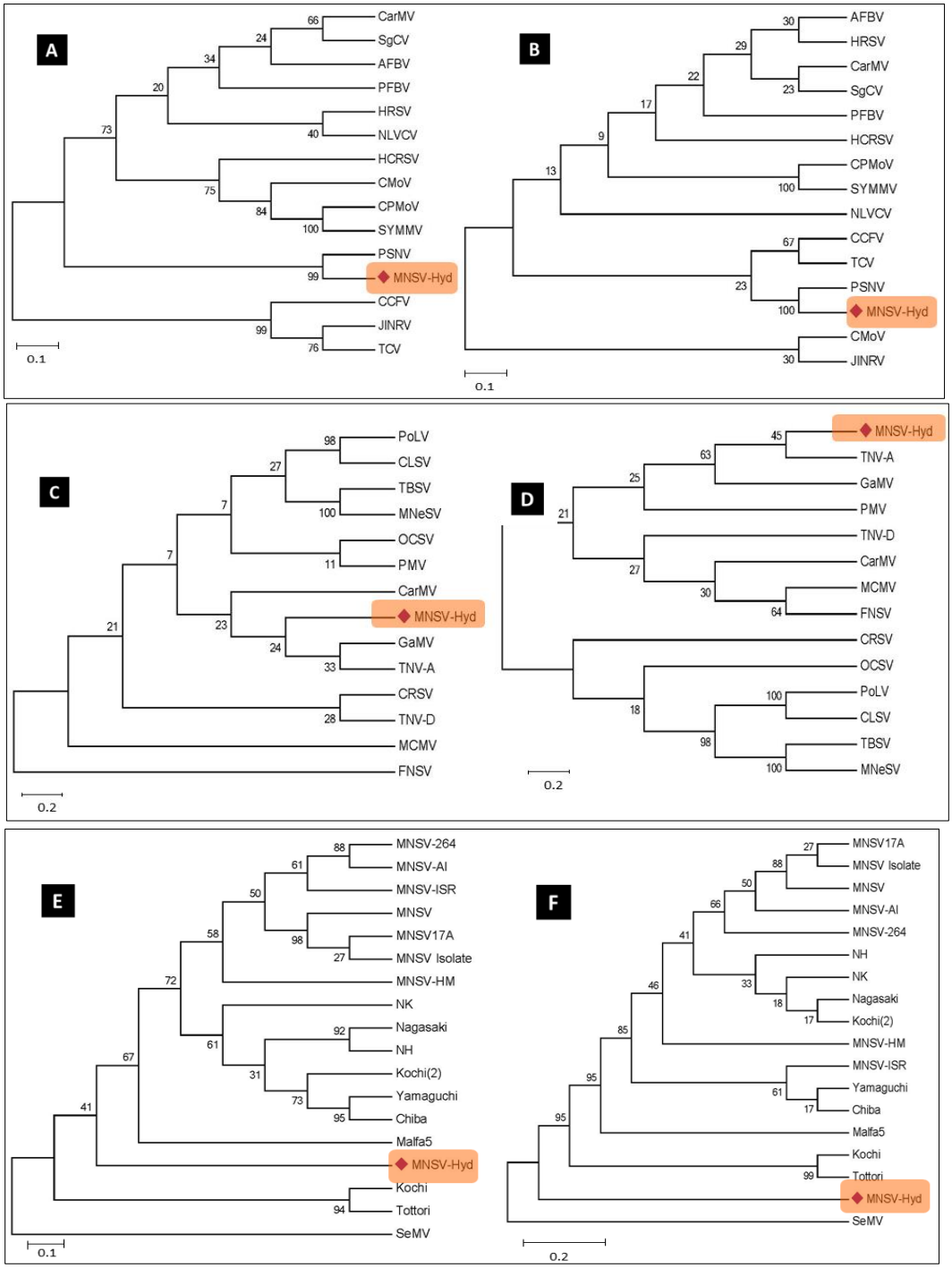

Fig-3.11: Representation of phylogenetic trees for MP gene with family, genus and MNSV isolates constructed by neighbor-joining method with 1000 bootstrap replicates using MEGA6. A, B is with family, Tombusviridae members; C, D is with genus, Carmovirus members; E, F is with MNSV isolates. A, C, E are at nucleotide level and B, D, F are at protein level. MNSV-Hyd is highlighted in all the cases. The distance bar is represented at the bottom of the tree. SeMV was used as out member.

3.3.7 (d) Taxonomic relationship of CP sequence

On assessment of CP homology trees with Tombusviridae members, MNSV-Hyd clusters with PMV and CLSV with 55 & 95 as boot strap values at nucleotide and protein levels respectively (fig-3.12A, B). MNSV-Hyd was clustered with CarMV on one hand at nucleotide level (fig-3.12A) where as in protein tree it was separated as individual branch (fig-3.12B). In case of Carmovirus members, the MNSV-Hyd clusters strongly with PSNV in both the levels. In nucleotide tree, MNSV-Hyd and PSNV are clustered on individual clade (fig-3.12C) whereas in protein homology tree, on one hand of the clade, MNSV-Hyd and PSNV are clustered and on the other hand CPMoV & SYMMV were clustered (fig-3.12D). In comparison with different MNSV strains, the MNSV-Hyd branched out as individual branch with 95 boot strap value (fig-3.12E). In this cluster, all the Spain isolates and Japan isolates were grouped separately as in case of other ORFs. At protein level, it relates to Japan watermelon isolates with boot strap value of 90 (fig-3.12F). The isolates, MNSV-17A, MNSV & MNSV isolate were separated as one branch which was not observed in nucleotide phylogenetic tree.

3.3.6 (e) Diversity analysis of 5' NCR

The phylogenetic trees with the non-coding region show lot of diversity. The branch length is highly variable in comparison with the trees constructed with the coding regions. In case of 5' NCR tree, all the Japan isolates and Spain isolates are grouped in one cluster indicating their homology based on the region. MNSV-264, Malfa5 strains branches separately, from other Spain isolates. MNSV-Hyd, Kochi & Tottori (watermelon isolates) groups as a separate clade from the other members with 97 boot strap value (fig-3.13). Within the same cluster also MNSV-Hyd shows lot of difference in the branch length indicating its diversity.

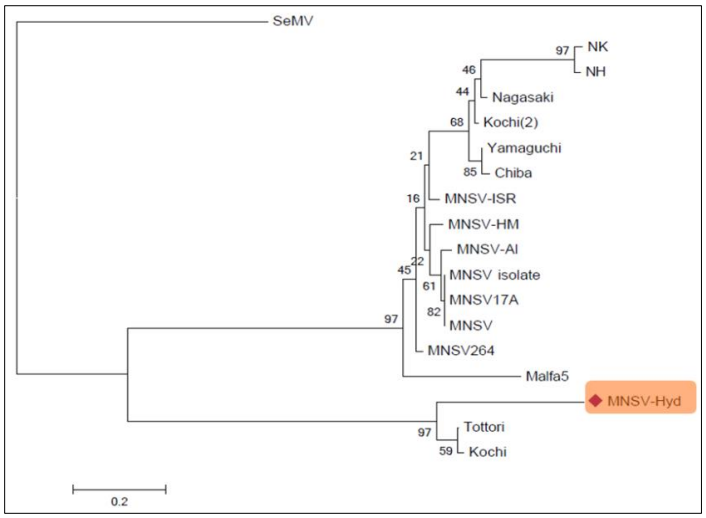

Fig-3.13: Phylogenetic comparison of 5' NCR of MNSV-hyd with the available MNSV isolates with NJ method. MNSV-Hyd was highlighted in the tree.

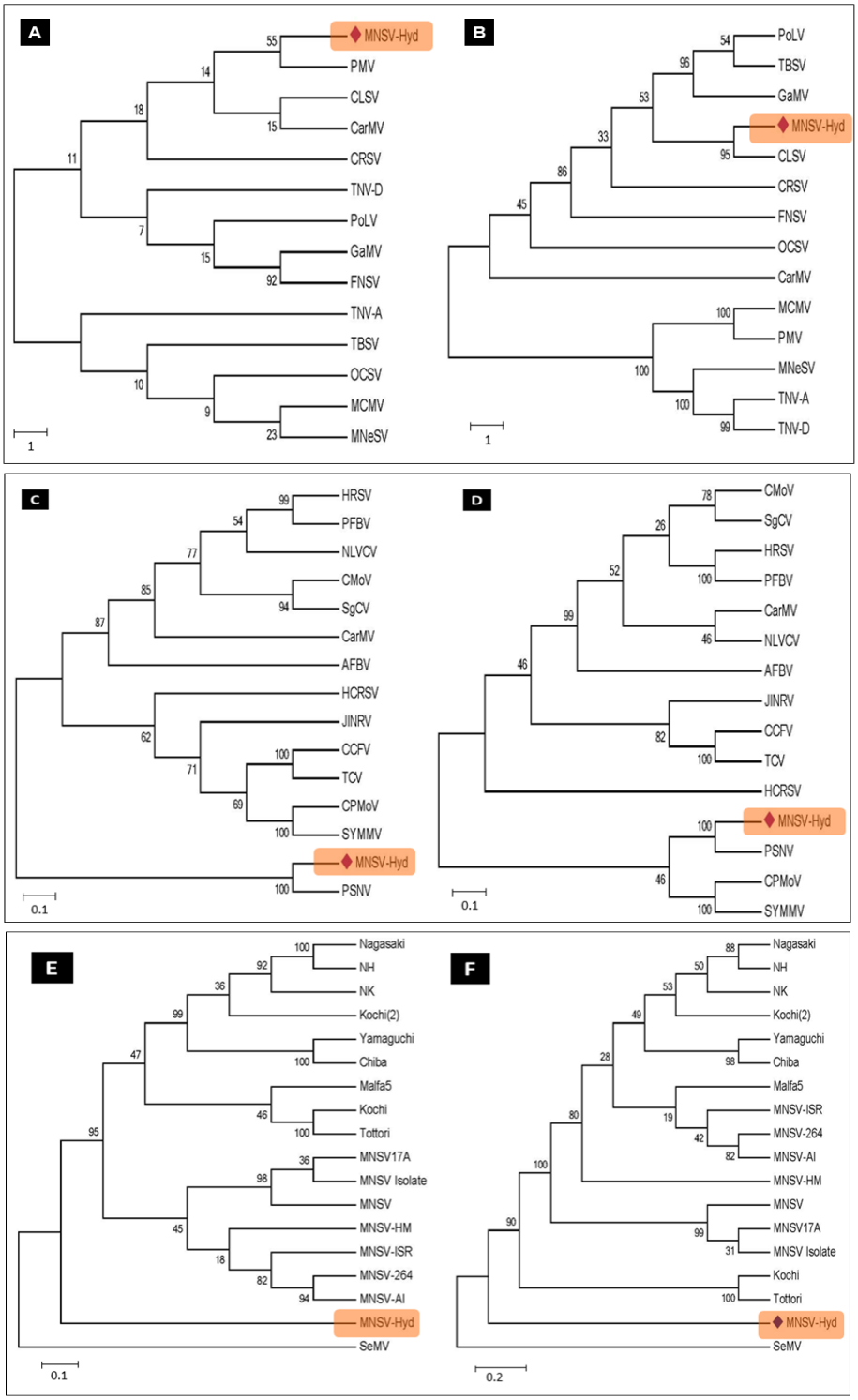

Fig-3.12: Diversity analysis of MNSV-Hyd CP sequence with family, genus and MNSV isolates constructed by neighbor-joining method with 1000 bootstrap replicates using MEGA6. A, B is with family, Tombusviridae members; C, D is with genus, Carmovirus members; E, F is with MNSV isolates. A, C, E are at nucleotide level and B, D, F are at protein level. MNSV-Hyd is highlighted in all the cases. The distance bar is represented at the bottom of the tree. SeMV was used as out member.

3.3.6 (f) Diversity analysis of 3' NCR

With phylogenetic tree constructed with 3' NCR, one separate group was formed with MNSV-Hyd, MNSV-264 (Spain isolate) and MNSV-Kochi & Tottori (Japan strains) (fig-3.14). MNSV-Hyd clustered with MNSV-264 strain indicating its homogeneity even though its relation was also observed with their close clustering. We haven't found similarity (bootstrap value) among the isolates at the 3' NCR, even though we used NJ method with 1000 replicates. Most of the MNSV isolates are variable at 3' NCR which can be observed in fig-3.14 unlike the 5' NCR (clustered based on regions in other ORFs).

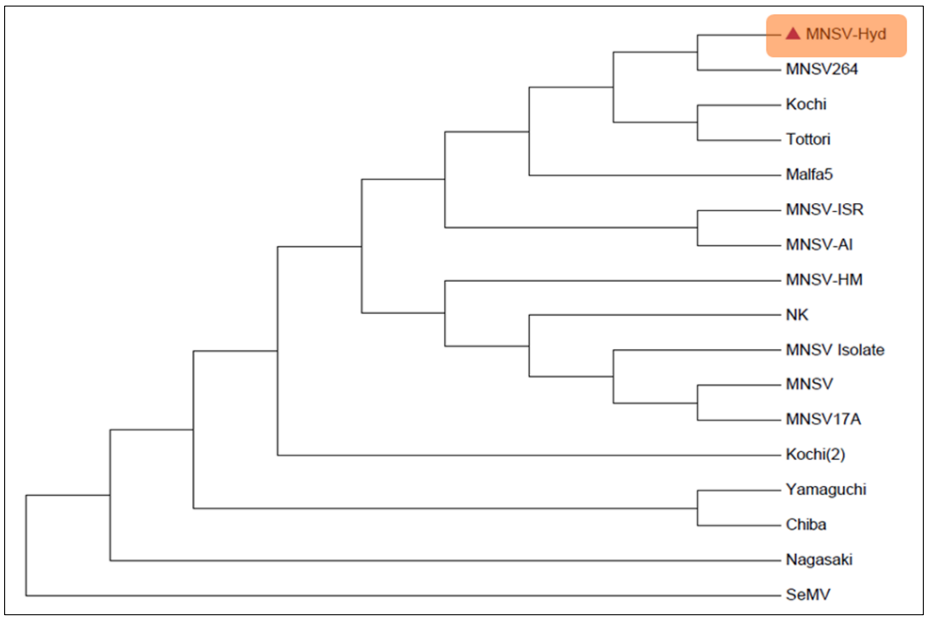

Fig-3.14: Phylogenetic comparison of 3' NCR of MNSV-hyd with the available MNSV isolates with NJ method. SeMV was used as out member. MNSV-Hyd was highlighted in the tree.

3.4 Discussion

The discovery of reverse transcriptase enzyme and PCR revolutionized the field of molecular virology by whole genome sequencing process including virus genomes. The first virus genome sequenced was that of a DNA virus, *Cauliflower mosaic virus* (CaMV) (Franck *et al*., 1980) and later the RNA virus, TMV (Goelet *et al*., 1982). From then several viruses are sequenced and used as molecular diagnostic tools in plant virology. Complete nucleotide sequence for 18 Carmoviruses are available in pubmed database. They include CarMV (Guilley *et al*., 1985), AnFBV (Adkins *et al*., 2006), NLVCV (Robertson *et al*., 2007), CCFV (Skotnicki *et al*., 1993), CPMoV (You *et al*., 1995), HCRSV (Huang *et al*.,

2000), CbMoV (Gulati-Sakhuja and Liu, 2010), JINRV (Takemoto *et al*., 2000), MNSV (Riviere and Rochon, 1990), PSNV (Suzuki *et al*., 2002), PFBV (Rico and Hernandez, 2004), SgCV (Weng and Xiong, 1997), TCV (Carrington *et al*., 1989), SYMMV (Nam *et al*., 2009), HSRV (Gulati-Sakhuja *et al*., 2011), GaMV (Ciuffreda *et al*., 1998), *Rosa rugosa leaf distortion virus* (RrLDV, Mollov *et al*., 2013) and *Rose yellow leaf virus* (RYLV, Mollov *et al*., 2014).

In the present chapter, the complete nucleotide sequence of MNSV-Hyd was determined by designing degenerate primers with reference to MNSV-A1 isolate as it was the first MNSV strain to have infectious clone (Diaz *et al*., 2003). Different regions of the MNSV-Hyd genome were amplified with great trouble using different primer sets in different combinations. The authentic end nucleotides of the viral genome were also confirmed by 3' & 5' RACE techniques (fig-3.4 and 3.5). More over the nucleotide sequence of the obtained fragments doesn't show similarity in NCBI blastn results. Only the translated protein sequence has similarity to the Carmovirus, MNSV watermelon strains Kochi & Tottori from Japan. It was reported that these two strains are also different from the other reported isolates of MNSV. These strains are unable to produce systemic infection on *Cucumis melo* (Ohki *et al*., 2008) which is consistent with our isolate (MNSV-Hyd). The NCBI blast data of the complete nucleotide sequence showed 75% homology with 52% of sequence coverage. The sequence coverage in the viral genome is in the RDRP region. The sequence coverage of MNSV-Hyd was more to the Spain isolates, A1, 264 & MNSV-Spain (fig-3.7).

The deduced genome organization of the new virus is similar to that of the reported MNSV genetic map with five ORFs and a leaky stop codon to translate the RDRP gene (largest protein, p89). The replicase function of the gene, p89 was confirmed by the presence of GDD motif which is a characteristic feature of the positive sense RNA viruses. The two sub-genomic RNA molecules are the characteristic feature of the Carmoviruses were also observed in the ds RNA profiling (Riviere and Rochon, 1990). The genome doesn't consist of cap at the 5' end and 3' end polyA tail which was confirmed by the 5' & 3' RACE methods respectively (Riviere and Rochon, 1990).

In comparison with the 12 different strains of Carmoviruses, MNSV-Hyd has more homology to PSNV in all the ORFs at protein level with maximum identity of 69% and RdRp and 7A has similarity at the nucleotide level also (tab-3.5). This proves the similarity

of the MNSV to PSNV which was reported earlier (Suzuki *et al*., 2002). The amino acid comparisons also proved that the identity is less in the p28 & CP region when compared to 7A and p89 genes (Suzuki *et al*., 2002). The identity was more with the MNSV isolates, Kochi, Tottori, 264, Malfa5 & A1 in both nucleotide and the protein comparisons (tab-3.5).

The taxonomic and phylogenetic relationship analysis to 12 virus species from all the genera in the family Tombusviridae showed its similarity to CarMV, type member of Carmovirus genus and with different members of genus it has similarity to PSNV among the Carmoviruses and clustered on separate branch with MNSV isolates (fig-3.9). Even though MNSV-Hyd shows homology to MNSV strains, more differences are observed at the nucleotide level indicating its diversity. All the individual gene trees showed lot of diversity at the nucleotide level with MNSV isolates. In most of the cases of phylogenetic analysis it is either clustering with watermelon strains of Japan or on an individual branch. The diversity was mainly observed in the p28 region, CP region and 3' NCR of MNSV-Hyd which might be the regions that may play an important role in host-pathogen interaction.

The specific primers designed to the MNSV-A1 template (tab-3.2; 1-22 primers) and to family members (tab-3.1;3-12) have never yielded us the positive results of amplification. Even after several trials of PCR in different combinations we were not able to amplify the desired regions. This difficulty in amplification process is due to the diversity in the virus at nucleotide level where we were not able to see the significant blast search of the sequenced fragments with blastn.A single nucleotide change *Hop stunt viroid* (HSVd) alters the cachexia symptoms in the citrus host. The pathogenic and the non-pathogenic strains of HSVd differ in the 'cachexia expression motif' by five to six nucleotides. It was shown that the changes in the motif play a major role in the symptom expression (Serra *et al*., 2008). The 3' NCR is responsible for the replication in *N. benthamiana* was proved in MNSV-264 isolate (Nieto *et al*., 2006). The clustering of the MNSV-Hyd with MNSV-264 was observed in the phylogenetic tree constructed for the 3' NCR unlike the other trees (Kochi, Tottori). F3.7This might be the region which is causing variation in the host range (Miras *et al*., 2014) of MNSV-Hyd (Fabaceae members, Chenopodaceae members, *Mimordica charantia* and *N. benthamiana*) with comparison of the other MNSV isolates from Japan and Spain (narrow host range restricted to Cucurbitaceae members). At the 5' NCR regions, even the MNSV-Hyd clustered with watermelon strains of Japan the branch length was more indicating its divergence from all the reported strains. The length of the NCRs is more

variable in MNSV-Hyd in comparison to reported isolates (tab-3.7). At the 5' end the NCR is more as in case of Kochi and Tottori in comparison to other isolates. But the 3' NCR is smaller than the reported isolates (tab-3.7A, B). Might these NCRs are responsible for the diversity in the host range of the virus (Miras *et al*., 2014) but need to be tested with swapping of the regions with other strains. We can observe the diversity in the NCRs in molecular evolutionary trees with less or no bootstrap values on the branch (fig-3.13; 3.14).

A

Name of the strain	No.of nts in 5'NCR
MNSV-Hyd	244
Kochi	268
Tottori	268
264	323
Yamaguchi	280
Nagasaki	282
Kouchi	282
Chiba	281
MNSV-17A	279
MNSV isolate	275
MNSV-ISR	279
Malfa5	287
HM	279
A1	280

B

Name of the strain	No.of nts in 5'NCR
MNSV-Hyd	98
Kochi	93
Tottori	93
264	87
Yamaguchi	88
Nagasaki	89
Kouchi	89
Chiba	89
MNSV-17A	86
MNSV isolate	86
MNSV-ISR	88
Malfa5	84
HM	88
A1	88

Tab-3.7: Difference in the nucleotides of NCR of MNSV-Hyd with the other isolates. A) Representation of number of nucleotides in 3' NCR; B) Representation of number of nucleotides in 5' NCR of different isolates.

Monopartite viruses are not that evolved in comparison to multipartite viruses. The mutation rates are more in RNA viruses with larger genomes. The smaller genomes can replicate effectively without the interference of recombination. Due to the segmentation in the genome, the replication could be faster with its own regulatory sequences (Navarro *et al*., 2013). The smaller genomes are more stable with low packaging density which is not observed in monopartite viruses. Due to these reasons a great variation was observed in the architecture of the genome of viruses, polarity in case of RNA viruses and in the genome size. All these will provide us an opportunity to study about the various molecular aspects and virus etiology by constructing infectious clones (chapter-4).

Virus species always consists of variations and not uniform population and termed as quasispecies (Domingo *et al*., 2006; Hull, 2014). Several new viruses are reported now-a-days due to their variations in genetic sequences and are left without being classified which is important for the development of disease control strategies (Hull, 2014). The different criteria used for the classification of the newly identified virus as a strain or isolate. They include nucleic acid sequence variation, molecular evolutionary trees, architecture of the virus particle, electrophoretic mobility, serological properties and biological criteria like macroscopic symptoms, cytological effects, host range, type of transmission and cross protection (Hull, 2014).

Till today there is no single assay system or the test to confirm the virus as an isolate or a strain. Based on the percentage of differences in the above parameters, the virus in the present work was identified as a new strain of MNSV from India. Here, both the biological characteristics of the virus (from chapter-2) and the molecular parameters from the present chapter were considered and compared to that of the reported MNSV isolates and assumed it to be a new strain rather than isolate. To our knowledge, it was the first report of MNSV from the Indian shores.

CHAPTER-4

Construction of full length infectious clone using agrobacterium T-DNA transient expression based approach

4.1 Introduction

The study of the plant RNA viruses was made easier with the discovery of the reverse genetics approach since mid-1980s. Forward genetics is the study of natural phenotype by manipulating the organism genotype whereas reverse genetics approach is the study of induced variation within the specific gene and to conclude gene function. This is the key step that helps the scientists to develop the infectious cloning technology and to study the role of each gene by mutational studies and gene silencing mechanisms In spite of the general genome organization and replication of the viruses, the mutational studies (deletions, insertions, substitutions), complementation tests, host-pathogen interactions, mechanism of defective interfering RNA (DI), satellite RNA genesis, antiviral strategies and preparation of new viral vectors can be studied with the construction of the infectious cDNA clones (*in vivo*)/transcripts (*in vitro*) (Voinnet *et al*., 2003).

Infectious transcripts/cDNA clones are nothing but the biologically amplifiable synthetic molecules, and are subjected to the RNA recombination events or genetic modifications. Infectious clones were generated by cloning the viral genome under the control of bacteriophage RNA promoters like T7, SP6, or T3 for *in vitro* assay (Chapman, 2008) or under the constitutive promoter such as *Cauliflower mosaic virus* (CaMV) 35S promoter for *in vivo* assay (Gopinath *et al*., 2005). For RNA viruses, cDNA clones of the complete genome serve as templates for the construction of infectious clones. The first plant virus which has the infectious clone was *Brome mosaic virus* (BMV, Ahlquist *et al*., 1984). After that infectious transcripts were produced for another two viruses TMV and ToMV (*Tomato mosaic virus*) under modified lambda promoter. The additional nucleotides at the 5' end and 3' end have lethal effect on the infectious clone even after the change of promoter to SP6/T7 bacteriophage RNA promoters. Moreover, the transcription kits are costly which is not affordable by the researcher and handling of RNA transcripts for mechanical inoculation is also a challenging task.

Therefore efforts were made to find cheaper and robust technique for the infection than *in vitro* method. The outcome of the efforts was the infectious cDNA clones (icDNA) were constructed in the binary vectors under the constitutive promoter at 5' end. The non-viral nucleotides at the 3' end of the genome were removed by adding the self-cleavage sequence of a ribozyme. As in previous constructs the infectivity depends on the authentic end nucleotide of the genome at 5' end after the promoter sequence (Marillonnet *et al*., 2005).

Several methods are in use to deliver the infectious clones into plants. Mechanical inoculation, agroinfiltration and biolistics are the common methods employed for whole plant inoculation whereas electroporation, microinjection and liposome mediated injections are employed for the inoculation of protoplasts (Nagyova and Subr, 2007). In mechanical inoculation, the plants are mechanically damaged with the help of abrasive and helps in the direct inoculation of nucleic acid material. The biolistic and microprojectile bombardment are used earlier which are costly and later replaced by the agrobacterium T-DNA based transient expression system (Chapman, 2008). The functional analysis of the transgene in stable transformation is very grueling, time consuming (even few years) and labor demanding processes. Stable transformations are even effected by the gene insertions and copy number of the inserted genes (Wroblewski *et al*., 2005).

Agroinfiltration is a transient expression system where plants were infiltrated using the ability of agrobacterium to infect plants and to release its T-DNA present in the right and left boarders in to the cell nucleus (Marillonet *et al.,* 2005). Agrobacterium based binary vectors are widely used for delivery of the infectious clones into the plant cell. This method has been used for infecting both DNA & RNA viruses (Chiba, 2006) and monopartite & multipartite viruses (Ratcliff *et al*., 2001; Liu and Lomonossoff, 2002). In addition to the viral functions to be observed at the cellular level, cultured tissues and whole plant level expression was also observed using the viral vectors in a process known magnifection which is highly helpful in antibody expression (Marillonet *et al.,* 2005; Giritch *et al*., 2006). The transient expression system is effective in tobacco (Sheludko *et al*., 2006), grapevine (Santos-Rosa *et al*., 2008), lettuce, tomato, *Arabidopisis* (Wroblewski *et al*., 2005), switchgrass (Vander Gheynst *et al*., 2008), radish, pea, lupine and flax (Van der Horn *et al*., 2000), Rice (Purkayastha et al., 2010), *Cyamposis tetragonaloba* (Govind *et al*., 2012) and in many plants after that. Among all the hosts, tobacco can be readily transformed by the Ti plasmid derivatives and the whole plant contains the insert gene. This technique is used in

plant biology to provoke the transient expression of genes in the plant or to produce the desired protein. The foreign gene was inserted into T-DNA of the agrobacterium; the culture was infiltrated into the leaf such that each cell will receive multiple copies of T-DNA molecules from the culture and then monitoring the transgene expression during the next few days (Annamalai *et al*., 2005; Gopinath *et al*., 2005). This process is relatively a simple process which decreases the time required for testing the transgene and stands as a best method to evaluate the potential of the transgene (Leckie and Stewart, 2011). Unlike the mechanical inoculation, handling of the agrobacterium culture is easy and can manipulate the infection by increasing or decreasing the culture density (Gopinath *et al*., 2005).

With this background the main objective of this chapter is set to construct an infectious clone for MNSV-Hyd which was easily manipulated consecutively that will facilitate to study the etiology of the pathogen and to perform functional analysis of individual genes which also helps in development of antiviral approaches. The construction of icDNA molecule in binary vector under the constitutive promoter is the most time consuming step in the agroinfiltration assay system.

4.2 Methods

4.2.1 (a) Restriction digestion and ligation

In order to construct a full length infectious clone to MNSV-Hyd, unique restriction sites are identified with in the overlapping region of the two clones that should not cut elsewhere in the sequence. The plasmids containing the two fragments to be joined were digested with the respective unique restriction enzymes for 2 h (section 3.2.9) and the inserts were ligated (section 3.2.5) into appropriate vectors.

4.2.1 (b) Primer overlap extension PCR

The sequence of interest was added to the desired fragment through the primer in PCR amplification process. This method was employed to introduce rhybozyme sequence at the end of the genome. A new primer was designed with 15 extra nucleotides to be added and 20-25 nt overlap of the desired fragment. The second primer will be the same that was used for the amplification of the insert in the template clone. The ribozyme sequence was added to the 3' end of the viral genome by primer extension PCR using the forward primer ODT2 (tab-4.3, primer-8) and the reverse primer (MRZI, tab-5.1, primer-7) that will bind to 3' end of the sequence with 15 nt of ribozyme sequence overhang. The PCR amplified product was gel extracted (section 4.2.5) and used as template for the second round of PCR.

The second reverse primer, MRZ2 (tab-5.1, primer-8) with overlapping sequence to the MRZI primer that binds to 3' end of the template. Now, the amplified PCR product consists of 3' overhang of ribozyme sequence was gel extracted and cloned into pGEMT-Easy vector (according to 4.2 protocols). Six positive clones were sequence confirmed for the presence of ribozyme and the resultant clones are designated as p3'RZ.

4.2.2 PCR based site directed mutagenesis

Two mutagenic primers of 30 nt, forward and reverse were designed on the opposite strands in the region of point mutation to be incorporated (tab-4.1). Mutation was incorporated in the forward primer with 30 nucleotides of binding capacity. The high fidelity PCR with vent polymerase was carried out in 50 µl reaction with 2U of enzyme, 3 µg of plasmid bearing the insert as template. The reaction mixture contains 5 µl of 10X buffer, 4 µl of 100 ng/µl concentration primers, 1µl of 25 mM dNTPs and 0.5 µl of 25 mM $MgCl_2$. The PCR cycling conditions were at 94˚C for 5 min for one cycle, 20 cycles of 94˚C for 50 sec, annealing temperature of 55˚C for 1 min and at 68˚C for 1min/kb +1 min extra time limit. The obtained PCR product was precipitated with isopropanol at 13,000 rpm for 10 min at 4˚C. Supernatant was discarded and the pellet was washed with 70% ethanol, air dried and dissolved in 18 µl of 5 mM tris pH-7.0. The purified PCR product was digested with *Dpn*I enzyme for overnight at 37˚C (Kunkel, 1985). The digested product was transformed into DH5α strain of *E.coli* cells by heat shock method. The plasmids were isolated by alkaline lysis method from the transformed colonies and the positive clones with the desired mutation were confirmed by digesting with restriction site (in case of mutation of the restriction site) with proper controls or by sequencing the plasmids.

4.2.3 (a) Agro chemical competent cells preparation

Stored agobacterium glycerol stock was streaked for single colonies on fresh LB rifampicin plate and isolated single colony was inoculated into 2 ml of LB broth containing 25 µg/µl of rifampicin (A1.22) from fresh plate and incubated at 28˚C for 48 hr with shaking. 200 ml of LB broth containing rifampicin as antibiotic was inoculated with 2 ml of culture and incubated at 28˚C for 7-8 hrs until the culture reaches 0.6 OD at 600 nm. The flask was incubated on ice for 30 min and the cells were harvested by subjecting the culture to centrifugation at 3,000 rpm for 15 min at 4˚C. The supernatant was discarded and the pellet was re-suspended in 100 ml of 10 mM $CaCl_2$ properly. The culture was again

subjected to centrifugation at 3,500 rpm for 10 min at 4˚C. The supernatant was discarded and the pellet was re-suspended in 10 ml of 10 mM $CaCl_2$ containing 15% glycerol. 200 µl of competent cells were aliquoted in 1.5 ml microfuge tubes, frozen in liquid nitrogen and stored in -80˚C for future use.

Sl.No	Name of the primer	Sequence (5'-3')	Purpose
1	MSmaI KO+	GAC TCC AGA GTA ATC CCCTGG GCA ATA CTG AGA CG	Primers used for the silent mutation of *Xma*I at position 2710
2	MSmaI KO-	GCT CTC AGT ATT G CCCAGG GG ATT ACT CTG GAG TC	
3	Mase KO+	CCT GTT CAC CCT CGT C ATCAAT GC TAG CAC TGT TAC	Primers used for the silent mutation of *Ase*I at position 2979
4	Mase KO-	GTA ACA GTG CTA CG ATTGAT G ACG AGG GTG AAC AGG	
5	MCP Ase I KO-	GAG TTT AGT GAC TCC ATTGAT GAC CAC AGG AGC ATA AAC	Primers used for the silent mutation of *Ase*I at position 3810
6	MCP Ase I KO+	GAA TAT GCT CCT GTG GTC ATCAAT GGT GTC ACT AAA CTC	
7	MRZ1	CAG AAG ACA TGT GAA TCA TGT CTT GAT GGC GGG GCC ACT TAA GTG GCC TC	Ribozyme sequence added at the 3' end
8	MRZ2	GCC CGG GCC GTT TCG TCC TCA CGG ACT CAT CAG AAG ACA TGT GAA TCA TGT CTT GA	
9	Pcb301 BglII	GAT GAC CTG GTG CAT TGC AAA CGC TAG G	35S promoter added to the 5' end of the genome
10	35S MNSV NheI	GGA ATA GTG GCT AGC TAT CCC CTC TCC TCT CCA AAT GAA ATG AAC TTC CTT ATA ATG	

Tab-4.1: List of primers used in the present chapter.

4.2.3 (b) Freeze-thaw method

A tube of prepared chemical competent cells was obtained from -80˚C freezer and thawed by placing it on ice for 5 min. To it approximately 3-4 µg of binary plasmid DNA was added, mixed well by tapping gently and incubated on ice for 20 min. Then transformation was performed by placing the microfuge tubes in liquid nitrogen (liq. N_2) for 5 min and thawed it by placing it in 37˚C water bath for 5 min. This step was repeated twice and the microfuge tubes were incubated at 28˚C for 3 h by adding 1 ml of LB broth (without antibiotic). The culture was spun down at 8000 rpm for 2 min at 4˚C and the supernatant was discarded, the pellet was dissolved in 100 µl of LB broth and plated on to the LB medium containing appropriate antibiotics. The plate was incubated at 28˚C in inverted position (small colonies were visible on the 2^{nd} day).

4.2.4 Agroinfiltration

The freshly transformed and PCR confirmed single agrobacterium colonies were inoculated in 2 ml culture with LB-kanamycin and rifampicin antibiotics at 50 µg/ml concentration. The culture was grown at 28˚C for 36 h at 170 rpm. The grown culture was used as inoculum to inoculate 10 ml of LB-kanamycin and rifampcin as antibiotics supplemented with 0.2 ml of 500 mM MES buffer pH-5.85 and 1.3 µl of 150 mM acetosyrinzone. The inoculated broth was incubated for overnight to noon at 28˚C for optimum growth. The bacterial cells were harvested by subjecting to centrifugation at 6,000 rpm for 10 min at 4˚C. Supernatant was decanted and re-suspended the bacterial pellets in 1 ml of infiltration buffer (10 mM $MgCl_2$). The bacterial culture was inducted with 15 µl of 150 mM acetosyrinzone for overnight. The induced culture was used to infiltrate *N. benthamiana* plants (8-9 weeks old) at 0.3-0.5 OD at 600 nm (diluted with infiltration buffer). The culture was infiltrated on the abaxial surface of leaf using the blunt ended syringe without damaging the leaf. The plants were maintained at 25˚C with 16 h light and 8 h dark period (Gopinath *et al*., 2005). The results were analyzed after 24-36 h of post infiltration (hpi) by SDS-PAGE/western blotting and by Confocal laser scanning microscopy (CLSM) in case of GFP constructs.

4.2.5 Total RNA extraction

The leaf material was weighed (500 mg), placed in the cold motor and macerated with help of pestle by adding 5 ml of RNA extraction buffer (App. A1.23) to make it into slurry. 750 µl of slurry was collected into 2.0 ml microfuge tube and incubated at 42˚C for 20 min. Equal volume of water saturated phenol and chloroform (1:1 ratio) was added followed by vigorous mixing and separated by subjecting the tube to centrifugation at 14,000 rpm for 15 min at 4˚C. Without disturbing the tube after centrifugation, the aqueous phase was collected into sterile microfuge tube and the nucleic acid was precipitated by adding equal volume of ice cold isopropanol and 1/3rd volume of 4 M LiCl and incubated in -80°C for 10 min. The nucleic acid was pelleted by subjecting to centrifugation at 14,000 rpm for 20 min at 4˚C. Supernatant was discarded and the pellet was washed twice with 70% alcohol by spinning at 14,000 rpm for 10 min. The pellet was air-dried and dissolved in 50 µl of sterile milli-Q water. The integrity of the RNA samples was analyzed by 1% agarose gel electrophoresis (section 2.2.7).

4.2.6 Electro-elution of vector backbones

The vector backbones (especially higher molecular sizes) were prepared by digestion with the respective restriction enzymes. Upon completion of the restriction digestion, the mixture was subjected to 1% agarose gel electrophoresis and the vector backbones were gel extracted by following the electro-elution process. The backbones were excised from agarose gel and placed in a dialysis bag containing 2-3 ml of working concentration of TAE buffer (tank buffer, A1.29) that was sealed on one end. After placing the gel piece the other end of the dialysis bag was also sealed securely without leakage and air bubbles inside the bag. The bag was placed in the tank containing the TAE buffer on anode side (without floating in the buffer). The electrophoresis was conducted at 100 V for 1 h and the reverse flow of current was conducted for 30 sec. The bag was opened and the TAE buffer was collected into microfuge tubes. The DNA was precipitated with 1/3rd volume of 2.5 M sodium acetate and equal volume of isopropanol. The precipitation was enhanced by placing the tubes in -80˚C freezer for 10 min. The precipitated DNA was collected by subjecting to centrifugation at 13,000 rpm for 10 min. The pellet was washed with 70% ethanol and centrifuged at 13,000 rpm for 10 min. The pellet was air-dried and dissolved in 30-40 µl of 5 mM tris pH-7.4. The concentration of the eluted product was analyzed by Nanodrop (NanoDrop Technologies, Inqaba Biotechnical Industries (Pty) Ltd, SA) at 260 nm or by 1% agarose gel and used in the cloning.

4.2.7 Colony PCR

Sl. No	Primer Name	Sequence (5'-3')	Purpose
1F	Pcb301 209+	CCA TCG TTG AAG ATG CCT CTG	Used to amplify fragment-A
1R	M725 *Eco*RI-	CA GAA TTC AAA AGA GCC CGA CTC GTG	
2F	M1261*Hind*III+	GCA AGC TTG CGA ATC GCT TGA AGG ACT GGC	Used to amplify fragment-B
2R	M7B *Xhoba*I-	G CTC GAG TCT AGA TTA ACC ATC GCC ATT CGT TGA GAT TCC	
3F	M7A *Eco*RI+	C GAA TTC GAT GCT CAA CGA ACT GTA GAT C	Used to amplify fragment-C
3R	M3355 *Bam*HI-	CAGA CTC CAG AGT AAT CCC CGG GGC	
4F	MCP *Nco*I+	G CCATG GCG ATG GTT AAA CGC GCA AAC	Used to amplify fragment-D
4R	Mend *Xma*I	GCC CGG GCG GGG CCA CTT AAG TGGG CCT CAA TTC	
5	MCP*Xhoba*I-	G TCT AGA CTC GAG CTA TAC AAG GTA AGC TAC CTC ACT GG	Used to amplify CP

Tab-4.2: Specific primers designed to MNSV-Hyd

Confirmation of the transformed plasmid was performed through colony PCR according to Sambrook *et al*., 2001. Single isolated colony from the transformed plate was selected and picked the colony with sterile toothpick, streaked on fresh plate and the remaining colony was diluted in 200 µl of milliQ water. The diluted colony of 2 µl was used as template for PCR amplification and the remaining PCR conditions were same as described in 3.2.3a.

4.3 Results

4.3.1 Fusion of overlapping clones

As described in earlier chapter-4, the genome sequence of MNSV-Hyd was obtained in five different mother clones (tab-4.3) that encompass the complete genome. The clones were pTZ57R/T T/A cloning vector or pGEMT-Easy vector. The clones with 100% similarity were only selected for the construction of infectious clones.

We used two approaches to assemble the full length clone; 1) restriction digestion (4.2.1a) and 2) primer overlap extension PCR (4.2.1b). A serious consideration in selection of clones was that in the overlapping region of the adjacent clones 100% sequence homology was observed. We tried to choose the unique restriction sites within the overlapping sequence that did not cut anywhere in the selected two fragments. If we are not able to acquire any unique restriction site in the two fragments then we selected the subsequent sites to clone the fragments in two pieces in other cloning vectors with respective restriction sites. The full length infectious clone was obtained in different steps as shown in the diagram (fig-4.1) which will be described in later parts in a detailed way.

Fragment number	**Size of the fragment**	**Assigned name to the clone**	**Encompassing the region of the genome (nucleotide number)**
clone-1	0.8 kb	p5'TGN	(start) 1-770 nt
clone-2	1.2 kb	pTVR	750-1756 nt
clone-3	2 kb	pTNVR	1298-3405 nt
clone-4	1.2 kb	pTGC	2708-4127 nt
Clone-5	0.6 kb	p3'NCR	3719-4274 nt (end)

Tab-4.3: Representation of the mother clones that encompass the whole viral genome.

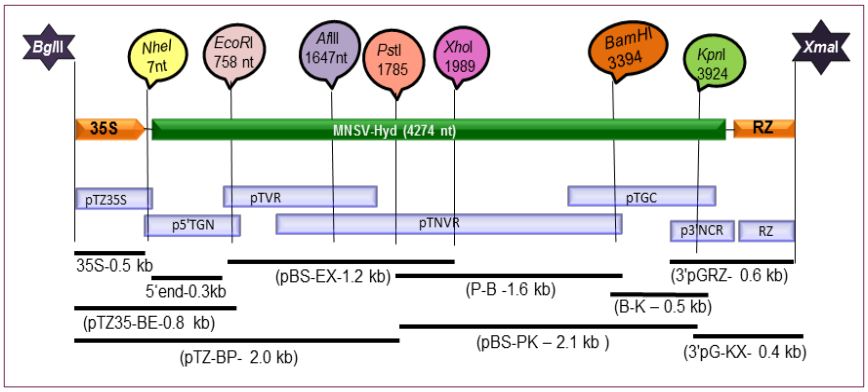

Fig-4.1: Pictorial representation of the unique restriction sites and the generation of different intermediate clones in the process of infectious clone construction. Gray color boxes are the representation of the mother clones of MNSV-Hyd with their respective nomenclature inside the box. Bars represent the intermediate clones and their sizes. 35S and RZ represents 35S double promoter at 5' end and ribozyme sequence at 3' end of the genome respectively.

4.3.2 Amplification and cloning of 3S promoter sequence

Initially 35S double promoter was added to the 5' end of the viral genome for efficient *in vivo* transcription process. The 35S double promoter having 550 bp was amplified from BMV R3 clone (Gopinath *et al*., 2005) as template with specific forward primer with *Bgl*II restriction site and the reverse primer having the extra 15 nt of MNSV 5' end sequence (tab-4.1; primers-9 and10) (fig-4.2A). The amplified PCR fragment was gel extracted (fig-4.2B) and ligated into pTZ T/A vector. The confirmed clones were designated as pTZ35S (fig-4.2C) and were sequence confirmed.

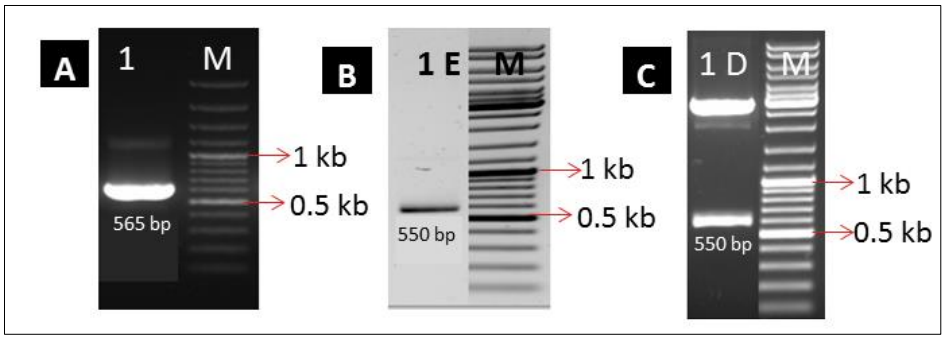

Fig-4.2: Amplification and cloning strategy of 35S promoter sequence from BMV R3 plasmid. A) PCR amplification of 565 bp product (550+15) with specific primers containing 15 nt overlap of MNSV 5' NCR sequence in the reverse primer; B) gel elution of PCR amplified product; C) cloning and restriction digestion of pTZ T/A clone for confirmation of positive clones.

4.3.3 (a) Step-1: Fusion of 35S promoter sequence to clone-1(p5'TGN)

This pTZ35S clone has 15 nt of overlapping sequence with the clone-1(p5'TGN) and it comprises of unique restriction site *Nhe*I within the overlapping region. The p5'TGN clone was digested with *Nhe*I and *Eco*RI restriction enzymes to release 0.75 kb fragment (fig-4.4B). The strategy used in the cloning process was represented in Fig-5.3. The pTZ35S plasmid containing the 35S double promoter gene was digested with *Nhe*I and *Eco*RI restriction enzymes (fig-4.4A) (clones are chosen in such a way that it consists of *Bgl*II and *EcoR*I enzymes at the opposite ends) and the digested backbone was electro eluted from the gel as described in 4.2.6 (fig-4.4C). The released insert from p5'TGN clone (0.75 kb) (fig-4.4D) was ligated into the prepared pTZ35S backbone (fig-4.4C). The ligated insert was confirmed by restriction enzyme digestion, *Bgl*II & *EcoR*I enzymes to release 1300 bp fragment (fig-4.4E). The resultant positive clone was named as pTZ35-BE.

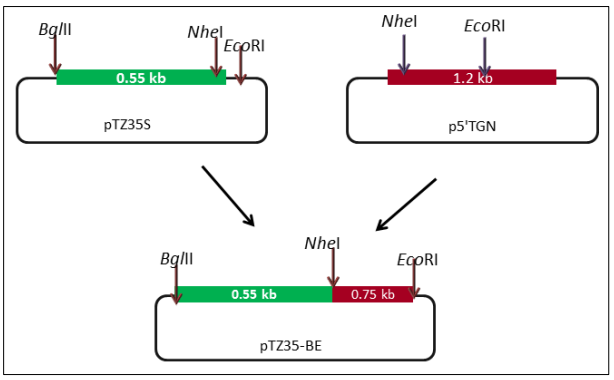

Fig-4.3: Strategy used for the fusion of 35S promoter sequence to clone-1(p5'TGN)

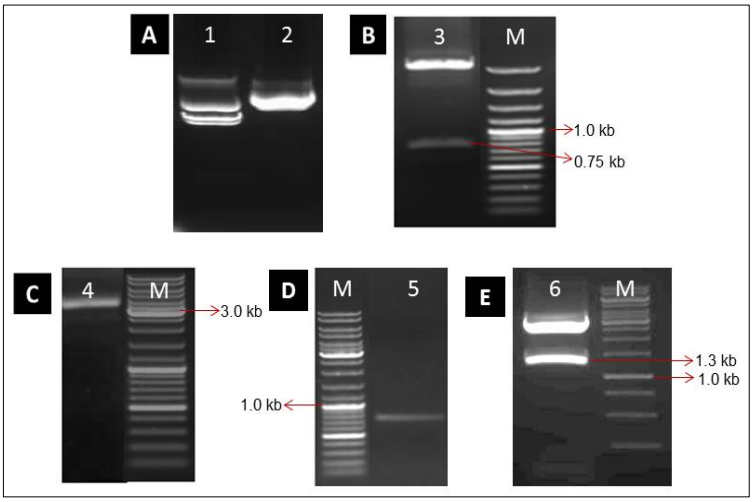

Fig-4.4: Cloning strategy of step-1. A) Vector backbone digestion, 1- Uncut pTZ35S clone, 2- pTZ35S plasmid digested with *Nhe*I and *EcoR*I to release~ 50 bp fragment. B) Digestion of p5'TGN clone with, 1- *Nhe*I and *EcoR*I to release 0.75 kb fragment, M- DNA marker. C) Electro-elution of pTZ35S vector backbone digested with *Nhe*I and *Eco*RI, D) gel extraction of 0.75 kb insert from p5'TGN, E) Confirmation of recombinant plasmid, pTZ35-BE by restriction digestion with *Bgl*II and *EcoR*I to release 1300 bp insert.

4.3.3 (b) Step 2: Fusion of fragments from pTVR and pTNVR clones

The clone-2 (pTVR) and clone-3 (pTNVR) are having the overlapping region of 456 nt and both the clones comprises of sequence from 750 to 3405 nt in the whole genome of MNSV-Hyd. The unique restriction site found in the overlapping region was *Afl*II. In clone, pTNVR two internal sites of *Eco*RI and *Hind*III were observed which cannot be used for the cloning purpose. Moreover none of the unique restriction sites were found at the end of the pTNVR clone. So, *XhoI* was used which is present in the middle of the gene (fig-4.5). The pTVR clone (clone-2) was digested with *Eco*RI and *Afl*II sites (fig-4.6A) and the pTNVR clone (clone-3) was digested with *Afl*II and *Xho*I (fig-4.6B), which are unique restriction sites in the respective clones.

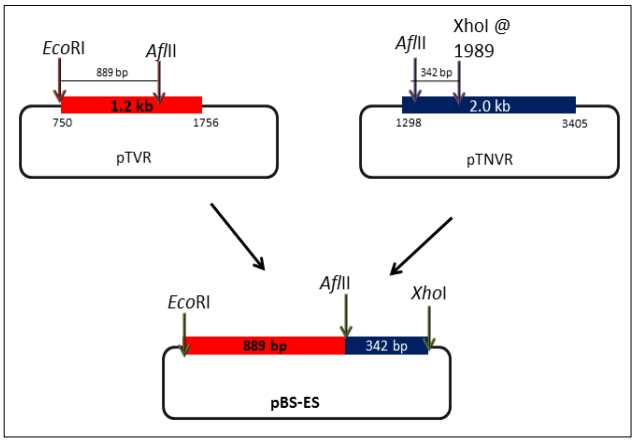

Fig-4.5: Strategy used for step-2 cloning. Region encompassing in the complete genome was represented to the bottom of the fragments. Digested fragment sizes were also represented between the restriction sites. pBS-pBS KS+ vector.

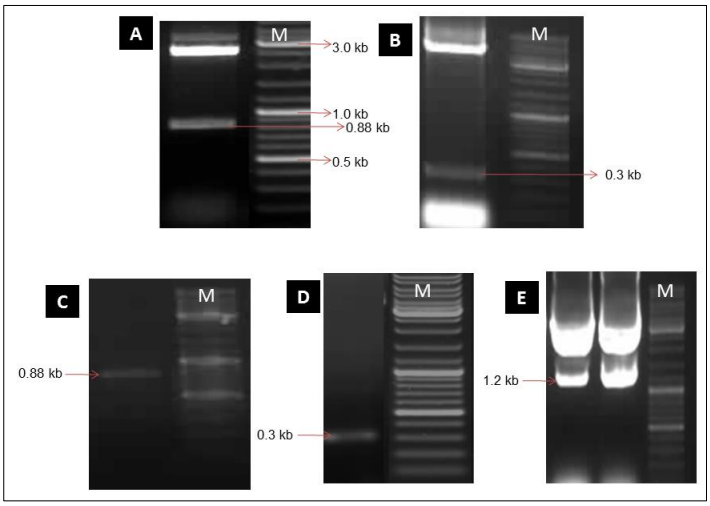

Fig-4.6: Fusion of fragments from pTVR and pTNVR clones. A) Digestion of pTVR clone with *Eco*RI and *Afl*II to release the insert of 889 bp, M- 1 kb DNA marker and size denoted on the right of it (same ladder used in all the gels); B) pTNVR clone digested with *Afl*II & *Xho*I (size- 342 bp); C) gel extracted 889 bp insert from pTVR clone; D) gel extracted 342 bp insert from pTNVR clone; E) restriction digestion analysis of the recombinant clone, pBS-EX clone with *Eco*RI & *Xho*I to release total size of 1231 bp.

These two fragments were eluted (fig-4.6C, D) and ligated into pBluescript KS+ vector (pBS+) backbone, which is also prepared by digestion with *Eco*RI and *Xho*I. The eluted inserts were ligated into the prepared pBS+ backbone. The ligated product was

transformed into DH5α cells and the clones having the insert of length of 1231 bp were selected as positive recombinant clones and named as pBS-EX (fig 4.6E).

4.3.3 (c) Step 3: Fusion of fragments from pTZ-BE and pBS-EX clones

Now both the above two fragments from the clones generated in step-1 and step-2 were ligated together into the pTZ T/A cloning vector (fig-4.7). The pTZ-BE clone was digested with *Bgl*II and *Eco*RI enzymes to release 1300 bp insert (fig-4.8A). The pBS-EX clone was cleaved with restriction enzymes *Eco*RI and *Pst*I to release 1023 bp insert (fig-4.8B).

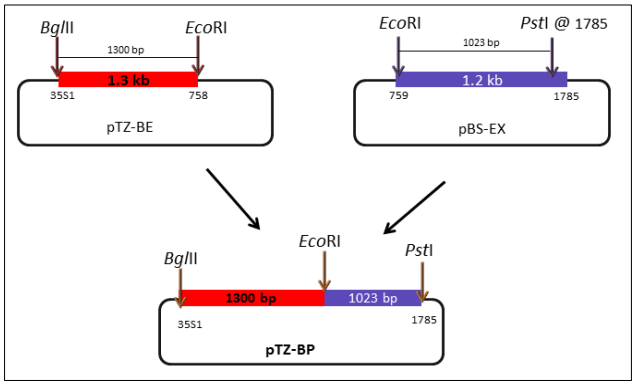

Fig-4.7: Strategy used for step-3 cloning. Region encompassing in the complete genome was represented to the bottom of the fragments. Digested fragment sizes were also represented between the restriction sites. 35S1- 35s promoter sequence first nt.

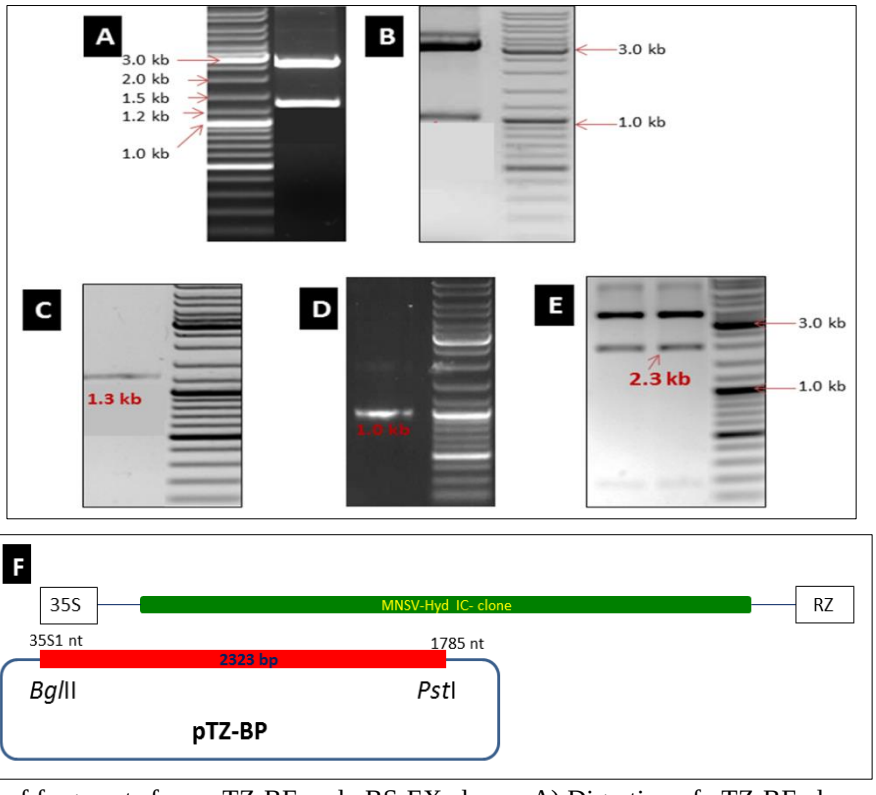

Fig-4.8: Fusion of fragments from pTZ-BE and pBS-EX clones. A) Digestion of pTZ-BE clone with *Bgl*II and *Eco*RI to release the insert of 1300 bp, M- 1 kb DNA marker and size denoted on the right of it (same ladder used in all the gels); B) pBS-EX clone digested with *Eco*RI and *Pst*I (size- 1023 bp); C) gel extracted 1.3 kb insert from pTZ-BE clone; D) gel extracted 1023 bp insert from pTZ-BE clone; E) restriction digestion analysis of the recombinant clone, pTZ-BP clone with *Eco*RI and *Pst*I to release total size of 2323 bp; F) Overview of the complete cloning in full length context after the three successive steps. The fusion fragment overlaps from 35S to 1785 nt in MNSV-Hyd sequence template.

Both the inserts were gel extracted using Nucleospin columns (fig-4.8C, D) according to mentioned protocol in section 3.2.5. pTZ T/A vector was digested with restriction enzymes *Bgl*II and *Pst*I and the resultant backbone was agarose gel extracted by following the protocol in section 4.2.7. The purified inserts were ligated into the prepared pTZ57R/T backbone digested with restriction enzymes *Bgl*II to *PstI* sites to release the fusion fragment of 2323 bp (fig-5.8E). The positive recombinant clones were designated as pTZ-BP. With this fusion fragment about half of the MNSV-Hyd sequence was cloned into pTZ clone using unique restriction sites (fig-4.8F).

4.3.3 (d) Step 4: Fusion of fragments from pTNVR and pTGC clones

To fuse the second half of the genome (fig-5.8F), two clones (pTNVR and pTGC) are selected,having overlapping region of 697 nt. The unique restriction site was identified as *Bam*HI in the overlapping region. Here, the pTNVR clone was digested with *Pst*I at the 5' region and with *Bam*HI on the 3' region to release the insert of size 1612 bp (fig-4.10A). The released fragment was purified through the columns from Nucleospin (fig-4.10C). The pTGC clone was digested with *Bam*HI and *Kpn*I restriction enzymes at 5' and 3' regions respectively and the released 535 bp fragment (fig-4.10B) was gel extracted (fig-4.10D). The vector pBS+ backbone was also digested with *Pst*I and *Kpn*I restriction enzymes. The eluted inserts were ligated into the prepared pBS+ backbone and transformed by following the standardized protocol. The recombinant positive plasmids were analyzed by restriction enzymes *Pst*I and *Kpn*I to release the fusion fragment of 2147 bp (fig-4.10E). The resultant positive clone having the insert from *Pst*I site to *Kpn*I site was named as pBS-PK (fig-4.10). The complete strategy was pictographically represented in fig-4.9.

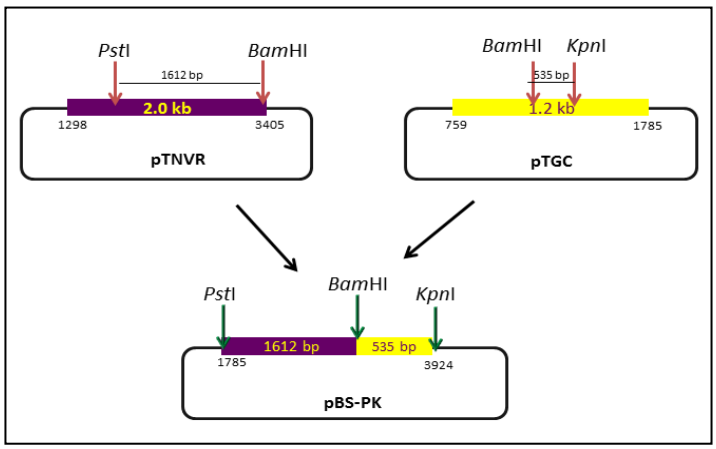

Fig-4.9: Strategy used for step-4 cloning of second half of MNSV-Hyd genome. Region encompassing in the complete genome was represented to the bottom of the fragments. Digested fragment sizes were also represented between the restriction sites.

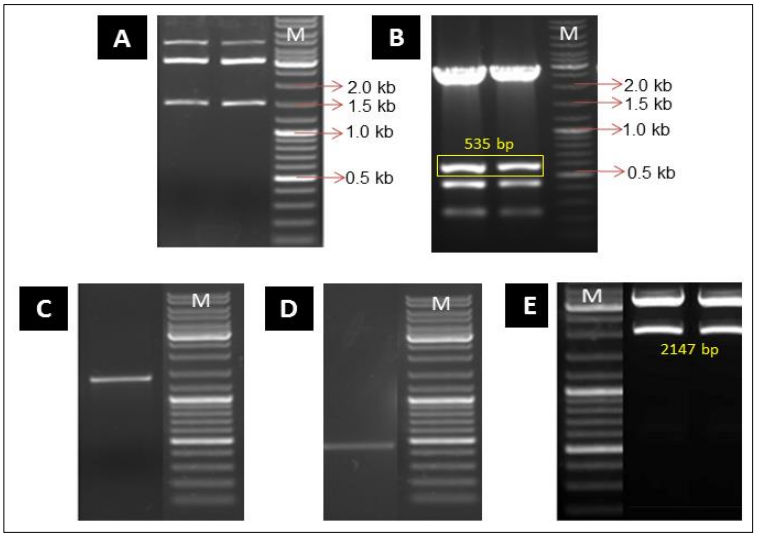

Fig-4.10: Cloning process to fuse the fragments from pTNVR and pTGC clones. A) Restriction digestion of pTNVR clone with *Pst*I & *Bam*HI (1612 nt), M- 1 kb ladder, sizes represented on the right side of the gel (same ladder was used in all the gels); B) restriction digestion of pTGC clone digested with *Bam*HI & *Kpn*I (different sizes were released due to the presence of same sites in pTZ T/A vector); selected fragment was shown in yellow box; C) gel extraction of 1612 bp fragment; D) gel extraction of 535 bp insert from pTGC clone; E) Recombinant clone consisting of 1612 & 535 bp fragments, release of 2147 bp fragment by digestion with *Pst*I & *Kpn*I enzymes.

4.3.3 (e) Step 5: Silent mutation of restriction sites in clone pBS-PK

Restriction site *Xma*I (CCCGGG) and two *Ase*I (ATTAAT) sites (both in CP region) in the clone pBS-PK were silent mutated as they interfere in further cloning manipulations. The mutagenic primers were designed in the respective sites as described in section 4.2.2.

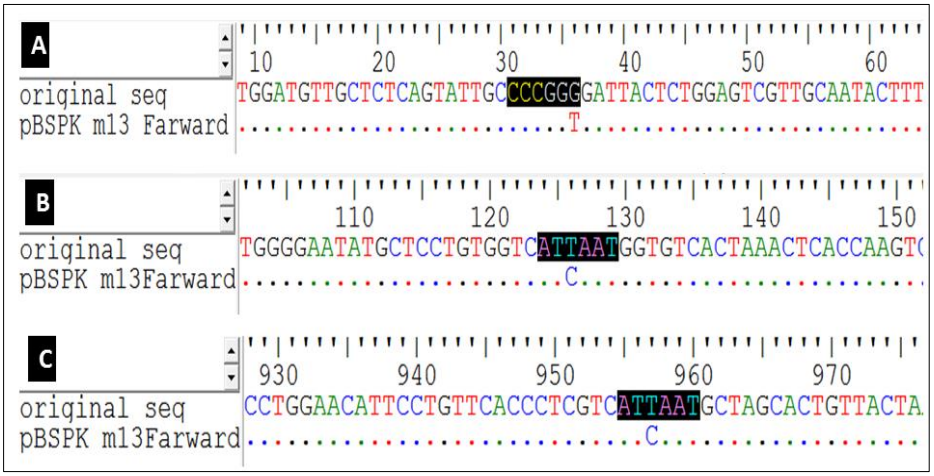

Fig-4.11: Comparison of pBS-PK-3ko clone sequence with original sequence of MNSV-Hyd using Bioedit software. One *Xma*I and two *Ase*I sites were silent mutated to avoid problems in cloning and construction of infectious clone to MNSV-Hyd. A) *Xma*I mutation at 2710 nt position; B) *Ase*I mutation at 2979 nt position; C) *Ase*I mutation at 3810 nt position.

Fig-4.12: Silent mutation comparison of pBS-PK-3ko clone with original amino acid sequence of MNSV-Hyd. A) Mutation of *Xma*I site at nucleotide position of 2710 in pBS-PK-3ko clone. B, D, F are original sequence with appropriate amino acid sequence of MNSV-Hyd; C) Mutation of *Ase*I site at nucleotide position of 2979 in pBS-PK-3ko clone; E) Mutation of *Ase*I site at nucleotide position of 3810 in pBS-PK-3ko clone. In the three mutations no change in the amino acid was observed indicating the authenticity of the clones. The restriction site was highlighted in blue color.

The primer sets 1&2, 3&4 and 5&6 (tab-4.1) were used for the mutagenesis of *Xma*I at position 2710 nt, *Ase*I at position 2979 nt and second *Ase*I at position 3810 nt respectively. The site CCCGGG was mutated to CCCTGG, *Ase*I site at 2979 was mutated to ATCAAT and *Ase*I at position 3810 was mutated to ATTGAT. In all these mutations, proper care is taken that there is no change in the amino acid translated and only the restriction site was knocked out (silent mutation). The mutagenesis was carried out with vent polymerase using pBS-PK clone as template. The resulted PCR amplified product was subjected to *Dpn*I digestion overnight and transformed into DH5α cells. The transformed colonies containing recombinant plasmids were analyzed by restriction digestion and confirmed by sequencing the clones on both the strands. The restriction site was mutated so that the respective restriction enzyme doesn't recognize the site for cleavage. pBS-PK clone consists of all the three point mutations was named as pBS-PK-3ko.

4.3.3 (f) Step 6: Fusion of ribozyme sequence to fragment in p3' NCR clone

Ribozyme (RZ) sequence of 47 nt length was added to the 3'end of the viral sequence by primer extension PCR following the protocol mentioned in section 4.2.1(b) (Gopinath et

al., 2005). After the second PCR reaction, the resultant PCR product (fig-4.13A) was gel extracted (fig-4.13B) and ligated into pGEMT-easy T/A cloning vector by following the standardized cloning protocols. The ligated mixture was transformed into DH5α cells of *E.coli* strain and the transformed colonies were confirmed by restriction digestion (fig-4.13C). The presence of ribozyme was checked by sequencing the recombinant clones of both the strands. The sequence confirmed clones with ribozyme (p3'RZ) without single nucleotide addition or deletion were used for the infectious clone construction. The p3'RZ clone was digested with *Kpn*I and *Xma*I restriction enzymes. The released 400 bp fragment (fig-5.13E) was gel extracted (fig-5.13E) and used in the infectious clone construction.

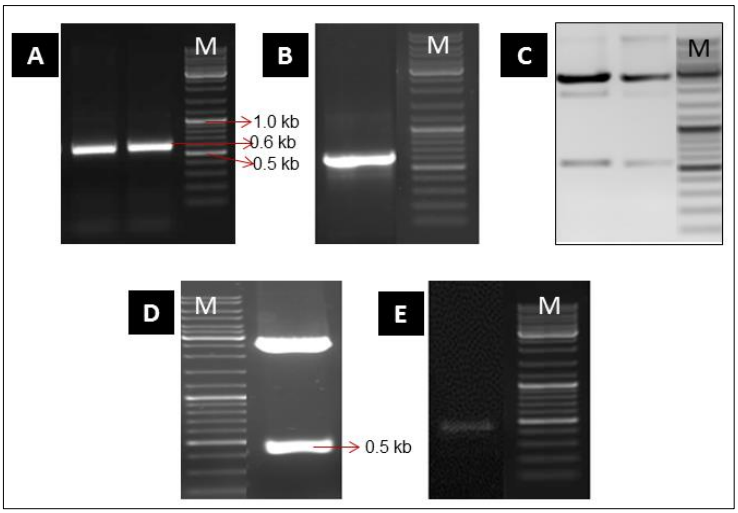

Fig-4.13: Cloning process to fuse ribozyme sequence to 3'pNCR clone. A) Primer extension PCR to add ribozyme to 3'pNCR clone (0.6 kb), M- 1 kb ladder, sizes represented on the right side of the gel (same ladder was used in all the gels); B) gel extraction of PCR amplified product using Nucleospin columns; C) confirmation of recombinant p3'RZ clones with ribozyme sequence by digestion with *Eco*RI; D) Restriction digestion of p3'RZ clone with *Kpn*I and *Xma*I sites (0.4 kb); E) Gel extraction of 0.4 kb insert digested from p3'RZ clone.

4.3.3 (g) Step 7: Preparation of binary vector backbone

The pCB301, binary vector is capable of replicating in DH5α bacterial cells and agrobacterium was selected for construction of MNSV-Hyd infectious clone which is of only 3.1 kb size. The pCB301 clone, BR3 (fig-5.14A, lane-1) consisting of BMV RNA3 insert (Gopinath *et al*., 2005) was transformed and enriched the plasmid by alkaline lysis method. The isolated plasmid was purified by Nucleospin plasmid isolation columns.

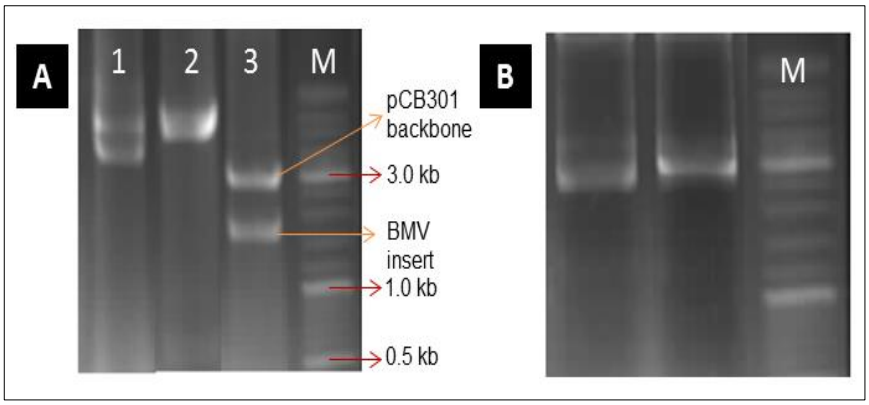

Fig-4.14: Preparation of binary vector backbone from BR3-pCB301. A) Preparation of binary backbone, pCB301; 1- Undigested binary plasmid, BR3, 2- linearized binary plasmid digested with *Bgl*II restriction enzyme, 3- Double digested plasmid with *Bgl*II and *Xma*I enzymes to release BMV insert, M- 1 kb DNA ladder (same ladder in both the gels); B) Electro eluted binary backbone (1, 2) digested with *Bgl*II and *Xma*I.

The backbone was prepared from the purified plasmids by digesting with the restriction enzymes *Bgl*II and *Xma*I restriction enzymes to release the BMV RNA3 insert (fig-5.14A). The backbone, pCB301-BX was purified from the gel by following the protocol mentioned in the section 5.2.7 (fig-5.14B). The gel eluted backbone was used for the ligation of the MNSV-Hyd inserts in the construction of infectious clone.

4.3.3 (h) Step 8: Ligation of fragments from pTZ-BP, pBS-PK-3ko and p3'RZ clones

In this step, the inserts from three major clones, pTZ-BP, pBS-PK-3ko and p3'RZ were ligated into the prepared binary backbone, pCB301-BX. The recombinant clone pTZ-BP was digested with *Bgl*II and *Pst*I to release the insert of size 1785 nt. The second clone consisting of 2147 nt length of insert was released by digesting the clone with restriction enzymes *Pst*I and *Kpn*I. The third recombinant clone, p3'RZ consisting of 3' NCR sequence along with the ribozyme sequence (392 nt length) was released from the clone by digesting with *Kpn*I and *Xma*I enzymes. All the three digested inserts were purified through the Nucleospin columns. The eluted plasmids were ligated into prepared binary vector backbone, pCB301-BX. The ligated products were transformed into DH5α cells by heat shock method of transformation. The transformed plasmids were analyzed for the recombinant clones containing the full length MNSV-Hyd sequence with 35S promoter on 5' end and ribozyme sequence on 3' end of the genome sequence (fig-4.15). The confirmed positive infectious clones of MNSV-Hyd were double confirmed by PCR amplification of individual genes. The individual coding regions, p28, MP, CP and 3'NCR including ribozyme were PCR amplified with the respective specific primers from the constructed

binary clones as templates. The restriction digestion analyzed and PCR confirmed infectious clones are sequenced completely and are designated as icMNSV-Hyd.

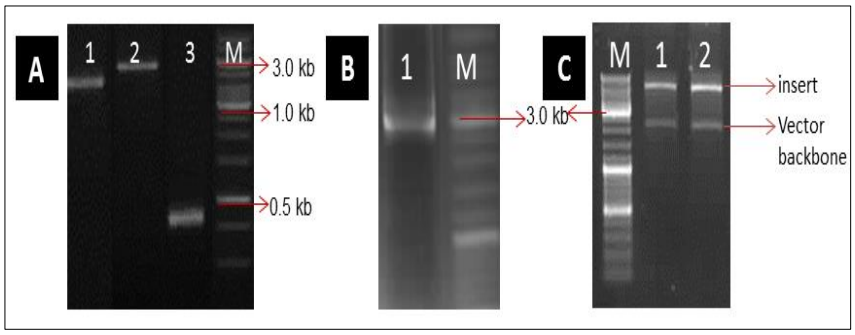

Fig-4.15: Cloning strategy of the complete MNSV-Hyd sequence into the binary backbone, pCB301. A) Eluted inserts, 1- insert of 1785 bp size consists of 5' end sequence from pTZ-BP clone digested with *Bgl*II and *Pst*I, 2- 2.1 kb insert consisting of middle part of MNSV-Hyd sequence from pBS-PK-3ko clone digested with *Pst*I and *Kpn*I, 3- 3' end sequence of MNSV-Hyd with ribozyme from p3'RZ clone of 400 bp size, M- 1 kb DNA ladder (same ladder used in all the gels); B) Electro-eluted binary plasmid vector backbone digested with *Bgl*II and *Xma*I, pCB301-BX; C) Restriction digestion of recombinant plasmids, icMNSV-Hyd with *Bgl*II and *Xma*I to release complete MNSV-Hyd sequence (total 4.6 kb insert = 35S promoter+4274 nt+RZ sequence) and binary backbone of 3.1 kb, 1, 2- positive recombinant clones that released complete MNSV-Hyd sequence.

4.4 Mobilization of the sequence confirmed clones into agrobacterium

The sequence confirmed positive clones are enriched and the plasmids were column purified using the Nucleospin plasmid columns. Six different individual colonies were selected for checking the infectious nature through agroinfiltration process. 10 µl of purified plasmids were transformed by freeze-thaw method into the prepared chemical competent agrobacterium cells (EHA105) (4.2.3).

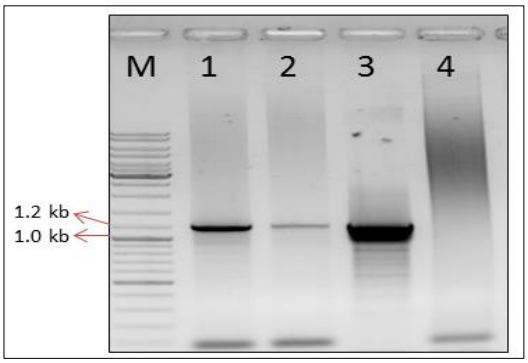

Fig-4.16: Colony PCR for the transformed agrobacterium colonies with icMNSV-Hyd clone by PCR amplification of MNSV-Hyd CP gene. M- 1 kb DNA ladder, Lanes: 1, 2- PCR from the agrobacterium colonies with specific primers, 3- positive control of CP fragment from pTGC clone, 4-negative control without template.

Transformed colonies were observed clearly on the LB kanamycin + rifampicin plates after 72 h of incubation at 28˚C. The observed colonies were confirmed by the colony PCR with

specific primer sets that are used to amplify CP region with specific primers designed in CP region (primers: CP+: and CP-:).

4.5 Agroinfiltration of icMNSV-Hyd clones

The PCR confirmed agrobacterium colonies from section 5.4 were used for the infiltration of the *N. benthamiana* plants (7 weeks old plants). The positive recombinant clones were processed as described under the section 5.2.4 in 10 ml cultures for the agro infiltration approach. All the agro cultures were grown at 28˚C at 170 rpm until optimum density was obtained and were induced with acetosyrinzone for overnight. Later, the density of the culture was measured at 595 nm using spectrophotometer. The culture was diluted to a final concentration of 0.3 OD with the infiltration buffer and infiltrated on abaxial side of *N. benthamiana* leaves using 2 ml syringe without needle. Each construct was infiltrated to at least three plants for confirmation and observed for the visible symptoms. The *N. benthamiana* plants were inoculated with pure virus culture to serve as positive control of the symptoms. All the plants were maintained at 24˚C with 16 h of photoperiod.

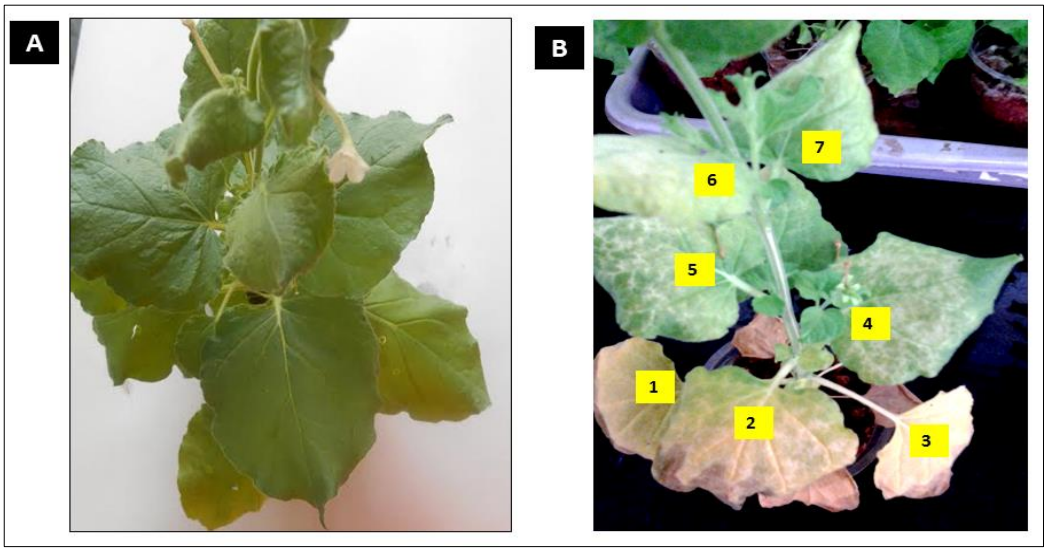

Fig-4.17: Infectivity of the constructed icMNSV-Hyd clones after 20 dpi. A) Control plant infiltrated with buffer alone; B) Visible symptom expression in infiltrated plants with recombinant icMNSV-Hyd clones. 1, 2, 3- Infiltrated leaves; 4, 5, 6 & 7- non-infiltrated systemic leaves.

The viral symptoms were observed on infiltrated plants with icMNSV-Hyd in 5 days delay to that of the control plant inoculated with the pure MNSV-Hyd virus (fig-4.17B). The chlorotic and blistering like symptoms were observed on the infiltrated plants as that of wild

type in the infiltrated leaves (fig-2.2 S, T) and systemic symptoms were also observed clearly as of wild type (fig-4.17B and fig-2.2 U).

4.6 Infectivity test

The infectivity test was performed by back inoculation of visible symptoms on infiltrated leaves on to indicator host (*P. vulgaris*) through mechanical inoculation. The systemic infection of the virus was also confirmed by back inoculation of the systemic symptomless leaves on to the indicator host. The necrotic symptoms (same as wild type) were visible on the 3rd dpi on the indicator host with the back inoculation test with all the infiltrated and the systemic leaves (data not shown).

In order to confirm the constructs one more time, agrobacterium was isolated from the infiltrated and systemic leaves. Agrobacterium was isolated by grinding small piece of the infiltrated leaf in 1 ml of sterile distilled water and plated 40 µl on LB kanamycin plates. After the appearance of colonies (48 h later) plasmids were isolated from the agrobacterium colonies and confirmed by colony PCR. Approximately 20 colonies were used for the transformation and plasmids were enriched. Approximately 1.5 kb fragment was amplified with specific primer sets 3 and 6 (tab-3.3) (fig-4.18A).

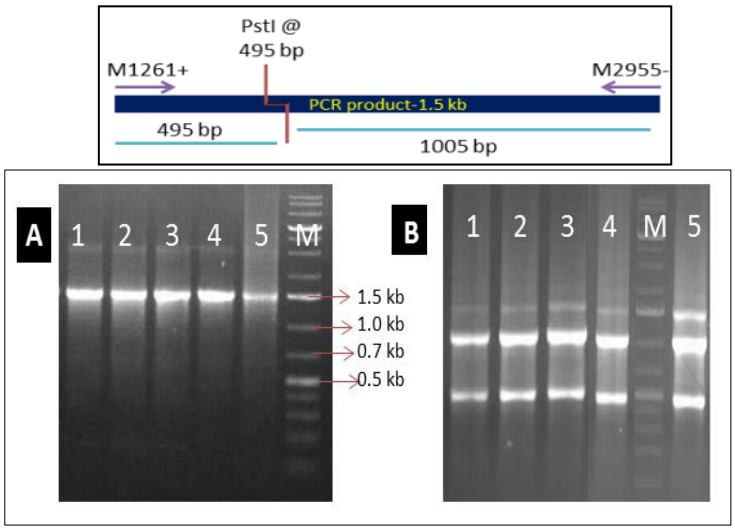

Fig-4.18: Confirmation of the infiltrated constructs from infiltrated plants (N. benthamiana). A) 1.5 kb fragment was PCR amplified with specific primers set (tab-4.3, primers-3 and 6), 1- pTNVR plasmid used as positive control, 2, 3- PCR from agrobacterium plasmid isolated from infiltrated leaves, 4 and 5- PCR from the agrobacterium plasmid isolated from systemic leaves; Top panel: shows the digestion pattern of PCR product; B) Digestion of the amplified PCR product with *Pst*I at 495 bp to release approximately 500 bp fragment and 1 kb fragment, 1, 2- infiltrated leaves, 3, 4- systemic leaves and 5- positive control; M- 1 kb DNA ladder (same ladder in both the gels).

The amplified PCR products were confirmed by internal restriction enzyme *Pst*I at 495 bp

where the positive products were cleaved into two fragments to obtain 0.45 kb and 1 kb (fig-4.18B and top panel). With this we are sure that there is no contamination which is a major problem with agrobacterium culture.

4.7 Confirmation of transcripts in the infiltrated plants

For confirmation of transcripts, total RNA was isolated from the infiltrated and systemic leaves as mentioned under the section 4.2 (fig-4.19). Pure virus inoculated leaves were also included in the RNA extraction process as positive controls. The isolated RNA was used for the first strand cDNA synthesis with end reverse primer as described in section 3.2. Different regions were amplified using synthesized cDNAs as templates with specific primer (4.4) sets in PCR by following the standardized conditions mentioned in 2.3. Expected sized fragments were amplified same as that of the wild type (fig-4.20). All the fragments were further confirmed by the internal restriction sites in the respective fragments (data not shown). Same results were obtained from all the 10 plants tested each time (data not shown).

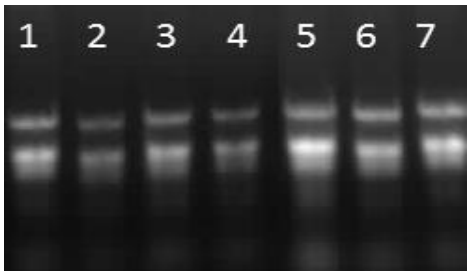

Fig-4.19: Total RNA isolated from the infiltrated *N. benthamiana* plants. 1-3: icMNSV-Hyd infiltrated leaves, 4 -6: Uninfiltrated systemic leaves, 7- wild type.

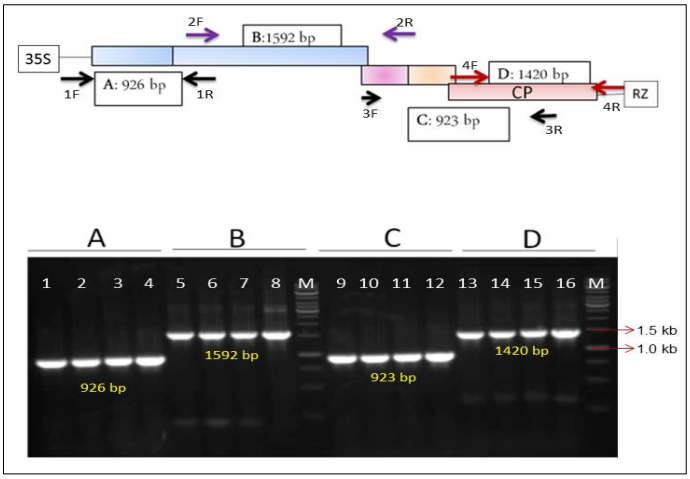

Fig-4.20: Confirmation of the transcripts in the infiltrated and systemic leaves by RT-PCR approach. Top panel: pictorial representation of the MNSV-Hyd genome map and the primers used in the confirmation by RT-PCR. Lower gel: Analysis of the PCR amplification on 1% agarose gel. A-D: different regions amplified in the complete MNSV-Hyd genome as represented in the top picture. The size of the fragments was also represented in the top picture. A: 5' end of the genome of 926 bp with primers; B: 1592 bp fragment with primers; C: 923 bp fragment with primers; D: 1420 bp fragment at 3' end of the genome with primers. Lanes: 1, 5, 9, 13- PCR with RNA isolated from infiltrated leaves; 2, 3, 6, 7, 10, 11, 14, 15- PCR with RNA isolated from systemic leaves; 4, 8, 12, 16- wt control; M- DNA ladder.

4.8 Discussion

Construction of infectious clones has become a regular laboratory process with the advent of molecular biology as they serve as important tools to study molecular processes like replication, host-virus interaction and in recent biotechnological studies (Junqueira *et al*., 2014; Lindbo, 2007). Apart from that the viral vectors can also be constructed which is helpful for the expression of recombinant proteins (viral & non-viral) and biopharmaceuticals in bulk at cheaper cost (Klimyuk *et al*., 2008; Gleba *et al*., 2007). The plants are used as biofactories for the production of foreign genes (Vadim *et al*., 2008). Multiple proteins can be coexpressed in plants and as well as heterologous protein are also produced in plants (Priti *et al*., 2010) using the viral vectors which help in decreasing the cost of the product (Bedoya *et al*., 2010). For example the production of the human harmones in industries is very expensive so, if we are able to produce them in plants using viral vectors and agroinfiltration process where we can produce in larger volumes and also cost effective (Gils *et al*., 2005; Hefferon *et al*., 2012). The high levels of agrobacterium culture should be infiltrated to increase the levels of expression in the host cell (Lindbo, 2007). It was also proven that the production of recombinant proteins in the plants was more efficient for proper folding and activity when compared to protein produced in *E. coli* or yeast (Popescu *et al*., 2007). Construction of infectious clone is the first and foremost step in the study of functional genomics of any organism with many future applications.

The obtained overlapping mother clones from the previous chapter-4 were used for the construction of the infectious cDNA molecule and the *in vivo* transient expression system (agroinfiltration) was used for the assessment of the clone (Gopinath *et al*., 2005). This agroinfiltration system is the most reliable, robust and less expensive method which can be used in Indian conditions when compared to that of the *in vitro* run off transcription systems. The transcription kits are costly which are not affordable and at the same way handling of the RNA molecules is a big challenging task in the *in vitro* systems. In case of agrobacterium, once we are successful in construction of binary clone (pCB301) and mobilization of the plasmid into agrobacterium (EHA105) then the remaining processes will be taken care by agrobacterium cell machinery in the plant cell nuclei. The detrimental effects of RNA can be lessening as RNA is synthesized inside the cell.

Using the unique restriction sites present in the overlapping regions of the mother clones, the full length infectious cDNA molecule was constructed to MNSV-Hyd. The 35S promoter from the CaMV was fused on the 5' end of the viral genome for efficient transcription through PCR based approach. The ribozyme sequence was added at the 3' end

of the genome from the *Avacado sunblotch viroid* (ASBVd) for generation of the unit length molecules by primer extension PCR.

The wild type viral symptoms were observed in the icDNA molecule infiltrated *N. benthamiana* leaves (fig-5.10). The systemic infection in the leaves was observed in 5-6 days delay when compared to that of the wild type virus inoculation. The severity of the symptoms was more in case of the cDNA infiltrated leaves (agroinfiltration) when compared to that of the virus inoculated leaves (mechanical inoculation). It was also showed that the agroinfiltration is highly efficient than mechanical inoculation where only few cells will receive the infectious molecule. In mechanical inoculation the leaf has to be damaged by an abrasive and then the inoculum was inoculated on the surface of the leaf. But in agro-infiltration, the virus culture was directly infiltrated into the interstitial spaces of the leaf with the help of a syringe. So, the availability of the transgene/RNA was more in the agroinfiltration approach than to the mechanical inoculation (Boyer and Haenni, 1994). The expression levels are also altered by increasing or decreasing the agrobacterium inoculum concentration levels (Lindbo, 2007). So, each and every cell will be flushed with several copies of recombinant T-DNAs harboring the MNSV-Hyd icDNA.

It has been reported that the presence of non-viral nucleotides at the 5' end of the genome completely abolishes or reduces the infectivity but at 3' end it is tolerable to some extent (Boyer and Haenni, 1994). Short 3' extensions of 1-7 nt have no influence on the biological activity of the clone (Dawson *et al*., 1986) where as long extensions abolishes the infectivity (Dzianott and Bujarski, 1989). In *Poliovirus*, presence of poly-A tail at the 3' end of *in vitro* produced poliovirus transcript has increased infectivity (Sarnow *et al*., 1989). Upto +19 nt extensions were tolerated by BMV RNA transcripts *in vitro* and +22 nt *in vivo* was observed (Ishikawa *et al*., 1997; Annamalai and Rao, 2005). Ishikawa *et al*., (1997) proved that in yeast cells, the 3' extensions are highly sensitive. 3' and 5' end nucleotides repair *in vivo* was also proposed by Govind *et al*., (2012). The 5' extensions of 1 or 2 nucleotides also decrease the infectivity of the clone and 14-17 nts completely abolishes the infectivity (Heaton *et al*., 1989). But the *in vivo* transcripts of *Beet necrotic yellow vein virus* (BNYVV) can tolerate up to 40 nt at 5' end but not infectious *in vitro*. The non-viral nucleotides have less effect on plant viruses in comparison to animal viruses (Boyer and Heanni, 1994).

The infectivity was assessed by the back inoculation of the symptoms on to the indicator host, *P. vulgaris*, by colony PCR from the agrobacterium isolated from infiltrated plants and RT-PCR. All the genes and NCRs in the viral genome are amplified through RT-

PCR and confirmed (fig-5.20). With this we are sure that the constructed infectious clone was proficiently inserted into the host cell, transcribed and translated in the host cell. Once we have the working infectious cDNA molecule in hand, the functional analysis of the virus can be carried out easily by agroinfiltration approach. The role of the individual viral gene/ protein can be known which is helpful for the establishment of the control strategies for viruses as they are the damaging factors of the agriculture.

In the earlier chapter, diversity of MNSV-Hyd from the reported isolates shown that it was geographically different isolate from India. The high degree of variability can be studied in case of MNSV-Hyd using this infectious clone.

CHAPTER-5

Elucidation and in planta analysis of virus encoded proteins as GFP chimeras through confocal laser scanning microscopy

5.1 Introduction

Regulation of gene expression which extended to gene sub-cellular localization studies is the dominant subject in the modern day molecular biology. The use of reporter genes has occupied an indispensable place in the study of gene expression and as well as localization. Reporter genes are the genes whose products can be easily monitored or assayed without the background interference of the host. Once the reporter assay is developed for a gene then it will be employed for different kind of genes without wasting time for the assay development for each gene, which is very difficult and laborious. Different ways are in use to study the gene expression and localization using the reporter genes. Fusions of reporter genes to constitutive promoters, for example, it has been instrumental in the development of many transformation methods, as well as the routine monitoring of transformation experiments. While such use of reporter genes *per se* is not directly related to gene expression studies, it is a prerequisite, since the use of reporter genes is only possible in systems where transformation is available (Chiu *et al*., 1996).

Provided that transformation is available, reporter genes can facilitate and expand the ways in which regulation of gene expression can be studied. The precise fusion of a reporter gene to a regulatory sequence provides many insights to the complex gene regulation processes. For example, fusions to reporter genes to gene of interest can be designed to help characterize the specific signals that exert controls on the initiation of transcription (e.g. promoters, enhancers, repressor binding sequences); stability, transport or processing of mRNAs (e.g. 5'- and 3'- untranslated regions, introns and alternative mRNA splicing, or polyadenylation signals); translation efficiency (e.g. the context surrounding translation initiation site, or specific mRNA secondary structures); protein degradation (e.g. stabilizing and destabilizing N-terminal amino acids) (Sheen *et al*., 1995).

To unravel the role and localization of virus encoded genes, histochemical staining with β-glucuronidase (GUS) was used as marker in the last decade. GUS as a reporter gene has been extensively used in analyzing expression levels by different promoters in plant.

This is an *in vivo* expression system used in analysis of highly sensitive and weak promoters also due to its stability (Weinmann *et al*., 1994; Jefferson *et al*., 1987). Another assay system that is most widely used is the Luciferase system where the Lucifereases are the class of enzymes that generate light through chemical transformations of number of substrates. Luciferase also offers the most rapid and sensitive assay (Brandes *et al*., 1996) in plants with less background reaction as plants contain less or no endogenous luciferase (Nass and Scheel, 2001). These are labile and have short life (Pazzagli *et al*., 1992). The main disadvantage of these two systems is the inherent destructive method which is relatively complicated and depends on multiple reagents, there by data normalization is difficult.

Green fluorescent protein (GFP) from *Aequorea victoria*, a jelly fish is the most commonly used reporter gene in plants. The major advantage of this system is that it is strong fluorescent protein, doesn't require any substrates or co-factors and is non-destructive method of *in vivo* reporter in plants and tolerates the N-terminal and as well as C-terminal fusions (Kain *et al*., 1995). It is also used as tool in gene trafficking and sub-cellular localization of proteins where it can be monitored in living organisms, avoiding fixation and staining artifacts (Chalfie *et al*., 1994). Based on all these advantages it has been proved that GFP can be used as reporter gene to study viral infection process, cell-to-cell movement and sub cellular localization of the viral encoded proteins (Baulcombe *et al*., 1995; Oparka *et al*., 1996; Santa Cruz *et al*. 1996). It is non-toxic, highly stable inside the cell and photo bleaches slowly keeping it appropriate condition for long term in vivo fluorescence imaging. With this non-destructive imaging technique it has been proved to study the spread of viruses at single cell level and in whole plant scenario using confocal laser scanning microscopy (Oparka *et al*., 1997). This technique made possible and gain insights to study the role of viral specific genes in viral infection processes.

The increased popularity of fluorescent protein has greatly simplified the genetic engineering of GFP where it is expressed as a free protein in the cell (Baulcombe *et al*., 1995). This led to development of improved versions like mGFP5, mGFP5-ER- a plant intron was removed and targeted to endoplasmic reticulum (ER) (Haseloff *et al*., 1997). Brighter and more soluble red and blue shifted GFP variants- eGFP, YFP (yellow fluorescent protein), CFP (cyan fluorescent protein) (Reichel *et al*., 1996; Davis and Vierstra, 1998) are also available. Fluorescent proteins from other sources like RFP (Red

fluorescent protein) from *Discosoma* species, is more soluble and has been demonstrated working well in plants (Jach *et al*., 2001; Dietrich and Maiss, 2003; Hanson and Kohler, 2001; Day *et al*., 2001).

After a virus particle introduced into the cell, their progeny move from one cell to another cell using the unique cell organelle called plasmodesmata. The virus requires the viral encoded proteins called movement proteins (MP) for gating mechanism and its translocation from cell-to-cell (Carrington *et al*., 1996). The systemic infection of the virus through the intracellular networking was also proved by using reporter genes that target the particular organelle (Harries *et al*., 2009a; Harries *et al*., 2010). Even silencing activity of the viral proteins with different reporter gene is also possible (Voinnet, 2001). The role of individual viral proteins was analyzed by using viral vectors and deletion studies (Santa cruz *et al*., 1996). The plant viral vectors are also used for the transient expression of foreign proteins *in planta* (Scholthof and Scholthof, 1996; Gils *et al*., 2005; Giritch *et al*., 2006; Marillonnet *et al*., 2005).

It has been proved that plant viral encoded proteins use different host cell organelles for the replication in the process of infection. BMV, CPMV, ToRSV targets to endoplasmic reticulum (ER) for their replication. The regions important for the their targeting are also identified in many viruses (Carette *et al*., 2002 a, b; den Boon *et al*., 2001; Zhang and Sanfacon *et al*., 2006; Pouwels *et al*., 2002). The *Cauliflower mosaic virus* movement protein (CaMV-p6) can form motile inclusion bodies associating with ER that traffic along the microfilaments and stabilize microtubules (Harries *et al*., 2009a). TMV-MP associates and accumulates the microtubules during its movement (Curin *et al*., 2007). Different types of movement protein trafficking was initially explained by Carrington *et al*., 1996. The C-terminal hydrophobic domain of the *Papaya ringspot virus* (PRSV) P3 protein (plays a role in formation of viral replication complex) has shown to target ER (Eiamtanasate *et al*., 2007). *Tobacco vein mottle virus* (TVMV) P3 protein interacts with CI protein in cytoplasm (Rodriguez-Cerezo *et al*., 1993). The P3 protein of *Tobacco etch virus* (TEV) is associated with viral NIa and NIb proteins in the nucleus (Langenberg and Zhang, 1997). TEV-P3 protein forms mobile inclusions and traffics along actin microfilaments and plays a dual role in virus movement and replication (Cui *et al*., 2010). It was shown that *Potato virus-Y* coat protein (PVY-CP) has action in chloroplasts may contribute to symptom development in

infection (Naderi and Berger, 1997). The replication proteins (P1 and P2) of *Alfalfa mosaic virus* (AMV) are localized into tonoplasts for the virus replication process even P1 is found in other organelles (Heijden *et al*., 2001). The replication protein, P33 of *Tobacco bushy stunt virus* (TBSV) localizes to peroxisomes to ER sorting pathway (McCartney *et al*., 2005). The 66 kDa replication protein of TYMV targets to chloroplast envelope for its action (Prodhomme *et al*., 2003). The cytopathological vesicles formed from the outer nuclear membrane were also observed in *Pea enation mosaic virus* (PEMV) (Powell *et al*., 1977). The localization of 36 kDa protein of *Carnation italian ringspot virus* (CIRSV) to mitochondria was also shown using GFP chimeras (Rubino *et al*., 2001). The membrane modifications that are required by the viruses in the plant cell are like: alpha-like viruses replicate along the ER invaginations, flavi-like viruses replicate along organellar membranes, Bromoviruses and Tombusviruses need ESCRT (endosomal sorting complexes required for transport) for their replication (Barajas *et al*., 2009).

The present chapter discusses about the localization patterns of the MNSV-encoded proteins in the plant cell (*N. benthamiana*) using GFP chimeras.

5.2 Methods

5.2.1 Preparation of the binary vector backbone

The binary vector, pCB302 plasmid containing the BMV insert (Gopinath *et al*., 2005) was used for the construction of fusion clones. The vector contains CaMV 35S double promoter and a 5' untranslated leader sequence from *Tobacco etch virus* and a 3' 35S terminator and it has kanamycin as selectable marker with 7.0 kb size. The plasmid was transformed into DH5α cells of *E.coli* by heat shock transformation (3.2.8). The transformed colonies were enriched in LB media and plasmids were isolated by alkaline lysis method (3.2.9). The binary plasmids were digested with *Nco*I and *Xba*I restriction enzymes to release the BMV insert. The vector backbone was gel extracted by electro elution method (4.2.6) and used for the cloning.

5.2.2 Construction of GFP clones

GFP was amplified with the primers 21 and 22 (tab-5.1) which consists of restriction

sites on both primers that are helpful for the 5' and 3' fusions using mGFP5 clone (Gopinath *et al*., 2005) as template. The primer, NEH-GFP1+ (21) has *Nco*I, *Eco*RI and *Hind*III restriction enzymes that are added on the 5' end of GFP and KPBSX-GFP1- (22) has *Kpn*I, *Pst*I, *Bam*HI, stopcodon and *Xba*I sites on the 3' end of GFP gene. The PCR amplification was performed with *Pfu* enzyme at conditions: 94˚C for 5 min of one cycle and 30 cycles of 94˚C- 50 sec, 57˚C-30sec, 68˚C-1 min and 1 cycle of final extension for 10 min at 68˚C. The PCR amplified product was analyzed, agarose gel extracted and poly 'A' was added to the insert using *Taq* polymerase at 72˚C for 2 hrs. The insert was cloned into pTZ T/A cloning vector by cloning manipulations. The resultant clone was designated as MCS-GFP.

In the same way another clone, NX-GFP-EX was prepared with *Nco*I and *Xho*I (primer 17) on 5' and *Eco*RI and *Xba*I (primer 18) (tab-5.1) on 3' ends of the GFP gene respectively.

Sl. No	Name of the Primer	Sequence (5'-3')	Purpose
1	*Kpn*I P28	CGG TAC CGC TAC TGC AAT GAA TAC TAT GGG G	Used in p28 chimera construction
2	p28 *Xho-Xba*I	CTC TAG ACT CGA GCT AGT TGA CAA GCC TGA AGG CCT TCC AGT C	
3	M7a*Eco*RI+	C GAA TTC GAT GCT CAA CGA ACT GTA GAT C	Used in p7A chimera construction
4	M7a*Xbaho*I-	G CTC GAG TCT AGA TCA GAA GTT AAA ATT AAT TTT AAC TTT G	
5	M7b*Eco*RI+	C GAA TTC GGG TGT GGA TGT TGC TCT CAG	Used in p7B chimera construction
6	M7b*Xbaho*I-	G CTC GAG TCT AGA TTA ACC ATC GCC ATT CGT TGA GAT TCC	
7	MCP *Pst*I+	G CTG CAG GCG ATG GTT AAA CGC GCA AAC	Used in CP chimera construction
8	MCP*Xhoba*I-	G TCT AGA CTC GAG CTA TAC AAG GTA AGC TAC CTC ACT GG	
G+	GFP325+	GTG CTA CAC CCT CGT CAA CAG	Used in sequencing of the binary clones
G-	GFP325-	CCG TCC TCC TTG AAA TCG ATT C	
G1	GFPNEH	GCC ATG GGA TCC GAA TTC AGT AAA GGA GAA GAA CTT TTC ACT GG	Used in GFP clone (MCS-GFP) construction
G2	GFPKPB*X	GGG CTC GAG AGT AAA GGA GAA GAA CTT TTC ACT GGT ACC TGC AGG ATC TGA CTC TGA G	
G3	GFP*Ncxho*+	GCC ATG GGG CTC GAG AGT AAA GGA GAA GAA CTT TTC ACT GG	Used in GFP clone (NX-GFP-EX) construction
G4	GFP*EcoXba*-	G TCT AGA TTA GAA TTC AAG CTC ATC ATG TTT GTA TAG TTC ATC C	

Tab-5.1: List of primers used in the present chapter. * -represents presence of stop codon. Restriction sites were underlined.

5.2.3 Construction of GFP chimeras

5.2.3 (a) Construction of p28 chimera

The p28 gene was amplified with the specific set of primers 1 and 2 (tab-5.1) with *Taq* polymerase and at same PCR conditions as in 5.2.2 (GFP amplification). The amplified genes were cloned into pTZ T/A cloning vector and the positive clones were confirmed by restriction digestion with *Eco*RI and *Hind*III (data not shown). The p28 insert was digested with *Kpn*I and *Xba*I. The GFP clone, NX-GFP-EX was digested with *Nco*I and *Kpn*I restriction enzymes. The released inserts 28 and GFP was gel extracted, analyzed and cloned into pCB302, binary vector backbone (5.2.1) for the N-terminal GFP p28 clone (G-28) (fig-5.1).

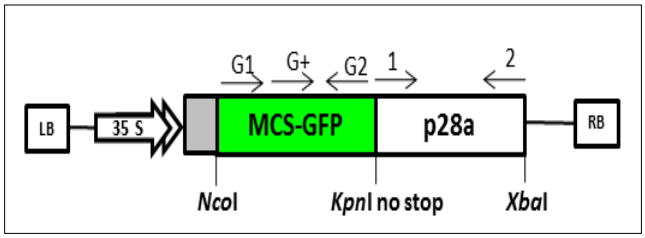

Fig-5.1: Pictorial representation of cloning strategy used for construction of GFP-28 chimera. G1, G2, G+, 1 and 2 are primers used in cloning as represented in tab-5.1. Here and at other places LB, RB, 35S represents left and right boarders, 35S double promoter respectively. The restriction sites used in the cloning were represented in the figure and direction of the primers was denoted by an arrow with primer number on the arrow.

5.2.3 (b) Construction of 7A chimera

The 7A gene was amplified with the specific primer sets 3 and 4 (tab-5.1) as described in 5.2.2 except the annealing temperature at 58˚C and extension temperature at 72˚C with *Taq* polymerase. The amplified gene was cloned into pTZ T/A cloning vector from Fermentas. The 7A clone was digested with *Eco*RI and *Xba*I restriction enzymes and insert was gel extracted. The GFP clone, NX-GFP-EX was digested with *Nco*I and *Eco*RI (G-NE) (for N-terminal GFP fusion clone). For N' GFP fusion, 7A and G-NE inserts were ligated and cloned into pCB302 (5.2.1) (G-7A) (fig-5.2).

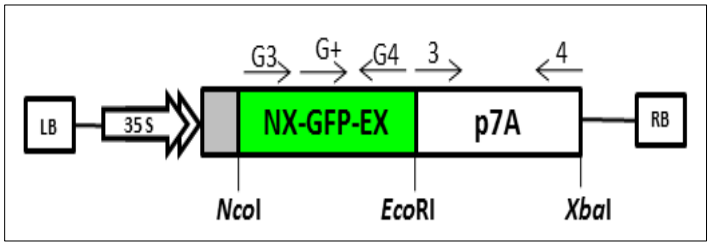

Fig-5.2: Pictorial representation of cloning strategy used for construction of GFP-7A1 chimera. G3, G4, G+, 3 and 4 are primers used in amplification of GFP and 7A genes. The restriction sites used in the cloning were represented in the figure and direction of the primers was denoted by an arrow with primer number on the arrow.

5.2.3 (c) Construction of 7B chimera

Towards the construction of 7B chimera, the 7B gene was amplified with the primers 5 and 6 (tab-5.1), using *Taq* polymerase with PCR conditions same as with 7A gene and cloned into pGEMT-Easy vector. The positive 7B clone was digested with *Eco*RI and *Xba*I restriction enzymes and the inserts 7B and G-NE was gel extracted, analyzed and cloned into pCB302. The resultant positive clones were designated as G-7B. The construct was confirmed by restriction digestion and by sequencing the constructs on both the strands (fig-5.3).

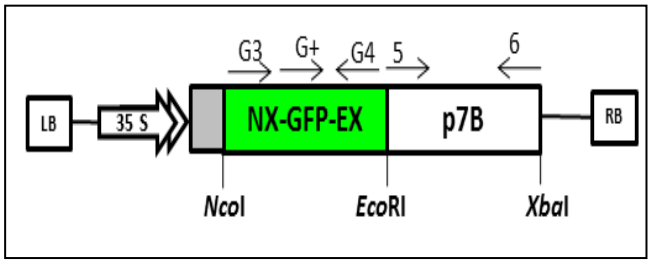

Fig-5.3: Pictorial representation of cloning strategy used for construction of GFP-7B chimera. G3, G4, G+, 5 and 6 are primers used in amplification of GFP and 7A genes respectively. The restriction sites used in the cloning were represented in the figure and direction of the primers was denoted by an arrow with primer number on the arrow.

5.2.3 (d) Construction of CP chimera

Firstly, the cloning of CP gene into T/A vector was performed by amplifying the gene with specific primers, 7 and 8 (tab-5.1) with *Taq* polymerase under the same amplification conditions under 5.2.3b except the extension time for 2 min 20 sec. The PCR product was cloned into pTZ T/A vector and clone was digested with *Pst*I and *Xba*I

restriction enzymes. Parallely, MCS-GFP construct was digested with *Nco*I and *Pst*I. Both the inserts were gel extracted and cloned into pCB302 binary vector (5.2.1) for the N-terminal GFP-CP chimera (G-CP). The construct was confirmed through restriction digestion and PCR amplification. The fusion junction was confirmed by sequencing the clones on both the strands (fig-5.4).

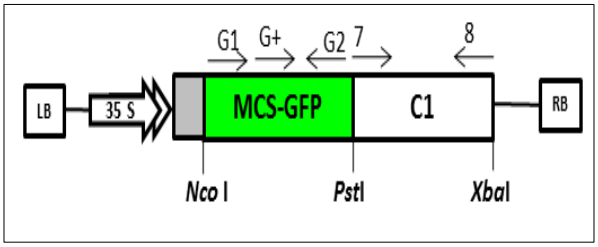

Fig-5.4: Pictorial representation of cloning strategy used for construction of GFP-CP chimera. G1, G2, G+, 7 and 8 are primers used in amplification of GFP and CP genes respectively. LB, RB, 35S: left and right boarders, 35S double promoter respectively. The restriction sites used in the cloning were represented in the figure and direction of the primers was denoted by an arrow with primer number on the arrow.

5.2.4 Transformation of GFP chimeras into agrobacterium

The GFP chimeras were mobilized into agrobacterium C58C1 strain by following the procedure mentioned under section 4.2.3. The agrobacterium colonies were confirmed by colony PCR for the respective construct and positive clones were used for the infiltration.

5.2.5 Agroinfiltration and transient expression

Respective GFP chimeras are infiltrated into individual plants and observed under Confocal laser scanning microscopy (CLSM) after 36 h and 48 h of post infiltration (hpi) process. Prior to the preparation of the sample, the slides were painted with the clear nail polish in rectangular shape to form a small trough and allowed to dry completely. After proper incubation time, small piece of the leaf in the infiltrated area was excised using a scalpel and placed in the prepared trough on the slide. Small water droplet was placed on the leaf and was covered with coverslip without entrapping the air bubbles. The cover slip was fixed by placing small droplets of nail polish at the edges of the cover slip. Allowed it to air dry completely for 10-15 min and then analyzed under the CLSM at wavelength 417. The localization results were scored and analyzed along with the positive controls, mGFP5 and mGFP5er.

5.2.5 Prediction of mitochondrial targeting sequence

The determined DNA sequence of p28 gene was translated into protein sequence using (http://bioinformatics.picr.man.ac.uk/research/software/tools/sequenceconverter.html) the online software tools and subjected to MITOPROTII version 1.1, a tool used for predicting the mitochondrial targeting sequence. Mito Prot calculates the N-terminal protein region that can support a mitochondrial targeting sequence and the cleavage site. It searches for the existence of two close Glu or Asp within a determined distance. A typical MTS contain several positively charged residues and hydrophobic residues which electrophoretically promote transfer of proteins across the membrane. Mitochondrial targeting sequence should at least contain 2 positively charged residues with increase in hydrophobicity; the possibility of importing a protein also diminishes.

5.3 Results

All the confirmed constructs through internal restriction digestion (fig-5.5) and sequencing were mobilized into C58C1 strain of agrobacterium (5.2.4) and the transformed colonies were confirmed by performing colony PCR, The PCR confirmed colonies were used in the agroinfiltration (5.2.5) process. The localization of the each MNSV-Hyd gene was determined by the GFP fluorescence by infiltration of the individual genes. The localization of the two MPs was also checked by infiltrating individual constructs and as well as by coinfiltration of the two constructs mixed in equimolar ratios. Each construct was infiltrated to a minimum of two plants and the experiments were repeated four times.

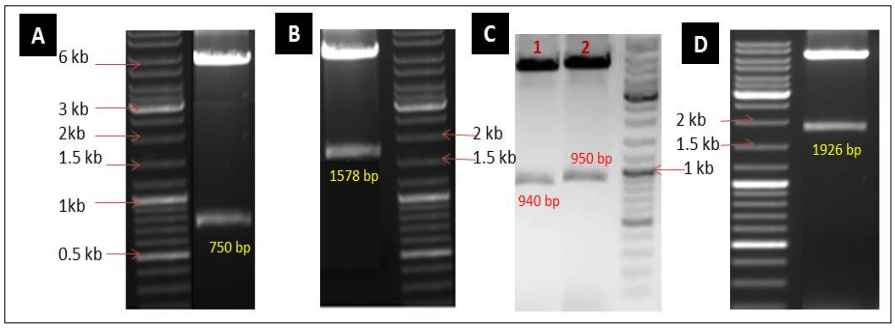

Fig-5.5: Confirmation of fusion chimeras along with positive control (mGFP5) by restriction digestion. A) Digestion of mGFP5 binary plasmid with *Nco*I and *Xba*I to release 750 bp fragment, B) digestion of G-28 construct with *Nco*I and *Xba*I restriction enzymes to release 1578 bp fragment (750+828), C) digestion of G-7A and G-7B constructs with *Nco*I and *Xba*I restriction enzymes to release approximately 950 (750+200) (lane-2) and 940 bp (750+189) (lane-1) fragments respectively, D) digestion of G-CP construct with *Nco*I and *Xba*I restriction enzymes to release 1926 bp fragment (750+1176).

5.3 (a) Localization of mGFP5

In the case of plants infiltrated with wild type GFP construct (mGFP5) fluorescence was observed all along the cell wall presumably near the plasma membrane which is where the cytoplasm is thinly spread (0.5 micron thickness) along with the membrane. The fluorescence was found all over the cell including cytoplasmic strands in closer view indicating its soluble nature in the cell (fig-5.6-panel-1 and 2). In the higher magnification, fluorescence was observed in the nucleoplasm of the nucleus but not into nucleolus (fig-5.6, panel-3).

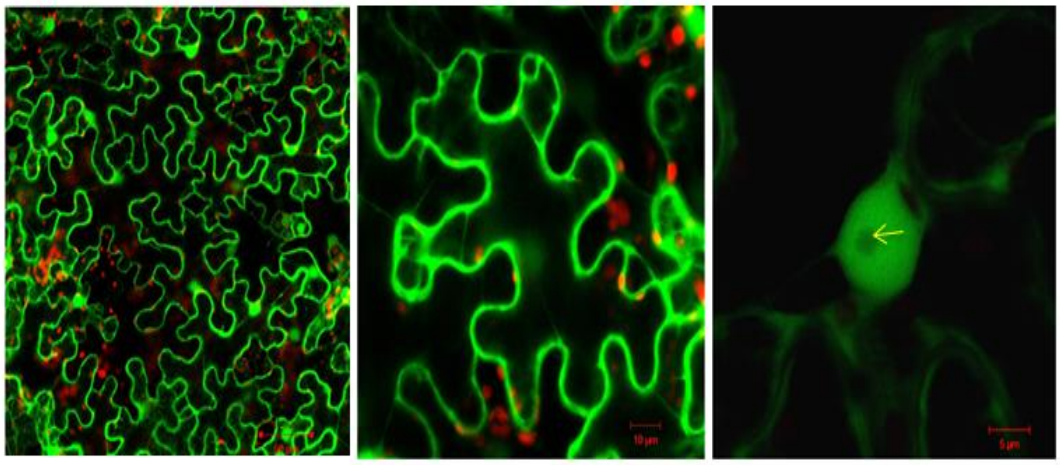

Fig-5.6: Confocal imaging od positive control mGFP5. Panel-1: GFP fluorescence was observed uniformly in all the cells along the cell wall at 20 µm magnification; panel-2: at 10 µm magnification GFP fluorescence was observed in single cell indicating the soluble nature; panel-3: fluorescence of the mGFP5 was observed in the nucleus at 5 µm magnification where no GFP signal was found in the nucleolus (indicated by yellow colored arrow). Red color is the auto-fluorescence of chloroplasts in the cells.

5.3 (b) Localization of GFP-28 chimera

Transient expression of GFP-28 fusion protein fluorescence was very faint but it was along the cell wall which needs to be reconfirmed with another construct where GFP is fused at the C-terminus of the p28 proteins (p28-GFP). The fluorescence was observed as aggregates in all the cells (fig-5.7).

The literature pertaining to p28 has revealed that the presence of mitochondrial targeting sequence in the gene (Ohki *et al*., 2010). The *insilico* analysis of p28 gene using MitoProtII 1.1 has revealed the presence of mitochondrial targeting signal (MTS) (fig-5.8) on amino-terminal.

Dr. Naresh Babu's research group has demonstrated the targeting of p28-GFP to mitochondrial in HELA cells (unpublished data) (fig-5.9, left panel) and this is also confirmed by mitochondrial marker. This construct has GFP fused at the C-terminus of p28 and analyzed in HELA cells. Cyclophilin D was used as positive control where the fluorescence was observed in red color (fig-5.9, middle panel). The overlay image of p28-GFP fluorescence and cyclophilin-D was observed in bright yellow color indicating the fluorescence localizing to mitochondria (fig-5.9, right panel).

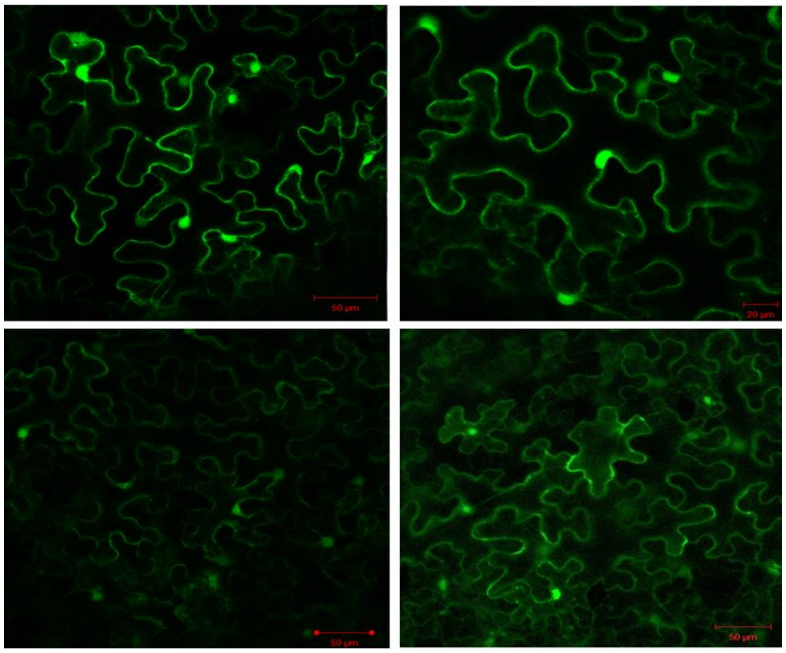

Fig-5.7: GFP fluorescence of GFP-28 chimera was observed all along the cell wall where the fluorescence was very weak. Fluorescence was also observed as aggregates which might be rough endoplasmic reticulum (RER).

5.3 (c) Localization of GFP-7A chimera

No fluorescence was observed in G-7A chimera within first 36 h (data not shown). However, GFP fluorescence was observed along the cell wall after 48 hpi (fig-5.10A1) and fluorescence was observed faintly in the cell walls of epidermal cells (fig-5.10A2). In closer magnification, bright GFP fluorescence signal was found in the guard cells of stomata and in the chloroplasts (fig-5.10B). The auto-fluorescence of chloroplasts was used as the internal marker for identifying the chloroplasts (fig-5.10, B, C). The overlay image of GFP and auto

fluorescence was observed as yellow color. The fluorescence of the chloroplasts and the subsidiary cells was observed uniformly in majority of the documentations.

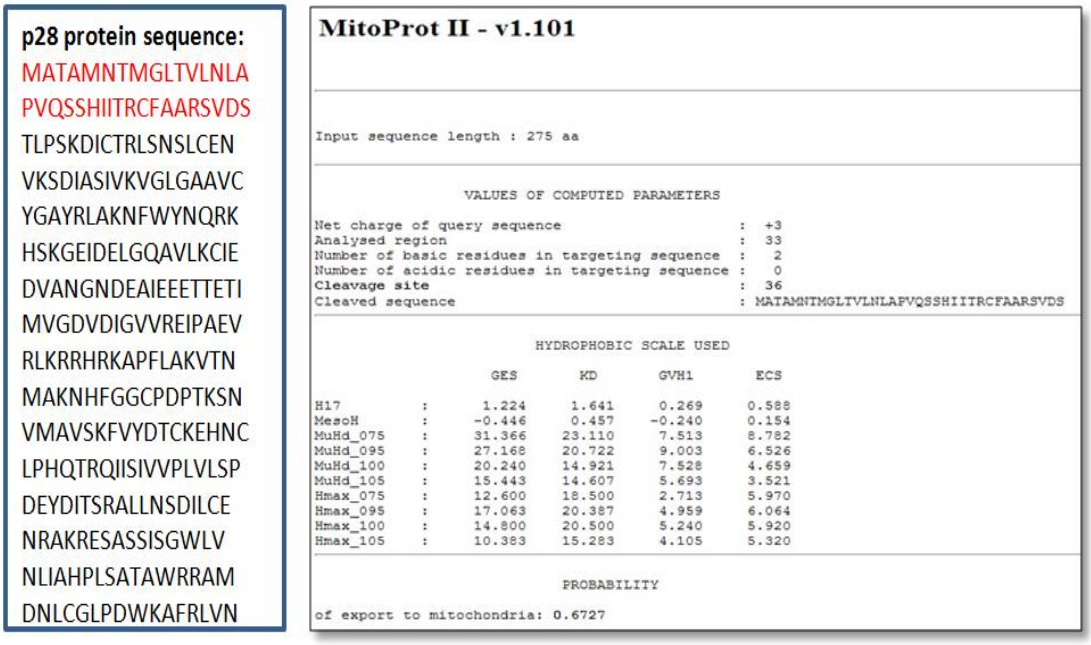

p28 protein sequence:
MATAMNTMGLTVLNLA
PVQSSHIITRCFAARSVDS
TLPSKDICTRLSNSLCEN
VKSDIASIVKVGLGAAVC
YGAYRLAKNFWYNQRK
HSKGEIDELGQAVLKCIE
DVANGNDEAIEEETTETI
MVGDVDIGVVREIPAEV
RLKRRHRKAPFLAKVTN
MAKNHFGGCPDPTKSN
VMAVSKFVYDTCKEHNC
LPHQTRQIISIVVPLVLSP
DEYDITSRALLNSDILCE
NRAKRESASSISGWLV
NLIAHPLSATAWRRAM
DNLCGLPDWKAFRLVN

MitoProt II - v1.101

Input sequence length : 275 aa

VALUES OF COMPUTED PARAMETERS

Net charge of query sequence	: +3
Analysed region	: 33
Number of basic residues in targeting sequence	: 2
Number of acidic residues in targeting sequence	: 0
Cleavage site	: 36
Cleaved sequence	: MATAMNTMGLTVLNLAPVQSSHIITRCFAARSVDS

HYDROPHOBIC SCALE USED

	GES	KD	GVH1	ECS
H17 :	1.224	1.641	0.269	0.588
MesoH :	-0.446	0.457	-0.240	0.154
MuHd_075 :	31.366	23.110	7.513	8.782
MuHd_095 :	27.168	20.722	9.003	6.526
MuHd_100 :	20.240	14.921	7.528	4.659
MuHd_105 :	15.443	14.607	5.693	3.521
Hmax_075 :	12.600	18.500	2.713	5.970
Hmax_095 :	17.063	20.387	4.959	6.064
Hmax_100 :	14.800	20.500	5.240	5.920
Hmax_105 :	10.383	15.283	4.105	5.320

PROBABILITY

of export to mitochondria: 0.6727

Fig-5.8: Confirmation of the mitochondrial targeting sequence using MitoProtII version 1.1 software. left panel showing the p28 sequence highlighting MTS in red color, right panel showing the details obtained in the MitoProtII software after the analysis of the result.

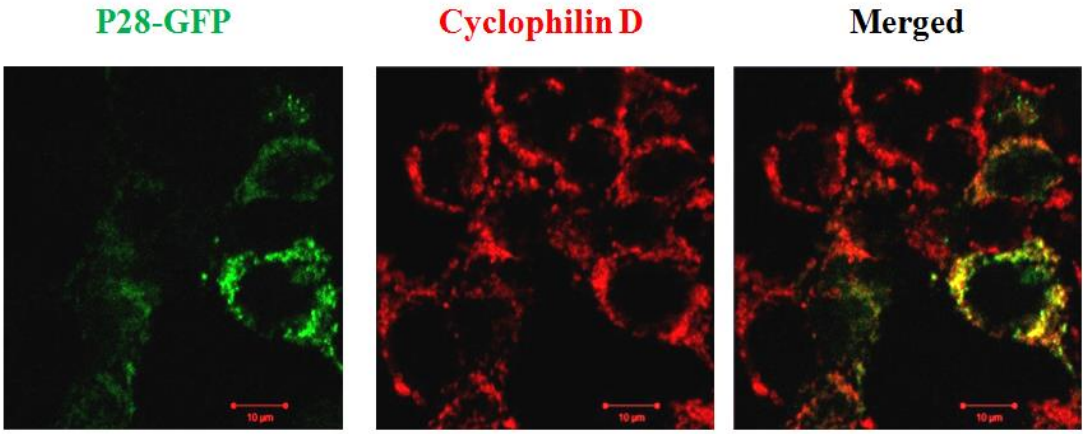

Fig-5.9: Subcellular localization of p28-GFP gene in HELA cells. Left panel: p28-GFP chimera localization in the HELA cells as GFP fluorescence, middle panel: Cyclophilin D in red fluorescence targeting mitochondria, panel-3: merged image (right panel) showing the mitochondria target in the yellow color.

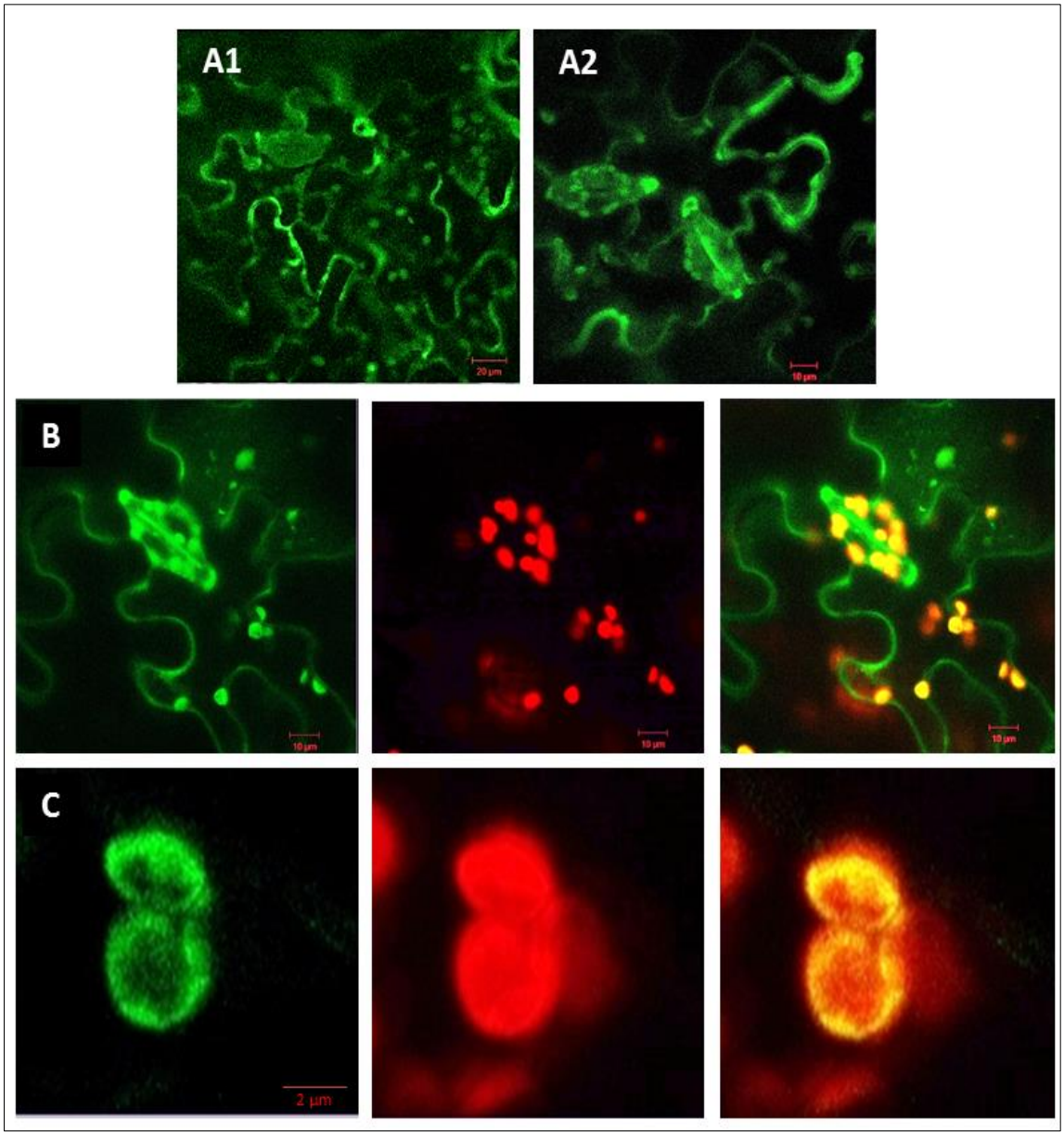

Fig-5.10: Subcellular localization of GFP-7A construct in *N. benthamiana*. A1) GFP-7A fluorescence was observed in the epidermal cells, A2) fluorescence in subsidiary cells and guard cells; B) panel-1: closer view of guard cells, Panel-2: autofluorescence of chloroplasts in the guard cells, panel-3: overlay image of the GFP and auto-fluorescence was observed in yellow color. C) Closer view of the chloroplasts was shown with GFP fluorescence and autofluorescence (panel-2). The overlay image was shown in the yellow color (panel-3).

5.3 (d) Localization of GFP-7B chimera

Transient expression of G-7B fusion construct, GFP fluorescence was observed as aggregates in all the cells after 36 hpi (fig-5.11A). Even after 48 hpi, the localization was not observed but stronger intense aggregates were observed in the cells (fig-5.11B). Auto

fluorescence of chloroplasts was observed in red color. In closer magnification of single aggregate (at 2 µm) was observed always in closer proximity to nucleus (N) and presumed to be rough endoplasmic reticulum (RER) and failed to localize to other cell organelles. No fluorescence was found in the nucleus in closer magnification (fig-5.11C).

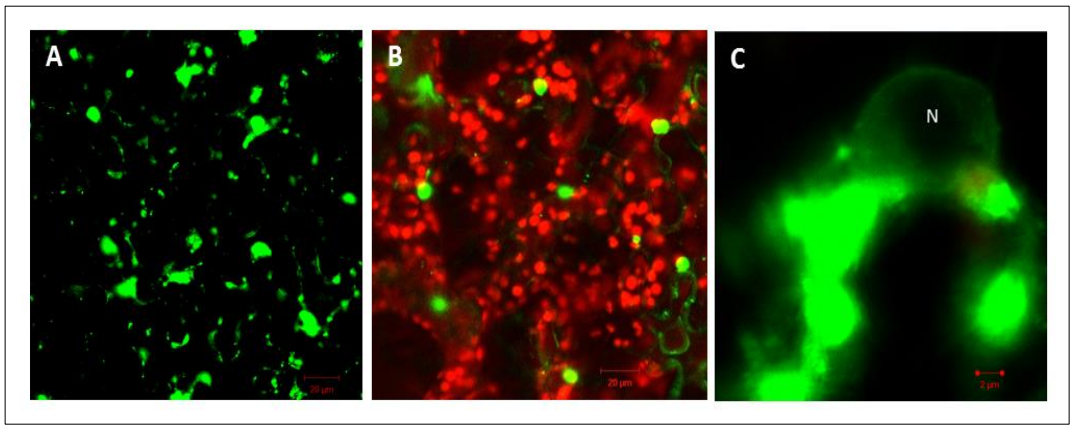

Fig-5.11: Subcellular localization of GFP-7B construct after 36 hpi in *N. benthamiana* plants. A) Fluorescence was observed as discrete spots all over the cells in 36 hr pi. B) Aggregates of GFP fluorescence after 48 hpi not targeting the organelles but formed larger aggregates, auto fluorescence of chloroplasts was observed in red color, C) Closer view of single aggregate at 2µm magnification where we observed the fluorescence around the nucleus (N) which we assume it as RER. The fluorescence was not observed in the nucleus (N).

5.3 (e) Co-infiltration of GFP-7A and GFP-7B chimeras fusion chimeras

Individual agro constructs (G-7A and G-7B) were mixed and infiltrated into the same leaf in equimolar concentrations [both are dyads of MP known as double gene block (DGB) proteins]. With this combination the GFP fluorescence was observed as fluorescent spots after 36 hpi (fig-5.12A) and enhanced GFP fluorescence was observed as distinct punctate spots along the cell walls which might be the modified plasmodesmata's all along cell wall (fig-5.12B). With this set of infiltration no fluorescence was observed as in chloroplasts or stomatal guard cells (fig-5.10) as in GFP-7A infiltration. In closer view the punctuate spots was also observed in bright field images also (fig-5.12C). However, we may need to use a marker protein which localizes to plasmodesmata as are in the process of procuring it. These results demonstrate that G-7A and G-7B interactions are a must to dock the movement protein complex to the plasmodesmata.

5.3 (f) Localization of GFP-CP chimera

In case of G-CP fusion chimera, the fluorescence was found all along the cell wall (presumably near the plasma membrane) after 36 hpi indicating its soluble nature (fig-5.13A). In most cases of localization, we could able to see clear signal along the cytoplasmic strands in form of network (fig-5.13B) which could be smooth ER (SER) indicating that the synthesized coat protein might be using SER for its intra-cellular trafficking (need to be confirmed through markers). In some planes, small fluorescent round structures were also observed uniformly in all the cells (fig-5.13C) which need to be studied further.

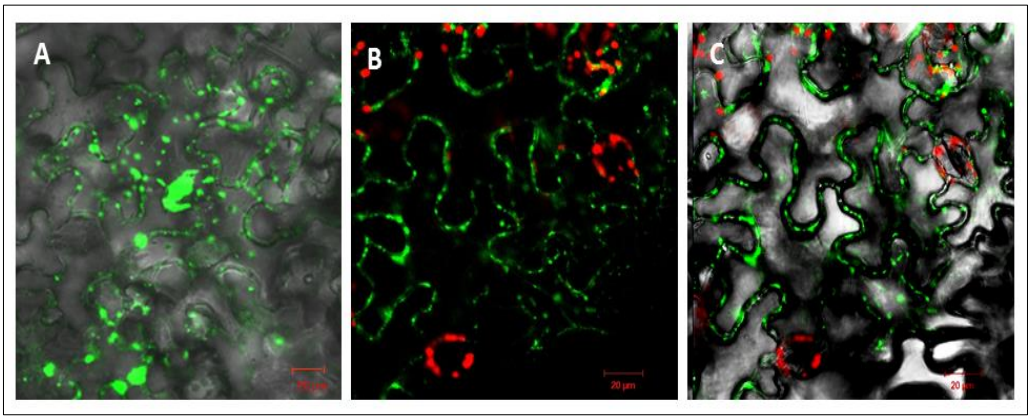

Fig-5.12: Subcellular co-localization of co-infiltrated GFP-7A and GFP-7B constructs. A) Bright field image of fluorescence was observed as fluorescence spots all over the cell 36 hpi, B) Fluorescence was observed clearly as the punctuate spots along the cell wall which might be plasmodesmata after 48 hpi, auto fluorescence of the chloroplasts was observed in red color, C) After 40 hpi the punctuate spots are clearly observed along the cell wall where cell boundary is clearly observed in bright field image.

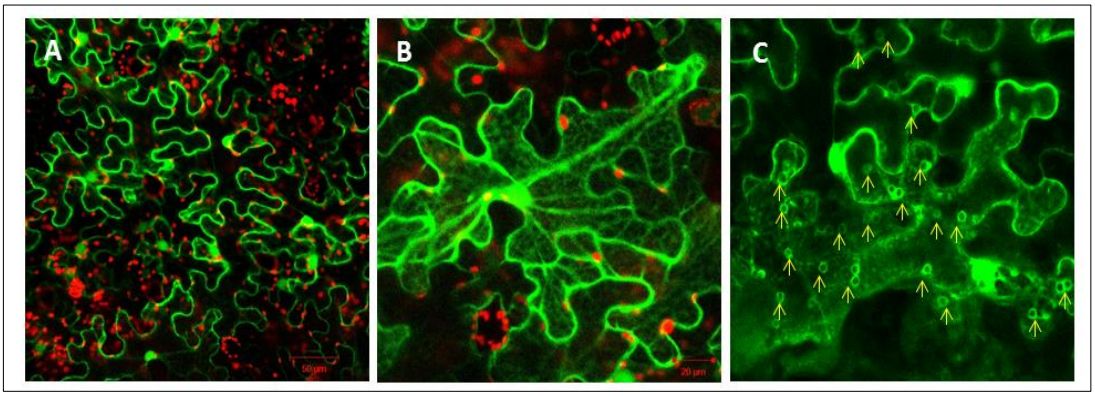

Fig-5.13: Sub cellular localization of GFP-CP chimera. A) In low magnification the fluorescence was observed uniformly along the cell wall indicating its soluble nature, B) In closer view (20 µm magification) of a single cell, we can see the fluorescent network in a cell that is seen clearly in all cells which could be SER, auto fluorescence of the chloroplasts was observed in red color C) Small unknown round fluorescent structures were also observed in the cells in further magnification in some planes (indicated by yellow colored arrows).

5.4 Discussion

Subcellular localization of individual viral genes was elucidated using green fluorescence protein, GFP. GFP was isolated from the jelly fish which is very advantageous over GUS for the *in planta* studies (Kain and Li *et al*., 2005). It is the most widely used non-destructive method to study *in vivo* gene expression. Transient expression system (agroinfiltration) which is harmless, biodegradable, robust and simple procedure even can be employed for increasing the yield of the required proteins using viral vectors for the analysis of the viral GFP chimeras in the present chapter (Marillonnet *et al*., 2005; Gopinath *et al*., 2005). In order to visualize diverse viral genes during infection process, we have constructed GFP chimeras of all the MNSV encoded genes on the 5' end of the gene in binary vector, pCB302.

The second transmembrane domain in the p29 gene of MNSV-A1 strain was proved to be localizing to mitochondria even though its specific function was not known (Mochizuki *et al*., 2008). Though we failed to see the localization of N-terminal GFP fused p28 chimera (G-28) of MNSV-Hyd to the specific organelle we are able to identify MTS through insilico analysis. The 35 aa MTS was predicted in the p28 gene of MNSV-Hyd on the N-terminal region (fig-5.8). Initially we have constructed GFP-28 chimera in binary vector, however we are able to observe very faint signal along with the cell wall including bright fluorescent patches in individual cells. Since, we have blocked the N-terminal MTS with GFP fusion the synthesized fusion protein may not be targeted to mitochondria, probably it may require free N-terminus for other interactions. However, 28-GFP construct developed by Dr. Naresh Babu Sepuri's has rightly targeted to mitochondria as has been demonstrated by the cyclophilin-D marker in Hela cells. This means that we need to generate 28-GFP construct to demonstrate the mitochondrial targeting of p28 gene and further characterize the gene functionally. We are in the process of constructing 28-GFP construct and functional analysis is in the process.

Literature of MNSV revealed that two small proteins in the central region of the viral genome are enough to support the viral movement in the host by acting *in trans* by mutational studies and GFP chimeras (Genoves *et al*., 2006). The first protein 7A is RNA binding protein (Navarro *et al*., 2006) and the second one is membrane bound (Martinez-Gil *et al*., 2007). In case of MNSV-Hyd, infiltration of GFP-7A construct alone localized to

stomatal guard cells mainly to the chloroplasts in 48 hpi and GFP-7B alone was observed all along the cell as strong fluorescent aggregates where there is no localization to a particular organelle after in 48 hpi. Nevertheless, co-infiltration of both GFP-7A and GFP-7B chimeras was observed as fluorescent punctate spots along the cell wall which could be the modified plasmodesmata and is the characteristic feature of MP. Localization of GFP-7A to chloroplasts was not observed in co-infiltration. This gives a lead that interaction of both the proteins at a particular movement in and requires for localizing to plasmodesmata which is not observed in the individual protein characterization. This also needs to be analyzed further by fusing different reporter genes (RFP-7A/GFP-7A and RFP-7B/GFP-7B) to study further about this interaction.

The CP of MNSV apart from the structural function, it is also plays a role in symptom control and systemic movement. It also acts silencing suppressor protein which can delay the RNA silencing in host plant, *N. benthamiana* but not prevent the PTGS in transient expression. The activity of the protein is 10 folds weaker than HC-Pro as measured by mRNA accumulation of GFP on 5^{th} day of infiltration (Genoves *et al*., 2006). In MNSV-Hyd, infiltration of GFP on the N-terminal of CP gene (G-CP) showed fluorescence along the cell wall and the fluorescence of the cytoplasmic network was also clearly observed in the cells. These cytoplasmic connections could be SER which needs to be validated through markers where CP is using SER for its intracellular trafficking. Apart from that some unknown cell organelles (small fluorescent bodies) were observed in some planes which also need to be validated by using markers. The localization study of the individual genes was the primary step to delineate the molecular pathways of the viral replication and trafficking.

The biologically active infectious clone of MNSV-Hyd in the previous chapter and localization study of the viral proteins in the present chapter are handy to study host-pathogen interactions of MNSV-Hyd can pave the way for the functional analysis of MNSV-Hyd genes and their roles on diverse viral processes so efficiently.

SUMMARY

Summary

During the field surveys in 2009 in Rangareddy district of newly formed Telangana state, a new virus named *Melon necrotic spot virus* (designated MNSV-Hyd) was identified on *Cucumis melo* crop with symptomology ranging from severe mosaic symptoms to death of the whole plant.

The thesis discussed about the biological and molecular characteristics of the new virus which proceeds with the construction of infectious cDNA clone, development of in vivo assay system, agroinfiltration and partly studied about the subcellular localization of the virus encoded proteins using GFP chimeras. The biological properties of the new virus include icosahedral symmetry with 28 nm diameter when observed under TEM by negative staining process, 44 kDa of CP on SDS-PAGE with 4.3 kb monopartite, positive sense single stranded RNA genome. The ds RNA profiling of the virus showed three major bands, one genomic and two sub-genomic molecules. The virus was reacted positively with antisera against MNSV procured from Japan in DIBA and western analysis. The possible role of the seed in the virus transmission was not observed in ELISA. The new virus has extended host range to *N. benthamiana* and most of the Fabaceae hosts which are non-hosts for all MNSV reported strains.

The complete genome sequence of MNSV-Hyd was established in five independent overlapping clones by molecular biology cloning techniques. The full length nucleotide sequence was submitted in Genbank with accession number JX879088. The NCBI-blast analysis of nucleotide sequence doesn't show homology with any of the reported viruses rather contained short regions of identity (mainly in RdRp and MP) with MNSV strains kochi & tottori from Japan with 54% identity. The linear genetic map of the virus was deduced which encodes five proteins, p28, p89, 7A, 7B and p42. The RDRP protein, p89 is formed as the result of read through stop codon after p28 gene has GDD motif which is involved in replicase activity, 7A & 7B proteins are involved in the cell-to-cell movement and p42 protein is the structural protein implicate in the virion formation. In the diversity analysis, it was observed that MNSV-Hyd as a new strain of MNSV rather than an isolate with only 55% of similarity with other MNSV strains & isolates.

Full length infectious cDNA clone to MNSV-Hyd (ic MNSV-Hyd) was constructed which serves as tool to study the viral genome, gain insights in to the genome organization, virus gene functions and gene expression studies. The infectious clone was

constructed by fusing 35S double promoter on the 5' end of the genome for efficient transcription and a ribozyme at the 3' end of the genome for generation of unit length molecules. Proficient infection was observed in the ic MNSV-Hyd clone agroinfiltrated N. benthamiana plants similar to that of wild type infection. To our knowledge, this is the second infectious cDNA clone generated in Indian sub-continent for the RNA virus.

The sub cellular localization of the MNSV-Hyd encoded proteins were also studied as GFP chimeras using confocal laser scanning microscopy. The GFP fluorescence of chimera G-28 gene was observed very faintly where it was difficult to study localization of the gene. *In silico* analysis of p28 gene showed the presence of mitochondrial targeting sequence at the 5' end of the gene which needs the further analysis by *in planta* studies. The GFP fluorescence was observed in the stomatal guard cells with G-7A chimera and localization was not observed except the discrete fluorescent spots in case of G-7B chimera. It was proved that interaction of 7A and 7B proteins in MNSV-Hyd is required for the viral cell-to-cell movement by co-infiltration study and as well as by individual chimeras. The CP protein fluorescence was observed all over the cell indicating its soluble nature and the cellular network which might be the SER was observed in all the cells. The small fluorescent bodies were observed in all the cells which need to be further validated by organelle markers.

Based on biological characters, host range studies, genome organization, NCBI-blast results and diversity analysis, MNSV-Hyd is member of Carmovirus and it might be a new strain of MNSV from Indian sub-continent for the first time.

REFERENCES

&

APPENDICES

References

Abou-Jawdah, Y., Sobh, H., Ei-Zammar, S., Fayyad, A., Lecoq, H., 2000. Incidence and management of cucurbits in Lebanon. Crop protection 19; 217-224.

Adkins, S., Hammond, J., Gera, A., Maroon-Lango, C. J., Sobolev, I., Harness, A., Zeiden, M., Spiegel, S., 2006. Biological and molecular characterization of a novel Carmovirus isolated from Angelonia. Phytopathol. 96 (5); 460-467.

Agrios, G. N., 2005. How plants defend themselves against pathogens. In: Dreibelbris D (ed), plant pathology. 5th edition, Elsevier, San Diego, CA; 922.

Ahlquist, P., French, R., Janda, M., Sue Lesch-Friest, L., 1984. Multiple component RNA plant virus infection derived from viral cDNA. Proc. Natl. Acad. Sci 81; 7066-7070.

Ali Sevik, M., Toksoz, Y., 2008. Occurrence of Squash mosaic virus (SqMV) Infecting pumpkin and squash growing in Samsun, Turkey. J. Turk. Phytopathol. 37 (1); 15-25.

Andret-Link, P., Fuchs, M. 2005. Transmission specificity of plant viruses by vectors. J. Plant. Pathol. 87 (3); 153-165.

Annamalai, P., Rao, A.L., 2005. Replication independent expression of genome components and capsid protein of *Brome mosaic virus in planta*: a functional role for viral replicase in RNA packaging. Virol. 338; 96-111.

Arslan1, D., Legendre1, M., Seltzer, V., Abergel, C. and Claverie, J. M. 2011. Distant Mimivirus relative with a larger genome highlights the fundamental features of Megaviridae. Proc. Natl. Acad. Sci. 108 (42); 17486-1749.

Avgelis, A., 1985. Occurance of *Melon Necrotic Spot Virus* in Crete (Greece). Phytopath 114; 365-372.
Barajas, D., Jiang, Y., Nagy, P. D., 2009. A Unique Role for the Host ESCRT Proteins in replication of *Tomato bushy stunt virus.* PLOS Pathogen 5 (12); 1-13.

Baulcombe, D. C., Chapman, S. N., Santa Cruz, S., 1995. Jelly fish green fluorescent protein as a reporter for virus infections. The Plant. J. 7 (6); 1045-1053.

Bedoya, L., Martínez, F., Rubio, L., Jose-Antonio Daros., 2010. Simultaneous equimolar expression of multiple proteins in plants from a disarmed potyvirus vector. J. Biotech. 150; 268-275.

Boonrod, K., Chotewutmontri, S., Galetzka, D., Krczal, G., 2005. Analysis of tombusvirus revertants to identify essential amino acid residues within RNA-dependent RNA polymerase motifs. J. Gen. Virol. 86; 823-826.

Boyer, J., Haenni, A., 1994. Infectious transcripts and cDNA clones of RNA viruses. Virology 198, 415-426.
Brandes, C., Plautz, J. D., Stanewsky, R., Jaison, C. F., Straume, M., Wood, K. V., Kay, S. A., Hall, J. C., 1996. Novel features of Drosophila period transcription revealed by real time luciferase reporting. Neuron 16 (4); 687-692.

Bryan, G. T., Gardner, R. C., Forster, R. L. S., 1992. Nucleotide sequence of the coat protein gene of a strain of clover yellow vein virus from New Zealand: conservation of a stem-loop structure in the 3' region of potyviruses Arch. virol. 124;133-146.

Burdon, J. J., 1987. Diseases and Plant Population Biology. Cambridge: Cambridge Univ. Press. 208.
Carrington, J. C., Heaton, L. A., Zuidema, D., Hillman, B. I., Morris, T. J., 1989. The genome structure of *Turnip Crinkle Virus*. Virology 170 (1); 219-226.

Burgyan, J., Horynik, C., Szittya, G., Silhavy, D., Bisztray, G., 2000. The ORF-1 products of tombusviruses play a crucial role in lethal necrosis of viral-infected plants. J. Virol. 74 (23); 10873-10881.

CABI (2010) *Melon necrotic spot virus* [Distribution map]. Distribution Maps of Plant Diseases 2010 No. October pp. Map 1089 (Edition 1).
Campbell, R. N., Sim, S. T., Lecoq, H., 1995. Virus transmission by host specific strains of *Olphidium bornovanus* and *Olphidium brassicae*. Eur. J. Pl. Pathol. 101; 273-182.

Campbell, R. N., Wipf-scheibel, C., Lecoq, H., 1996. Vector-assisted seed transmission of *Melon necrotic spot virus* in melon. Phytopathol 86, 1294-1298.

Canizares, M. C., Marcos, J. F., Pallas, V., 2001. Molecular variability of twenty-one geographically distinct isolates of *Carnation Mottle Virus* (CarMV) and phylogenetic relationships within the Tombusviridae family. Arch. Virol 146; 2039-2051.

Carette, J. E., Van Lent, J., MacFarlane, S. A., Wellink, J., Van Kammen, A., 2002a. *Cowpea mosaic virus* 32- and 60-kilodalton replication proteins target and change the morphology of endoplasmic reticulum membranes. J. Virol. 76; 6293-6301.

Carette, J. E., Verver, J., Martens, J., Van Kampen, T., Wellink, J., Van Kammen, A., 2002b. Characterization of plant proteins that interact with *Cowpea mosaic virus* '60K' protein in the yeast two-hybrid system. J. Gen. Virol. 83; 885-893.

Carrington, J. C., Heaton, L. A., Zuidema, D., Hillman, B. I., Morris, T. J., 1989. The genome structure of *Turnip Crinkle Virus*. Virology 170 (1); 219-226.

Carrington, J. C., Kasschau, K. D., Mahajan, S., K., Schaad, M. C., 1996. Cell-to-cell and long distance transport of viruses in plants. The plant cell 8; 1669-1681.

Chalfie, M., Tu, Y., Euskirchen, G., Ward, W. W., Prasher, D. C., 1994. Green fluorescent protein as a marker for gene expression. *Science* 263; 802-805.

Chao, C. H., Chen, T,C., Kang, Y,C., Li, J, T., Huang, L,H., Yeh, S,D., 2010. Characterization of *Melon Yellow Spot Virus* infecting cucumber in Taiwan. Plant Phytology Bulletin 19; 41-52.

Chapman, 2008. Construction of infectious clones for RNA viruses: TMV. In: Foster, G. D., Johansen, I. E., Hong, Y., Nagy, P.D., eds. Plant Virology Protocols: from viral sequence to protein function. Humana Press, Totowa, NJ, USA.

Chen, T. C., Lu, Y.Y., Cheng, Y.H., Chang, C.A., Yeh, S.D., 2008. *Melon necrotic spot virus* in watermelon: a first record from Taiwan. Plant Pathol. 57; 765.

Chiba, M., Reed, J. C., Prokhnevsky, A. I., Chapman, E. J., Mawassi, M., Koonin, E. V., Carrington, J. C., Dolja, V. V., 2006. Diverse suppressors of RNA silencing enhance agroinfection by a viral replicon. Virology 346; 7-14.

Chiu, W. L., Niwa, Y., Zeng, W., Hirano, T., Kobayashi, H., Sheen, J., 1996. Engineered GFP as a vital reporter in plants. Current Biology 6 (3); 325-330.

Choi, G. S., Kim, J. H., Kim, J. S., 2003. Characterization of *Melon necrotic spot virus* isolated from muskmelon. Plant Pathol. J. 19; 123-127.

Christensen, N. M., Faulkner, C., Oparka, K., 2009. Evidence for unidirectional flow through plasmodesmata. Plant Physiol 150; 96-104.

Citovsky, V., Wong, M. L., Shaw, A. L., Prasad, B. V. V., Zambryski, P. 1992. Visualization and characterization of *tobacco mosaic virus* movement protein binding to single-stranded nucleic acids. Plant Cell. 4 (4); 397-411.

Ciuffreda, P., Rubino, L., Russo, M., 1998. Molecular cloning and complete sequence of *Galinsoga mosaic virus* genome RNA. Arch. Virol. 143; 173-180.

Cohen, Y., Gisel, A. & Zambryski, P. C., 2000. Cell-to-cell and systemic movement of recombinant green fluorescent protein-tagged *Turnip crinkle viruses*. Virology 273; 258-266.
Coudriet, D. L., Kishaba, A.N & Carroll, J.E., 1979. Transmission of *Muskmelon necrotic spot virus* in muskmelons by cucumber beetles. J. Eco. Entom. 72; 560-561.

Coutts, B. A., Kehoe, M. A., Webster, C. G., Wylie, S. J., Jones, R. A. C., 2011. *Zucchini yellow mosaic virus*: biological properties, detection procedures and comparison of coat protein gene sequences. Arch Virol 156; 2119-2131.

Cowan, G. H., Lioliopoulou, F., Ziegler, A., Torrance, L., 2002. Subcellular localization, protein interactions and RNA binding of *Potato mop-top virus* triple gene block proteins. Virology 298 (1); 106-115.

Cui, X., Wei, T., Chowda-reddy, R. V., Sun, G., Wang, A., 2010. The *Tobacco etch virus* P3 protein forms mobile inclusions via the early secretory pathway and traffics along actin microfilaments. Virol. 3917 (1); 56-63.

Curin, M., Ojangu, E. L., Trutnyeva, K., Ilau, B., Truve, E., Waigmann, E., 2007. MPB2C, a microtubule - associated plant factor, is required for microtubular accumulation of *Tobacco mosaic virus* movement protein in plants. Plant Physiol. 143 (2); 801-811.

Davis, S. J., Vierstra, R. D., 1998. Soluble and highly fluorescent variants of green fluorescent protein for use in higher plants. Plant Mol. Bio. 36; 521-528.

Dawson WO, Beck DL, Knorr DA, Grantham GL. 1986. cDNA cloning of the complete genome of *Tobacco mosaic virus* and production of infectious transcripts. Proc. Natl. Acad. Sci 3; 1832- 1836.

Day, T. A., 2001. Multiple trophic levels in UV-B assessments- completing the ecosystem. New Phytologist 152 (2); 183-186.

De Carlo, S., Harris, J. R., 2011. Negative staining and cryonegative staining of macromolecules and viruses for TEM. Micro 42; 117-131.

den Boon, J. A., Chen, J., Ahlquist, P., 2001. Identification of sequences in *Brome mosaic virus* replication protein 1a that mediate association with endoplasmic reticulum membranes. J. Virol. 75; 12370-12381.

Diaz, J. A., Bernal, J. J., Moriones, E., Aranda, M. A., 2003. Nucleotide sequence and infectious transcripts from a full-length cDNA clone of the Carmovirus *Melon necrotic spot virus*. Arch Virol 148; 599-607.

Diaz, J. A., Nieto,C., Moriones, E., Truniger,V., Aranda, M.A., 2004. Molecular Characterization of a *Melon necrotic spot virus* strain that overcomes the resistance in melon and non-host Plants. MPMI. 17 (6); 668-675.

Dietrich, C., Maiss, E., 2003. Fluorescent labelling reveals spatial separation of potyvirus populations in mixed infected *Nicotiana benthamiana* plants. J. Gen. Virol. 84 (10); 2871-2876.

Diez, J., Marcos, J. F., Pallas, V., 1998. Carmovirus isolation and RNA extraction. Methods in molecular biology. 81; Plant virology protocols: From virus isolation to transgenic resistance. Edited by: Foster, G. D., Taylor, S. C., Humana Press Inc., Totowa, NJ.

Diveki, Z., Salanki, K., Balazs, E., 2004. The necrotic pathotype of the *Cucumber mosaic virus* (CMV) Ns strain is solely determined by amino acid 461 of the 1a protein. MPMI 17 (8); 837-845.

Dodds, J. A., 1993. ds RNA in diagnosis. In: Mathews R.E.F. (ed). Diagnosis of plant virus diseases. 273-294. CRC Press. Boca Raton, USA.

Domingo, E., 1997. RNA virus mutations and fitness for survival. Ann. Rev, Micro. 51; 151-178.

Domingo, J. L., 2006. Polychlorinated diphenyl ethers (PCDEs): environmental levels, toxicity and human exposure. A review of the published literature. Environ. Int. 32; 121-127.

Dzianott, A. M., Bujarski, J. J., 1989. Derivation of an infectious viral RNA by autolytic cleavage of in vitro transcribed viral cDNAs. PNAs 86 (13); 4823-4827.

Edwardson, J. R., and R. G. Christie. 1991. Cucumoviruses, CRC Handbook of viruses infecting legumes, CRC Press, Boca Raton, Fla ; 293-319.

Eiamtanasate, S., Juricek, M., Yap, Y. K., 2007. C-terminal hydrophobic region leads PRSV P3 protein to endoplasmic reticulum. Virus genes 35; 611-617.
Epel, B. L., 2009. Plant viruses spread by diffusion on ER-associated movement-protein-rafts through plasmodesmata gated by viral induced host beta-1,3-glucanases.Semin. Cell Dev. Biol. 20;1074-1081.

Fang, L., Coutts, R. H. A., 2013. Investigations of the *Tobacco necrosis virus* D p60 replicase protein. PLOS One 8 (11); 1-10.

Fattouh, F. A., 2003. Double infection of cucurbit host by *Zucchini yellow mosaic virus* and *Cucumber mosaic virus*. Pak. J. PhytoPathol.2; 85-90.

Fernandez-salas, E., Sagar, M., Cheng, C., Yuspa, S. H., Weinberg, W. C., 1999. P53 and tumor necrosis factor α regulate the expression of a mitochondrial chloride channel protein. J. Bio. Chem. 274; 36488-36497.

Forner, J., Binder, S., 2007. The red fluorescent protein eqFP611: application in subcellular localization studies in higher plants. BMC Plant Biology 7 (28); 1-12.

Forterre, P., 2010. "Gaint viruses: Conflicts in revisiting the virus concept", Intervirology 53; 362-378.

Franck, A., Jonard, G., Richards, K., Hirth, L. and Guilley, H., 1980. Nucleotide sequence of *Cauliflower mosaic virus* DNA. Cell 21; 285-294.

Garcia-Arenal, F., Fraile, A., Malpica, J. M., 2001. Variability and genetic structure of plant virus populations. Annu. Rev. Phytopathol. 39;157-186.

Gelvin, S. B., 2003. Transformation: the biology behind the *Agrobacterium*-mediated plant "Gene-Jockeying" Tool. Microbiol. Mol. Biol. Rev. 67(1); 16-37.

Genoves, A., Navarro, J.A., Pallas, V., 2006. Functional analysis of five melon necrotic spot genome encoded proteins. J. Gen. Virol. 87; 2371-2380.

Genoves, A., Navarro, J.A., Pallas, V., 2009. A Self-interacting carmovirus movement protein plays a role in binding of viral RNA during cell-to-cell movement and shows an actin cytoskeleton movement in cell periphery. Virol. 395; 133-142.

Genoves, A., Navarro, J. A., Pallas, V., 2010. The Intra- and intercellular movement of *Melon Necrotic Spot Virus* depend on the active secretory pathway. MPMI 23(3), 263-267.

Genoves, A., Pallas, V., Navarro, J. A., 2011. Contribution of topology determinants of a viral movement protein to its membrane association, intracellular traffic, and viral cell-to-cell movement. J. Virol. 85 (15); 7797-7809.

Gerdes, H. H., Kaether, C., 1996. Green fluorescent protein applications in cell biology. FEBS Letters 389; 44-47.

Ghasemzadeh, A., Bashir, N. S., Masoudi, N., 2012. Sequencing part of *Watermelon mosaic virus* genome and phylogenetical comparison of 5 isolates with other isolates from world. J. Agric. Food. Tech. 2 (6); 93-101.

Gheysen, G., Geert, A., Van Montagu, M., 1998. *Agrobacterium* mediated plant transformation: a scientifically intriguing story with significant applications. In: K. Lindsey (Ed.), Transgenic Plant Research, Harwood Academic Publishers, Amsterdam, 1-33.

Gibbs, A., 1999. Evolution and origins of tobamoviruses. Phil. Trans. R. Soc. Lond. B 354; 593-602.

Gils, M., Kandzia, R., Marillonnet, S., Klimyuk, V., Gleba, Y., 2005. High-yield production of authentic human growth hormone using a plant virus-based expression system. Plant Biotech. J. 3; 613-620.

Giritch, A., Marillonnet, S., Engler, C., Van Eldik, G., Botterman, J., Klimyuk, V., Gleba, Y., 2006. Rapid high yield expression of full size IgG antibodies in plants coinfected with non- competing viral vectors. PNAS 103 (40); 14701-14706.

Gleba, Y., Klimyuk, V., Marillonnet, S., 2007. Viral vectors for the expression of proteins in plants. Curr. Opin. biotechnology 18 (2); 134-141.

Goelet, P., Lomonossoff, G. P., Butler, P. J. G., Akam, M. E., Gait, M. J., and Karn, J., 1982. Nucleotide sequence of tobacco mosaic virus RNA. Proc. Natl. Acad. Sci. USA 79; 5818- 5822.

Gonazalez-Garza, R., Gumpf, D. J., Kishaba, A. N., Bohn, G. W., 1979. Identification, seed transmission, and host range pathogenicity of a California isolate of *Melon necrotic spot virus*. Phytopathol. 69; 340-345.

Goodin, M. M., Zaitlin, D., Naidu, R. A., Lommel, S. A., 2008. *Nicotiana benthamiana*: its history and future as a model for plant pathogen interactions. MPMI 21 (8); 1015-1026.

Gopinath, K., Dragnea, B., and Kao, C. 2005. Interaction between *Brome mosaic virus* proteins and RNAs: Effects on RNA replication, protein expression, and RNA stability. J. Virol. 79;14222- 14234.

Gosalvez-Bernal, B., Genoves, A., Navarro, J. A., Pallas, V., Sanchez-Pina, M. A., 2008. Distribution and pathway for phloem dependent movement of *Melon necrotic spot virus* in melon plants. Mol. Plant. Pathol. 9 (4); 447-461.

Govind, K., Makinen, K., Savitri, H. S., 2012. *Sesbania mosaic virus* infectious clone: possible mechanism of 5' and 3' end repair and role of poly protein processing in viral replication. PLOS One 7 (2); 1-13.

Gu, Q. S., Bao, W. H., Tian, Y. P., Prins, M., Yang, H. X., Lu, J., Liu, L. F., Peng, B., 2008. *Melon necrotic spot virus* newly reported in China. *New Disease Reports* 16; 16.

Guilley, H., Carrington, J. C., Balazs, E., Jonard, G., Richards, K., Morris, T.J., 1985. Nucleotide sequence and genome organization of *Carnation mottle virus*. Nucl. Acids. Res. 13 (18); 6663-6677.

Gulati-Sakhuja, A., Liu, H. Y., 2010. The complete nucleotide sequence and genome organization of *Calibrachoa mottle virus*, a new species in the genus Carmovirus of the family, Tombusviridae.Virus. Res. 147 (2); 216-223.

Gulati-Sakhuja, A., Rains, L., Tian, T., Liu, H. Y., 2011. The complete nucleotide sequence and genome organization of a novel carmovirus-*honeysuckle ringspot virus* isolated from honeysuckle. Arch. Virol.156 (9);1635-1640.

Hall, T. 1999. Bio Edit: a user-friendly biological sequence alignment editor and analysis program for Windows 95/98/NT. Nucleic Acids Symposium Series 41, 95-98.

Hamilton, R. I., Edwardson, J. R., Francki, R. I. B., Hsu, H. T., Hull, R., Koenig, R., Milne, R. G., 1981. Guidelines for the identification and characterization of plant viruses. J. gen. virol. 54; 223-241.

Han, S. S., Yoshida, K., Karasev, A. V., Iwanami, T., 2002. Nucleotide sequence of Japanese isolate of *Squash mosaic virus*. Arch Virol 147; 437-443.

Hanson, M. R., Kohler, R. H., 2001. GFP imaging: methodology and application to investigate cellular compartmentation in plants. J. Exp. Bot. 52 (356); 529-539.

Harries, P. A., Palanichelvam, K., Yu, W., Schoelz, J. E., Nelson, R. S., 2009a. The *Cauliflower Mosaic Virus* protein P6 forms motile inclusions that traffic along actin microfilaments and stabilize microtubules. Plant physiology. 149; 1005-1016.

Harries, P. A., Park, J. W., Sasaki, N., Ballard, K. D., Maule, A. J., Nelson, R. C., 2009b. Differing requirements for actin and myosin by plant viruses for sustained intercellular movement. PNAS 106 (41); 17594-17599.

Harries, P. A., Schoelz, J. E., Nelson, R. S., 2010. Intracellular transport of viruses and their components: utilizing the cytoskeleton and membrane highways. MPMI 23 (11); 1381-1393.

Harries, P., Ding, B., 2011. Cellular factors in plant virus movement: At the leading edge of macromolecular trafficking in plants. Virol. 411, (2); 237-243.

Haseloff, J., Kirby, R. S., Prasher, D. C., Hodge, S., 1997. Removal of a cryptic intron and sub cellular localization of green fluorescent protein are required to mark transgenic *Arabidopsis* plant brightly. Proc. Natl. Acad. Sci. 94 (6); 2122-2127.

Haupt, S., Cowan, G. H., Ziegler, A., Roberts, A. G., Oparka, K. J., Torrance, L., 2005. Two plant viral movement proteins traffic in the endocytic recycling pathway. The plant cell 17 (1); 1164-1181.

Heaton, L. A., Carrington, J.C., Morris, T. J., 1989. *Turnip crinkle virus* infection from RNA synthesized in vitro. Virol. 170; 214-218.

Hefferon, K. L., 2012. Plant virus expression vectors set the stage as production platforms for biopharmaceutical proteins. Virol. 433; 1-6.

Heijden, M. W. V. D., Jan Carette, E., Reinhoud, P. J., Haegi, A., Bol, J. F., 2001. *Alfalfla mosaic virus* replicase proteins P1 & P2 interact and co localize at the vacuolar membrane. J. Virol. 75 (4); 1879-1887.

Hellens, R. P., Edwards, E. A., Leyland, N. R., Bean, S., Mullineaux, P. M., 2000. pGreen: a versatile and flexible binary Ti vector for *Agrobacterium*-mediated plant transformation. Plant Mol. Biol. 42; 819-832.

Herrera, J. A.,Cebrian, M. C., Jorda, C., 2006. First Report of *Melon necrotic spot virus* in Panama. Plant disease 90 (9); 1261.

Herranz, M. C., Pallas, V., 2004. RNA binding properties and mapping of RNA binding domain from the movement protein of the *Prunus necrotic ring spot virus*. J. Virol. 85 (3); 761-768.

Hessa, T., White, S. H., Von Heijne, G., 2005. Membrane insertion of a potassium channel voltage sensor. Science 307 (5714); 1427.

Hobbs, H. A., Reddy, D. V. R., Rajeshwari, R., Reddy, A. S., 1987. Use of antigen coating method and protein coating ELISA procedures for detection of three peanut viruses. Plant Dis. 71; 747-749.

Hofmann, C., Niehl, A., Sambade, A., Steinmetz, A., Heinlein, M., 2009. Inhibition of *Tobacco mosaic virus* movement by expression of an actin-binding protein. Plant physiol. 149; 1810-1823.

Horvath, J., 1993. Host plants in diagnosis. Diagnosis of plant virus diseases edited by Matthews. R. E. F. CRC Press, Boca Raton, Florida, USA; 15-48.

Hu, X., Meacham, T., Ewing, L., Gray, S. M., Karasev, A. V. 2009. A novel recombinant strain of *Potato virus* Y suggests a new viral genetic determinant of vein necrosis in tobacco. Virus Research 143: 68-76.

Huang, M., Koh, D. D. Y., Weng, L. J., Chang, M. L., Yap, Y. K., 2000. Complete nucleotide sequence and genome organization of *Hibiscus chlorotic ringspot virus*, a new member of Carmovirus: evidence for the presence and expression of two novel open reading frames. J.Virol 74; 3149-3155.

Hull, R., 2014. Matthew's Plant virology, 5th Edition, Academic Press, San Diego, CA.

Ishikawa, M., Janda, M., Krol, M. A., Ahlquist, P., 1997. *In vivo* DNA expression of functional *Brome mosaic virus* RNA replicons in *Sacchromyces cerevisiae*. J. Virol. 71; 7781-7790.

Jach, G., Binot, E., Frings, S., Luxa, K., Schell, J., 2001. Use of red fluorescent protein from *Discosoma* sp. as a reporter for plant gene expression. The plant J. 28 (4); 483-491.

Jackson, A. O., Lim, H. S., Bragg, J., Ganesan,U., Lee, M. Y., 2009. Hordeivirus replication, movement, and pathogenesis. Ann. Rev. Phytopathol. 47; 385-422.

Jefferson, R. A., 1987. Assaying chimeric genes in plants: the GUS gene fusion system. Plant Mol. Biol. Rep. 5; 387-405.

Joensuu, J. J., Conley, A. J., Lienemann, M., Brandle, J. E, Linder, M. B., Menassa, R., 2010. Hydrophobin fusions for high-level transient protein expression and purification in *Nicotiana benthamiana*. Plant Physiol 152; 622-633.

Johenson, L. K, Carrington, J. C, 2001. Silencing on the spot induction and suppression of RNA silencing in the agrobacterium mediated transient expression system. Plant physiology 126; 930-938.

Junqueira, B. R. T., Nicolini, C., Lucinda, N., Orílio, A. F.,Nagata, T., 2014. A simplified approach to construct infectious cDNA clones of a Tobamovirus in a binary vector. J. Virol. Methods 198; 32-36.

Kain, S. R., Adams, M., Kondepudi, A., Yang, T. T., Ward, W. W., Kitts, P., 1995. Green fluorescent protein as a reporter of gene expression and protein localization. Biotech. 19 (4); 650-655.

Kain, S., Li, X., 2005. Rapidly degrading GFP (Green Florescent Protein): Properties, Applications, and Protocols. Biotechniques 19 (4); 650-654.

Kang, B. C., Yeam, I., Jahn, M. M., 2005. Genetics of plant virus resistance. Ann. Rev. Phytopathol. 43; 581-621.

Kasteel, D. T., Van der wel, N. N., Jansen, K. A., Goldbach, R, W., Van Lent, J, W., 1997. Tubule forming capacity of the movement proteins of *Alfalfa mosaic virus* and *Brome mosaic virus*. J. Gen. Virol. 78 (8); 2089-2093.

Kehr, J., Buhtz, A., 2008. Long distance transport and movement of RNA through the phloem. J. Exper. Botany 59, (1); 85-92.

Kido, K., Mochizuki, T., Matsuo, M., Tanaka, C., Kubota, K., Ohki, T., Tsuda, S., 2008a. Functional degeneration of the resistance gene nsv against *Melon necrotic spot virus* at low temperature. Eur. J. Plant Pathol. 121; 189-194.

Kido, K., Tanaka, C., Mochizuki, T., Kubota, K., Ohki, T., Ohnishi, J., Knight, L. M., Tsuda, S., 2008b. High temperatures activate local viral multiplication and cell-to-cell movement of *Melon necrotic spot virus* but restrict expression of systemic symptoms. Phytopathol 98 (2); 181-186.

King, A. M. Q., Adams, M. J., Carstens, E. B., Lefkowitz, E. J. editors., 2012. Virus Taxonomy Ninth Report of the International Committee On Taxonomy of Viruses. San Diego, CA: Elsevier Academic Press. 1327.

Kiraly, L., Cole, A. B., Bourque, J. E., Schoelz, J. E., 1999. Systemic cell death is elicited by the interaction of a single gene in *Nicotiana clevelandii* and gene VII of *Cauliflower mosaic virus*. MPMI 12 (10); 919-925.

Kishi, K., 1966 Necrotic spot of melon, a new virus disease. Ann. Phytopathol. Soc. Japan. 32; 138-144.

Klimyuk, V., Marillonnet, S.,Knablein, J., Mc Caman, M., Gleba, Y., 2008. Modern biopharmaceuticals. : Design, development and optimization. Chapter-6: Production of recombinant proteins in plants 893-917.

Koonin, E. V. and Dolja, V. V. 1993. Evolution and taxonomy of positive-stranded RNA viruses: Implication of comparative analysis of amino acid sequences. Crit. Rev. Biochem. Mol. Biol. 28; 375-430.

Kovalev, N., Pogany, J., Nagy, P. D., 2014. Template role of double-stranded RNA in Tombusvirus replication. J. Virol. 88 (10); 5638-5651.

Kubo, C., Nakazono-Nagaoka, E., Hagiwara, K., Kajihara, H., Takeuchi, S., Matsuo, K., Lchiki, T. U., Omura, T., 2005. New severe strains of *Melon necrotic spot virus*: symptomatology and sequencing. Plant Pathol. 54; 615-620.

Kunkel, T. A., 1985. Rapid and efficient site-specific mutagenesis without phenotypic selection. Proc. Natl. Acad. Sci. 82(2); 488-92.

La Scola, B., Audic, S., Robert, C., Jungang, L., de Lamballerie, X., Drancourt, M., Birtles, R., Claverie, J. M., Raoult, D., 2003. A Giant virus in Amoeba. Science 299; 2033.

Langenberg, W. G., Zhang,L., 1997. Immunocytology shows the presence of *Tobacco etch virus* P3 protein in nuclear inclusions. J stru. Bio. 118 (3); 243-247.

Lathman, L. J., Jones,R. A. C., 2001. Incidence of virus infection in experimental plots commercial crops and stocks of cool season crop legumes. Aus. J. Agri. Res. 52; 414-424.

Leckie, B. M., Stewart, C. N., 2011. Agroinfiltration is a technique for rapid assays for evaluating candidate insect resistance transgenes in plants. Plant Cell Rep. 30; 325-334.
Lecoq, H., and Desbiez, C., (ed) 2012. Viruses of cucurbit crops in the Mediterranean region: An ever changing picture. Advances in virus research. First edition, Elsevier, San Diego, CA; 68-114.

Lecoq, H., Dafalla, G. A., Mohammed, Y. F., Ali, H. M., Wipf-Scheibel, C., Desbiez, C., Eljacj. E., Omara, S. K., Pitrat, M., 1994. Survey of viral diseases infecting cucurbit crops in eastern, central and western Sudan. University of Khartoum, Jour. Agr. Sci. 2; 67-82.

Lim, H.S., Bragg, J. N., Ganesan, U., Ruzin, S., Schichnes, D., Lee, M. Y., Vaira, A. M., Ryu, K. M., Hammond, J., Jackson, A. O., 2009. Subcellular localization of *Barley stripe mosaic virus* triple gene block proteins. J. Virol. 83 (8); 9432-9448.

Lindbo, J. A., 2007. TRBO: A high efficiency *Tobacco mosaic virus* RNA-based over expression vector. Plant Physiol. 145; 1232-1240.

Liu, L., Kloepper, J. W., Tuzun, S., 1995. Induction of systemic resistance in cucumber against Fusarium wilt by plant growth promoting Rhizobacteria. Phytopathol. 85 (6); 695-698.

Liu, L., Lomonossoff, G. P., 2002. Agroinfection as a rapid method for propagating *Cowpea mosaic virus* based constructs. J. Virol. Meth. 105 (2); 343-348.

Lokesh, G. L., Gopinath, K., Satheshkumar, P. S., Savitri, H.S., 2001. Complete nucleotide sequence of Sesbania mosaic virus: a new virus species of the genus *Sobemovirus.* Archives of virology 146 (2); 209-223.

Lommel, S. A., Martelli, G. P., Rubino, L. & Russo, M., 2005.Eighth Report of the International Committee on Taxonomy of Viruses, edited by C. M. Fauquet, M. A. Mayo, J. Maniloff, U. Desselberger & L. A. Ball, pp. 907–936. New York: Academic Press.

Lucas, W. J., 1995. Plasmodesmata: Intercellular channels for macromolecular transport in plants. Curr. Opin. Cell. boil. 7, 673-680.

Lucas, W. J., 2006. Plant viral movement proteins: Agents for cell-to-cell trafficking of viral genomes. Virol. 344; 169-184.

Malpica, J. M., Fraile, A., Moreno, I., Obies, C. I., Drake, J. W.,García-Arenal, F., 2002. The Rate and character of spontaneous mutation in an RNA Virus. Genetics 162 (4); 1505-1511.

Marillonnet, S., Theoringer, C., Kandzia, R., Klimyuk, V., and Gleba, Y., 2005. Systemic *agrobacterium tumefaciens*-mediated Transfection of viral replicons for effective transient expression in plants. Nat. Biotech 23 (6); 718-723.

Martinez-Gil, L., Sauri, A., Vilar, M., Pallas, V., Mingarro, I., 2007. Membrane insertion and topology of the 7B movement protein of *Melon necrotic spot virus*. Virology 367 (2); 348- 357.

Martínez-Turino, S., Hernández, C., 2012. Analysis of the subcellular targeting of the smaller replicase protein of *Pelargonium flower break virus*. Virus Research 163; 580-591.

Mary, C., 2012. Gaint viruses revive old questions about viral origins, Science 2; 1035.
Massumi, H., Samei, A., Pour, A. H., Shaabanian, M., 2007. Occurance, distribution and relative incidence of seven viruses infecting green-house grown cucurbits in Iran. Plant disease 91 (2); 158-163.

Matsuo, K., Kameya-Iwaki, M., Ota, T., 1991. Two new strains of *Melon necrotic spot virus*. Ann. Phytopathol. Soc. Japan 57; 558-67.

Matthieu, L., Bartoli. J., Shmakova, L., Sandra, J., Labadie, K., Adrait. A., Magali, L., Olivier, P., Lionel, B., Bruley, C., Yohann, C., Elizaveta, R., Chantal, A. and J. Michel, J. C., 2014. Thirty-thousand-year-old distant relative of giant icosahedral DNA viruses with a Pandoravirus morphology. Proc. Natl. Acad. Sci.111 (11); 4274-4279.

Maule, A. J., 2008. Plasmodesmata: structure, function and biogenesis. Curr. Opin. Plant Biol. 11; 680-686.

McCartney, A. W., Greenwood, J. S., Fabian, M. R., White, K. A., Mullen, R. T., 2005. Localization of *Tomato bushy stunt virus* replication protein P33 reveals a peroxisome to endoplasmic reticulum sorting pathway. The plant cell 17 (12); 3513-3531.
McKinney, H. H., 1935. Evidence of virus mutation in the common mosaic of tobacco. J. Agric. Res. 51; 951-81.

Milne, R. H., and Howie, A., 1984. Electron microscopy of copper oxidation. Philosophical magazine A 49 (5); 665-682.

Min-Ryu, C., Anand, A., Li Kang., Mysore, S.K., 2004. Agrodrench: a novel and effective agroinoculation method for virus induced gene silencing in roots and divers Solanaceous species. The Plant J. 40; 322-331.

Mitra, R., Krishnamurthy, K., Blancaflor, E., Payton, M., Nelson, R. S., Verchot-Lubicz, J., 2003. The *potato virus x* TGBp2 protein association with the endoplasmic reticulum plays a role in but is not sufficient for viral cell-to-cell movement. Virology 312, (1); 35-48.

Miras, M., Sempere, R. N., Kraft, J. J., Miller, W. A., Aranda, M. A., Truniger, V., 2014. Interfamiliar recombination between viruses led to acquisition of a novel translation-enhancing RNA element that allows resistance breaking. New Phytologist. 202 (1); 233-246.

Mo, X. H., Chen, Z. B., Chen, J. P., 2011. Molecular identification and phylogenetic analysis of a viral RNA associated with the Chinese tobacco bushy top disease complex. Ann Appl Biol 158; 188-193.

Mochizuki, T., Hirai, K., Kanda, A., Ohnishi, J., Ohki, T., Tsuda, S., 2009. Induction of necrosis via mitochondrial targeting *Melon Necrotic Spot Virus* Replication protein p29 by its second transmembrane domain. Virol. 390; 239-249.

Mochizuki, T., Ohnishi, J., Ohki, T., Kanda, A., Tsuda, S., 2008. Amino acid substitution in the coat protein of *Melon Necrotic Spot Virus* causes loss of binding to the surface of *Olpidium bornovanus* zoospores. J Gen Plant Pathol. 74; 176-81.

Mollov, D., Ben Lockhart., Zlesak, D. C., 2013. Complete nucleotide sequence of *Rosa rugosa leaf distortion virus*, a new member of the family Tombusviridae. Arch Virol 158; 2617-2620.

Mollov, D., Ben Lockhart., Zlesak, D. C., 2014. Complete nucleotide sequence of *Rose yellow leaf virus*, a new member of the family Tombusviridae. Arch Virol.

Morozov, S. Y., Solovyev, A. G., 2003. Triple gene block: modular design of a multifunctional machine for plant virus movement. J. Gen. Virol. 84 (6); 1351-1366.

Morris, T. S, 2001. Tombusviruses. In: Maloy, O. T, Murray, T. D, eds. *Encyclopedia of Plant Pathology* 2. New York, USA: John Wiley and Sons, 1031-1034.

Morris, T. J., Dodds, J. A. 1979. Isolation and analysis of double-stranded RNA from virus-infected plant and fungal tissue. Phytopathol. 69, (8); 854-858.

Naderi, M., Berger, P. H., 1997. Effects of chloroplast targeted *Potato virus* Y coat protein on transgenic plants. Physiol. Mol. Plant. Physiol. 50 (2); 67-83.

Nagy, P. D., Barajas, D., Pogany, J., 2012. Host factors with regulatory roles in Tombusvirus replication. Curr. Opin. Biol. 2; 691-698.

Nagy, P. D., Pogany, J., 2000. Partial purification and characterization of *Cucumber necrosis virus* and *Tomato bushy stunt virus* RNA-dependent RNA polymerases: Similarities and differences in template usage between Tombusvirus and Carmovirus RNA-dependent RNA polymerases. Virol. 276 (2); 279-288.

Nagy, P. D., Pogany, J., 2010. Global genomics and proteomics approaches to identify host factors as targets to induce resistance against *Tomato bushy stunt virus*. Adv. Vir. Res. 76; 123-177.

Nagy, P. D., Pogany, J., 2011. The dependence on viral RNA replication on co-opted host factors. Nature Rev. Microbiol. 10; 137-149.

Nagyova, A., Subr, Z., 2007. Infectious full length clones of plant viruses and their use for construction of viral vectors. Acta Virol. 51; 223-227.

Naidu, R. A, Hughes, J. D. A., 2003. Methods for the detection of plant viral diseases in plant virology in sub-Saharan Africa, Proceedings of plant virology, IITA, Ibadan, Nigeria. Eds. Hughes JDA, Odu B, 233-260.

Nam, M., Kim, S. M., Domier, L. L., Koh, S., Moon, J. K., Choi, H.S., Kim, H.G., Moon, J. S., Lee, S. H., 2009. Nucleotide sequence and genome organization of of a newly identified member of thegenus Carmovirus, *Soy-bean yellow mottle mosaic virus* from Soybean. Arch. Virol. 154; 1679-1684.

Narayanaswamy, P., 2008. Molecular Biology in plant pathogenesis and disease management. Microbial plant pathogens. Volume-1, Springer science + business media, 8.

Nass, N., Scheel, D., 2001. Enhanced luciferin entry causes rapid wound-induced light emission in plants expressing high levels of luciferase. Planta 212; 149-154.

Navarro, J. A. S., Zwart, M. P., Elena, S. F., 2013. Effects of the number of genome segments on primary and systemic infections with a multipartite plant RNA virus. J. Virol. 87 (19); 10805- 10815.

Navarro, J. A., Carring, A., Climent, J., Sauri, A., Martinez-Gil, L., Mingarro, I., Pallas, V., 2006. RNA-binding properties and membrane insertion of *Melon Necrotic Spot Virus* (MNSV) double gene block movement proteins. Virol. 356; 57-67.

Nayudu, M. V., 2008. Plant Viruses, Tata McGraw-Hill Education, 7 West Patel Nagar, New Delhi, India .

Niehl, A., and Heinlein, M. 2011. Cellular pathways for viral transport through plasmodesmata. Protoplasma. 248: 75-99.

Nieto, C., Morales, M., Orjeda, G., Clepet, C., Monfort, A., Sturbois, B., Puigdomenech, P., Pitrat, M., Caboche, M., Dogimont, C., Garcia-Mas, J., Aranda, A. M., Bendahmane, A., 2006. An eIF4E allele confers resistance to an uncapped and non-polyadenylated RNA virus in melon. Plant J. 48, 452-462.

Nishiguchi, M., Motoyoshi, F., Oshima, N., 1978. Behavior of a temperature sensitive strain of *Tobacco mosaic virus* in tomato leaves and protoplasts. J. Gen. virol. 39; 53-61.

Nishiguchi, M., Motoyoshi, F., Oshima, N., 1980. Further investigation of a temperature sensitive strain of *Tobacco mosaic virus*: its behavior in tomato leaf epidermis. J. Gen. Virol. 46; 497-500.

Noueiry and Ahlquist. 2003. Brome mosaic virus RNA replication: Revealing the Role of the Host in RNA virus Replication. Annual Review of Phytopathol. 41; 77-98

O'Reilly., Kao, C. C., 1998. Analysis of RNA dependent RNA polymerase structure and function as guided by known polymerase structures and computer predictions of secondary structures. Virology 252; 287-303.

Ohki, T., Akita, F., Mochizuki, T., Kanda, A., Sasaya, T., Tsuda, S., 2010. The protruding domain of the coat protein of *Melon Necrotic Spot Virus* is involved in compatibility with and transmission by the fungal vector Olpidium bornovanus. Virol. 402; 129-134.

Ohki, T., Sako, I., Kanda, A., Mochizuki, T., Honda,Y., and Tsuda, S., 2008. A new strain of *Melon necrotic spot virus* that is unable to systemically infect *Cucumis melo*. Phytopathology 98, 1165-1170.

Ohshima, K., Ando, T., Motomura, N., Matsuo, K., Sako, N., 2000. Comparative study on genome of two Japanese Melon necrotic spot isolates. Acta. Virol. 44 (66); 309-314.

Oparka, K. J., 2004. Getting the message across: how do plant cells exchange macromolecular complexes? Cell 8 (1); 33-41.

Oparka, K. J., Boevink, P., Santa cruz, S., 1996. Study of movement of plant viruses using green fluorescent protein. Trends in plant Science 1 (12); 412-418.

Oparka, K. J., Prior, D. A. M., Santa cruz, S., Padgett, H. S., Beachy, R. N., 1997. Gating of epidermal plasmodesmata is restricted to the leading edge of expanding infection sites of *Tobacco mosaic virus.* The Plant J. 12 (4); 781-789.

Ozeki, J., Takahashi, S., Komatsu, K., Kagiwada, S., Yamashita, K., Mori, T., Hirata, H., Yamaji, Y., Ugaki, M., Namba, S., 2006. A single amino acid in the RNA-dependent RNA polymerase of *Plantago asiatica mosaic virus* contributes to systemic necrosis. Arch. Virol. 151; 2067-2075.

PaDIL., 2013. Plant pest and Diease Image Library. Banded cucumber beetle *Diabrotica balteata* and western spotted cucumber beetle *Diabrotica undecimpunctata*. (www.padil.gov.au/pests-and-diseases/Pest/Main/135549).

Panaviene, Z., Baker, J. M., Nagy, P. D., 2003. The overlapping RNA binding domains of p33 and p92 replicase proteins are essential for tombusvirus replication. Virol. 308 (1); 191-205.

Pathak, K. B., Jiang, Z., Ochanine, V., Sharma, M., Pogany, J., Nagy, P. D., 2013. Characterization of dominant-negative and temperature sensitive mutants of tombusvirus replication proteins affecting replicase assembly. Virol. 437; 48-61.
Pathak, K. B., Pogany, J., Xu, K., white, A, K., Nagy, P. D., 2012. Defining the roles of *cis*-acting RNA elements in Tombusvirus replicase assembly *in vitro*. J. Virol. 86 (1); 156-171.

Pazzagli, M., Devine, J. H., Peterson, D. O., Baldwin, T.O., 1992. Use of bacterial and firefly luciferases as reporter genes in DEAE-dextran mediated transfection of mammalian cells. Analyt. Biochem. 204 (2); 315-323.

Pearson, H., 2008. Virophage suggests viruses are alive. Nature, 454; 677.

Peiro, A., Martinez-Gil, L., Tamborero, S., Pallas, V., Navarro, J. A. S., Mingarro, I., 2014. The *Tobacco mosaic virus* movement protein associates with but does not integrate into biological membranes. J. Virol. 88 (5); 3016-3026.

Peng, J. C., Yeh, S. D., Huang, L. H., Li, J. T., Cheng, Y. F., Chen, T. C., 2011. Emerging threat of thrips borne *Melon Yellow Spot Virus* on melon and water melon in Taiwan. Eur. J. Plant. Pathol 130; 205-214.

Pennisi, E., 2013. Ever-bigger viruses shake tree of life, Science 341; 226.

Philippe, N., Matthieu, L., Gabriel, D., Yohann, C., Olivier, P., Magali, L., Arslan, D., Virginie, S., Lionel, B., Christophe, B., Garin, J., Claverie, J. M. Chantal, A., 2013. Pandoraviruses: Amoeba Viruses with Genomes Up to 2.5 Mb Reaching That of Parasitic Eukaryotes. Sci. 341; 281-286.

Popescu, S. C., Popescu, G. V., Bachan, S., Zhang, Z., Seamy, M., Gerstein, M., Snyder, ., Dinesh-Kumar, S. P., 2007. Differential binding of calmodulin-related proteins to their targets revealed through high density Arabidopsis protein microarrays. PNAs 104 (11); 4730-4735.

Pouwels, J., Van Der Krogt, G. N. M., Van Lent, J., Bisseling, T., Wellink, J., 2002. The cytoskeleton and secretory pathway are not involved in targeting the *Cowpea mosaic virus* movement protein to the cell periphery. Virology 297; 48-56.

Powell, C. A., De Zoeten, G. A., Gaard, G., 1977. The localization of *Pea enation mosaic virus*- induced RNA-dependent RNA polymerase in infected peas. Virology 78 (1); 135-143.

Prasher, D. C., Eckenrode, V. K., Ward, W. W., Prendergast, F. G., Cormier, M. J., 1992. Primary structure of the *Aequorea victoria* green-fluorescent protein. *Gene* 111; 229-233.

Priti, N. D., Srivastava, N., Padh, H., 2010. Production of heterogenous proteins in plants: Strategies for optimal expression. Biotechnology advances 28; 427-435.

Prodhomme, D., Jakubiec, A., Tournier, V., Drugeon, Gabriele, Jupin, I., 2003. Targetting of the *Turnip Yellow mosaic virus* 66 K replication protein to the chloroplast envelope is mediated by the 140 K protein to the chloroplast envelope is mediated by 140 K protein. J. Virol. 77 (17); 9124-9135.

Provvidenti, R., 1996, Disease caused by viruses. In: Zitter TA, Hopkins, DL, Thomas, CE, Compendium of cucurbit diseases. St Paul, MN, USA, APS Press, 37-45.

Purkayastha, A., Mathur, S., Verma, V., Sharma, S., Dasgupta, I., 2010. Virus-induced gene silencing in rice using a vector derived from a DNA virus. Planta 232;1531-1540.

Rajendran, K. S., Pogany, J., Nagy, P. D., 2002. Comparison of *Turnip Crinkle Virus* RNA-dependent RNA polymerase preparations expressed in *Escherichia coli* or derived from infected plants. J. Virol. 76 (4); 1707-1717.

Ranjith, C. T., Gopinath, K., Jacob, A. N. K., Srividhya, V., Elango, P., Savitri, H.S., 1998. Genomic sequence of physalis mottle virus and its evolutionary relationship with other Tymoviruses. Archives of virology 143 (8); 1489-1500.

Ratcliff, F., Martin Hernandez, A. M., Baulcombe, D. C., 2001. *Tobacco rattle virus* as a vector for analysis of gene function by silencing. Plant. J. 25 (2); 237-245.

Reichel, C., Mathur, J., Eckes, P., Langenkemper, K., Koncz, C., Schell, J., Reiss, B., Mass, C., 1996. Enhanced green fluorescence by the expression of an *Aequorea victoria* green fluorescent protein mutant in mono and dicotyledonous plant cells. PNAS 93 (12); 5888-5893.

Reingold, V., Lachman, O., Blaosov, E. and Dombrovsky, A., 2014. Seed disinfection treatments do not sufficiently eliminate the infectivity of *Cucumber green mottle mosaic virus* (CGMMV) on cucurbit seeds. Plant Pathology (Online version before inclusion in a issue). Doi: 10.1111/ppa.12260.

Restrepo-Hartwig, M. A., Ahlquist, P., 1996. *Brome mosaic virus* helicase and polymerase proteins co-localize on the endoplasmic reticulum at sites of viral RNA synthesis. J. Virol. 70 (12); 8908-8916.

Restrepo-Hartwig, M. A., Ahlquist, P., 1999. *Brome mosaic virus* RNA replication proteins 1a and 2a co-localize and 1a independently localizes on yeast endoplasmic reticulum. J. Virol. 73 (12); 10303-10309.

Ribeiro, D., Borst, J. W., Goldbach, R., Kormelink, R., 2009. Tomato spotted wilt virus nucleocapsid protein interacts with both viral glycoproteins Gn and Gc in planta. Virol. 383; 121-130.

Ribeiro, D., Foresti, O., Denecke, J.,Wellink, J., Goldbach, R., Kormelink, R. J. M., 2008. *Tomato spotted wilt virus* glycoproteins induce the formation of endoplasmic reticulum and golgi derived pleomorphic membrane structures in plant cell. J. Gen. Virol. 89 (8); 1811-1818.

Rico, P., Hernandez, C., 2009. Characterization of the subgenomic RNAs produced by *Pelargonium flower break virus*: Identification of two novel RNA species. Virus Res. 142, 100-107.

Riviere, C. J., Pot, J., Tremaine, J.H., Rochon, D.M., 1989. Coat protein of *Melon Necrotic Spot Carmovirus* is more similar to those of Tombusviruses than those of Carmoviruses. J Gen. Virol. 70, 3033-3042.

Riviere, C. J., Rochon, D.M., 1990. Nucleotide sequence and genomic organization of *Melon Necrotic Spot Virus*. J. Gen. Virol. 71, 1887-1896.

Robertson, N. L., 2004. Biology of a new virus isolated from *Lupinus nootkatensis* plants in Alaska. Plant pathology 53 (5); 569-576.

Robertson, N. L., Corte, F., Pare, C., Leblanc, E., Bergeron, M. G., Leclere, D., 2007. The complete nucleotide sequence of *Nootka lupine vein-clearing virus*. Virus genes 35; 807-814.

Rochon, D. A., Kakani, K., Robbins, M., Reade, R., 2004. Molecular aspects of plant virus transmission by *Olpidium* and *Plasmodiophorid* vectors. Annu. Rev. Phytopathol. 42; 211-241.

Rodriguez-Cerezo, E., Ammar, E. D., Pirone, T. P., Shaw, J. G., 1993. Association of the non-structural P3 viral protein with cylindrical inclusions in potyvirus infected cells. J Gen Virol. 74; 1945.

Rodriguez-Hernandez, A. M., Gosalvez, B., Sempere, R. N., Burgos, L., Aranda, M. A., Truniger, V., 2012. Melon RNA interference (RNAi) lines silenced for Cm-elF4E show broad virus resistance. Mol. Plant. Pathol. 13 (7); 755-763.

Romay, G., Lecoq, H., Geraud-Pouey, F., Chirinos, D. T., Desbiez, C., 2014. Current status of cucurbit viruses in Venezuela and characterization of Venezuelan isolates of *Zucchini yellow mosaic virus*. Plant Pathology 63; 78-87.

Romero-Brey, I., Bartenschlager, R., 2014. Membranous replication factories induced by plus- strand RNA viruses Viruses 6; 2826-2857.

Roossinck, M. J., 2013. Plant virus ecology. PLOS Pathogen 9 (5); 1-3.

Rott, M. E., Tremaine, J. H., Rochon, D. M., 1991. Nucleotide sequence of *Tomato ringspot virus* RNA-2. J. gen. virol 72 (7);1505-1514.

Rua, M. A., Pollina, E. C., Power, A. G., Mitchell, C. E., 2011. The role of viruses in biological invasions: friend or foe? Curr. Opin. Virol. 1; 68-72.

Rubino, L., Weber-Lotfi, F., Dietrich, A., Stussi-Garaud, C., Russo, M., 2001. The open reading frame-1encoded ('36K') protein of *Carnation Italian ringspot virus* localizes to mitochondria. J. Gen. Virol. 82 (1); 29-34.

Sambrook, J., Fritsch, E. F., Maniatis, T. 2001. Molecular cloning: A laboratory Manual (2).Cold Spring Harbor Laboratory, Cold Spring Harbor, New York.

Samuels, T. D., Ju, H. J., Ye, C. M., Motes, C.M., Blancaflor, E.B., Verchot-Libicz, J., 2007. Subcellular targeting and interactions among the *Potato virus* X TGB protein. Virology. 367 (2); 375-389.

Sang-Min, C., Vaidya, M., and Tzfira, T., 2006. Agrobacterium is not alone: gene transfer to plants by viruses and other bacteria. TRENDS in plant Science 11(1); 1-4.

Santa cruz, S., Chapman, S., Robert, A. G., Roberts I. M., Prior, D. A. M., Oparka, K. J., 1996. Assembly and movement of a plant virus carrying a green fluorescent protein over coat. PNAS 93; 6286-6290.

Santos-Rosa, M., Poutaraud, A., Merdinoglu, D., Mestre, P., 2008. Development of a transient expression system in grapevine via agro-infiltration. Plant Cell Rep. 27; 1053-1063.

Sarnow, P., 1989. Translation of glucose-regulated protein 78/immunoglobulin heavy-chain binding protein mRNA is increased in poliovirus-infected cells at a time when cap-dependent translation of cellular mRNAs is inhibited. PNAs 86 (15); 5795-5799.

Satyanarayana, T., Gowda, S., Ayllon, M.A., Dawson, W.O., 2003. Frameshift mutations in infectious cDNA clones of *Citrus tristeza virus*: A strategy to minimize the toxicity of viral sequences to *Escherichia coli* .Virology 313; 481-491.

Schepetilnikov, M. V., Solovyev, A. G., Gorshkova, E. N., Schiemann, J., Prokhnevsky, A. I., Dolja, V. V., Morozov, S. Y., 2008. Intracellular targeting of a Hordeiviral membrane- spanning movement protein: sequence requirements and involvement of an unconventional mechanism. J. Virol. 82 (3); 1284-1293.

Scholthof, H. B., Scholthof, K. G., 1996. Plant virus gene vectors for transient expression of foreign proteins in plants. Ann. Rev. Phtopathol. 34; 299-323.

Scholthof, H. B., Scholthof, K. G., Kikkert, M., Jackson, J.O., 1995. *Tomato Bushy stunt virus* spread is regulated by two nested genes that function in cell-to-cell movement and host dependent systemic invasion. Virology 213 (2); 425-438.

Serra, P., Gago, S., Duran-Vila, N., 2008. A single nucleotide change in *Hop stunt viroid* modulates citrus cachexia symptoms. Virus research 138; 130-134.

Serva, S., Nagy, P. D., 2006. Proteomics analysis of the Tombusvirus replicase: HSP 70 Molecular chaperone is associated with the replicase and enhances viral RNA replication. J. Virol. 80 (5); 2162-2169.

Sheen, J., Hwang, S., Niwa, Y., Kaboyashi, H., Galbraith, D. W., 1995. Green-fluorescent protein as a new vital markerin plant cells. Technical advance 8 (5); 777-784.

Sheludko, Y. V., Sindarovska, Y. R., Gerasymenko, I. M., Bannikova, M. A., 2006. Comparison of several *Nicotiana* species as host for high-scale Agrobacterium-mediated transient expression. Biotechnol. Bioeng 96; 608–614.

Skotnicki , M. L., Mackenzie, A. M., Torronen, M., Gibbs, A. J., 1993. The genome sequence of *Cardamine chlorotic fleck Carmovirus*. J. Gen. Virol. 74; 1933-1937.

Stewart, C. N., 2008. Plant biotechnology and genetics: principles, techniques and applications. John Wiley & Sons, Inc., Hoboken, New Jersey. 1-365.

Suzuki, S., Hase, S., Takahashi, H., Ikegami, M., 2002. The genome organizations of *Pea stem necrosis virus* and its assignment to the genus Carmovirus. Intervirology 45; 160-163.

Takemoto, Y., Kanehira, T., Shinohara, M., Yamashita, S., Hibi, T., 2000. The nucleotide sequence and genome organization of *Japanese iris necrotic spot virus*, a new species in the genus Carmovirus. Arch. Virol. 145; 651-657.

Tian, T., Posis, K., Maroon-Lango, C. J., Mavrodieva, V. J., Haymes, S., Pitman, T. L., Falk, B. W., 2014. First report of *Cucumber green mottle mosaic virus* on melon in the United States. Plant disease 98 (8); 1163.

Traynor, P., Young, B. M., Ahlquist, P.,1991. Deletion analysis of *Brome mosaic virus* 2a protein: Effects on RNA replication and systemic spread. J. Virol. 65; 2807-2815.

Tribodet, M., Glais, L., Karlan, C., Jacquot, E., 2005. Characterization of *Potato virus*-Y molecular determinants involved in the vein necrosis symptom induced by PVY isolates infected *N. tabacum* cv. Xanthi. J. Gen. Virol. 86; 2101-2105.

Tzanetakis, I. E., Martin, R. R., 2008. A new method for extraction of double-stranded RNA from plants. J. Virol. Methods 149; 167–170.

Tzfira, T., and Citovsky, V. 2006. *Agrobacterium*-mediated genetic transformation of plants: biology and biotechnology. Curr. Opin. Biotechnol. 17; 147-154.

Tzfira, T., and Citovsky, V. 2008. Agrobacterium: From Biology to Biotechnology. Springer, New York. 1-734.

Vadim, M., Farrance, C, E., Green , B, J., Yusibov, V., 2008. Plants as biofactories. Biologicals 36 (6); 354-358.

Vaghchhipawala, Z., Mysore, K.S., 2008. Agroinoculation: A simple procedure for systemic infection of plants with viruses. in: Foster G, editor. Plant Virology Protocols: From viral sequence to protein function. Humana press, Totowa, NJ 451; 555-562.

Van Bakoven, H., Verver, J., Wellinck, J., van Kammen, A., 1993. Protoplasts transiently expressing the 200K coding sequence of *cowpea mosaic virus* B-RNA support replication of M-RNA. J. Gen. Virol 74; 2233-2241.

Van der Horn, R. A. L., Laurent, F., Roth, R., De Wit, P. J., 2000. Agroinfiltration is a versatile tool that facilitates comparative analysis of Avr9/Cf-9-induced and Avr4/Cf-4-induced necrosis. Mol. Plant Microbe Interact 13; 439-446.

Van Regenmortel, M. H. V., Fauquet, C. M., Bishop, D. H. L., Carstens, E., Estes, M. K., Lemon, S., Maniloff, J., Mayo, M. A., McGeoch, D., Pringle, C. R., Wickner, R. B., 2000. Virus Taxonamy, Seventh report of the International committee on Taxonomy of Viruses. Academic Press, New York.

Van Wezel, R., Liu, H., Tien, P., Stanely, J., Hong, Y., 2001. Gene C2 of the monopartite geminivirus *Tomato yellow leaf curl virus*-China encodes a pathogenicity determinant that is localized in the nucleus. Mol Plant Microbe Interact 14 (9); 1125-1128.

VanderGheynst, J. S, Guo, H. Y., Simmons, C. W., 2008. Response surface studies that elucidate the role of infiltration conditions on *Agrobacterium tumefaciens*-mediated transient transgene expression in harvested switchgrass (*Panicum virgatum*). Biomass Bioenergy 32; 372-379.

Vilar, M., Sauri, A., Marcos, J. F., Mingarro, I., Perez-Paya, E., 2005. Transient structural ordering of the RNA binding domain of *Carnation mottle virus* p7 movement protein modulates nucleic acid binding. ChemBioChem 6 (8); 1391-1396.

Vogel, F., Hofius, D., Sonnewald, U., 2007. Intracellular trafficking of *Potato leafroll virus* movement protein in transgenic Arabidopsis. Traffic 8; 1205-1214.
Voinnet, O., 2001. RNA silencing as a plant immune system against immune system against viruses. Trends. Genet. 17 (8); 449.

Voinnett, O., Rivas, S., Mestre, P., Baulcombe, D., 2003. An enhanced transient expression system in plants based on suppression of gene silencing by the p19 protein of *Tomato bushy stunt virus*. Plant. J. 3; 259-73.

Wada, Y., Tanaka, H., Yamashita, E., Kubo, C., Ichiki-Uehara, T., Nakazono-Nagaoka, E., Omura, T., and Tsukihara, T., 2008. The structure of *Melon necrotic spot virus* determined at 2.8A° resolution. Acta Cryst. F64, 8-13.

Waigmann, E., Ueki, S., Trutnyeva, K., Citovsky, V., 2004. The ins and outs of non-destructive cell-to-cell and systemic movement of plant viruses. Crit. Rev. Plant Sci. 23 (3); 195-250.

Wang, Y., Ding, B., 2010. Viroids: Small Probes for Exploring the Vast universe of RNA Trafficking in Plants. Journal of Integrative Plant Biology 52 (1); 28-39.

Wang, Y., Xiao, M., Zhang, W., Luo, J., Bao, K., Nie, M., Chen, J., Li, B., 2007. Mutational analysis of the GDD sequence motif of the *Classical swine fever virus* RNA-dependent RNA virus. Virus genes 34; 63-65.

Wang, Y., Gaba, V., Yang, J., Palukaitis, P., Gal-On, A., 2002. Characterization of synergy between *Cucumber mosaic virus* and Potyviruses in cucurbit hosts. Phytopathol. 92 (1); 51-58.

Weber, F., Wagner, V., Rasmussen, S. B., Hartmann, R., Paludan, S. R., 2006. Double-stranded RNA is produced by positive-strand RNA viruses and DNA viruses but not in detectable amounts by negative-strand RNA viruses. J. Virol. 80 (10); 5059-5064.

Weinmann, P., Gossen, M., Hillen, W., Bujard, H., Gatz, C., 1994. A chimeric transactivator allows tetracycline-responsive gene expression in whole plants. *Plant J*. 5; 559-569.

Weng, Z., Xiong, Z., 1997. Genome Organization and gene expression of *Saguaro cactus Carmovirus*. J Gen Virol. 78, 525-534.

Wiedenmann, J., Oswald, F., Nienhaus, G. U., 2009. Fluorescent proteins for live cell imaging: opportunities, limitations, and challenges. Life 61(11); 1029-1042.

Wright, K. M., Wood, N. T., Roberts, A. G., Chapman, S., Boevnik, P., Mackenzie, K. M., Oparka, K. J., 2007. Targeting of TMV movement protein to plasmodesmata requires the actin/ER network; Evidence from FRAP. Traffic 8 (1); 21-31.

Wroblewski, T., Tomczak, A., Michelmore, R., 2005. Optimization of Agrobacterium-mediated transient assays of gene expression in lettuce, tomato, and Arabidopsis. Plant Biotechnol. J. 3; 259-273.

Yakoubi, S., Desbiez, C., Fakhfakh, H., Wipf-Scheibel, C., Marrakchi, M., Lecoq, H., 2008. First Report of *Melon Necrotic Spot Virus* on melon in Tunisia. Plant Pathol. 57, 386.

Yang, T. T., Cheng, L., Kain, S. R., 1996. Optimized codon usage and chromophore mutations provide enhanced sensitivity with the green fluorescent protein. Nucleic Acids Res 24; 592-4593.

Yang, Y., Li, R., Qi, M., 2000. In vivo analysis of plant promoters and transcription factors by agroinfiltration of tobacco leaves. Plant J 22; 543-551.

Yoshida, K., Goto, T., Nemoto, M., Tsuchizaki, T., 1980. Five viruses isolated from melon (*Cucumis melo* L.) in Hokkaido. Ann. Phytopath. Soc. Jpn. 46; 339-348.

You, X. J., Kim, J. W., Stuart, G. W., Bozarth, R. Z., 1995. The complete sequence of *Cowpea mottle virus* and its assignment to genus Carmovirus. J. Gen. Virol. 76 (11); 2841-2845.

Yu, H. H., Wong, S. M., 1998. Synthesis of biologically active cDNA clones of *cymbidium mosaic potexvirus* using a population cloning strategy. Arch. Virol. 143; 1617-1620.

Yuan, X. F., Shi, K. R., Young, M. Y. L., Simon, A. E., 2010. The terminal loop of a 3' proximal hairpin plays a critical role in replication and the structure of the 3' region of *Turnip crinkle virus*. Virology 402, 271-280.
Yamshchikov, V. F., Wengler, G., Perelygin, A. A., Brinton, M. A., Compans, R. W., 2001. An infectious clone of the West Nile Flavivirus. Virology 281 (2); 294-304.

Yuan, Z. C.,Williams, M., 2012. A really useful pathogen, *Agrobacterium tumefaciens.* The Plant Cell 24(10); 1012.

Yuki, V. A., Rezende, J. A. M., Kitajima, E. W., Barroso, P. A. V., Kuniyuki, H., Pavan, M. A., 2000. Occurance, distribution and relative incidence of five viruses infecting in the state of Sao Paulo, Brazil. Plant disease 84 (5); 516-520.

Zamyatnin, A. A., Solovyev, A. G., Savenkov, E. I., Germundsson, A., Sandgren, M., Valkonen, J. P. T., Morozov, S. Y., 2004. Transient coexpression of individual genes encoded by the triple gene block of *Potato mop-top virus* reveals requirements for TGBp1 trafficking. MPMI 17 (8); 921-930.
Zell, R., Krumbholz, A., Wutzler, P., 2008. Impact of global warming on viral diseases: what is the incidence? Current opinion in biotechnology 19 (6); 652-660.

Zhang, G., Sanfacon, H., 2006. Characterization of membrane association domains within the *Tomato ringspot nepovirus* X2 protein, an endoplasmic reticulum targeted polytopic membrane protein. J. Virol. 80 (21); 10847-10857.

A1.1 Acetosyrinzone- 150 mM

Dissolve 294.3 mg of acetosyrinzone in 10 ml of DMSO

A1.2 Acrylamide:bisacrylamide

Acrylamide- 29.2 gm
Bis acrylamide-0.8 gm
Dissolve in 100 ml of autoclaved double distilled water. Don't autoclave.

A1.3 Ammonium acetate-5M

Ammonium acetate – 38.55 gm
Make up with double distilled water – 100 ml
Don't autoclave

A1.4 Ammonium sulphate-55%

55gm of ammonium sulphate
100 ml of double distilled water
Dissolve completely by stirring, autoclave and store.

A1.5 Buffer-A

100mM CaCl2,70mM MnCl2, 70mM of sodium acetate; Sodium acetate was first dissolved in Milli Q water, pH was adjusted to 5.5 and the rest of the salts were added & filter sterilized

A1.6 Buffer-B

Buffer-A containing 15% glycerol was filter sterilized and used directly

A1.7 Blocking buffer

5 gm of milk powder (Nestle/Amul) was dissolved in 100 ml of 1X TBS

A1.8 Carbonate buffer

Na_2CO_3 – 1.59 gm
$NaHCO_3$ – 2.93 gm
Dissolve and make up to 1000 ml with double distilled water

A1.9 Compositions of different percentages of gels

	Stacking Gel	Resolving Gel		
	4%	7.5%	12%	X%
30% Acrylamide/bis	1.32 ml	2.5 ml	4.0 ml	0.33•X ml
0.5 M Tris-HCl, pH 6.8	2.52 ml	–	–	–
1.5 M Tris-HCl, pH 8.8	–	2.5 ml	2.5 mnl	2.5 ml
10% SDS	100 µl	100 µl	100 µl	100 µl
Distilled deionized water	6 ml	4.85 ml	3.35 ml	7.35 – (0.33•X) ml
TEMED	10 µl	5 µl	5 µl	5 µl
10% APS	50 µl	50 µl	50 µl	50 µl
Total Volume	10 ml	10 ml	10 ml	10 ml

A1.10 Destaining solution

20 ml Methanol
10 ml glacial acetic acid
70 ml double distilled water
Mix well

A1.11 Inoculation buffer

20 mM potassium phosphate buffer (prepare from stock-1M) and
0.01% β-mercapto ethanol

A1.12 Lammeli sample Dye pH-6.8 (LSD)

Distilled water – 20 ml
1.5 M Tris-HCl pH-6.8 – 5 ml
Glycerol – 4 ml
10% SDS – 8 ml
2-ME – 2 ml
0.05% bromophenol blue – 1.5 ml
Make up the volume to 50 ml with distilled water

A1.13 Loading dye-6X

1X TAE buffer – 8 ml
Glyceral (20%) – 2 ml
0.1% Bromophenol blue – 100 µ

A1.14 PBS-10X

NaCl – 80 gm
Na2PO4.2H2O – 14.4 gm
KH2PO4 – 0.2 gm
KCl – 0.2 gm
Make up to 1000 ml with distilled water

A1.15 PBS-T

500 µl of tween-20 in 1000 ml of 1X PBS

A1.16 PBS-TPO

100 ml of PBS-T
PVP – 2 gm
Ovalbumin – 0.2 gm

A1.17 Plasmid isolation buffer - P1

50mM Tris-HCl pH-8.0
10mM EDTA pH-8.0

A1.18 Plasmid isolation buffer – P2

200mM NaOH
1% SDS

A1.19 Plasmid isolation buffer – P3

3M potassium acetate; pH-5.5

A1.20 Potassium phosphate buffer

Stock-1: Prepare 1M K_2HPO_4 = 174.18 gm in 1L distilled water
Stock-2: Prepare 1M KH_2PO_4 = 136.09 gm in 1L distilled water
Mix 80.2 ml of stock-1 and 19.8 ml of stock-2 and make up the volume to 1L with distilled water to get Potassium phosphate buffer of pH-7.4.

A1.21 Resolving buffer

1.5 M Tris-HCl – 18.1 gm of Tris base
60 ml distilled water, adjust pH-8.8 with HCl, make up volume to 100 ml, autoclave and store.

A1.22 Rifampicin

Dissolve 50 mg in DMSO

A1.23 RNA Extraction buffer (Gopinath *et al.*, 2005)

0.1M glycine pH 9.2
40 mM EDTA
100 mM NaCl
2% SDS
0.05% bentonite

A1.24 SDS running buffer-10X

Tris base – 15.1 gm
Glycine – 72 gm
SDS- 5 gm
Dissolve and make up the volume to 1000 ml with double distilled water

A1.25 Stacking buffer

1.5 M Tris-HCl – 18.1 gm of Tris base in 60 ml distilled water, adjust pH-6.8 with HCl, make up volume to 100 ml, autoclave and store.

A1.26 Staining solution

100 mg of Coomassie R-250
40 ml of methanol

Dissolve completely and then add
10 ml of glacial
50 ml of double distilled water

A1.27 Substrate buffer for western

15 mg of BCIP in 1 ml of DMFO
30 mg of NBT in 1 ml of 70% DMFO

A1.28 Substrate buffer for ELISA

9.7% diethanolamine,
50 mg p-nitrophenyl phosphate pH 9.8

A1.29 TAE-50X

Tris base – 242 gm
EDTA – 17.8 gm
Glacial acetic acid – 57.10 ml
Water – 752 ml

A1.30 TBS-10X

Tris base – 12.1 gm
NaCl – 148.2 gm
Dissolve and make up to 1000 ml
with double distilled water

A1.31 TBS-T

500 µl of tween-20 in 1000 ml of 1X TBS

A1.32 Western transfer buffer

Tris base – 30.2 gm
Glycine – 144 gm
Dissolve and make up to 1000 ml
with double distilled water

A1.33 Total soluble protein buffer

50 mM Tris Acetate pH7.4,
10 mM $MgCl_2$,
250 mM KCl,
20% glycerol
1 mM PMSF
1 mM DTT

Complete nucleotide sequence of MNSV-Hyd (Acc. No: JX879088)